Bremen 2022
Cover illustration by Santos Benito Orodea

David Benito Merino | Archaea and bacteria mediating anaerobic alkane degradation at its upper temperature limit

David Benito Merino

Archaea and bacteria mediating anaerobic alkane degradation at its upper temperature limit

Archaea and bacteria mediating anaerobic alkane degradation at its upper temperature limit

Dissertation

in fulfillment of the requirements for the degree of Doctor of Natural Sciences

– Dr. rer. nat. –

Faculty of Geosciences, University of Bremen

David Benito Merino

Bremen, December 2022

The research presented in this thesis was conducted between September 2018 and December 2022 in the HGF MGP Bridge Group for Deep-Sea Ecology and Technology at the Max Planck Institute for Marine Microbiology in Bremen, under the leadership of Prof. Dr. Antje Boetius and the direct supervision of Dr. Gunter Wegener. This thesis is framed in the program of the International Max Planck Research School of Marine Microbiology (mar*mic*).

Author: David Benito Merino

ORCID: 0000-0002-1453-7330

Max Planck Institute for Marine Microbiology, Bremen

Faculty of Geosciences, University of Bremen

First reviewer: Prof. Dr. Antje Boetius

Faculty of Geosciences, University of Bremen

Alfred Wegener Institute, Helmholtz Center for Polar and Marine Research, Bremerhaven

Max Planck Institute for Marine Microbiology, Bremen

Second reviewer: Dr. Cornelia Welte

Radboud University Nijmegen, The Netherlands

First examiner: Prof. Dr. Kai-Uwe Hinrichs

Second examiner: Dr. Gunter Wegener

Date of the doctoral defence: 17th February 2023

Im Zweifel für Verzärtelung
und für meinen Knacks,
für die äußerste Zerbrechlichkeit,
für einen Willen wie aus Wachs.
(...)
Im Zweifel für Ziellosigkeit
(...)

Tocotronic, „Im Zweifel für den Zweifel“

Index

Summary

Deep in the seafloor, geothermal heat transforms organic matter into alkanes and other petroleum compounds. These compounds migrate towards the sediment surface, where microorganisms consume them as carbon and energy source. In marine sediments, alkane degradation is predominantly coupled to sulfate reduction. This process is largely performed by archaea of the phylum Halobacteriota with methyl/alkyl-coenzyme M reductases (Mcr/Acr), which form syntrophic consortia with sulfate-reducing bacteria (SRB). Most of these organisms degrade alkanes shorter than pentane and at temperatures of maximum 60°C. In my thesis project, I cultured and characterized novel Mcr/Acr-encoding archaea and associated SRB from sediments of the Guaymas Basin (Gulf of California) beyond this temperature limit.

Chapter 2 (Manuscript I) describes a novel consortium mediating anaerobic methane oxidation (AOM) at 70°C. The consortium consists of anaerobic methanotrophic archaea of the group ANME-1c and the thermophilic SRB *Candidatus* Thermodesulfobacterium torris. The ANME-1c is an ancestral ANME-1 clade that retains some characteristics of their thermophilic alkane-degrading relatives. The association of ANME-1c with Thermodesulfobacteria likely relies on direct interspecies electron transfer (DIET) via cytochromes. **Chapter 3** (Manuscript II) describes the enrichment of Acr-encoding archaea of the phylum Hadarchaeota, which grow on the long-chain alkane hexadecane. *Candidatus* Cerberiarchaeum oleivorans and genomes from the same family encode the complete pathway for alkane degradation, which is not present in other Hadarchaeota. We propose that this Hadarchaeota family acquired some of the pathways for alkane degradation via horizontal gene transfer from other subsurface archaea. **Chapter 4** (Manuscript III) shows that pathways related to DIET are widespread in Thermodesulfobacteria of marine environments. This suggests that other Thermodesulfobacteria species are potential syntrophic partners for anaerobic oxidation of alkanes.

In **Chapter 5**, I discuss the findings of this thesis in the context of the evolution of archaea and alkane metabolisms. Acr-encoding archaea and associated SRB might occupy a broader variety of niches than previously thought. In summary, my thesis expands the occurrence of anaerobic methane and long-chain alkane metabolisms towards higher temperatures, now including archaea of the phylum Hadarchaeota.

Zusammenfassung

Tief im Meeresboden werden organische Stoffe durch geothermische Wärme in Alkane und andere Erdölverbindungen umgewandelt. Diese wandern in Richtung der Sedimentoberfläche, wo Mikroorganismen sie als Kohlenstoff- und Energiequelle nutzen. In marinen Sedimenten ist der Abbau von Alkanen in erster Linie an die Sulfatreduktion gekoppelt. Diese Alkane werden von Archaeen aus den Halobacteriota abgebaut, welche diese Substrate mit Methyl/Alkyl-Coenzym-M-Reduktasen (Mcr/Acr) aktivieren. Die Archaeen formen syntrophe Konsortien mit sulfatreduzierenden Bakterien (SRB). Die meisten dieser Organismen bauen Alkane kürzer als Pentan (C_5) und auf Temperaturen niedriger als 60°C ab. In meiner Dissertation beschreibe ich neuartige Mcr/Acr-tragendende Archaeen und deren Partnerbakterien, die ich aus Sedimenten des Guaymas-Beckens (Golf von Kalifornien) kultiviert habe. Die Resultate verschieben die zuvor gekannten Temperaturgrenzen.

Kapitel 2 (Manuskript I) beschreibt ein neuartiges Konsortium, dass unter anaeroben Bedingungen und einer Temperatur von 70°C Methan oxidiert. Das Konsortium besteht aus anaeroben methanotrophen Archaeen der Gruppe ANME-1c und dem thermophilen SRB *Candidatus* Thermodesulfobacterium torris. Bei ANME-1c handelt es sich um eine ursprüngliche ANME-1 Variante, die einige markante Merkmale ihrer thermophilen, alkanabbauenden Verwandten in sich trägt. Die Assoziation von ANME-1c mit Thermodesulfobacteria beruht vermutlich auf einer Form des direkten Elektronentransfers zwischen verschiedenen Arten? (DIET), welche über Cytochrome katalysiert wird. **Kapitel 3** (Manuskript II) beschreibt die Anreicherung von Acr-kodierenden Archaeen des Phylums Hadarchaeota, die auf dem langkettigen Alkan Hexadekan wachsen. *Candidatus* Cerberiarchaeum oleivorans und Genome aus der gleichen Familie kodieren den kompletten Weg zum Alkanabbau, der in anderen Hadarchaeota nicht vorhanden ist. Wir vermuten, dass diese Hadarchaeota-Familie einige der Stoffwechselwege für den Alkanabbau durch horizontalen Gentransfer von anderen unterirdischen Archaeen erworben hat. **Kapitel 4** (Manuskript III) zeigt, dass DIET-verwandte Stoffwechselwege in Thermodesulfobacteria von marinen Umgebungen weit verbreitet sind. Dies deutet darauf hin, dass weitere Arten aus der Gruppe der Thermodesulfobacteria das Potential haben, als syntrophe Partner für die anaerobe Oxidation zu leben.

In **Kapitel 5** diskutiere ich die Ergebnisse dieser Arbeit im Zusammenhang mit der Evolution von Archaeen und dem Alkanstoffwechsel. Acr-kodierende Archaeen und assoziierte SRB könnten eine breitere Palette von Nischen besetzen als bisher angenommen. Zusammenfassend lässt sich sagen, dass meine Arbeit das Vorkommen anaerober Methan- und langkettiger Alkan-Stoffwechsel auf höhere Temperaturen ausweitet und nun auch Archaeen des Stammes Hadarchaeota einschließt.

List of abbreviations

Acr	alkyl-coenzyme M reductase
ANI	average nucleotide identity
ANKA	anaerobic multicarbon alkane-degrading archaea
ANME	anaerobic methanotrophic archaea
AOM	anaerobic oxidation of methane
Aor	tungsten-containing aldehyde ferredoxin oxidoreductase
Apr	adenylylsulfate reductase
Ass	alkylsuccinate synthase
ATP	adenosine triphosphate
C	carbon
CARD-FISH	catalyzed reporter deposition-fluorescent in situ hybridization
Cbc	cytochrome *bc*
Cdh/Acs	carbon monoxide dehydrogenase/acetyl-coenzyme A synthase complex
CH_4	methane
CLR	center-log ratio
CO	carbon monoxide
CO_2	carbon dioxide
CoA	coenzyme A
COG	cluster of orthoulogous groups
CoM	coenzyme M
DAPI	4',6-diamidino-2-phenylindole
DIET	direct interspecies electron transfer
DNA	deoxyribonucleic acid
Dsr	dissimilatory sulfite reductase
Etf	electron transfer flavoprotein
FA	formamide
$FADH_2$/FAD	flavin adenine dinucleotide (reduced/oxidized)
Fd	ferredoxin
Fla	archaeal flagellum protein
Fqo	F_{420}:quinone oxidoreductase
GTDB	Genome Taxonomy Database
H_2	dihydrogen, molecular hydrogen
H_4MPT	tetrahydromethanopterin
Hdr	coenzyme B-coenzyme M heterodisulfide reductase
HMM	hidden Markov model
MAG	metagenome-assembled genome
Mch	methenyltetrahydromethanopterin cyclohydrolase
Mcr	methyl-coenzyme M reductase
Mer	N^5,N^{10}-methylene-H_4MPT reductase
MF	methanofuran
MHC	multiheme *c*-type cytochrome

Mtr	Na^+-translocating methyl-H_4MPT coenzyme M methyltransferase
mWL	methyl-branch Wood-Ljungdahl pathway
NADH/NAD^+	nicotinamide adenine dinucleotide (reduced/oxidized)
Nuo	NADH:ubiquinone oxidoreductase
Oet	outer membrane-bound extracellular electron transfer conduit
Omc	outer-membrane cytochromes
PCR	polymerase chain reaction
Pil	bacterial pilus protein
Qmo	quinone-modifying oxidoreductase
Qrc	quinone reductase complex
R/V	research vessel
RNA	ribonucleic acid
rRNA	ribosomal RNA
RT	room temperature
rTCA cycle	reductive tricarboxylic acid cycle
S^0	elemental sulfur
S^{2-}	sulfide
Sat	sulfate adenylyltransferase
SINA	SILVA Incremental Aligner
SO_4^{2-}	sulfate
SRB	sulfate-reducing bacteria
TCA cycle	tricarboxylic acid cycle / Krebs cycle
WL pathway	Wood-Ljungdahl pathway / reductive acetyl-coenzyme A pathway

Introduction and aims of the thesis

1.1. Microbial life in heated environments

Temperature is a key parameter that affects the activity and presence of microbes in the environment, and shapes their evolution (Brock, 1978a). High temperatures in an ecosystem can be caused by solar energy, anthropogenic activities or geothermal activity, the latter being the most prevalent (Brock, 1978b; Wiegert, 2001). Below the surface, the Earth's temperature increases on average 25°C with every kilometre of depth. The subsurface is regarded as a hot and nutrient-limited environment (Gold, 1992; Colman et al., 2017) yet contains a large number of prokaryotes (Whitman et al., 1998; Parkes et al., 2000; Kallmeyer et al., 2012). Some hot environments exist at shallower depths in marine and terrestrial settings, associated with local geothermal activity. Heated environments are habitats for thermophilic archaea and bacteria. Thermophiles are adapted to temperatures above 50°C, whereas hyperthermophiles have growth optima above 80°C (Holden, 2009). Many thermophiles are archaea (Rampelotto, 2013). In fact, the current record of thermophily is held by *Methanopyrus kandleri*, a marine methanogen that can grow at 122°C (Takai et al., 2008). In this introduction, I will cover deep-sea environments and, specifically, hot deep-sea environments and their microbial communities.

The deep-sea as habitat of microorganisms

The seafloor represents 67% of the Earth's surface. In the dark seabed, photosynthesis does not occur. A small fraction of the organic matter fixed in the photic zone sediments to the seafloor, where it sustains the activity of heterotrophic organisms (Jørgensen and Boetius, 2007). Within the seafloor, the quality and quantity of organic carbon decreases with depth, accompanied by a decrease in microbial cell numbers (Parkes et al., 2000). The degradation of organic matter in the seafloor is coupled to the reduction of terminal electron acceptors, following the order of decreasing redox potential (Figure 1). Oxygen and nitrate are often depleted within a few centimetres. Below this zone, oxidized metals (manganese and iron), sulfate and carbon dioxide are electron acceptors, and fermentative reactions appear as electron sinking mechanisms (Froelich et al., 1979; Jørgensen, 2006). This utilization cascade of electron acceptors translates into lesser favourable reactions (i.e., the free energy yield decreases with decreasing redox potential). The reduced products of these reactions accumulate and diffuse upwards where microorganisms can reoxidize them.

Methanogenesis, sulfate reduction and fermentation are key processes in the anoxic seafloor and in the sediment subsurface (D'Hondt et al., 2002; Teske and Sørensen, 2008). Methanogens belong exclusively to the domain *Archaea* and populate anoxic environments where electron acceptors other than CO_2 are scarce (Thauer et al., 2008; Offre et al., 2013). CO_2 reduction by methanogenesis produces methane that

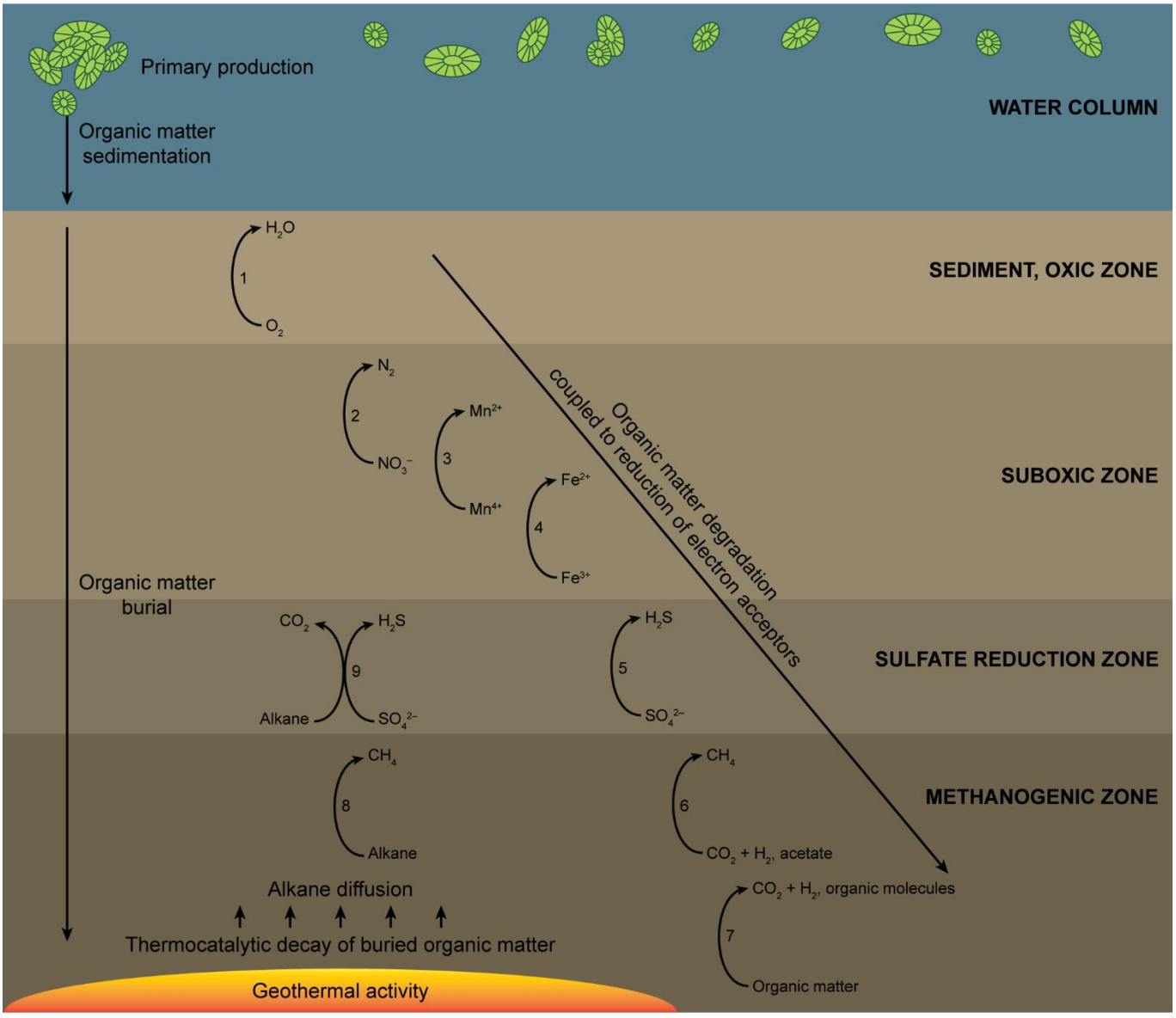

Figure 1. Oxidation of organic matter and alkanes in marine sediments. Organic matter produced by phototrophs in the lit ocean sinks to the seafloor and gets buried upon sedimentation. Microbes degrade organic matter sequentially in aerobic respiration (1), nitrate respiration (2), manganese reduction (3), iron reduction (4), sulfate reduction (5), methanogenesis (6) and fermentation (7). Buried organic matter exposed to geothermal gradients decays into alkanes and other hydrocarbons. Alkane oxidation occurs coupled to methanogenesis (8), or to sulfate reduction (9). Figure adapted from (Jørgensen, 2006).

diffuses towards the sediment surface. In the sulfate-methane transition zone (SMTZ), methane is reoxidized with sulfate as electron acceptor, in a process known as anaerobic oxidation of methane (AOM) (Boetius and Knittel, 2010). Anaerobic methane-oxidizing archaea (ANME) catalyse AOM, and coexist with bacteria that use sulfate as terminal electron acceptor (Knittel and Boetius, 2010). AOM occurs in a variety of deep-sea habitats such as mud volcanoes, cold seeps, methane hydrates, hydrothermal systems and subsurface sediments (Boetius and Knittel, 2010). There is even evidence for AOM at temperature up

to temperatures of 80°C (Kallmeyer and Boetius, 2004; Holler et al., 2011), but the responsible organisms for AOM at these temperature were unknown.

Hydrothermal vents and hot springs

Hydrothermal vents are geological features where heated fluids from the deep seafloor are expelled into the ocean. Most hydrothermal vents happen at mid-ocean ridges and others are formed at back arc spreading centres, volcanic arcs and intraplate volcanoes (German and Lin, 2004; Beaulieu and Szafrański, 2020). At mid-ocean ridges, the tectonic plates diverge as new oceanic crust is created at the rupture. Back arc basins and volcanic arcs form at subduction zones and are also associated with hydrothermalism (Stern, 2002). Hydrothermal activity also occurs at intraplate volcanoes, both in the ocean and in continents. At hydrothermal sites, hot fluids are released into the water column (Corliss et al., 1979; Rona et al., 1986; Pedersen et al., 2010).

The heated fluids contain varying amounts of reduced compounds including sulfide, hydrogen gas, ammonia, methane and reduced metals supporting chemosynthetic animal and microbial benthic communities (Corliss et al., 1979; Brooks et al., 1990; Kelley et al., 2002). In addition, some vents expel fatty acids and multicarbon alkanes. These compounds are formed sequentially by thermocatalytic decay and thermal decarboxylation of organic matter (Des Marais et al., 1981; Martens, 1990). Short-chain fatty acids are present in natural oil reservoirs and their detection serves to localize the reservoirs (Collins, 1975). It has been postulated that lipids subjected to chemical reactions above 115°C are the major precursors of petroleum (Collins, 1975).

The Guaymas Basin hydrothermal system

The Guaymas Basin is located in the Gulf of California at a depth of 2000 m (Figure 2) (Simoneit et al., 1990; Teske et al., 2016). The Basin is part of the boundary between the Pacific and North American tectonic plates. These two plates diverge, which produces transform faults and active spreading centres. The Guaymas Basin is covered with a thick layer (hundreds of meters) of organic-rich sediment (Simoneit et al., 1990). The sediment is mainly formed of diatom ooze from the photosynthetically productive surface waters and terrigenous material from coastal runoff (Calvert, 1966).

The Guaymas Basin is a sedimentary hydrothermal system, where hot magmatic sills intrude into the sediment, heating it up to 200–300°C (Calvert, 1966; Kawka and Simoneit, 1987; Teske and Carvalho, 2020). The heat results in the thermocatalytic decay of sedimented organic matter, and releases petroleum compounds such as methane, gaseous alkanes, long-chain alkanes and aromatic hydrocarbons (Figure 1)

(Simoneit and Lonsdale, 1982; Kawka and Simoneit, 1987; Bazylinski et al., 1988; Simoneit et al., 1988; Welhan, 1988; Milkov, 2005; Stolper et al., 2014). Hydrothermal circulation transports the hydrocarbon-rich fluids towards the sediment surface. The Guaymas Basin has some classic hydrothermal vents, but due to the thick sediment layer, diffuse venting is prevalent. The geothermal activity in the sediment forms methane and short-chain gaseous alkanes (up to 4 carbon atoms) over short geological times (Simoneit et al., 1990; Teske and Carvalho, 2020). In upper sediment layers, these hydrocarbons meet gradients of different electron acceptors and can serve as carbon and energy sources for the microbial communities (Rueter et al., 1994; Teske et al., 2002). Hydrocarbon oxidation is mainly coupled to sulfate reduction, which produces sulfide. At the sediment surface, the formed sulfide is oxidized by aerobic sulfide-oxidizing bacteria, for example filamentous *Beggiatoaceae* (Figure 2C). These bacteria accumulate sulfur granules intracellularly and form thick white and yellow mats on the surface (Teske et al., 2016). In fact, the presence of these mats in the sediment's surface are a proxy for sulfate-reduction activity in deeper layers.

For this thesis, I used material from two sampling campaigns in the Guaymas Basin. During the R/V *Atlantis* expeditions AT37-06 (December 2016) and AT42-05 (November 2018), the submersible *Alvin* was used to retrieve sediment cores from the Basin. In the laboratory, I used sediment samples to establish anoxic enrichment cultures growing on alkanes and I characterized the microbial communities that developed therein.

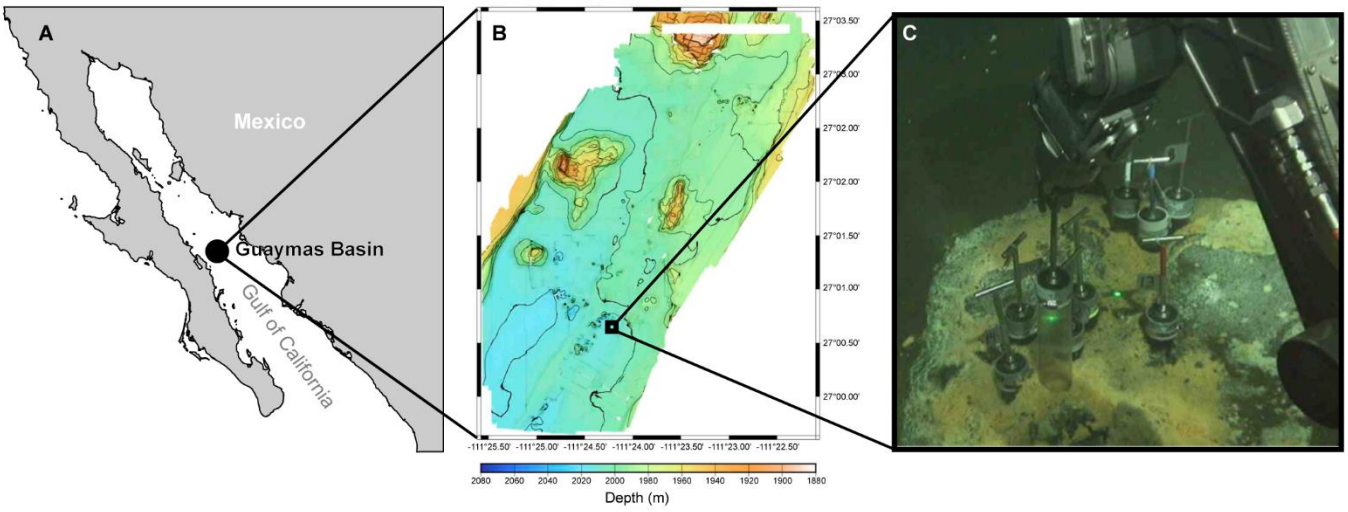

Figure 2. The Guaymas Basin hydrothermal system. A. Location of the Guaymas Basin in the Gulf of California (Mexico). **B.** Bathymetric map of the Guaymas Basin. **C.** The submersible *Alvin* sampling push cores from a sediment covered by *Beggiatoaceae*, at 2013 m depth (R/V *Atlantis* expedition AT42-05). Figures and photos courtesy of Andreas Teske and Hanna Zehnle.

1.2. The biogeochemistry of alkanes

Hydrocarbons consist solely of carbon (C) and hydrogen (H) atoms and form the largest part of coal, crude oil and natural gas. The use of hydrocarbons as fossil fuels during the industrial and market capitalism eras has on one side increased the gross domestic product, while on the other side triggering global warming by greatly increasing atmospheric CO_2 (Hall et al., 2003). It is questionable whether gross domestic product is an appropriate measurement of wellbeing in light of the current climate crisis (Masood, 2022). The use and further development of renewable energies alternative to fossil fuels, and other measures like economic degrowth are necessary to tackle the causes and effects of climate change (Ripple et al., 2020; Hickel et al., 2022; Schipper et al., 2022). Apart from the societal importance, hydrocarbons are one of the most abundant organic molecules in the biogeosphere (Wilkes and Schwarzbauer, 2010). In marine systems, hydrocarbons are found in oil reservoirs, petroleum seeps, hydrothermal systems and gas hydrates (Teske and Carvalho, 2020). According to the bonds present in their chemical structure, hydrocarbons can be divided into saturated, unsaturated and aromatic hydrocarbons. Here, I will explain the chemistry and origin of linear saturated hydrocarbons as well as their significance in natural environments.

Physicochemical properties of *n*-alkanes

n-Alkanes (hereafter referred to as "alkanes") are linear saturated hydrocarbons with the general formula C_nH_{2n+2}. Alkanes cover a wide span of molecules depending on the number of carbon atoms: methane (CH_4, C_1 alkane) and the multicarbon alkanes (MC-alkanes), which I further discriminate into gaseous short-chain alkanes (C_2 to C_4, i.e., ethane, propane and butane), mid-chain alkanes (C_5 to $C_{\leq 14}$) and long-chain oil alkanes ($C_{>14}$). Even though alkanes are energy-rich compounds, they are chemically unreactive, due to their stable covalent bonds (Widdel and Musat, 2010b). The lack of reactivity of alkanes explains their name *paraffins* (from Latin *parum*, too little, and *affinis*, related or having affinity, therefore *low affinity*) (Wilkes and Schwarzbauer, 2010).

In alkanes, C atoms combine one 2*s* and three 2*p* orbitals to form an sp^3 hybrid orbital (Figure 3A) (Wilkes and Schwarzbauer, 2010; Bruice, 2013). The sp^3 orbital can form four covalent σ-bonds in a tetrahedral disposition (Figure 3B). In alkanes, the C-C are σ-bonds between sp^3 orbitals and the C-H bonds are σ-bonds between an sp^3 orbital of C and the 1*s* orbital of H (Figure 3C). The similar electronegativity of C (2.55) and H (2.20) results in a symmetric distribution of the electrons in the hybrid sp^3 orbitals forming non-polar σ-bonds. This apolarity makes C atoms in alkanes rather inaccessible to chemical reactions (Wilkes and Schwarzbauer, 2010).

Because viscosity increases with chain length (Wilkes and Schwarzbauer, 2010), oil alkanes (e.g. more than 10 carbon atoms) are basically insoluble and diffuse at slower rates in hydrothermal systems (Simoneit et al., 1988; Didyk and Simoneit, 1990). In contrast, the high gas pressure of short-chain alkanes and especially methane in systems like the Guaymas Basin keeps them dissolved in hydrothermal fluids (Simoneit et al., 1988; Didyk and Simoneit, 1990).

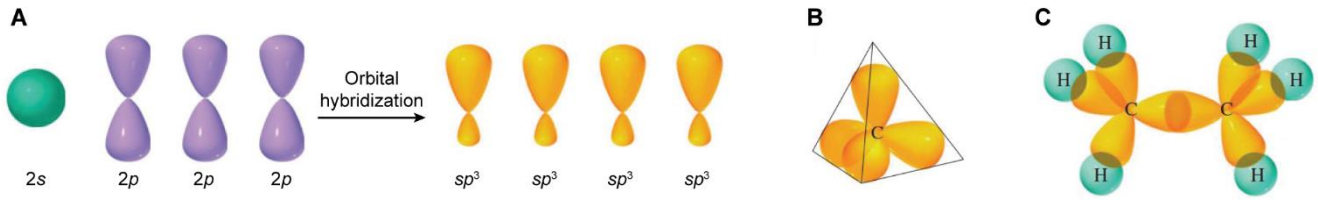

Figure 3. Geometry of carbon orbitals and covalent bonds in alkanes. A. In a carbon atom, one 2*s* and three 2*p* orbitals hybridize to form four sp^3 orbitals. **B.** Hybrid sp^3 orbitals orient towards the corners of a regular tetrahedron. **C.** In alkanes like ethane (C_2H_6), covalent bonds are formed by overlapping of carbon sp^3 orbitals to form C-C bonds or overlapping of carbon sp^3 orbitals with a hydrogen 1*s* orbital to form C-H bonds. Figure adapted from (Bruice, 2013).

Origin of alkanes on Earth

Alkanes form primarily under anoxic conditions in the Earth's subsurface. They are of either abiotic, thermocatalytic or biotic origin. Most abiotic alkanes form during the serpentinization of ultramafic rocks (Berndt et al., 1996; Kelley, 1996; Proskurowski, 2010). On modern Earth, however, this pathway is of minor importance (Sherwood Lollar et al., 2002). Thermogenic alkanes are formed when buried organic matter is exposed to high temperatures and pressures (Wilkes and Schwarzbauer, 2010). On modern Earth, most methane by anaerobic methanogenic archaea. Some long-chain alkanes are also found in plant leaf waxes (Wilkes and Schwarzbauer, 2010). Minor amounts of methane and short-chain alkanes are formed as metabolic side products of aerobic microorganisms such as cyanobacteria (Karl et al., 2008).

Methane, the simplest of alkanes, is an abundant low-molecular weight organic compound on Earth and the main constituent of natural gas (Wilkes and Schwarzbauer, 2010). Methane is a greenhouse gas 25 times more potent than CO_2 and its concentration in the atmosphere has tripled in the last 300 years. In the atmosphere, however, methane is less abundant than CO_2. Atmospheric methane derives from anthropogenic and natural sources. Anthropogenic activities account for approximately 50% of the methane emissions (Saunois et al., 2020). Global methane sinks are slightly smaller than the sources and,

therefore, methane levels have steadily increased in the atmosphere since pre-industrial times (Conrad, 2009).

Microbial methanogenesis is a major source of methane on Earth, and it contributes to approximately 70% of the global methane emissions to the atmosphere (Conrad, 2009). Microbial methanogenesis occurs in a variety of anoxic environments, such as freshwater sediments, wetlands, marine sediments, anaerobic digesters and ruminants' rumens (Conrad, 2009). In the ocean, most of the biogenic methane is produced in benthic systems (Reeburgh, 2007). However, almost the totality of methane mobilized from gas hydrates and produced by benthic methanogens is efficiently consumed by methanotrophs in the sediments and in the water column (Reeburgh, 2007; Conrad, 2009). Consequently, the oceans are a minor source of atmospheric methane (Reeburgh, 2007).

Long-chain alkanes are a major component of crude oil. Alkanes form in sedimentary basins over geological time scales. There, organic matter produced in the photic zone sediments to the seafloor, where it suffers biochemical transformations, burial and thermal degradation (Tissot and Welte, 1984). The first step of petroleum formation is *diagenesis*, in which sedimented organic matter is degraded by microbial activity. The recalcitrant fraction of polymeric organic molecules that endures biochemical degradation receives the name of *kerogen* (Tissot and Welte, 1984; Wilkes and Schwarzbauer, 2010). Upon further sedimentation, burial depth of kerogen increases. *Catagenesis* is the second and main step of petroleum formation, when kerogen is exposed at high temperatures and pressures, releasing crude oil and natural gas hydrocarbons. At greater depths or in locations with a strong geothermal gradient, *metagenesis* of kerogen occurs. At this stage, methane is the only compound released from kerogen (Tissot and Welte, 1984).

1.3. Microbial oxidation of alkanes

Alkanes contain reduced carbons and thus can serve as carbon and electron source for many microorganisms, which have developed metabolic pathways to utilize them since the early Earth. Before alkanes can be metabolized, they require an enzymatic activation or functionalization. Due to their lack of chemical reactivity, the alkane activation represents a challenge for microorganisms. The activation of alkanes is a reaction that attacks the C-H bond (Widdel and Musat, 2010a; Rabus et al., 2016). The dissociation of the C-H bond is an energy costly process (Widdel and Musat, 2010b; Rabus et al., 2016). The H is subsequently replaced by a more polar group, making the molecule more prone to chemical reactions and ready for microbial oxidation.

Aerobic oxidation of alkanes

Under oxic conditions, aerobic bacteria oxidize alkanes to CO_2. The first step is the activation of the alkane with a monooxygenase (Wang and Shao, 2013). Monooxygenases reduce molecular oxygen (O_2) with NADH to form oxygen in the peroxide state (O_2^{2-}). Peroxide derives into an intermediate reactive oxygen species that attacks the alkane to form an alcohol (Widdel and Musat, 2010a). The activation of methane by methane monooxygenases produces methanol, that is subsequently oxidized to formaldehyde, formate and CO_2. Alkane monooxygenases (hydroxylases) that activate short-chain alkanes are related to methane monooxygenases, whereas those for longer alkanes belong to different classes (Rojo, 2010). The resulting alkanol (i.e., an alkane with a hydroxyl group at the terminal carbon) is successively oxidized to an aldehyde and a carboxylic acid (fatty acid), and then completely oxidized to CO_2 via the β-oxidation pathway (Rojo, 2010; Wang and Shao, 2013).

Aerobic methane oxidizing bacteria (MOB) belong to the classes Alpha- and Gammaproteobacteria (phylum Proteobacteria), to the phylum Verrucomicrobiota and to the candidate species *Candidatus* Methylomirabilis oxyfera (phylum Methylomirabilota, former NC10) (Kalyuzhnaya et al., 2019). MOB are widespread in freshwater systems where methane is available (Kalyuzhnaya et al., 2019), and they have been detected in some benthic and pelagic marine environments (Tavormina et al., 2008). Aerobic non-methane alkane oxidizers belong to the classes Gammaproteobacteria (phylum Proteobacteria) and Bacilli (Firmicutes), and are involved in bioremediation of oil spills (Wang and Shao, 2013). One remarkable example is the marine bacterium *Alkanivorax*, capable of utilizing alkanes ranging from C_5 to C_{36} (Liu and Shao, 2005). *Alkanivorax* are present in low abundances in seawater but proliferate after oil spills (Kasai et al., 2002).

Anaerobic oxidation of alkanes in bacteria

Anaerobic bacteria use at least three different mechanisms to activate alkanes: (i) addition to fumarate, (ii) hydroxylation during denitrification and (iii) anaerobic hydroxylation followed by carboxylation (Callaghan, 2013). The nitrate reducer HdN1 (Gammaproteobacteria) apparently uses the "intra-aerobic" mechanism of alkane activation, producing intracellular O_2 during denitrification (So et al., 2003). This pathway has been confirmed for the methanotroph *Ca.* Methylomirabilis oxyfera (Ettwig et al., 2010). In denitrifying alkanotrophs, an alkane hydroxylase uses the intracellular O_2 to activate mid- and long-chain alkanes (Zedelius et al., 2011). Another mechanism for alkane activation is the anaerobic hydroxylation by an ethylbenzene dehydrogenase (EBDH)-like complex (Callaghan, 2013). The activation is followed by an oxidation of the hydroxyl group and a carboxylation. This pathway has been proposed for the sulfate

reducer *Desulfococcus oleovorans* Hxd3 (Callaghan, 2013). Homologs of EBDH and key products found in oil reservoirs provide further evidence for this pathway (Shou et al., 2021).

However, the most common anaerobic activation mechanisms for non-methane alkanes is the addition to fumarate (Widdel and Musat, 2010a). This reaction has been observed for short- and long-chain *n*-alkanes (Callaghan, 2013), and is catalyzed by alkylsuccinate synthases (Ass) or methylalkylsuccinate synthases (Mas) (Grundmann et al., 2008; Callaghan et al., 2010). These enzymes activate the alkanes preferentially at the subterminal carbon by a glycyl radical reaction and subsequently add the alkyl group to the double bond of fumarate, forming a (1-methylalkyl)succinate (Figure 4A) (Rabus et al., 2001; Buckel and Golding, 2006). The (1-methylalkyl)succinate is then ligated to coenzyme A (CoA) and, after a molecular reorganization and a decarboxylation reaction, it is oxidized in the β-oxidation pathway (Wilkes and Rabus 2020).

Fumarate addition is spread among several microbial lineages of nitrate- and sulfate-reducing bacteria (SRB) (Callaghan, 2013). The pathway is prevalently associated with sulfate-reducing Desulfobacterota (Widdel et al., 2010; von Netzer et al., 2013). This mechanism has been demonstrated for long-chain alkanes and short-chain alkanes down to butane and propane, whereas ethane or methane activation via Ass has not been reported (Kniemeyer et al., 2007; Widdel et al., 2010; Jaekel et al., 2013). The hyperthermophilic sulfate-reducing archaeon *Archaeoglobus fulgidus* also uses Ass to activate long-chain alkanes (Khelifi et al., 2014) and it is thought that the *ass* genes were acquired via horizontal gene transfer from SRB.

In deep sediment layers or oil reservoirs where terminal electron acceptors other than CO_2 are depleted, some alkanotrophic bacteria ferment the alkanes to acetate and hydrogen. These bacteria establish syntrophic associations with methanogenic archaea that grow on the fermentation products (Zengler et al., 1999; Jones et al., 2008; Gieg et al., 2014; Toth and Gieg, 2018; Liu et al., 2020b). This syntrophy makes both partners interdependent, and allows them to metabolize substrates which they could not utilize on their own (Schink, 1997; Orphan, 2009).

Anaerobic oxidation of alkanes in archaea

Biogenic methane supports anaerobic communities in the subsurface. In marine sediments, most of this gas is consumed in deeper layers, where oxygen is not available. Anaerobic oxidation of methane (AOM) can occur coupled to the reduction of other electron acceptors, namely nitrate, ferric iron, manganese oxides and sulfate (Raghoebarsing et al., 2006; Beal et al., 2009; Knittel and Boetius, 2009; Haroon et al.,

2013; Ettwig et al., 2016; Leu et al., 2020). Because sulfate is the most abundant electron acceptor in seawater, sulfate-dependent AOM is prevalent in marine sediments. AOM removes more than 90% of the methane produced in the seafloor (Hinrichs and Boetius, 2002; Reeburgh, 2007).

The enzyme methyl-coenzyme M reductase (Mcr) is central in anoxic methane metabolism and is exclusively encoded by archaea. Methanogenic archaea use Mcr in the final step of methanogenesis to reduce methyl-CoM to methane (Thauer, 2019). In contrast, ANME use highly similar variants of this enzyme for the first step of AOM (Thauer, 2011; Scheller et al., 2020). The activation of methane as methyl-CoM is the rate-limiting step in AOM (Scheller et al., 2010; Thauer, 2011). ANME run the methanogenesis pathway in the oxidative direction (i.e. reverse methanogenesis) to completely oxidize methane to CO_2 (Thauer, 2011; Scheller et al., 2020). The occurrence of ANME in methanogenic sediments suggested that ANME include facultative methanogens (Lloyd et al., 2011; Kevorkian et al., 2021), yet no ANME have been cultured under methanogenic conditions.

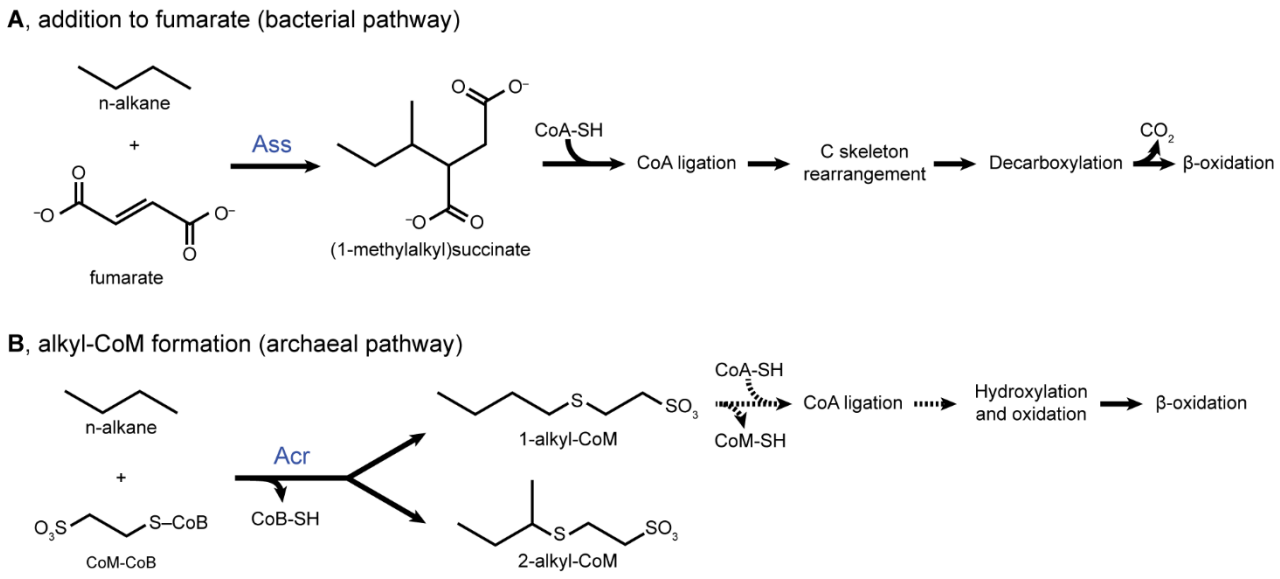

Figure 4. Main alkane-activating reactions in anaerobic microbes. The reactions are shown for the activation of butane. **A.** Anaerobic bacteria (mainly sulfate reducers) and the archaeon *Archaeoglobus fulgidus* activate alkanes via addition to fumarate. The reaction is catalyzed by alkylsuccinate synthases (Ass). The resulting alkylsuccinate is ligated to CoA and, after molecular rearrangement and decarboxylation, a fatty acid enters the β-oxidation. **B.** Anaerobic archaea use Mcr variants (Acr) to activate alkanes to alkyl-CoM. Two products are formed, with the CoM moiety in the first or second carbon. The alkyl group is transferred to CoA and oxidized to a carboxylic acid, which can enter the β-oxidation. The reactions marked with dashed arrows are hypothetical and have not been demonstrated *in vitro*.

Some archaea related to ANME use Mcr variants to activate short-chain alkanes to the corresponding alkyl-CoMs (Figure 4B). *Ca*. Syntrophoarchaeum activates propane and butane to propyl- and butyl-CoM, respectively (Laso-Pérez et al., 2016). Mcr variants were also shown to activate ethane in *Ca*. Ethanoperedens and *Ca*. Argoarchaeum (Chen et al., 2019; Hahn et al., 2020). I discuss the diversity and evolution of Mcr-encoding archaea, with a focus on divergent Mcr variants, in the following section in detail.

Table 1. Mcr/Acr-encoding archaea and their metabolisms. Table adapted from (Wang et al., 2020). Cultivation status: C=cultured (at least one instance in pure or enrichment culture), U=uncultured.

Organism	Mcr/Acr function	Electron acceptor	Partner bacteria	Cultivation status	References
Methanogens	CH_4 formation	CO_2	--	C	Reviewed in (Garcia et al., 2022)
Ca. Methanophagales (ANME-1)	CH_4 activation	SO_4^{2-}	*Ca.* Desulfofervidus, Seep-SRB2	C	(Hinrichs et al., 1999; Boetius et al., 2000; Krukenberg et al., 2018)
Ca. Methanocomedenaceaea, *Ca*. Methanomarinus (ANME-2a, 2b)		SO_4^{2-}	Seep-SRB1		(Orphan et al., 2002; Wang et al., 2014)
Ca. Methanogasteraceae (ANME-2c)		SO_4^{2-}	Seep-SRB1, SRB2		(Krukenberg et al., 2018; Wang et al., 2019a)
Ca. Methanoperedens (ANME-2d)		NO_3^-, Fe^{3+}, Mn^{4+}	--		(Haroon et al., 2013; Arshad et al., 2015; Cai et al., 2018; Leu et al., 2020)
ANME-3		SO_4^{2-}	Desulfobulbia, Seep-SRB1		(Niemann et al., 2006; Lösekann et al., 2007; Omoregie et al., 2008; Schreiber et al., 2010)
Ca. Ethanoperedens	Ethane activation	SO_4^{2-}	*Ca*. Desulfofervidus	C	(Hahn et al., 2020)
Ca. Argoarchaeum					(Chen et al., 2019)
Ca. Syntrophoarchaeales	Propane/butane activation	SO_4^{2-}	*Ca*. Desulfofervidus	C	(Laso-Pérez et al., 2016; Wang et al., 2019a)
Ca. Methanomethylicales	Unknown, Mcr-type	Unknown	--	U	(Vanwonterghem et al., 2016)
Ca. Nezhaarchaeales					(Hua et al., 2019; Wang et al., 2019b)
Ca. Korarchaeales					(McKay et al., 2019; Wang et al., 2019b)
Nitrososphaerales					(Hua et al., 2019)
Ca. Methanomixophus (Archaeoglobi)		Unknown/SO_4^{2-}			(Colman et al., 2019; Wang et al., 2019b; Liu et al., 2020a)
Ca. Methanoliparia	$C_{\geq 13}$ alkane activation and CH_4 formation	CO_2	--	C	(Borrel et al., 2019; Laso-Pérez et al., 2019; Zhou et al., 2022)
Ca. Bathyarchaeia	Unknown, Acr-type	Unknown	--	U	(Evans et al., 2015)
Ca. Hadarchaeota					(Hua et al., 2019; Wang et al., 2019b)
Ca. Helarchaeales					(Seitz et al., 2019)
Ca. Polytropus marinifundus (Archaeoglobi)					(Boyd et al., 2019; Wang et al., 2019b)

1.4. Diversity of Mcr-encoding archaea

Archaea coding for Mcr belong mainly to the phyla Halobacteriota and Methanobacteriota, which include all cultured methanogens and methanotrophs (Table 1). Mcr variants with strong sequence divergence to the ones used for methane metabolism (Figure 5) are responsible for the activation of non-methane alkanes to the corresponding alkyl-CoM. Highly divergent Mcr sequence variants were first found in metagenome-assembled genomes (MAGs) of subsurface Bathyarchaeota (Evans et al., 2015). Based solely on genomic evidence, the authors claimed that Bathyarchaea might use Mcr for methane metabolism. This was also the first instance of Mcr-encoding archaea from a phylum unrelated to known methanogens and ANME. Later on, culture- and metagenomics-based approaches showed that *Ca*. Syntrophoarchaeum use Bathyarchaea-like Mcr variants to activate short-chain alkanes (Laso-Pérez et al., 2016). Mcr variants were also shown to activate ethane in *Ca*. Ethanoperedens and *Ca*. Argoarchaeum (Chen et al., 2019; Hahn et al., 2020). The crystal structure of the *Ca*. Ethanoperedens Mcr has been characterized (Hahn et al., 2021). This evidence led to rename the divergent Mcrs to multicarbon-alkane Mcrs or alkyl-CoM reductases (Acrs) (Thauer, 2019; Wang et al., 2020; Lemaire and Wagner, 2022). Thanks to this evidence, an Acr encoded in a genome is an indication for potential multicarbon alkane metabolism (Wegener et al., 2022). This has led to describe numerous non-syntrophic and putative anaerobic multicarbon alkane-degrading archaea (ANKA).

Environmental metagenomics have revealed Mcr/Acr-encoding MAGs throughout the domain Archaea (Table 1). Acrs have been found in the class Archaeoglobi (phylum Halobacteriota) (Boyd et al., 2019), in the phylum Hadarchaea (Wang et al., 2019b) and in the class Helarchaeia (phylum Asgardarchaeota) (Seitz et al., 2019), as well as in the phylum Halobacteriota (Borrel et al., 2019; Laso-Pérez et al., 2019). Mcr-type sequences have been found within the phylum Thermoproteota in the orders *Ca*. Methanomethylicales (Vanwonterghem et al., 2016), *Ca*. Nezhaarchaeales (Hua et al., 2019; Wang et al., 2019b), *Ca*. Korarchaeales (McKay et al., 2019; Wang et al., 2019b) and Nitrososphaerales (Hua et al., 2019). Similar Mcr-type sequences were also found in an Archaeoglobi MAG (Colman et al., 2019; Wang et al., 2019b; Liu et al., 2020a). Most of these environmental MAGs have not been cultivated to date and their physiology remains inconclusive.

Methanogenic archaea

Methanogenesis is one of the most primitive metabolisms on Earth (Ueno et al., 2006). Methanogenic archaea were classified in two groups within the former phylum Euryarchaeota: Class I methanogens (orders Methanobacteriales, Methanococcales and Methanopyrales) and Class II methanogens (orders

Methanosarcinales, Methanomicrobiales and Methanocellales) (Bapteste et al., 2005; Gribaldo and Brochier-Armanet, 2006; Garcia et al., 2022). According to novel standardized taxonomy, Class I and II methanogens belong to the phyla Methanobacteriota and Halobacteriota, respectively (Rinke et al., 2021).

Methanogens mainly reduce CO_2 to methane using the methyl branch of the Wood-Ljungdahl pathway, including tetrahydromethanopterin S-methyltransferase (Mtr) and Mcr. In addition, methyl-reducing hydrogenotrophic methanogens of the order Methanomassiliicoccales (phylum Thermoplasmatota) and of the class Methanonatronarchaeia (phylum Halobacteriota) have been described, providing further evidence for the wide distribution and ancestral origin of methanogenesis in the Archaea (Borrel et al., 2013; Sorokin et al., 2017).

Some studies have suggested that Mcr was present in the common ancestor of Class I and II methanogens and Thermoproteota (Borrel et al., 2019; Wang et al., 2021). In fact, these two clades appear together in the phylogeny of Mcr (Figure 5). Notably, archaea of the DPANN superphylum (*Ca*. Diapherotrites, *Ca*. Parvarchaeota, *Ca*. Aenigmarchaeota, *Ca*. Nanohaloarchaeota and *Ca*. Nanoarchaeota) do not encode Mcr. According to some studies, DPANN are at the root of archaeal phylogeny and they would be close to the common ancestor of all archaea (Williams et al., 2017). However, this might be an artefact based on their fast evolutionary rates (Adam et al., 2017; Wang et al., 2021). Therefore, the ancestral origin of methanogenesis in Archaea is still a possible scenario and coincides with evidence on early biological methane formation on Earth (Ueno et al., 2006).

Anaerobic methanotrophic archaea

Since the discovery of the first microbial consortium mediating AOM (Boetius et al., 2000), our understanding of AOM has greatly increased thanks to the application of cultivation-dependent and -independent techniques. ANME perform AOM coupled to the reduction of sulfate or other electron acceptors. With the reconstruction of ANME genomes, it was shown that they use the methanogenesis pathway in reverse to oxidize methane to CO_2 (Krüger et al., 2003; Hallam et al., 2004; Meyerdierks et al., 2005, 2010). Three major clades of ANME have been described: ANME-2 and ANME-3 are included in the order Methanosarcinales and ANME-1 form the order Methanophagales. All ANME clades are comprised in the phylum Halobacteriota. All three ANME groups contain marine syntrophic archaea that coexist with SRB of the phylum Desulfobacterota (Knittel and Boetius, 2009, 2010). ANME-2d (*Ca*. Methanoperedens) are non-syntrophic and couple the oxidation of methane to the reduction of nitrate,

nitrite, ferric iron or manganese (Ettwig et al., 2010, 2016; Haroon et al., 2013; Arshad et al., 2015; Cai et al., 2018; Leu et al., 2020).

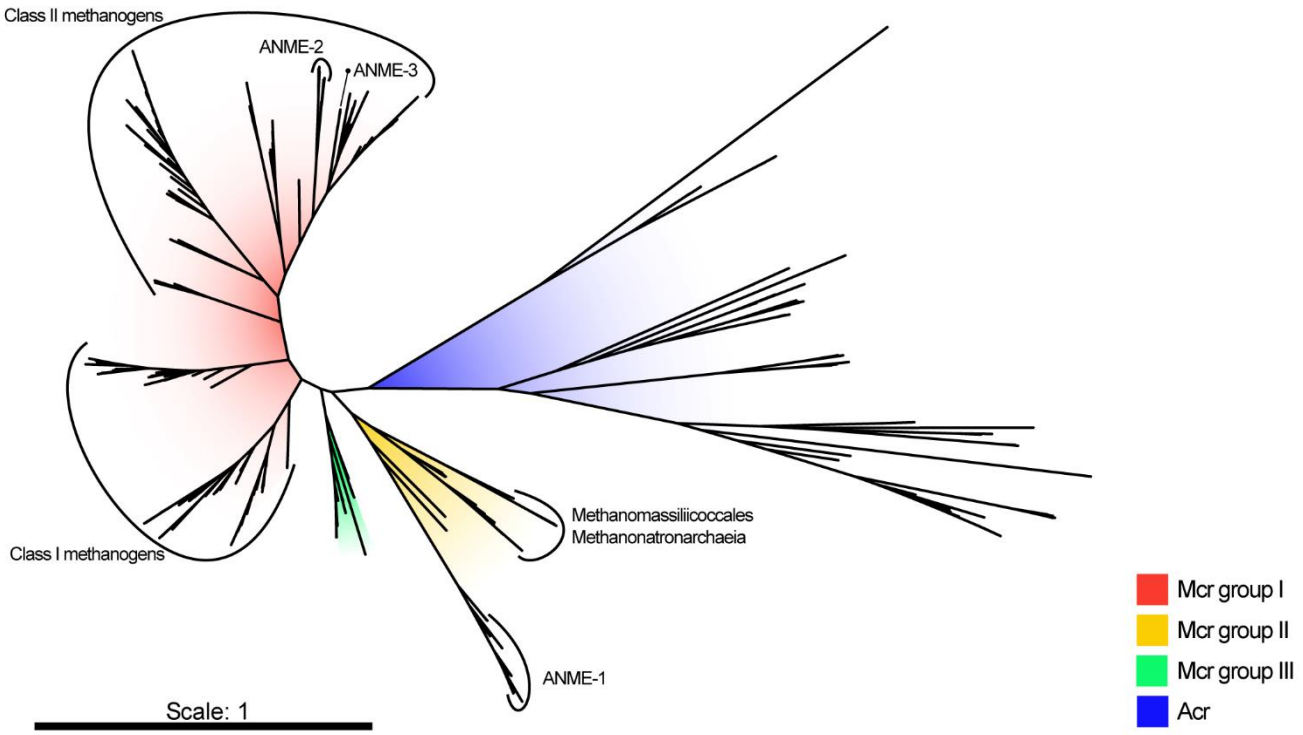

Figure 5. Diversity of methyl/alkyl-coenzyme M reductases. Mcrs are involved in methanogenesis and anaerobic methane oxidation and can be divided into three groups, according to (Garcia et al., 2022): group I contains mainly Mcrs of CO_2-reducing methanogens (class I and II), ANME-2 and ANME-3; group II contains Mcrs of methyl-reducing methanogens (Methanomassiliicoccales and Methanonatronarchaeia) and ANME-1; and group III contains Thermoproteota-like Mcr sequences, likely involved in methyl-reducing methanogenesis. The divergent Acr branch corresponds to alkanotrophic archaea (ANKA). The tree is a maximum likelihood phylogeny of McrA.

ANME-2 are relatively widely distributed in sulfate-methane transition zones of marine sediments (Boetius and Knittel, 2010). ANME-3 inhabit cold habitats like mud volcanoes and methane seeps (Niemann et al., 2006; Lösekann et al., 2007; Boetius and Knittel, 2010). In contrast, ANME-1 are meso- and thermophilic and specific to habitats such as hydrothermal vents (Boetius and Knittel, 2010). In general, ANME are widespread in anoxic marine sediments where methane diffuses from deeper layers (Boetius and Knittel, 2010; Ruff et al., 2015).

Up to date, AOM cultures between 20 and 60°C have been described (Figure 6) (Girguis et al., 2003; Nauhaus et al., 2007; Zhang et al., 2011; Holler et al., 2011; Haroon et al., 2013; Aoki et al., 2014; Wegener et al., 2016; Vaksmaa et al., 2017; Cai et al., 2018; Krukenberg et al., 2018; Leu et al., 2020).

Nevertheless, there is evidence that AOM happens at temperatures up to 85°C (Kallmeyer and Boetius, 2004; Holler et al., 2011; Adams et al., 2013) and environmental analyses have found ANME sequences and lipids in thermophilic systems (Schouten et al., 2003; Schrenk et al., 2004; Roussel et al., 2008). Thus, more thermophilic ANME or novel ANME lineages might exist.

Syntrophic alkane-degrading archaea

The first ANKA were discovered in sulfate-dependent AOM cultures transferred to a butane or propane atmosphere (Laso-Pérez et al., 2016). *Ca*. Syntrophoarchaeales form a sister order to *Ca*. Methanophagales (ANME-1). Similarly, *Ca*. Ethanoperedens are thermophilic ethane-oxidizing archaea from the order Methanosarcinales (Hahn et al., 2020). Both groups associate with the thermophilic SRB *Ca*. Desulfofervidus auxilii to perform thermophilic anaerobic oxidation of short-chain alkanes.

Ca. Syntrophoarchaea is present in hydrothermal systems and oil seeps like the Guaymas Basin and the Gulf of Mexico (Laso-Pérez et al., 2016, 2019; Dombrowski et al., 2017, 2018; Wang et al., 2019a). *Ca*. Ethanoperedens is also present in other cold environments like gas hydrates and mud volcanoes (Orcutt et al., 2010; Ruff et al., 2015; Hahn et al., 2020). At moderate temperatures, these ANKA might be outcompeted by alkane-oxidizing SRB (Kleindienst et al., 2014).

Methanogenic alkane-degrading archaea

As mentioned before, syntrophic consortia perform alkane fermentation coupled to methanogenesis and the reaction is feasible both at standard and culture conditions (Zengler et al., 1999). Interestingly, ANKA of the family *Ca*. Methanoliparia combine the two half reactions within one cell and they encode both an Mcr and an Acr (Borrel et al., 2019; Laso-Pérez et al., 2019). *Ca*. Methanoliparia grow on various long-chain alkanes, *n*-alkylbenzenes and *n*-alkylcyclohexanes, with alkane chain lengths ranging from C_{12} to $C_{>30}$ (Zhou et al., 2022). The Acr activates the alkanes to alkyl-CoM, which are subsequently oxidized via β-oxidation to produce acetyl-CoA. The β-oxidation also produces reduced cofactors (NADH and $FADH_2$). *Ca*. Methanoliparia then uses the Wood-Ljungdahl pathway in the reductive direction to reoxidize the reduced cofactors for methane production via Mcr.

Uncultured, putative alkane-degrading archaea

Bathyarchaeia MAGs BA1 and BA2 each encode one Acr (Evans et al., 2015). Although at the time of their discovery these Bathyarchaeia were linked to methane metabolism, we now can speculate that they are involved in anaerobic oxidation of alkanes. Indeed, they originate from Surat Basin (Australia), a

geological site containing hydrocarbon deposits. Acrs have also been found in the Hadarchaeota (Wang et al., 2019b), in the Helarchaeales (phylum Asgardarchaeota) (Seitz et al., 2019) and in an Archaeoglobi MAG (phylum Halobacteriota) (Boyd et al., 2019) (Table 1). Acr-encoding Hadarchaea originated from the Jinze hot spring (China) (Wang et al., 2019b). Helarchaeales and *Ca*. Polytropus marinifundus (Archaeoglobi) were found in hydrothermal vents in the Guaymas Basin and in the Juan de Fuca Ridge flank, respectively (Boyd et al., 2019; Seitz et al., 2019).

Ca. Polytropus is an Acr-encoding Archaeoglobi that takes its name "versatile" from the variety of electron-sinking mechanisms it encodes (Boyd et al., 2019). *Ca.* P. marinifundus encodes several multiheme cytochromes that might enable iron reduction or interspecies electron transfer. A nitrate reductase and a sulfur reductase-like complex would enable the use of nitrate or sulfur compounds as terminal electron acceptors (Boyd et al., 2019). In contrast, neither the Hadarchaea nor the Helarchaeia

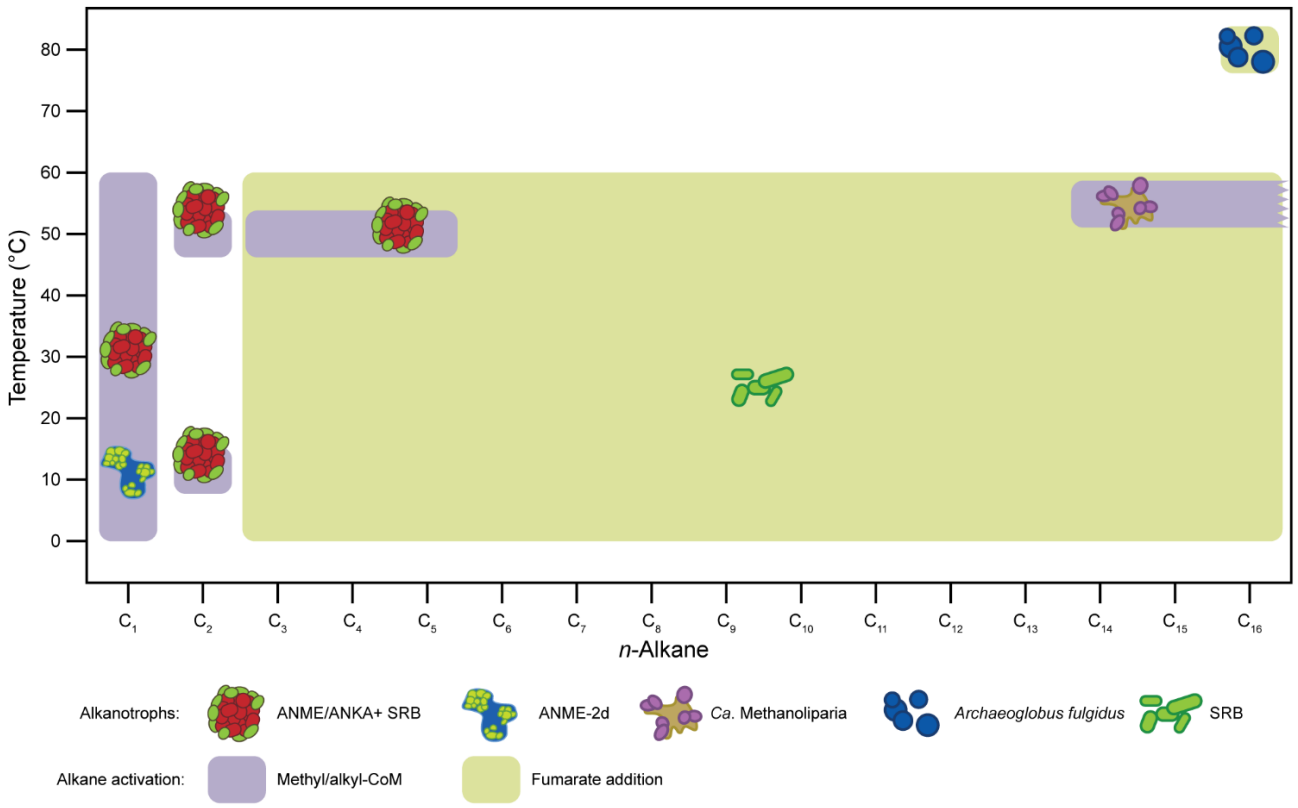

Figure 6. Growth temperature and substrates of cultured alkane oxidizers. The x-axis shows the chain length of the aliphatic alkane substrate and the y-axis shows the growth temperature. The shaded rectangles represent the mode of activation: in fumarate addition via alkylsuccinate synthases (bacterial pathway, in pale yellow) and activation via Mcr/Acr (archaeal pathway, in lilac). The hyperthermophilic archaeon *Archaeoglobus fulgidus* has been shown to activate long-chain alkanes via fumarate addition. The serrated edge of the *Ca*. Methanoliparia box represents the ability to activate alkanes longer than C_{16}. The known upper temperature limit of alkane degradation by ANKA is 60°C.

MAGs encode respiratory pathways or the traditional systems associated with syntrophy. A syntrophic mechanism based on the transfer of hydrogen to a partner hydrogenotrophic organism has been proposed (Seitz et al., 2019). However, more research is needed in order to understand the dynamics of hydrocarbon degradation by these organisms.

1.5. Diversity of sulfate-reducing partner bacteria

By its coupling to sulfate reduction, alkane oxidation becomes thermodynamically feasible. So far, only a single MAG of Archaeoglobi has been described, which codes for both Mcr and a dissimilatory sulfate-reduction pathway (Table 1) (Liu et al., 2020a). The other ANME/ANKA do not encode a dissimilatory sulfate-reduction pathway. Therefore, the cultured alkane oxidizing archaea partner with bacteria, which use the reducing equivalents released by the archaea for sulfate-reduction. The pathways for this electron exchange are not fully resolved. However, the tight nature of the partners suggest direct interspecies electron transport (DIET) (McGlynn et al., 2015; Wegener et al., 2015; Laso-Pérez et al., 2016; Hahn et al., 2020).

Sulfate reducers in AOM

According to genome-based phylogeny, all known partner SRB belong to the phylum Desulfobacterota (Parks et al., 2018) and are included within five distinct clades: Seep-SRB1a and Seep-SRB-1g (class Desulfobacteria), Seep-SRB2 (class Dissulfuribacteria), HotSeep-1 (class Desulfofervidia) and Seep-DBB (class Desulfobulbia) (Murali et al., 2022). Cold-adapted ANME-3 associate with Desulfobulbia SRB and Seep-SRB1a (Niemann et al., 2006; Lösekann et al., 2007; Schreiber et al., 2010). Psychro- and mesophilic ANME-1 and -2 form consortia with SRB of the groups Seep-SRB1 and Seep-SRB2 (Michaelis et al., 2002; Knittel et al., 2003, 2005; Boetius and Knittel, 2010; Schreiber et al., 2010; Ruff et al., 2015; Krukenberg et al., 2018; Metcalfe et al., 2020; Yu et al., 2021). These SRB appear to be solely syntrophic and isolation attempts have not been successful (Krukenberg et al., 2016).

Thermophilic ANME-1a that grow at 50 to 60°C form consortia with a single species of SRB, namely *Ca.* Desulfofervidus auxilii (HotSeep-1) (Wegener et al., 2015; Krukenberg et al., 2016, 2018). Interestingly, *Ca*. D. auxilii can grow alone using hydrogen as electron donor (Krukenberg et al., 2016). Comparative transcriptomics provided evidence on differential gene expression between hydrogenotrophic and AOM growth of *Ca*. D. auxilii. Extracellular multiheme cytochromes (MHC) and pilus genes were underexpressed during hydrogenotrophic growth compared to AOM (Wegener et al.,

2015). Extracellular MHC and cell appendages likely support DIET from ANME-1 to *Ca*. D. auxilii (Wegener et al., 2015; Krukenberg et al., 2018).

Partner sulfate reducers in AOA

Anaerobic multicarbon alkane oxidation by ANKA also occurs in syntrophy with SRB, except for the non-syntrophic *Ca*. Methanoliparia. Thermophilic *Ca*. Syntrophoarchaeum and *Ca*. Ethanoperedens form consortia with *Ca*. Desulfofervidus auxilii for the oxidation of short-chain alkanes up to 4 carbon atoms (Laso-Pérez et al., 2016; Hahn et al., 2020). Interestingly, the psychrophilic *Ca*. Argoarchaeum ethanivorans forms loose aggregates with an unidentified SRB (Chen et al., 2019). Whether the association of these ANKA with the partner SRB only depends on temperature, rather than being specific on the archaeal partner needs further investigation.

Other sulfate reducers in heated and oil-rich environments

In general, oil biodegradation in reservoirs can only occur at temperatures below 80°C, point where the oil becomes sterile according to the palaeopasteurization hypothesis (Head et al., 2010). Many SRB and sulfate-reducing archaea (SRA) thrive in hydrothermal, subsurface and oil-rich environments (Head et al., 2010; Colman et al., 2017; Gieg, 2018). In oil reservoirs, the production of sulfide by SRB and SRA leads to petroleum souring (Gieg et al., 2011). For example, the archaeon *Archaeoglobus fulgidus* was isolated from a marine hydrothermal vent and is able to oxidize alkanes using fumarate addition (Stetter et al., 1987; Khelifi et al., 2014), a pathway that is typical of anaerobic alkanotrophic bacteria (Callaghan et al., 2006). *A. fulgidus* strains have been repeatedly found in and isolated from high-temperature oil fields (Stetter et al., 1993; Gieg et al., 2011).

Thermodesulfobacteria is a class of thermophilic and hyperthermophilic Desulfobacterota that thrive at temperatures between 60 and 90°C. Several Thermodesulfobacteria strains have been isolated from hydrothermal vents, hot springs and oil reservoirs (Rosnes et al., 1991; Beeder et al., 1995; Sonne-Hansen and Ahring, 1999; Jeanthon et al., 2002; Moussard et al., 2004; Hamilton-Brehm et al., 2013). Interestingly, Thermodesulfobacteria were abundant in hot sediments of the Guaymas Basin in layers where ANME-1 were also present (Dombrowski et al., 2018).

1.6. Hypotheses and aims of the thesis

The diversity of Archaea involved in the anaerobic oxidation of alkanes, especially Acr-based alkane metabolism is currently a developing theme in microbiology. Most of the Acr sequences derive from environmental samples, so the concrete physiology of the corresponding ANKA remains unresolved. In particular, an environmental Acr sequence cannot be assigned to a specific alkane without the availability of pure cultures or enrichments. Furthermore, the association of ANKA/ANME with partner SRB seems to be specific on temperature. Again, cultivation in combination with meta'omics can aid us to explore this new diversity.

Before I started my thesis, microorganisms performing sulfate-dependent AOM were cultured between 4 and 60°C, and Acr-encoding Archaea growing on short-chain alkanes were cultured at temperatures ≤50°C. Archaea that use Acr for the activation of alkanes longer than butane had not been cultured. Thus, the aims of my thesis were: (i) to culture and characterize novel archaea and bacteria that perform AOM at close to the observed temperature maximum of AOM, and (ii) to test whether anaerobic archaea are able to grow on long-chain alkanes. For these aims, I incubated sediments from the Guaymas Basin with these two electron donors (methane or hexadecane) and sulfate as electron acceptor. I focused my research on testing the following hypotheses:

Novel ANME and SRB catalyze AOM at high temperatures

When I started my PhD, AOM cultures growing at temperatures up to 60°C were available. Short term incubations with sediments of the Guaymas Basin had shown that the range of AOM is between 4 and 70°C, with a maximum activity at 50°C (Holler et al., 2011).

In **Chapter 2**, I explored the known upper temperature limit of AOM, starting AOM enrichment cultures from Guaymas Basin sediment samples. This led to the discovery of ANME-1c, a thermophilic group of methanotrophs that associates with SRB of the family Thermodesulfobacteria to perform AOM at 70°C. This is the most thermophilic AOM culture available up to date.

Anaerobic archaea grow on long-chain alkanes

At the start of my PhD, an archaeal pathway had been described for the degradation of short-chain alkanes up to four carbon atoms. The pathway starts with alkane activation via Mcr variants (Acrs), yielding alkyl-CoMs (Laso-Pérez et al., 2016; Chen et al., 2019; Hahn et al., 2020). Furthermore, there was environmental evidence that *Ca*. Methanoliparia grew on oil alkanes (Laso-Pérez et al., 2019).

In **Chapter 3**, I describe the microbial communities in a culture amended with hexadecane as sole carbon/electron source and sulfate as electron acceptor. My work resulted in the enrichment of a Hadarchaeon that activates the long-chain alkane via Acr. In this Chapter, I assessed the evolution of alkane degradation pathways in the Hadarchaeota.

Syntrophic and free-living Thermodesulfobacteria have distinct genome features

During my PhD, I obtained thermophilic cultures that couple methane or hexadecane oxidation to sulfate reduction. Chapters 2 and 3 focus on the archaea that mediate alkane oxidation at high temperature (70°C). At the same time, novel syntrophic Thermodesulfobacteria were described. Research has pointed out the significance of cytochromes and cell appendages in DIET between ANME and SRB (McGlynn et al., 2015; Wegener et al., 2015; Krukenberg et al., 2018). Recently, comparative genomics has provided evidence on the physiological adaptations of syntrophic SRB in respect to free-living SRB (Murali et al., 2022).

Chapter 4 is a comparative study of the thermophilic Thermodesulfobacteria acting as partner bacteria of AOM/AOA with their free-living relatives. This helped clarify the genomic features present in syntrophic Thermodesulfobacteria and predict potentially syntrophic SRB in the Thermodesulfobacteria family.

References

Adam, P. S., Borrel, G., Brochier-Armanet, C., and Gribaldo, S. (2017). The growing tree of Archaea: new perspectives on their diversity, evolution and ecology. *ISME J.* 11, 2407–2425. doi: 10.1038/ismej.2017.122.

Adams, M. M., Hoarfrost, A. L., Bose, A., Joye, S. B., and Girguis, P. R. (2013). Anaerobic oxidation of short-chain alkanes in hydrothermal sediments: potential influences on sulfur cycling and microbial diversity. *Front. Microbiol.* 4, 110. doi: 10.3389/fmicb.2013.00110.

Aoki, M., Ehara, M., Saito, Y., Yoshioka, H., Miyazaki, M., Saito, Y., et al. (2014). A long-term cultivation of an anaerobic methane-oxidizing microbial community from deep-sea methane-seep sediment using a continuous-flow bioreactor. *PLoS One* 9. doi: 10.1371/journal.pone.0105356.

Arshad, A., Speth, D. R., De Graaf, R. M., Op den Camp, H. J. M., Jetten, M. S. M., and Welte, C. U. (2015). A Metagenomics-Based Metabolic Model of Nitrate-Dependent Anaerobic Oxidation of Methane by Methanoperedens-Like Archaea. *Front. Microbiol.* 6. doi: 10.3389/FMICB.2015.01423.

Bapteste, É., Brochier, C., and Boucher, Y. (2005). Higher-level classification of the Archaea: evolution of methanogenesis and methanogens. *Archaea* 1, 353. doi: 10.1155/2005/859728.

Bazylinski, D. A., Farrington, J. W., and Jannasch, H. W. (1988). Hydrocarbons in surface sediments from a Guaymas Basin hydrothermal vent site. *Org. Geochem.* 12, 547–558. doi: 10.1016/0146-6380(88)90146-5.

Beal, E. J., House, C. H., and Orphan, V. J. (2009). Manganese- and Iron-Dependent Marine Methane Oxidation. *Science (80-.).* 325, 184–187. doi: 10.1126/science.1169984.

Beaulieu, S. E., and Szafrański, K. M. (2020). InterRidge Global Database of Active Submarine Hydrothermal Vent Fields Version 3.4. *PANGAEA*. doi: 10.1594/PANGAEA.917894.

Beeder, J., Torsvik, T., and Lien, T. (1995). *Thermodesulforhabdus norvegicus* gen. nov., sp. nov., a novel thermophilic sulfate-reducing bacterium from oil field water. *Arch. Microbiol.* 164, 331–336. doi: 10.1007/BF02529979.

Berndt, M. E., Allen, D. E., and Seyfried, W. E. (1996). Reduction of CO2 during serpentinization of olivine at 300 °C and 500 bar. *Geology* 24, 351. doi: 10.1130/0091-7613(1996)024<0351:ROCDSO>2.3.CO;2.

Boetius, A., and Knittel, K. (2010). "Habitats of Anaerobic Methane Oxidizers," in *Handbook of Hydrocarbon and Lipid Microbiology*, ed. K. N. Timmis (Berlin, Heidelberg: Springer Berlin Heidelberg), 2193–2202. doi: 10.1007/978-3-540-77587-4_159.

Boetius, A., Ravenschlag, K., Schubert, C. J., Rickert, D., Widdel, F., Gieseke, A., et al. (2000). A marine microbial consortium apparently mediating anaerobic oxidation of methane. *Nature* 407, 623–626. doi: 10.1038/35036572.

Borrel, G., Adam, P. S., McKay, L. J., Chen, L.-X., Sierra-García, I. N., Sieber, C. M. K., et al. (2019). Wide diversity of methane and short-chain alkane metabolisms in uncultured archaea. *Nat. Microbiol.* 4, 603–613. doi: 10.1038/s41564-019-0363-3.

Borrel, G., O'Toole, P. W., Harris, H. M. B., Peyret, P., Brugère, J.-F., and Gribaldo, S. (2013). Phylogenomic Data Support a Seventh Order of Methylotrophic Methanogens and Provide Insights into the Evolution of Methanogenesis. *Genome Biol. Evol.* 5, 1769–1780. doi: 10.1093/gbe/evt128.

Boyd, J. A., Jungbluth, S. P., Leu, A. O., Evans, P. N., Woodcroft, B. J., Chadwick, G. L., et al. (2019). Divergent methyl-coenzyme M reductase genes in a deep-subseafloor Archaeoglobi. *ISME J.*, 1. doi: 10.1038/s41396-018-0343-2.

Brock, T. D. (1978a). "Introduction," in *Thermophilic Microorganisms and Life at High Temperatures*, ed. M. P. Starr (New York, NY: Springer), 1–11. doi: 10.1007/978-1-4612-6284-8_1.

Brock, T. D. (1978b). "The Habitats," in *Thermophilic Microorganisms and Life at High Temperatures*, ed. M. P. Starr (New York, NY: Springer), 12–38. doi: 10.1007/978-1-4612-6284-8_2.

Brooks, J. M., Wiesenburg, D. A., Roberts, H., Carney, R. S., MacDonald, I. R., Fisher, C. R., et al. (1990).

Salt, Seeps and Symbiosis in the Gulf of Mexico. *Eos, Trans. Am. Geophys. Union* 71, 1772. doi: 10.1029/EO071i045p01772.

Bruice, P. Y. (2013). *Organic Chemistry, 7th edition*. , ed. A. Jaworski Upper Saddle River, NJ: Pearson.

Buckel, W., and Golding, B. T. (2006). Radical enzymes in anaerobes. *Annu. Rev. Microbiol.* 60, 27–49. doi: 10.1146/annurev.micro.60.080805.142216.

Cai, C., Leu, A. O., Xie, G. J., Guo, J., Feng, Y., Zhao, J. X., et al. (2018). A methanotrophic archaeon couples anaerobic oxidation of methane to Fe(III) reduction. *ISME J. 2018 128* 12, 1929–1939. doi: 10.1038/s41396-018-0109-x.

Callaghan, A. V. (2013). Enzymes involved in the anaerobic oxidation of n-alkanes: from methane to long-chain paraffins. *Front. Microbiol.* 4, 1–9. doi: 10.3389/fmicb.2013.00089.

Callaghan, A. V., Davidova, I. A., Savage-Ashlock, K., Parisi, V. A., Gieg, L. M., Suflita, J. M., et al. (2010). Diversity of Benzyl- and Alkylsuccinate Synthase Genes in Hydrocarbon-Impacted Environments and Enrichment Cultures. *Environ. Sci. Technol.* 44, 7287–7294. doi: 10.1021/es1002023.

Callaghan, A. V., Gieg, L. M., Kropp, K. G., Suflita, J. M., and Young, L. Y. (2006). Comparison of mechanisms of alkane metabolism under sulfate-reducing conditions among two bacterial isolates and a bacterial consortium. *Appl. Environ. Microbiol.* 72, 4274–4282. doi: 10.1128/AEM.02896-05.

Calvert, S. E. (1966). Origin of Diatom-Rich, Varved Sediments from the Gulf of California. *J. Geol.* 74, 546–565. doi: 10.1086/627188.

Chen, S.-C., Musat, N., Lechtenfeld, O. J., Paschke, H., Schmidt, M., Said, N., et al. (2019). Anaerobic oxidation of ethane by archaea from a marine hydrocarbon seep. *Nat. 2019*, 1. doi: 10.1038/s41586-019-1063-0.

Collins, A. G. (1975). *Geochemistry of oilfield waters*. 1st ed. Amsterdam: Elsevier.

Colman, D. R., Lindsay, M. R., and Boyd, E. S. (2019). Mixing of meteoric and geothermal fluids supports hyperdiverse chemosynthetic hydrothermal communities. *Nat. Commun. 2019 101* 10, 1–13. doi: 10.1038/s41467-019-08499-1.

Colman, D. R., Poudel, S., Stamps, B. W., Boyd, E. S., and Spear, J. R. (2017). The deep, hot biosphere: Twenty-five years of retrospection. *Proc. Natl. Acad. Sci.* 114, 6895–6903. doi: 10.1073/pnas.1701266114.

Conrad, R. (2009). The global methane cycle: recent advances in understanding the microbial processes involved. *Environ. Microbiol. Rep.* 1, 285–292. doi: 10.1111/j.1758-2229.2009.00038.x.

Corliss, J. B., Dymond, J., Gordon, L. I., Edmond, J. M., von Herzen, R. P., Ballard, R. D., et al. (1979). Submarine Thermal Springs on the Galápagos Rift. *Science (80-.).* 203, 1073–1083. doi: 10.1126/science.203.4385.1073.

D'Hondt, S., Rutherford, S., and Spivack, A. J. (2002). Metabolic Activity of Subsurface Life in Deep-Sea Sediments. *Science (80-.).* 295, 2067–2070. doi: 10.1126/science.1064878.

Des Marais, D. J., Donchin, J. H., Nehring, N. L., and Truesdell, A. H. (1981). Molecular carbon isotopic evidence for the origin of geothermal hydrocarbons. *Nature* 292, 826–828. doi: 10.1038/292826a0.

Didyk, B. M., and Simoneit, B. R. T. (1990). Petroleum characteristics of the oil in a Guaymas Basin hydrothermal chimney. *Appl. Geochemistry* 5, 29–40. doi: 10.1016/0883-2927(90)90033-2.

Dombrowski, N., Seitz, K. W., Teske, A. P., and Baker, B. J. (2017). Genomic insights into potential interdependencies in microbial hydrocarbon and nutrient cycling in hydrothermal sediments. *Microbiome* 5, 106. doi: 10.1186/s40168-017-0322-2.

Dombrowski, N., Teske, A. P., and Baker, B. J. (2018). Expansive microbial metabolic versatility and biodiversity in dynamic Guaymas Basin hydrothermal sediments. *Nat. Commun.* 9, 4999. doi: 10.1038/s41467-018-07418-0.

Ettwig, K. F., Butler, M. K., Le Paslier, D., Pelletier, E., Mangenot, S., Kuypers, M. M. M., et al. (2010). Nitrite-driven anaerobic methane oxidation by oxygenic bacteria. *Nature* 464, 543–548. doi: 10.1038/nature08883.

Ettwig, K. F., Zhu, B., Speth, D., Keltjens, J. T., Jetten, M. S. M., and Kartal, B. (2016). Archaea catalyze iron-dependent anaerobic oxidation of methane. *Proc. Natl. Acad. Sci. U. S. A.* 113, 12792–12796. doi: 10.1073/pnas.1609534113.

Evans, P. N., Parks, D. H., Chadwick, G. L., Robbins, S. J., Orphan, V. J., Golding, S. D., et al. (2015). Methane metabolism in the archaeal phylum Bathyarchaeota revealed by genome-centric metagenomics. *Science (80-.).* 350, 434–438. doi: 10.1126/science.aac7745.

Froelich, P. N., Klinkhammer, G. P., Bender, M. L., Luedtke, N. A., Heath, G. R., Cullen, D., et al. (1979). Early oxidation of organic matter in pelagic sediments of the eastern equatorial Atlantic: suboxic diagenesis. *Geochim. Cosmochim. Acta* 43, 1075–1090. doi: 10.1016/0016-7037(79)90095-4.

Garcia, P. S., Gribaldo, S., and Borrel, G. (2022). Diversity and Evolution of Methane-Related Pathways in Archaea. *Annu. Rev. Microbiol.* 76. doi: 10.1146/annurev-micro-041020-024935.

German, C. R., and Lin, J. (2004). "The Thermal Structure of the Oceanic Crust, Ridge-Spreading and Hydrothermal Circulation: How Well do we Understand their Inter-Connections?," in *Geophysical Monograph Series*, eds. C. R. German, J. Lin, and L. M. Parson (Blackwell Publishing Ltd), 1–18. doi: 10.1029/148GM01.

Gieg, L. M. (2018). "Microbial Communities in Oil Shales, Biodegraded and Heavy Oil Reservoirs, and Bitumen Deposits," in *Microbial Communities Utilizing Hydrocarbons and Lipids: Members, Metagenomics and Ecophysiology* (Cham: Springer International Publishing), 1–21. doi: 10.1007/978-3-319-60063-5_4-1.

Gieg, L. M., Fowler, S. J., and Berdugo-Clavijo, C. (2014). Syntrophic biodegradation of hydrocarbon contaminants. *Curr. Opin. Biotechnol.* 27, 21–29. doi: 10.1016/j.copbio.2013.09.002.

Gieg, L. M., Jack, T. R., and Foght, J. M. (2011). Biological souring and mitigation in oil reservoirs. *Appl. Microbiol. Biotechnol.* 92, 263–282. doi: 10.1007/s00253-011-3542-6.

Girguis, P. R., Orphan, V. J., Hallam, S. J., and DeLong, E. F. (2003). Growth and methane oxidation rates of anaerobic methanotrophic archaea in a continuous-flow bioreactor. *Appl. Environ. Microbiol.* 69, 5472–5482. doi: 10.1128/AEM.69.9.5472-5482.2003.

Gold, T. (1992). The deep, hot biosphere. *Proc. Natl. Acad. Sci.* 89, 6045–6049. doi: 10.1073/pnas.89.13.6045.

Gribaldo, S., and Brochier-Armanet, C. (2006). The origin and evolution of Archaea: A state of the art. *Philos. Trans. R. Soc. B Biol. Sci.* 361, 1007–1022. doi: 10.1098/rstb.2006.1841.

Grundmann, O., Behrends, A., Rabus, R., Amann, J., Halder, T., Heider, J., et al. (2008). Genes encoding the candidate enzyme for anaerobic activation of n-alkanes in the denitrifying bacterium, strain HxN1. *Environ. Microbiol.* 10, 376–385. doi: 10.1111/j.1462-2920.2007.01458.x.

Hahn, C. J., Laso-Pérez, R., Vulcano, F., Vaziourakis, K.-M., Stokke, R., Steen, I. H., et al. (2020). "*Candidatus* Ethanoperedens," a thermophilic genus of archaea mediating the anaerobic oxidation of ethane. *MBio* 11, 1–18. doi: 10.1128/mBio.00600-20.

Hahn, C. J., Lemaire, O. N., Kahnt, J., Engilberge, S., Wegener, G., and Wagner, T. (2021). Crystal structure of a key enzyme for anaerobic ethane activation. *Science (80-.).* 373, 118–121. doi: 10.1126/science.abg1765.

Hall, C., Tharakan, P., Hallock, J., Cleveland, C., and Jefferson, M. (2003). Hydrocarbons and the evolution of human culture. *Nature* 426, 318–322. doi: 10.1038/nature02130.

Hallam, S. J., Putnam, N., Preston, C. M., Detter, J. C., Rokhsar, D., Richardson, P. M., et al. (2004). Reverse Methanogenesis: Testing the Hypothesis with Environmental Genomics. *Science (80-.).* 305, 1457–1462. doi: 10.1126/science.1100025.

Hamilton-Brehm, S. D., Gibson, R. A., Green, S. J., Hopmans, E. C., Schouten, S., van der Meer, M. T. J., et al. (2013). *Thermodesulfobacterium geofontis* sp. nov., a hyperthermophilic, sulfate-reducing bacterium isolated from Obsidian Pool, Yellowstone National Park. *Extremophiles* 17, 251–263. doi: 10.1007/S00792-013-0512-1.

Haroon, M. F., Hu, S., Shi, Y., Imelfort, M., Keller, J., Hugenholtz, P., et al. (2013). Anaerobic oxidation

of methane coupled to nitrate reduction in a novel archaeal lineage. *Nat. 2013 5007464* 500, 567–570. doi: 10.1038/nature12375.

Head, I. M., Larter, S. R., Gray, N. D., Sherry, A., Adams, J. J., Aitken, C. M., et al. (2010). "Hydrocarbon Degradation in Petroleum Reservoirs," in *Handbook of Hydrocarbon and Lipid Microbiology* (Berlin, Heidelberg: Springer Berlin Heidelberg), 3097–3109. doi: 10.1007/978-3-540-77587-4_232.

Hickel, J., Kallis, G., Jackson, T., O'Neill, D. W., Schor, J. B., Steinberger, J. K., et al. (2022). Degrowth can work — here's how science can help. *Nature* 612, 400–403. doi: 10.1038/d41586-022-04412-x.

Hinrichs, K.-U., and Boetius, A. (2002). "The Anaerobic Oxidation of Methane: New Insights in Microbial Ecology and Biogeochemistry," in *Ocean Margin Systems* (Berlin, Heidelberg: Springer Berlin Heidelberg), 457–477. doi: 10.1007/978-3-662-05127-6_28.

Hinrichs, K. U., Hayes, J. M., Sylva, S. P., Brewert, P. G., and DeLong, E. F. (1999). Methane-consuming archaebacteria in marine sediments. *Nature* 398, 802–805. doi: 10.1038/19751.

Holden, J. F. (2009). "Extremophiles: Hot Environments," in *Encyclopedia of Microbiology*, ed. M. Schaechter (Elsevier), 127–146. doi: 10.1016/B978-012373944-5.00281-9.

Holler, T., Widdel, F., Knittel, K., Amann, R., Kellermann, M. Y., Hinrichs, K.-U., et al. (2011). Thermophilic anaerobic oxidation of methane by marine microbial consortia. *ISME J.* 5, 1946–1956. doi: 10.1038/ismej.2011.77.

Hua, Z.-S., Wang, Y.-L., Evans, P. N., Qu, Y.-N., Goh, K. M., Rao, Y.-Z., et al. (2019). Insights into the ecological roles and evolution of methyl-coenzyme M reductase-containing hot spring Archaea. *Nat. Commun.* 10, 4574. doi: 10.1038/s41467-019-12574-y.

Jaekel, U., Musat, N., Adam, B., Kuypers, M., Grundmann, O., and Musat, F. (2013). Anaerobic degradation of propane and butane by sulfate-reducing bacteria enriched from marine hydrocarbon cold seeps. *ISME J.* 7, 885–895. doi: 10.1038/ismej.2012.159.

Jeanthon, C., L'Haridon, S., Cueff, V., Banta, A., Reysenbach, A.-L., and Prieur, D. (2002). Thermodesulfobacterium hydrogeniphilum sp. nov., a thermophilic, chemolithoautotrophic, sulfate-reducing bacterium isolated from a deep-sea hydrothermal vent at Guaymas Basin, and emendation of the genus Thermodesulfobacterium. *Int. J. Syst. Evol. Microbiol.* 52, 765–772. doi: 10.1099/00207713-52-3-765.

Jones, D. M., Head, I. M., Gray, N. D., Adams, J. J., Rowan, A. K., Aitken, C. M., et al. (2008). Crude-oil biodegradation via methanogenesis in subsurface petroleum reservoirs. *Nature* 451, 176–180. doi: 10.1038/nature06484.

Jørgensen, B. B. (2006). "Bacteria and Marine Biogeochemistry," in *Marine Geochemistry*, eds. H. D. Schulz and M. Zabel (Berlin/Heidelberg: Springer), 169–206. doi: 10.1007/3-540-32144-6_5.

Jørgensen, B. B., and Boetius, A. (2007). Feast and famine — microbial life in the deep-sea bed. *Nat. Rev. Microbiol.* 5, 770–781. doi: 10.1038/nrmicro1745.

Kallmeyer, J., and Boetius, A. (2004). Effects of Temperature and Pressure on Sulfate Reduction and Anaerobic Oxidation of Methane in Hydrothermal Sediments of Guaymas Basin. *Appl. Environ. Microbiol.* 70, 1231–1233. doi: 10.1128/AEM.70.2.1231-1233.2004.

Kallmeyer, J., Pockalny, R., Adhikari, R. R., Smith, D. C., and D'Hondt, S. (2012). Global distribution of microbial abundance and biomass in subseafloor sediment. *Proc. Natl. Acad. Sci.* 109, 16213–16216. doi: 10.1073/pnas.1203849109.

Kalyuzhnaya, M. G., Gomez, O. A., and Murrell, J. C. (2019). "The Methane-Oxidizing Bacteria (Methanotrophs)," in *Taxonomy, Genomics and Ecophysiology of Hydrocarbon-Degrading Microbes*, ed. T. J. McGenity (Cham: Springer International Publishing), 1–34. doi: 10.1007/978-3-319-60053-6_10-1.

Karl, D. M., Beversdorf, L., Björkman, K. M., Church, M. J., Martinez, A., and Delong, E. F. (2008). Aerobic production of methane in the sea. *Nat. Geosci.* 1, 473–478. doi: 10.1038/ngeo234.

Kasai, Y., Kishira, H., Sasaki, T., Syutsubo, K., Watanabe, K., and Harayama, S. (2002). Predominant growth of Alcanivorax strains in oil-contaminated and nutrient-supplemented sea water. *Environ.*

Microbiol. 4, 141–147. doi: 10.1046/J.1462-2920.2002.00275.X.

Kawka, O. E., and Simoneit, B. R. T. (1987). Survey of hydrothermally-generated petroleums from the Guaymas Basin spreading center. *Org. Geochem.* 11, 311–328. doi: 10.1016/0146-6380(87)90042-8.

Kelley, D. S. (1996). Methane-rich fluids in the oceanic crust. *J. Geophys. Res. Solid Earth* 101, 2943–2962. doi: 10.1029/95jb02252.

Kelley, D. S., Baross, J. A., and Delaney, J. R. (2002). Volcanoes, fluids, and life at mid-ocean ridge spreading centers. *Annu. Rev. Earth Planet. Sci.* 30, 385–491. doi: 10.1146/annurev.earth.30.091201.141331.

Kevorkian, R. T., Callahan, S., Winstead, R., and Lloyd, K. G. (2021). ANME-1 archaea may drive methane accumulation and removal in estuarine sediments. *Environ. Microbiol. Rep.* 13, 185–194. doi: 10.1111/1758-2229.12926.

Khelifi, N., Amin Ali, O., Roche, P., Grossi, V., Brochier-Armanet, C., Valette, O., et al. (2014). Anaerobic oxidation of long-chain n-alkanes by the hyperthermophilic sulfate-reducing archaeon, Archaeoglobus fulgidus. *ISME J.* 8, 2153–2166. doi: 10.1038/ismej.2014.58.

Kleindienst, S., Herbst, F. A., Stagars, M., Von Netzer, F., Von Bergen, M., Seifert, J., et al. (2014). Diverse sulfate-reducing bacteria of the Desulfosarcina/Desulfococcus clade are the key alkane degraders at marine seeps. *ISME J.* 8, 2029–2044. doi: 10.1038/ismej.2014.51.

Kniemeyer, O., Musat, F., Sievert, S. M., Knittel, K., Wilkes, H., Blumenberg, M., et al. (2007). Anaerobic oxidation of short-chain hydrocarbons by marine sulphate-reducing bacteria. *Nature* 449, 898–902. doi: 10.1038/nature06200.

Knittel, K., and Boetius, A. (2009). Anaerobic Oxidation of Methane: Progress with an Unknown Process. *Annu. Rev. Microbiol.* doi: 10.1146/annurev.micro.61.080706.093130.

Knittel, K., and Boetius, A. (2010). "Anaerobic Methane Oxidizers," in *Handbook of Hydrocarbon and Lipid Microbiology* (Berlin, Heidelberg: Springer Berlin Heidelberg), 2023–2032. doi: 10.1007/978-3-540-77587-4_147.

Knittel, K., Boetius, A., Lemke, A., Eilers, H., Lochte, K., Pfannkuche, O., et al. (2003). Activity, distribution, and diversity of sulfate reducers and other bacteria in sediments above gas hydrate (Cascadia margin, Oregon). *Geomicrobiol. J.* 20, 269–294. doi: 10.1080/01490450303896.

Knittel, K., Lösekann, T., Boetius, A., Kort, R., and Amann, R. (2005). Diversity and distribution of methanotrophic archaea at cold seeps. *Appl. Environ. Microbiol.* 71, 467–479. doi: 10.1128/AEM.71.1.467-479.2005.

Krüger, M., Meyerdierks, A., Glöckner, F. O., Amann, R., Widdel, F., Kube, M., et al. (2003). A conspicuous nickel protein in microbial mats that oxidize methane anaerobically. *Nature* 426, 878–881. doi: 10.1038/nature02207.

Krukenberg, V., Harding, K., Richter, M., Glöckner, F. O., Gruber-Vodicka, H. R., Adam, B., et al. (2016). *Candidatus* Desulfofervidus auxilii, a hydrogenotrophic sulfate-reducing bacterium involved in the thermophilic anaerobic oxidation of methane. *Environ. Microbiol.* 18, 3073–3091. doi: 10.1111/1462-2920.13283.

Krukenberg, V., Riedel, D., Gruber-Vodicka, H. R., Buttigieg, P. L., Tegetmeyer, H. E., Boetius, A., et al. (2018). Gene expression and ultrastructure of meso- and thermophilic methanotrophic consortia. *Environ. Microbiol.* 20, 1651–1666. doi: 10.1111/1462-2920.14077.

Laso-Pérez, R., Hahn, C., van Vliet, D. M., Tegetmeyer, H. E., Schubotz, F., Smit, N. T., et al. (2019). Anaerobic Degradation of Non-Methane Alkanes by "Candidatus Methanoliparia" in Hydrocarbon Seeps of the Gulf of Mexico. *MBio* 10, e01814-19. doi: 10.1128/mBio.01814-19.

Laso-Pérez, R., Wegener, G., Knittel, K., Widdel, F., Harding, K. J., Krukenberg, V., et al. (2016). Thermophilic archaea activate butane via alkyl-coenzyme M formation. *Nature* 539, 396–401. doi: 10.1038/nature20152.

Lemaire, O. N., and Wagner, T. (2022). A Structural View of Alkyl-Coenzyme M Reductases, the First

Step of Alkane Anaerobic Oxidation Catalyzed by Archaea. *Biochemistry* 61, 805–821. doi: 10.1021/acs.biochem.2c00135.

Leu, A. O., Cai, C., McIlroy, S. J., Southam, G., Orphan, V. J., Yuan, Z., et al. (2020). Anaerobic methane oxidation coupled to manganese reduction by members of the Methanoperedenaceae. *ISME J.* doi: 10.1038/s41396-020-0590-x.

Liu, C., and Shao, Z. (2005). Alcanivorax dieselolei sp. nov., a novel alkane-degrading bacterium isolated from sea water and deep-sea sediment. *Int. J. Syst. Evol. Microbiol.* 55, 1181–1186. doi: 10.1099/ijs.0.63443-0.

Liu, Y.-F., Chen, J., Zaramela, L. S., Wang, L.-Y., Mbadinga, S. M., Hou, Z.-W., et al. (2020a). Genomic and Transcriptomic Evidence Supports Methane Metabolism in Archaeoglobi. *mSystems* 5, 1–16. doi: 10.1128/mSystems.00651-19.

Liu, Y. F., Chen, J., Liu, Z. L., Shou, L. Bin, Lin, D. D., Zhou, L., et al. (2020b). Anaerobic degradation of paraffins by thermophilic Actinobacteria under methanogenic conditions. *Environ. Sci. Technol.* 54, 10610–10620. doi: 10.1021/ACS.EST.0C02071.

Lloyd, K. G., Alperin, M. J., and Teske, A. (2011). Environmental evidence for net methane production and oxidation in putative ANaerobic MEthanotrophic (ANME) archaea. *Environ. Microbiol.* 13, 2548–2564. doi: 10.1111/j.1462-2920.2011.02526.x.

Lösekann, T., Knittel, K., Nadalig, T., Fuchs, B., Niemann, H., Boetius, A., et al. (2007). Diversity and abundance of aerobic and anaerobic methane oxidizers at the Haakon Mosby Mud Volcano, Barents Sea. *Appl. Environ. Microbiol.* 73, 3348–3362. doi: 10.1128/AEM.00016-07.

Martens, C. S. (1990). Generation of short chain acid anions in hydrothermally altered sediments of the Guaymas Basin, Gulf of California. *Appl. Geochemistry* 5, 71–76. doi: 10.1016/0883-2927(90)90037-6.

Masood, E. (2022). GDP is getting a makeover — what it means for economies, health and the planet. *Nature* 611, 224–226. doi: 10.1038/d41586-022-03576-w.

McGlynn, S. E., Chadwick, G. L., Kempes, C. P., and Orphan, V. J. (2015). Single cell activity reveals direct electron transfer in methanotrophic consortia. *Nature* 526, 531–535. doi: 10.1038/nature15512.

McKay, L. J., Dlakić, M., Fields, M. W., Delmont, T. O., Eren, A. M., Jay, Z. J., et al. (2019). Co-occurring genomic capacity for anaerobic methane and dissimilatory sulfur metabolisms discovered in the Korarchaeota. *Nat. Microbiol.*, 1. doi: 10.1038/s41564-019-0362-4.

Metcalfe, K. S., Murali, R., Mullin, S. W., Connon, S. A., and Orphan, V. J. (2020). Experimentally-validated correlation analysis reveals new anaerobic methane oxidation partnerships with consortium-level heterogeneity in diazotrophy. *ISME J. 2020 152* 15, 377–396. doi: 10.1038/s41396-020-00757-1.

Meyerdierks, A., Kube, M., Kostadinov, I., Teeling, H., Glöckner, F. O., Reinhardt, R., et al. (2010). Metagenome and mRNA expression analyses of anaerobic methanotrophic archaea of the ANME-1 group. *Environ. Microbiol.* 12, 422–439. doi: 10.1111/j.1462-2920.2009.02083.x.

Meyerdierks, A., Kube, M., Lombardot, T., Knittel, K., Bauer, M., Glöckner, F. O., et al. (2005). Insights into the genomes of archaea mediating the anaerobic oxidation of methane. *Environ. Microbiol.* 7, 1937–1951. doi: 10.1111/J.1462-2920.2005.00844.X.

Michaelis, W., Seifert, R., Nauhaus, K., Treude, T., Thiel, V., Blumenberg, M., et al. (2002). Microbial Reefs in the Black Sea Fueled by Anaerobic Oxidation of Methane. *Science (80-.).* 297, 1013–1015. doi: 10.1126/science.1072502.

Milkov, A. V. (2005). Molecular and stable isotope compositions of natural gas hydrates: A revised global dataset and basic interpretations in the context of geological settings. in *Organic Geochemistry* (Elsevier Ltd), 681–702. doi: 10.1016/j.orggeochem.2005.01.010.

Moussard, H., L'Haridon, S., Tindall, B. J., Banta, A., Schumann, P., Stackebrandt, E., et al. (2004). Thermodesulfatator indicus gen. nov., sp. nov., a novel thermophilic chemolithoautotrophic sulfate-reducing bacterium isolated from the Central Indian Ridge. *Int. J. Syst. Evol. Microbiol.* 54, 227–

233. doi: 10.1099/ijs.0.02669-0.
Murali, R., Yu, H., Speth, D. R., Wu, F., Metcalfe, K. S., Crémière, A., et al. (2022). Physiological adaptation of sulfate reducing bacteria in syntrophic partnership with anaerobic methanotrophic archaea. *bioRxiv* 2022.11.23. doi: 10.1101/2022.11.23.517749.
Nauhaus, K., Albrecht, M., Elvert, M., Boetius, A., and Widdel, F. (2007). In vitro cell growth of marine archaeal-bacterial consortia during anaerobic oxidation of methane with sulfate. *Environ. Microbiol.* 9, 187–196. doi: 10.1111/j.1462-2920.2006.01127.x.
Niemann, H., Lösekann, T., De Beer, D., Elvert, M., Nadalig, T., Knittel, K., et al. (2006). Novel microbial communities of the Haakon Mosby mud volcano and their role as a methane sink. *Nat. 2006 4437113* 443, 854–858. doi: 10.1038/nature05227.
Offre, P., Spang, A., and Schleper, C. (2013). Archaea in Biogeochemical Cycles. *Annu. Rev. Microbiol.* doi: 10.1146/annurev-micro-092412-155614.
Omoregie, E. O., Mastalerz, V., de Lange, G., Straub, K. L., Kappler, A., Røy, H., et al. (2008). Biogeochemistry and Community Composition of Iron- and Sulfur-Precipitating Microbial Mats at the Chefren Mud Volcano (Nile Deep Sea Fan, Eastern Mediterranean). *Appl. Environ. Microbiol.* 74, 3198–3215. doi: 10.1128/AEM.01751-07.
Orcutt, B. N., Joye, S. B., Kleindienst, S., Knittel, K., Ramette, A., Reitz, A., et al. (2010). Impact of natural oil and higher hydrocarbons on microbial diversity, distribution, and activity in Gulf of Mexico cold-seep sediments. *Deep Sea Res. Part II* 57, 2008–2021. doi: 10.1016/j.dsr2.2010.05.014.
Orphan, V. J. (2009). Methods for unveiling cryptic microbial partnerships in nature. *Curr. Opin. Microbiol.* 12, 231–237. doi: 10.1016/j.mib.2009.04.003.
Orphan, V. J., House, C. H., Hinrichs, K.-U., McKeegan, K. D., and DeLong, E. F. (2002). Multiple archaeal groups mediate methane oxidation in anoxic cold seep sediments. *Proc. Natl. Acad. Sci.* 99, 7663–7668. doi: 10.1073/pnas.072210299.
Parkes, R. J., Cragg, B. A., and Wellsbury, P. (2000). Recent studies on bacterial populations and processes in subseafloor sediments: A review. *Hydrogeol. J.* 8, 11–28. doi: 10.1007/PL00010971.
Parks, D. H., Chuvochina, M., Waite, D. W., Rinke, C., Skarshewski, A., Chaumeil, P.-A., et al. (2018). A standardized bacterial taxonomy based on genome phylogeny substantially revises the tree of life. *Nat. Biotechnol.*, 1–9. doi: 10.1101/256800.
Pedersen, R. B., Rapp, H. T., Thorseth, I. H., Lilley, M. D., Barriga, F. J. A. S., Baumberger, T., et al. (2010). Discovery of a black smoker vent field and vent fauna at the Arctic Mid-Ocean Ridge. *Nat. Commun.* 1, 1–6. doi: 10.1038/ncomms1124.
Proskurowski, G. (2010). "Abiogenic Hydrocarbon Production at the Geosphere-Biosphere Interface via Serpentinization Reactions," in *Handbook of Hydrocarbon and Lipid Microbiology* (Berlin, Heidelberg: Springer Berlin Heidelberg), 215–231. doi: 10.1007/978-3-540-77587-4_14.
Rabus, R., Boll, M., Heider, J., Meckenstock, R. U., Buckel, W., Einsle, O., et al. (2016). Anaerobic Microbial Degradation of Hydrocarbons: From Enzymatic Reactions to the Environment. *J. Mol. Microbiol. Biotechnol.* 26, 5–28. doi: 10.1159/000443997.
Rabus, R., Wilkes, H., Behrends, A., Armstroff, A., Fischer, T., Pierik, A. J., et al. (2001). Anaerobic initial reaction of n-alkanes in a denitrifying bacterium: Evidence for (1-methylpentyl)succinate as initial product and for involvement of an organic radical in n-hexane metabolism. *J. Bacteriol.* 183, 1707–1715. doi: 10.1128/JB.183.5.1707-1715.2001.
Raghoebarsing, A. A., Pol, A., Van De Pas-Schoonen, K. T., Smolders, A. J. P., Ettwig, K. F., Rijpstra, W. I. C., et al. (2006). A microbial consortium couples anaerobic methane oxidation to denitrification. *Nature* 440, 918–921. doi: 10.1038/nature04617.
Rampelotto, P. H. (2013). Extremophiles and extreme environments. *Life* 3, 482–485. doi: 10.3390/LIFE3030482.
Reeburgh, W. S. (2007). Oceanic methane biogeochemistry. *Chem. Rev.* 107, 486–513. doi: 10.1021/cr050362v.

Rinke, C., Chuvochina, M., Mussig, A. J., Chaumeil, P.-A., Davín, A. A., Waite, D. W., et al. (2021). A standardized archaeal taxonomy for the Genome Taxonomy Database. *Nat. Microbiol.* 6, 946–959. doi: 10.1038/s41564-021-00918-8.

Ripple, W. J., Wolf, C., Newsome, T. M., Barnard, P., and Moomaw, W. R. (2020). World Scientists' Warning of a Climate Emergency. *Bioscience* 70, 8–12. doi: 10.1093/BIOSCI/BIZ088.

Rojo, F. (2010). "Enzymes for Aerobic Degradation of Alkanes," in *Handbook of Hydrocarbon and Lipid Microbiology* (Berlin, Heidelberg: Springer Berlin Heidelberg), 781–797. doi: 10.1007/978-3-540-77587-4_59.

Rona, P. A., Klinkhammer, G., Nelsen, T. A., Trefry, J. H., and Elderfield, H. (1986). Black smokers, massive sulphides and vent biota at the Mid-Atlantic Ridge. *Nat. 1986 3216065* 321, 33–37. doi: 10.1038/321033a0.

Rosnes, J. T., Torsvik, T., and Lien, T. (1991). Spore-Forming Thermophilic Sulfate-Reducing Bacteria Isolated from North Sea Oil Field Waters. *Appl. Environ. Microbiol.* 57, 2302–2307. doi: 10.1128/aem.57.8.2302-2307.1991.

Roussel, E. G., Bonavita, M.-A. C., Querellou, J., Cragg, B. A., Webster, G., Prieur, D., et al. (2008). Extending the Sub-Sea-Floor Biosphere. *Science (80-.).* 320, 1046–1046. doi: 10.1126/science.1154545.

Rueter, P., Rabus, R., Wilkest, H., Aeckersberg, F., Rainey, F. A., Jannasch, H. W., et al. (1994). Anaerobic oxidation of hydrocarbons in crude oil by new types of sulphate-reducing bacteria. *Nat. 1994 3726505* 372, 455–458. doi: 10.1038/372455a0.

Ruff, S. E., Biddle, J. F., Teske, A. P., Knittel, K., Boetius, A., and Ramette, A. (2015). Global dispersion and local diversification of the methane seep microbiome. *Proc. Natl. Acad. Sci. U. S. A.* 112, 4015–20. doi: 10.1073/pnas.1421865112.

Saunois, M., Stavert, A. R., Poulter, B., Bousquet, P., Canadell, J. G., Jackson, R. B., et al. (2020). The Global Methane Budget 2000–2017. *Earth Syst. Sci. Data* 12, 1561–1623. doi: 10.5194/essd-12-1561-2020.

Scheller, S., Ermler, U., and Shima, S. (2020). "Catabolic Pathways and Enzymes Involved in Anaerobic Methane Oxidation," in *Anaerobic Utilization of Hydrocarbons, Oils, and Lipids* (Cham: Springer International Publishing), 31–59. doi: 10.1007/978-3-319-50391-2_3.

Scheller, S., Goenrich, M., Boecher, R., Thauer, R. K., and Jaun, B. (2010). The key nickel enzyme of methanogenesis catalyses the anaerobic oxidation of methane. *Nature* 465, 606–608. doi: 10.1038/nature09015.

Schink, B. (1997). Energetics of syntrophic cooperation in methanogenic degradation. *Microbiol. Mol. Biol. Rev.* 61, 262–280. doi: 10.1128/mmbr.61.2.262-280.1997.

Schipper, E. L. F., Revi, A., Preston, B. L., Carr, E. R., Eriksen, S. H., Fernández-Carril, L. R., et al. (2022). "Climate Resilient Development Pathways," in *IPCC, 2022: Climate Change 2022: Impacts, Adaptation and Vulnerability. Contribution of Working Group II to the Sixth Assessment Report of the Intergovernmental Panel on Climate Change*, eds. H.-O. Pörtner, D. C. Roberts, M. Tignor, E. S. Poloczanska, K. Mintenbeck, A. Alegría, et al. (Cambridge, UK and New York, NY, USA: Cambridge University Press), 2655–2807. doi: 10.1017/9781009325844.

Schouten, S., Wakeham, S. G., Hopmans, E. C., and Damsté, J. S. S. (2003). Biogeochemical evidence that thermophilic archaea mediate the anaerobic oxidation of methane. *Appl. Environ. Microbiol.* 69, 1680–1686. doi: 10.1128/AEM.69.3.1680-1686.2003.

Schreiber, L., Holler, T., Knittel, K., Meyerdierks, A., and Amann, R. (2010). Identification of the dominant sulfate-reducing bacterial partner of anaerobic methanotrophs of the ANME-2 clade. *Environ. Microbiol.* 12, no-no. doi: 10.1111/j.1462-2920.2010.02275.x.

Schrenk, M. O., Kelley, D. S., Bolton, S. A., and Baross, J. A. (2004). Low archaeal diversity linked to subseafloor geochemical processes at the Lost City Hydrothermal Field, Mid-Atlantic Ridge. *Environ. Microbiol.* 6, 1086–1095. doi: 10.1111/J.1462-2920.2004.00650.X.

Seitz, K. W., Dombrowski, N., Eme, L., Spang, A., Lombard, J., Sieber, J. R., et al. (2019). Asgard archaea capable of anaerobic hydrocarbon cycling. *Nat. Commun.* 10, 1822. doi: 10.1038/s41467-019-09364-x.

Sherwood Lollar, B., Westgate, T. D., Ward, J. A., Slater, G. F., and Lacrampe-Couloume, G. (2002). Abiogenic formation of alkanes in the Earth's crust as a minor source for global hydrocarbon reservoirs. *Nature* 416, 522–524. doi: 10.1038/416522a.

Shou, L. Bin, Liu, Y. F., Zhou, J., Liu, Z. L., Zhou, L., Liu, J. F., et al. (2021). New evidence for a hydroxylation pathway for anaerobic alkane degradation supported by analyses of functional genes and signature metabolites in oil reservoirs. *AMB Express* 11. doi: 10.1186/s13568-020-01174-5.

Simoneit, B. R. T., Kawka, O. E., and Brault, M. (1988). Origin of gases and condensates in the Guaymas Basin hydrothermal system (Gulf of California). *Chem. Geol.* 71, 169–182. doi: 10.1016/0009-2541(88)90113-1.

Simoneit, B. R. T., and Lonsdale, P. F. (1982). Hydrothermal petroleum in mineralized mounds at the seabed of Guaymas Basin. *Nature* 295, 198–202. doi: 10.1038/295198a0.

Simoneit, B. R. T., Lonsdale, P. F., Edmond, J. M., and Shanks, W. C. (1990). Deep-water hydrocarbon seeps in Guaymas Basin, Gulf of California. *Appl. Geochemistry* 5, 41–49. doi: 10.1016/0883-2927(90)90034-3.

So, C. M., Phelps, C. D., and Young, L. Y. (2003). Anaerobic transformation of alkanes to fatty acids by a sulfate-reducing bacterium, strain Hxd3. *Appl. Environ. Microbiol.* 69, 3892–3900. doi: 10.1128/AEM.69.7.3892-3900.2003.

Sonne-Hansen, J., and Ahring, B. K. (1999). Thermodesulfobacterium hveragerdense sp.nov., and Thermodesulfovibrio islandicus sp.nov., Two Thermophilic Sulfate Reducing Bacteria Isolated from a Icelandic Hot Spring. *Syst. Appl. Microbiol.* 22, 559–564. doi: 10.1016/S0723-2020(99)80009-5.

Sorokin, D. Y., Makarova, K. S., Abbas, B., Ferrer, M., Golyshin, P. N., Galinski, E. A., et al. (2017). Discovery of extremely halophilic, methyl-reducing euryarchaea provides insights into the evolutionary origin of methanogenesis. *Nat. Microbiol.* 2, 17081. doi: 10.1038/nmicrobiol.2017.81.

Stern, R. J. (2002). Subduction zones. *Rev. Geophys.* 40, 3-1-3–38. doi: 10.1029/2001RG000108.

Stetter, K. O., Huber, R., Blöchl, E., Kurr, M., Eden, R. D., Fielder, M., et al. (1993). Hyperthermophilic archaea are thriving in deep North Sea and Alaskan oil reservoirs. *Nature* 365, 743–745. doi: 10.1038/365743a0.

Stetter, K. O., Lauerer, G., Thomm, M., and Neuner, A. (1987). Isolation of Extremely Thermophilic Sulfate Reducers: Evidence for a Novel Branch of Archaebacteria. *Science (80-.).* 236, 822–824. doi: 10.1126/science.236.4803.822.

Stolper, D. A., Lawson, M., Davis, C. L., Ferreira, A. A., Neto, E. V. S., Ellis, G. S., et al. (2014). Formation temperatures of thermogenic and biogenic methane. *Science (80-.).* 344, 1500–1503. doi: 10.1126/science.1254509.

Takai, K., Nakamura, K., Toki, T., Tsunogai, U., Miyazaki, M., Miyazaki, J., et al. (2008). Cell proliferation at 122°C and isotopically heavy CH 4 production by a hyperthermophilic methanogen under high-pressure cultivation. *Proc. Natl. Acad. Sci.* 105, 10949–10954. doi: 10.1073/pnas.0712334105.

Tavormina, P. L., Ussler, W., and Orphan, V. J. (2008). Planktonic and Sediment-Associated Aerobic Methanotrophs in Two Seep Systems along the North American Margin. *Appl. Environ. Microbiol.* 74, 3985–3995. doi: 10.1128/AEM.00069-08.

Teske, A., De Beer, D., McKay, L. J., Tivey, M. K., Biddle, J. F., Hoer, D., et al. (2016). The Guaymas Basin hiking guide to hydrothermal mounds, chimneys, and microbial mats: Complex seafloor expressions of subsurface hydrothermal circulation. *Front. Microbiol.* 7, 1–23. doi: 10.3389/fmicb.2016.00075.

Teske, A., Hinrichs, K.-U., Edgcomb, V., Gomez, A. D. V., Kysela, D., Sylva, S. P., et al. (2002). Microbial Diversity of Hydrothermal Sediments in the Guaymas Basin: Evidence for Anaerobic

Methanotrophic Communities. *Appl. Environ. Microbiol.* 68, 1994–2007. doi: 10.1128/AEM.68.4.1994.

Teske, A. P., and Carvalho, V. (2020). *Marine Hydrocarbon Seeps*. , eds. A. Teske and V. Carvalho Cham: Springer International Publishing doi: 10.1007/978-3-030-34827-4.

Teske, A., and Sørensen, K. B. (2008). Uncultured archaea in deep marine subsurface sediments: Have we caught them all? *ISME J.* 2, 3–18. doi: 10.1038/ismej.2007.90.

Thauer, R. K. (2011). Anaerobic oxidation of methane with sulfate: on the reversibility of the reactions that are catalyzed by enzymes also involved in methanogenesis from CO_2. *Curr. Opin. Microbiol.* 14, 292–299. doi: 10.1016/J.MIB.2011.03.003.

Thauer, R. K. (2019). Methyl (Alkyl)-Coenzyme M Reductases: Nickel F-430-Containing Enzymes Involved in Anaerobic Methane Formation and in Anaerobic Oxidation of Methane or of Short Chain Alkanes. *Biochemistry* 58, 5198–5220. doi: 10.1021/acs.biochem.9b00164.

Thauer, R. K., Kaster, A. K., Seedorf, H., Buckel, W., and Hedderich, R. (2008). Methanogenic archaea: ecologically relevant differences in energy conservation. *Nat. Rev. Microbiol. 2008 68* 6, 579–591. doi: 10.1038/nrmicro1931.

Tissot, B. P., and Welte, D. H. (1984). *Petroleum Formation and Occurrence*. Berlin, Heidelberg: Springer Berlin Heidelberg doi: 10.1007/978-3-642-87813-8.

Toth, C. R. A., and Gieg, L. M. (2018). Time Course-Dependent Methanogenic Crude Oil Biodegradation: Dynamics of Fumarate Addition Metabolites, Biodegradative Genes, and Microbial Community Composition. *Front. Microbiol.* 8, 1–16. doi: 10.3389/fmicb.2017.02610.

Ueno, Y., Yamada, K., Yoshida, N., Maruyama, S., and Isozaki, Y. (2006). Evidence from fluid inclusions for microbial methanogenesis in the early Archaean era. *Nature* 440, 516–519. doi: 10.1038/nature04584.

Vaksmaa, A., Guerrero-Cruz, S., van Alen, T. A., Cremers, G., Ettwig, K. F., Lüke, C., et al. (2017). Enrichment of anaerobic nitrate-dependent methanotrophic 'Candidatus Methanoperedens nitroreducens' archaea from an Italian paddy field soil. *Appl. Microbiol. Biotechnol.* 101, 7075–7084. doi: 10.1007/s00253-017-8416-0.

Vanwonterghem, I., Evans, P. N., Parks, D. H., Jensen, P. D., Woodcroft, B. J., Hugenholtz, P., et al. (2016). Methylotrophic methanogenesis discovered in the archaeal phylum Verstraetearchaeota. *Nat. Microbiol.* 1, 16170. doi: 10.1038/nmicrobiol.2016.170.

von Netzer, F., Pilloni, G., Kleindienst, S., Krüger, M., Knittel, K., Gründger, F., et al. (2013). Enhanced Gene Detection Assays for Fumarate-Adding Enzymes Allow Uncovering of Anaerobic Hydrocarbon Degraders in Terrestrial and Marine Systems. *Appl. Environ. Microbiol.* 79, 543–552. doi: 10.1128/AEM.02362-12.

Wang, F.-P., Zhang, Y., Chen, Y., He, Y., Qi, J., Hinrichs, K.-U., et al. (2014). Methanotrophic archaea possessing diverging methane-oxidizing and electron-transporting pathways. *ISME J.* 8, 1069–1078. doi: 10.1038/ismej.2013.212.

Wang, W., and Shao, Z. (2013). Enzymes and genes involved in aerobic alkane degradation. *Front. Microbiol.* 4, 116. doi: 10.3389/fmicb.2013.00116.

Wang, Y., Feng, X., Natarajan, V. P., Xiao, X., and Wang, F. (2019a). Diverse anaerobic methane- and multi-carbon alkane-metabolizing archaea coexist and show activity in Guaymas Basin hydrothermal sediment. *Environ. Microbiol.* 21, 1344–1355. doi: 10.1111/1462-2920.14568.

Wang, Y., Wegener, G., Hou, J., Wang, F., and Xiao, X. (2019b). Expanding anaerobic alkane metabolism in the domain of Archaea. *Nat. Microbiol.* 4, 1. doi: 10.1038/s41564-019-0364-2.

Wang, Y., Wegener, G., Ruff, S. E., and Wang, F. (2020). Methyl/alkyl-coenzyme M reductase-based anaerobic alkane oxidation in archaea. *Environ. Microbiol.* 00. doi: 10.1111/1462-2920.15057.

Wang, Y., Wegener, G., Williams, T. A., Xie, R., Hou, J., Tian, C., et al. (2021). A methylotrophic origin of methanogenesis and early divergence of anaerobic multicarbon alkane metabolism. *Sci. Adv.* 7, 1–12. doi: 10.1126/sciadv.abj1453.

Wegener, G., Krukenberg, V., Riedel, D., Tegetmeyer, H. E., and Boetius, A. (2015). Intercellular wiring enables electron transfer between methanotrophic archaea and bacteria. *Nature* 526, 587–590. doi: 10.1038/nature15733.

Wegener, G., Krukenberg, V., Ruff, S. E., Kellermann, M. Y., and Knittel, K. (2016). Metabolic capabilities of microorganisms involved in and associated with the anaerobic oxidation of methane. *Front. Microbiol.* 7, 1–16. doi: 10.3389/fmicb.2016.00046.

Wegener, G., Laso-Pérez, R., Orphan, V. J., and Boetius, A. (2022). Anaerobic Degradation of Alkanes by Marine Archaea. *Annu. Rev. Microbiol.* 76, 553–577. doi: 10.1146/annurev-micro-111021-045911.

Welhan, J. A. (1988). Origins of methane in hydrothermal systems. *Chem. Geol.* 71, 183–198. doi: 10.1016/0009-2541(88)90114-3.

Whitman, W. B., Coleman, D. C., and Wiebe, W. J. (1998). Prokaryotes: The unseen majority. *Proc. Natl. Acad. Sci. U. S. A.* 95, 6578. doi: 10.1073/PNAS.95.12.6578.

Widdel, F., Knittel, K., and Galushko, A. (2010). "Anaerobic hydrocarbon-degrading microorganisms: an overview," in *Handbook of Hydrocarbon and Lipid Microbiology*, ed. K. N. Timmis (Berlin, Heidelberg: Springer Berlin Heidelberg), 1998–2021. doi: 10.1007/978-3-540-77587-4.

Widdel, F., and Musat, F. (2010a). "Diversity and Common Principles in Enzymatic Activation of Hydrocarbons," in *Handbook of Hydrocarbon and Lipid Microbiology* (Berlin, Heidelberg: Springer Berlin Heidelberg), 981–1009. doi: 10.1007/978-3-540-77587-4_70.

Widdel, F., and Musat, F. (2010b). "Energetic and Other Quantitative Aspects of Microbial Hydrocarbon Utilization," in *Handbook of Hydrocarbon and Lipid Microbiology* (Berlin, Heidelberg: Springer Berlin Heidelberg), 729–763. doi: 10.1007/978-3-540-77587-4_57.

Wiegert, R. G. (2001). "High-Temperature Ecosystems," in *Encyclopedia of Biodiversity* (Elsevier), 111–120. doi: 10.1016/B978-0-12-384719-5.00206-9.

Wilkes, H., and Schwarzbauer, J. (2010). "Hydrocarbons: An Introduction to Structure, Physico-Chemical Properties and Natural Occurrence," in *Handbook of Hydrocarbon and Lipid Microbiology*, ed. K. N. Timmis (Berlin, Heidelberg: Springer Berlin Heidelberg), 1–48. doi: 10.1007/978-3-540-77587-4_1.

Williams, T. A., Szöllősi, G. J., Spang, A., Foster, P. G., Heaps, S. E., Boussau, B., et al. (2017). Integrative modeling of gene and genome evolution roots the archaeal tree of life. *Proc. Natl. Acad. Sci.* 114, E4602–E4611. doi: 10.1073/pnas.1618463114.

Yu, H., Skennerton, C. T., Chadwick, G. L., Leu, A. O., Aoki, M., Tyson, G. W., et al. (2021). Sulfate differentially stimulates but is not respired by diverse anaerobic methanotrophic archaea. *ISME J.* 16, 168–177. doi: 10.1038/s41396-021-01047-0.

Zedelius, J., Rabus, R., Grundmann, O., Werner, I., Brodkorb, D., Schreiber, F., et al. (2011). Alkane degradation under anoxic conditions by a nitrate-reducing bacterium with possible involvement of the electron acceptor in substrate activation. *Environ. Microbiol. Rep.* 3, 125–135. doi: 10.1111/j.1758-2229.2010.00198.x.

Zengler, K., Richnow, H. H., Rosselló-Mora, R., Michaelis, W., and Widdel, F. (1999). Methane formation from long-chain alkanes by anaerobic microorganisms. *Nature* 401, 266–269. doi: 10.1038/45777.

Zhang, Y., Maignien, L., Zhao, X., Wang, F., and Boon, N. (2011). Enrichment of a microbial community performing anaerobic oxidation of methane in a continuous high-pressure bioreactor. *BMC Microbiol.* 11, 2–9. doi: 10.1186/1471-2180-11-137.

Zhou, Z., Zhang, C., Liu, P., Fu, L., Laso-Pérez, R., Yang, L., et al. (2022). Non-syntrophic methanogenic hydrocarbon degradation by an archaeal species. *Nature* 601, 257–262. doi: 10.1038/s41586-021-04235-2.

Deep-branching ANME-1c archaea grow at the upper temperature limit of anaerobic oxidation of methane

David Benito Merino, Hanna Zehnle, Andreas Teske, Gunter Wegener

published in

Frontiers in Microbiology

23 September 2022

DOI: 10.3389/fmicb.2022.988871

Deep-branching ANME-1c archaea grow at the upper temperature limit of anaerobic oxidation of methane

David Benito Merino[1,2*], Hanna Zehnle[1,2,3], Andreas Teske[4], Gunter Wegener[1,3*]

[1]Max Planck Institute for Marine Microbiology, Bremen, Germany

[2]Faculty of Geosciences, University of Bremen, Bremen, Germany

[3]MARUM, Center for Marine Environmental Sciences, University of Bremen, Bremen, Germany

[4]Department of Earth, Marine and Environmental Sciences, University of North Carolina at Chapel Hill, Chapel Hill, NC, USA

*** Correspondence:**

David Benito Merino, dbenito@mpi-bremen.de

Gunter Wegener, gwegener@mpi-bremen.de

Keywords: anaerobic oxidation of methane, ANME-1, archaea, deep sea, hydrothermal vents

Abstract

In seafloor sediments, the anaerobic oxidation of methane (AOM) consumes most of the methane formed in anoxic layers, preventing this greenhouse gas from reaching the water column and finally the atmosphere. AOM is performed by syntrophic consortia of specific anaerobic methane-oxidizing archaea (ANME) and sulfate-reducing bacteria (SRB). Cultures with diverse AOM partners exist at temperatures between 12°C and 60°C. Here, from hydrothermally heated sediments of the Guaymas Basin, we cultured deep-branching ANME-1c that grow in syntrophic consortia with *Thermodesulfobacteria* at 70°C. Like all ANME, ANME-1c oxidize methane using the methanogenesis pathway in reverse. As an uncommon feature, ANME-1c encode a nickel-iron hydrogenase. This hydrogenase has low expression during AOM and the partner *Thermodesulfobacteria* lack hydrogen-consuming hydrogenases. Therefore, it is unlikely that the partners exchange hydrogen during AOM. ANME-1c also does not consume hydrogen for methane formation, disputing a recent hypothesis on facultative methanogenesis. We hypothesize that the ANME-1c hydrogenase might have been present in the common ancestor of ANME-1 but lost its central metabolic function in ANME-1c archaea. For potential direct interspecies electron transfer (DIET), both partners encode and express genes coding for extracellular appendages and multiheme cytochromes. *Thermodesulfobacteria* encode and express an extracellular pentaheme cytochrome with high similarity to cytochromes of other syntrophic sulfate-reducing partner bacteria. ANME-1c might associate specifically to *Thermodesulfobacteria*, but their co-occurrence is so far only documented for heated sediments of the Gulf of California. However, in the deep seafloor, sulfate–methane interphases appear at temperatures up to 80°C, suggesting these as potential habitats for the partnership of ANME-1c and *Thermodesulfobacteria*.

Introduction

In anoxic deep-sea sediments, the greenhouse gas methane is produced abiotically by thermocatalytic decay of buried organic matter or biotically by methanogens (Whiticar, 1999). Anaerobic oxidation of methane (AOM) mitigates the flux of methane to the water column and eventually to the atmosphere by consuming 90% of the methane produced in the deep sediments (Hinrichs and Boetius, 2002; Reeburgh, 2007; Regnier et al., 2011). In marine sediments, AOM primarily couples to sulfate reduction in a 1:1 stoichiometry:

$$CH_4 + SO_4^{2-} \rightarrow HS^- + HCO_3^- + H_2O. \qquad (1)$$

AOM is mediated by anaerobic methanotrophic archaea (ANME) that oxidize methane to CO_2 by reversing the methanogenesis pathway (Hallam et al., 2004; Meyerdierks et al., 2010; Wang et al., 2014). ANME do not encode respiratory pathways, but they pass the reducing equivalents liberated during AOM to sulfate-reducing partner bacteria (SRB), forming characteristic consortia (Boetius et al., 2000; Michaelis et al., 2002; Orphan et al., 2002; McGlynn et al., 2015; Wegener et al., 2015). The nature of this syntrophic association and the mechanisms involved in the transfer of reducing equivalents from ANME towards SRB are not completely resolved at the molecular level. Originally, it was proposed that the archaeal partners produce molecular hydrogen that is consumed by the bacterial partners (Hoehler et al., 1994). However, most ANME do not code for hydrogenases (Chadwick et al., 2022). Previous studies support the hypothesis of direct interspecies electron transfer (DIET) involving multiheme cytochromes and pilus proteins (Meyerdierks et al., 2010; McGlynn et al., 2015; Wegener et al., 2015). The partner SRBs use the AOM-derived electrons for anaerobic respiration with sulfate as final electron acceptor (Boetius et al., 2000; Wegener et al., 2015; Laso-Pérez et al., 2016). The limited energy yield of sulfate-dependent AOM (equation (1), $\Delta G^{\circ\prime} = -16.67$ kJ mol^{-1} at standard conditions and $\Delta G = -20$ to -40 kJ mol^{-1} in marine AOM habitats) needs to be shared between ANME and their syntrophic partner SRB (Thauer, 2011).

ANME inhabit a variety of marine habitats including cold seeps (Boetius et al., 2000; Orphan et al., 2001), mud volcanoes (Niemann et al., 2006), gas hydrates (Lanoil et al., 2001; Orcutt et al., 2004), hydrothermal vents (Inagaki et al., 2006; Biddle et al., 2012) and deep subsurface sediments (Roussel et al., 2008). ANME are polyphyletic and fall into three distinct phylogenetic groups (ANME-1, ANME-2 and ANME-3). ANME-3 often dominate AOM at mud volcanoes, where they form consortia with *Desulfobulbus*-related bacteria (Niemann et al., 2006; Lösekann et al., 2007). Cultivation attempts of ANME-3 have not been successful so far. ANME-2 are globally distributed in a variety of benthic habitats and are typically

found associated with *Desulfosarcina*/*Desulfococcus* bacteria (DSS, Seep-SRB1 and Seep-SRB2 clades) (Knittel et al., 2003, 2005; Boetius and Knittel, 2010). ANME-2 are dominant at cold seeps with high methane fluxes and temperatures below 20 °C (Knittel et al., 2005). Cultivation attempts at temperatures ≤ 20 °C resulted in the enrichment of ANME-2c (Holler et al., 2009; Wegener et al., 2016).

ANME-1 prevail in most deep sulfate-methane transition zones (SMTZs) (Ishii et al., 2004; Niemann et al., 2005; Treude et al., 2005), in hydrothermally heated sediments in the Guaymas Basin (Teske et al., 2002; Schouten et al., 2003; Ruff et al., 2015; Dombrowski et al., 2018), and in the Auka vent field, in the Pescadero Basin (Gulf of California) (Speth et al., 2022). Meso- and thermophilic AOM cultures have been obtained from Guaymas Basin sediments at 37, 50 and 60°C (Holler et al., 2011; Wegener et al., 2016). These cultures consisted of ANME-1a and HotSeep-1 (*Ca.* Desulfofervidus) as partner bacteria. *Ca.* Desulfofervidus sequences are also found *in situ* at these sites (McKay, 2014; Dowell et al., 2016).

Previous short-term incubations revealed AOM activity at temperatures up to 75°C or 85°C, but the microorganisms performing AOM under these conditions were not assessed (Kallmeyer and Boetius, 2004; Holler et al., 2011; Adams et al., 2013). Here, we obtained an active AOM culture at 70°C (AOM70) from Guaymas Basin hydrothermal sediments consisting of a previously uncultured ANME-1 subgroup (Teske et al., 2002) and an apparently obligate syntrophic *Thermodesulfobacterium* partner. We describe their function and interaction based on physiological experiments and molecular data.

Materials and Methods

Sediment collection and enrichment culture setup

Sediment push cores from gas-rich hydrothermal vents of the Guaymas Basin (Gulf of California) were collected by the submersible *Alvin* at 2013 m depth during RV *Atlantis* cruise AT42-05 (November 2018). Sediments for this AOM enrichment came from cores 4991-13 and 4991-14 in the Cathedral Hill area (27°00.6848’ N, 111° 24.2708’ W) collected on Nov. 17, 2018 in an area covered by dense orange-white *Beggiatoaceae* mats, where temperatures at 50 cm depth reached at least 80 °C. On board sediment samples were transferred to glass bottles sealed with butyl rubber stoppers, the headspace was exchanged to argon. Sediments were stored at 4°C until further processing. Sediment slurries were prepared following protocols previously described (Laso-Pérez et al., 2018). Anoxic sediments were mixed with sulfate-reducer medium (Widdel and Bak, 1992) in a 1/10 ratio (v/v) in serum vials sealed with rubber stoppers. The headspace of the serum vials was replaced with 2 atm methane:CO_2 (90:10). The dry weight of the original slurries was 60 g L^{-1}. The slurries were incubated at 70°C in the dark. Methane-dependent sulfide

production was measured with the copper sulfate assay (Cord-Ruwisch, 1985). Incubations with methane-dependent sulfide productions at 70°C are referred to as AOM70 culture. These cultures were diluted 1/5 with new medium when sulfide levels reached >10 mM. Cultures were virtually sediment-free after four dilutions.

DNA extraction and long-read sequencing

DNA samples for long-read sequencing were prepared according to previous protocols with few modifications (Zhou et al., 1996; Hahn et al., 2020). In short, 50 mL culture were collected in a Falcon tube and biomass was pelleted by centrifugation at RT (4000 rpm for 20 min). After removing the supernatant, 800 µL extraction buffer was added (100 mM tris-HCl, 100 mM sodium EDTA, 100 mM sodium phosphate, 1.5 M NaCl, 1% CTAB, pH 8). For physical lysis of cell envelopes, the pellet suspension was frozen twice in liquid nitrogen and thawed in water bath at 65 °C. For enzymatic lysis, 1000 µL extraction buffer with 60 µL proteinase K (20 mg mL^{-1}) was used at 37°C for 1.5 h with constant shaking. Chemical lysis was done with 300 µL 20% SDS at 65°C for 2 h. Cell debris was pelleted again by centrifugation at RT (13000 × *g* for 20 min). The clear supernatant was transferred to a new tube and 2 mL of chloroform-isoamyl alcohol (16:1, v:v) were added. The samples were mixed by inverting the tubes and centrifuged at RT (13000 × *g* for 20 min). The aqueous phase was transferred to a new tube and mixed with 0.6 volumes isopropanol. DNA was precipitated overnight at –20°C. After precipitation, DNA was re-dissolved at 65°C in a water bath for 5 min and samples were centrifuged at RT (13000 × *g* for 40 min). Supernatant was removed and the pellet was washed with ice-cold 80% ethanol. Samples were centrifuged at 13000 × *g* for 10 min and the ethanol was removed. Dried pellets were resuspended in 100 µL PCR-grade water. Long-read (>10 kb) genomic DNA was sequenced on a Sequel IIe (Pacific Biosciences) at the Max Planck Genome Centre in Cologne. Read length distributions and abundances are compiled in Supplementary Table 1.

RNA extraction and short-read shotgun sequencing

Triplicates of 30 mL culture were filtered onto 0.2 µL polycarbonate filters under gentle vacuum. Filters were soaked immediately with RNAlater (Invitrogen) preheated at 70 °C for 10-15 min. RNAlater was removed by filtration and the filters were stored at –20 °C until further processing. For RNA extraction, ¼ of a filter was put into a bead-beating tube (Lysing Matrix E, MPBio) together with 600 µL RNA lysis buffer (Quick-RNA MiniPrep kit, Zymo Research). Tubes were vortexed at maximum speed for 20 min. Biomass was pelleted by centrifugation at RT (10000 × *g* for 5 min). The supernatant was collected and RNA was extracted with the Quick-RNA MiniPrep kit (Zymo Research) including a DNA digestion step

with DNase I. Total RNA libraries were sequenced in an Illumina HiSeq2500 machine at the Max Planck Genome Centre (Cologne, Germany). We obtained 4 Mio 2×250 bp paired-end reads.

Metagenome and metatranscriptome analysis

Metagenomic long-reads were assembled using Flye v. 2.9 (Kolmogorov et al., 2020). Shotgun metatranscriptomic short reads were quality trimmed using BBduk from the BBtools package v. 38.87* with the parameters minlength=50 mink=6 hdist=1 qtrim=r trimq=20. Metagenomic reads were mapped to the general assembly. Long reads were mapped using minimap2 v. 2.21 (Li, 2018) with default parameters. Open reading frames in metagenomic contigs were predicted with prodigal v. 2.6.3 (Hyatt et al., 2010) and genes were annotated with PFAMs, TIGRFAMs, COGs, KEGGs and RNAmmer (Kanehisa and Goto, 2000; Haft et al., 2001; Lagesen et al., 2007; Galperin et al., 2015; Mistry et al., 2021). CXXCH motifs in putative multiheme cytochromes were searched with a custom script**. Predicted hydrogenase sequences were classified into subgroups with the hydrogenase database (HydDB) (Søndergaard et al., 2016). Subcellular localisation of heme-containing proteins and hydrogenases was predicted with PSORTb 3.0 (Yu et al., 2010). Metagenomic binning based on differential coverage across metagenomic samples was done with maxbin v 2.2.7 (Wu et al., 2016). Bins were manually refined in anvi'o v. 6 (Eren et al., 2015, 2020) by removing contigs with low coverage from high-coverage bins.

Triplicate metatranscriptomes were mapped to curated bins using bowtie 2 (Langmead and Salzberg, 2012). The rRNA and tRNA gene sequences were removed before calculating gene expression levels. Center-log ratio (CLR) values for relative gene expression were calculated according to the formula:

$$CLR_i = log_2 \frac{x_i}{L_i \sqrt[n]{x_1 \times x_2 \times \ldots \times x_n}} \qquad (2),$$

where x_i are the reads mapped to a specific gene and L_i is the length of the gene in kbp. A 0.5 factor was added to read-mapping values to avoid zero values.

To analyse the similarity of cytochrome-like proteins in ANME-1 and sulfate-reducing bacteria, amino acid sequences from sulfate-reducing partner bacteria genomes were downloaded from NCBI (Krukenberg et al., 2016, 2018). BLAST databases were created from the cytochrome sequences in the

* https://sourceforge.net/projects/bbmap/

** https://github.com/dbenitom/Metagenomics_scripts/blob/main/CXXCH_search_anvio_import.sh

reference SRB genomes using makeblastdb (BLAST v. 2.10.1) (Altschul et al., 1990). Cytochrome-like proteins in AOM70 cultures were queried against the custom database with BLASTp v 2.5.

Community composition and phylogenetic analyses based on the 16S rRNA gene

16S rRNA genes from long-read metagenomic assemblies were extracted with Metaxa2 (Bengtsson-Palme et al., 2015). Full-length 16S rRNA gene sequences were aligned to the SILVA database release 138.1 using the SINA aligner within the ARB software (Ludwig et al., 2004; Pruesse et al., 2012; Quast et al., 2013). Long reads were mapped against 16S rRNA genes using minimap2 (Li, 2018). Shotgun metatranscriptomic reads were aligned to 16S rRNA gene using bowtie2 (Langmead and Salzberg, 2012). Maximum-likelihood 16S rRNA phylogenetic trees with selected ANME or *Thermodesulfobacteria* sequences were calculated using RAxML with 1000 bootstraps and a 50% frequency base filter (Stamatakis, 2014).

Phylogenomic and phylogenetic analyses

Archaea and Bacteria genomes were downloaded from public databases (Supplementary Table 3). For ANME-1 phylogenomic analysis, the genomes were annotated with HMMs of 38 conserved archaeal marker genes (Supplementary Table 3) (Darling et al., 2014). For *Thermodesulfobacteria*, the genomes were annotated with HMMs of 71 conserved bacterial marker genes (Rinke et al., 2013). The amino acid sequences of each set were aligned and concatenated using MUSCLE (Edgar, 2004). Maximum likelihood phylogenomic trees were calculated with IQTree using the –test option to estimate the best substitution model for each protein in the partition file and using 100 bootstraps (Chernomor et al., 2016; Kalyaanamoorthy et al., 2017; Minh et al., 2020). Reference hydrogenase sequences (Supplementary Table 5) were downloaded from the hydrogenase database (HydDB) (Søndergaard et al., 2016). ANME-1 hydrogenases and reference hydrogenases were aligned with muscle (Edgar, 2004). Maximum likelihood phylogenetic trees of the alignment were calculated with IQTree with 100 bootstraps (Chernomor et al., 2016; Kalyaanamoorthy et al., 2017; Minh et al., 2020). Trees were visualised and edited on the Interactive Tree Of Life (iTOL) online server (Letunic and Bork, 2011).

Catalyzed reporter deposition-fluorescent *in situ* hybridization (CARD-FISH)

To prepare CARD-FISH samples, 5 mL culture were fixed at 1% formaldehyde concentration over night at 4°C. Fixed samples were sonicated (15 s, 30% power, 20% cycle) to detach cells from sediment particles to detach larger aggregates. Samples were then filtered onto 0.2 µm polycarbonate filters and fixed with 0.2% low-melting agarose before CARD-FISH. Samples were stored at –20°C until further processing.

CARD-FISH was performed as described previously (Pernthaler et al., 2002). In short, endogenous peroxidases were inactivated with a solution of 0.15% H_2O_2 in methanol for 30 min at RT. Cell walls were permeabilized with lysozyme (Sigma Aldrich, 10 mg mL^{-1} lysozyme in 50 mM EDTA, 100 mM Tris-HCl; 60 min incubation at 37°C), proteinase K (15 µg mL^{-1} proteinase K in 50 mM EDTA, 100 mM Tris-HCl, 500 mM NaCl; 10 min incubation at RT) and HCl (0.1 M HCl; 1 min incubation at RT). Horseradish peroxidase-labelled probes were diluted in hybridisation buffer at the adequate formamide concentration for each probe (Supplementary Table 2). Probes were hybridized at 46°C for 2 h. Signal amplification with fluorescent tyramides was done for 45 min at 46°C. For double hybridizations, peroxidases of the prior hybridisation step were inactivated by incubating the filter in 0.30% H_2O_2 in methanol for 30 min at RT.

Quantification of methane and hydrogen in AOM cultures

For cultures under AOM conditions, hydrogen formation in the headspace was measured by gas chromatography coupled to reducing compound photometry (RCP, Peak Performer 1 RCP, Peak Laboratories). For cultures under methanogenic conditions, methane formation in the headspace was measured via gas chromatography and flame ion detection (GC-FID, Focus GC, Thermo).

Results and Discussion

AOM enrichment cultures at 70°C

A slurry produced from hydrothermally-heated sediments from the Guaymas Basin and sulfate-reducer medium was supplemented with a methane:CO_2 headspace and incubated at 70°C. These incubations showed methane-dependent sulfate reduction, as measured by an increase of sulfide in the medium (Figure 1B and Supplementary Figure 1). These incubations produced sulfide 12 to 15 mM sulfide within about 100 days. The slurries were diluted 1/10 (v/v) in fresh SRB medium, and a fresh methane:CO_2 headspace was added and the incubation was proceeded. After four additional incubation and dilution steps, the produced AOM70 cultures were virtually sediment-free, contained microbial aggregates visible with the naked eye and produced approximately 100 µmol sulfide L^{-1} d^{-1}. To our knowledge, this is the first long-term cultivation of AOM-performing microorganisms above 60°C. The culture showed strongly decreased sulfide production at 60°C. It tolerated a transfer to 75°C, but became inactive at 80°C, confirming prior results on the upper temperature limit of AOM made in short-term incubations with Guaymas Basin sediments (Holler et al., 2011; McKay et al., 2016).

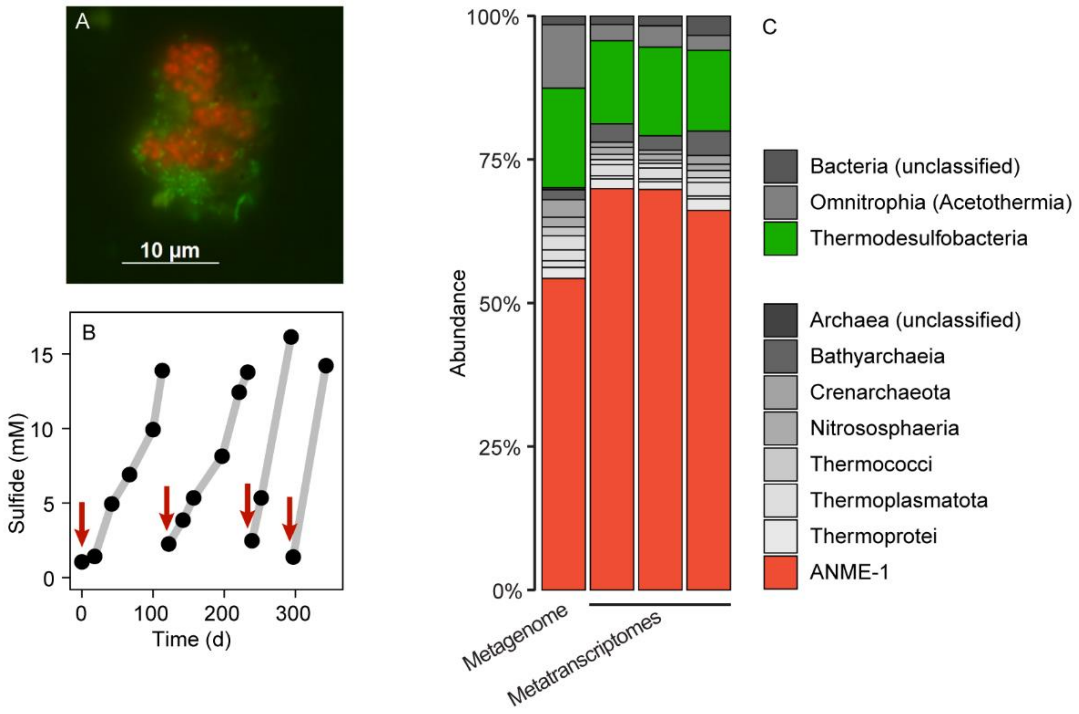

Figure 1. Microbial composition and growth of thermophilic AOM cultures. A. CARD-FISH on AOM aggregates with the probes EUB388 I-III (green) and ANME-1-389 (red). Bacteria (green) and archaea (red) form shell-type consortia. **B.** Methane-dependent sulfide production in AOM cultures. The red arrows indicate when culture medium was replaced. **C.** 16S rRNA gene relative abundance in long-read metagenomic reads and shotgun metatranscriptomic reads (triplicate metatranscriptomes). The enrichment is dominated by ANME-1 and sulfate reducers of the class Thermodesulfobacteria. Other bacteria and archaea such as Acetothermia and Bathyarchaeia are side community members from original sediment samples.

Thermophilic AOM community at 70°C

To resolve the microbial community composition of the AOM70 culture, we obtained a long-read metagenome and triplicate short-read metatranscriptomes. The community consisted mainly of ANME-1 (~50% relative abundance of mapped reads) and *Thermodesulfobacteria* (~20% relative abundance) based on 16S rRNA gene fragments recruited from the metagenome (Figure 1C) that were rare in the original sediment samples (Supplementary Figure 2). Metatranscriptomic samples were also dominated by ANME-1 (~70% relative abundance) and *Thermodesulfobacteria* (~15% relative abundance), forming the active AOM community at 70°C. Both the metagenome and metatranscriptome revealed noticeable populations of Bathyarchaeota and Acetothermia (<10% relative abundance of mapped reads). Yet, we were not able to reconstruct MAGs of these organisms; hence, their potential functions are unknown. Previous studies suggest that these organisms ferment or oxidize biomolecules produced by the AOM community (Kellermann et al., 2012; Dombrowski et al., 2017; Hao et al., 2018; Zhu et al., 2022).

After long-read metagenome assembly and binning, we obtained two high quality MAGs of the two members of the AOM consortium (Table 1). The *Thermodesulfobacterium* MAG has a size of 1.7 Mbp and GC content of 29%. The bin is almost complete (98.6%) and has no contamination based on the presence of 104 bacterial single-copy marker genes (CheckM) (Parks et al., 2015). The ANME-1 bin has a size of 1.5 Mbp and a GC content of 47.8%. The bin is 90.8% complete and has contamination of 7.9% based on 149 archaeal marker genes (CheckM) (Parks et al., 2015).

Table 1. Metagenome-assembled genomes retrieved from AOM70 enrichment cultures.

	***Ca.* Thermodesulfobacterium**	**ANME-1c (*Ca.* Methanophagales)**
No. of contigs	4	16
Genome size	1.702 Mbp	1.493 Mbp
L50/N50	2/808,565 bp	5/109,767 bp
GC content	29.0%	47.8%
Completeness*	98.6%	90.8%
Contamination*	<1%	7.89%

* Completeness and contamination were calculated with CheckM.

We attempted to visualize the enriched ANME-1 using a previously established probe targeting the whole ANME-1 clade (ANME-1-350, Supplementary Table 2) (Boetius et al., 2000). *In situ* hybridization with the ANME-1-350 failed, because the probe has two mismatches with the 16S rRNA sequence of the enriched ANME-1. The 16S rRNA gene of this ANME-1 belong to a clade ancestral to all ANME-1a/b, namely ANME-1c (Supplementary Figure 4 and discussion below) (Laso-Pérez et al., 2022). A newly developed ANME-1-389 probe specifically binds to ANME-1c cells. Because the probes available for partner SRB do not target the 16S rRNA sequence of *Thermodesulfobacteria*, we designed three candidate probes to target this clade (Supplementary Table 2). Unfortunately, none of these probes hybridized the 16S rRNA of this organism after various CARD-FISH attempts (Supplementary Table 2). *Thermodesulfobacteria* are likely the partner bacteria of ANME-1c during AOM at 70°C based on the abundance of bacterial cells and their gene content (see discussion below). Furthermore, all genes coding for dissimilatory sulfate reductase (*dsr*) in the metagenome belong to the *Thermodesulfobacterium* MAG. Double hybridization with the ANME-1c and the general bacterial probes (Supplementary Table 2) revealed a dominance of "shell-type" aggregates consisting of ANME-1c and partner bacteria (Figure 1A and Supplementary Figure 3). These consortia consist of clumps of ANME-1c cells, surrounded by smaller

rod-shaped bacterial cells. These shell-type aggregates differ from the predominantly mixed-type aggregates of moderately thermophilic consortia growing at 50-60°C (Holler et al., 2011; Wegener et al., 2015). A shell-type growth morphology is often observed in cold-adapted ANME (Knittel et al., 2005). The reason for the different association types is unknown.

Phylogeny of deep-branching ANME-1c

On the basis of whole genome comparison, the ANME-1 population detected in the AOM70 culture falls into the recently named ANME-1c clade (Figure 2A) (Laso-Pérez et al., 2022; Speth et al., 2022).The ANME-1c group is basal to its sister groups ANME-1a and ANME-1b within the order ANME-1 (*Ca.* Methanophagales). The 16S rRNA gene phylogenetic tree supports this phylogenetic placement (Supplementary Figure 4). ANME-1c belong to the class Syntrophoarchaeia with the ANME-1, *Ca.* Syntrophoarchaeales and *Ca.* Alkanophagales. Considering an average nucleotide identity (ANI) of <83% for distinct species and >95% for same species (Jain et al., 2018) the ANME-1c clade consists of two distinct species clusters (Supplementary Figure 5). The ANME-1c MAG from the AOM70 culture belongs to the cluster of *Ca.* Methanoxibalbensis ujae from Pescadero Basin (Laso-Pérez et al., 2022). ANME-1c 16S rRNA gene sequences have been detected in hydrothermal sediments of the Guaymas Basin and the Juan de Fuca Ridge (Supplementary Figure 4) (Teske et al., 2002; Merkel et al., 2013; McKay et al., 2016), and a MAG of the ANME-1c clade (accessions: SAMN09215218, GCA_003661195.1) was derived from Guaymas Basin hydrothermal sediments (Dombrowski et al., 2018). ANME-1c are also present in rock samples from hydrothermal fields in Pescadero Basin (Gulf of California) (Speth et al., 2022). The ANME-1c clade was originally named “ANME-1b” by Teske and coworkers to differentiate this lineage from previously described cold-seep ANME-1 (Teske et al., 2002) and later renamed to ANME-1Guaymas because it was predominantly recovered from Guaymas Basin (Biddle et al., 2012; Merkel et al., 2013; Dowell et al., 2016). These sequences originate from sediment cores with sulfate-reducing activity at temperatures between 65 and 90°C, showing that these archaea are likely all thermophiles (Biddle et al., 2012). Furthermore, the high GC content (>60%) of ANME-1c 16S rRNA genes indicates that these archaea might have temperature optima in the upper range of thermophily above 70°C (Merkel et al., 2013).

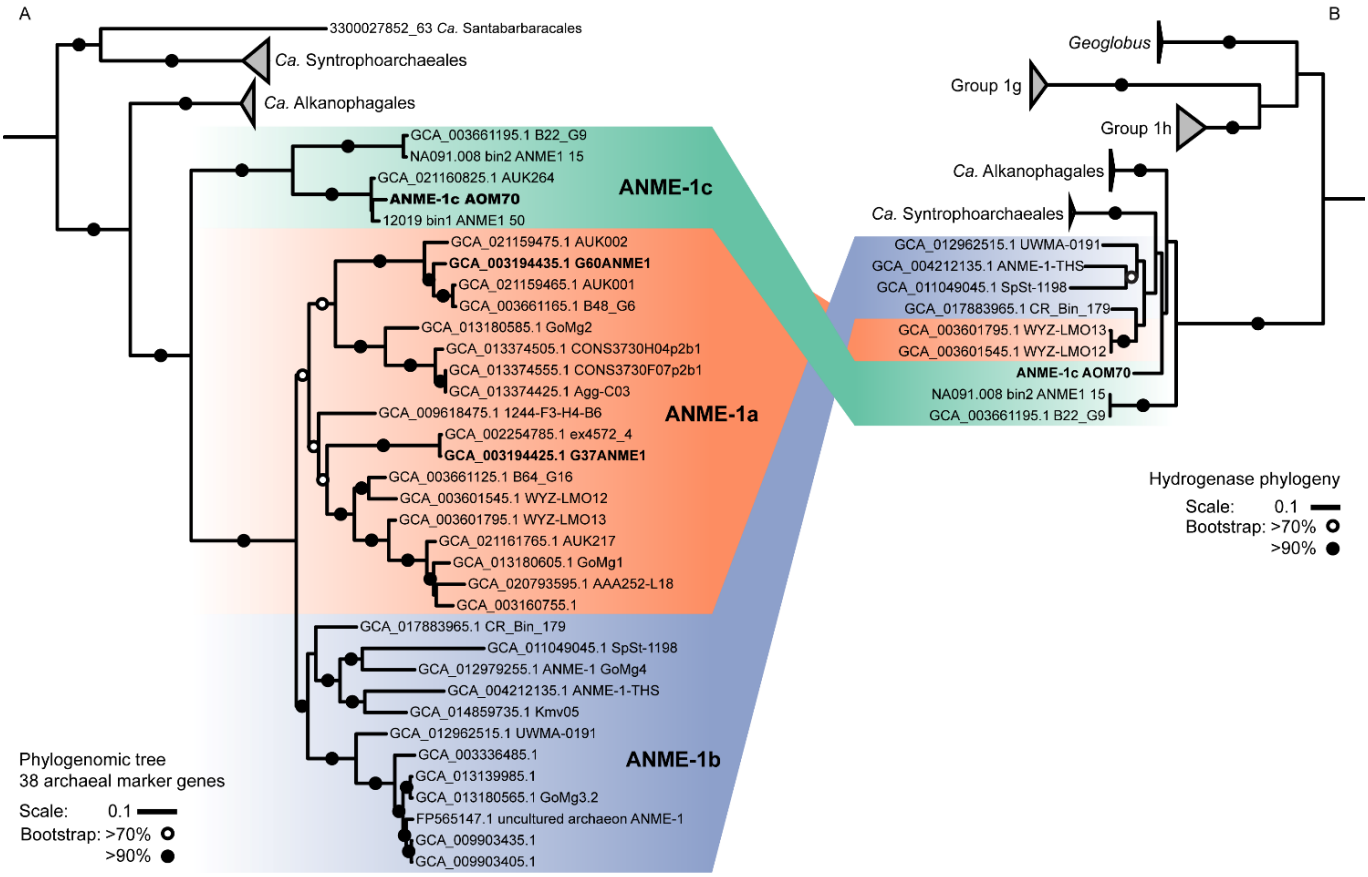

Figure 2. ANME-1 phylogenomic tree and hydrogenase phylogeny. A. Phylogeny of ANME-1 order (*Ca.* Methanophagales) with related *Ca.* Alkanophagales, *Ca*. Syntrophoarchaeales and *Ca*. Santabarbaracales. Maximum likelihood phylogenomic tree based on an alignment of 38 archaeal conserved genes from 55 genomes (Supplementary Table 3). *Geoglobus* sequences were the outgroup to set the tree root (not shown). **B.** Hydrogenase phylogeny. ANME-1, *Ca.* Alkanophagales and *Ca.* Syntrophoarchaeales hydrogenases are located at the base of groups 1g and 1h of NiFe hydrogenases. A complete hydrogenase tree is shown in Supplementary Figure 11. MAGs from cultured ANME are depicted in bold. Shading in both trees indicates the three subdivisions of the ANME-1: ANME-1c, ANME-1a and ANME-1b. ANME-1 AOM70 is the genome discussed in the main text. Scales indicate nucleotide substitution per site. Bootstrap support is based on 100 iterations above 70% and above 90%.

Genomic and metabolic features of ANME-1c

ANME-1c codes for a complete methanogenesis pathway including a canonical methane-active Mcr (Figure 3). The *mcr*ABC genes in ANME-1c have the highest expression (CLR > 7) among all genes in the dataset. This high expression of *mcr* confirms previous transcriptomic work in ANME (Haroon et al., 2013; Krukenberg et al., 2018). The activation of methane is the rate-limiting step of AOM, and ANME would promote this reaction by producing large amounts of Mcr (Scheller et al., 2010; Thauer, 2011). Similar to other ANME-1 archaea, ANME-1c does not encode a N^5,N^{10}-methylene-H_4MPT reductase (*mer*). This gene might be substituted by a 5,10-methylenetetrahydrofolate reductase (*met*) (Stokke et al.,

2012; Krukenberg et al., 2018). The function of this bypass has not been verified yet. All other genes of the methanogenesis pathway show a relatively high expression with CLR values between 0.1 and 3.4 (Supplementary Table 4), supporting a catabolic function of the encoded genes. ANME-1c encodes and expresses the methanogenesis-related membrane-bound complex H^+-translocating F_{420}:quinone oxidoreductase (*fqo*) that catalyses the transfer of electrons from reduced cofactors to the quinone pool (Pereira et al., 2011). ANME-1c encodes an ATP synthase, which is a common feature in ANME to enable the oxidative phosphorylation of ATP, coupled to the influx of protons. ANME-1c encodes a sulfate adenylyltransferase (*cys*N) (low expression, CLR = –0.02) and an adenylylsulfate kinase (*cys*C) (high expression, CLR=2.21) that could be used for assimilatory sulfate metabolism, but it lacks the key genes for dissimilatory sulfate reduction. The ANME-1c MAG lacks a complete nitrogenase operon, suggesting it is incapable of nitrogen fixation. The capability for nitrogen fixation has been shown only in ANME-2 archaea but not in ANME-1 (Dekas et al., 2009, 2015; Orphan et al., 2009; Krukenberg et al., 2018). The nitrogenase subunits *nif*DH detected in ANME-1c and other ANME-1 genomes (Meyerdierks et al., 2010) are likely paralogs of *cfb*CD because they are located in an operon with genes encoding the biosynthetic pathway of coenzyme F_{430} (Zheng et al., 2016; Moore et al., 2017). Coenzyme F_{430} functions as a prosthetic group that binds to the active site of McrA, and is therefore a key molecule for methanogens and methanotrophs (Friedmann et al., 1990; Ermler et al., 1997; Shima et al., 2012).

ANME-1c likely performs autotrophic carbon fixation via the carbon monoxide dehydrogenase/acetyl-CoA synthase complex (Cdh/Acs) (Kellermann et al., 2012). All the *cdh* transcripts are highly abundant (CLR between 0.4 and 2.0, Supplementary Table 4), supporting the use of this pathway for autotrophy. ANME-1c does not encode other complete carbon fixation pathways. The reductive tricarboxylic acid (rTCA) cycle is incomplete, lacking the key enzyme pyruvate carboxylase. The rTCA cycle genes have relatively low expression (CLR –0.7 to 1.8, Supplementary Table 4). Enzymes of this pathway may play a role in the biosynthesis of cell building blocks (Meyerdierks et al., 2010). Like all ANME-1, ANME-1c contains a β-oxidation pathway. The phylogenetically related multi-carbon alkane oxidizers, *Ca.* Syntrophoarchaeales, *Ca.* Alkanophagales and *Ca.* Santabarbaracales harbor several copies of the β-oxidation genes and use the encoded pathway to split alkane-derived acyl-CoA into acetyl-CoA units (Laso-Pérez et al., 2016; Wang et al., 2021). However, the expression of β-oxidation genes in ANME-1c is relatively low, especially the first two reactions (CLR –0.2 to 0.5, Supplementary Table 4). Furthermore, ANME-1c lacks the electron transfer flavoprotein (*etf*AB) needed to oxidize acyl-CoA to enoyl-CoA. Hence, β-oxidation may not serve a catabolic function in ANME-1c, but play a role in biosynthesis of cell compounds. Wang and colleagues suggested that the ancestor of Syntrophoarchaeia (family including

ANME-1, *Ca.* Syntrophoarchaeales and *Ca.* Alkanophagales) activated multi-carbon alkanes with their multicarbon-alkane specific Mcr (Acrs) forming the corresponding alkyl-CoM as intermediate (Laso-Pérez et al., 2016; Wang et al., 2021). It was proposed that ANME-1 acquired a methane-activating Mcr from methylotrophic methanogens, likely from the clade *Ca.* Methanofastidiosa/*Ca.* Nuwarchaeia, and later lost the *acr* genes (Borrel et al., 2019; Wang et al., 2021).

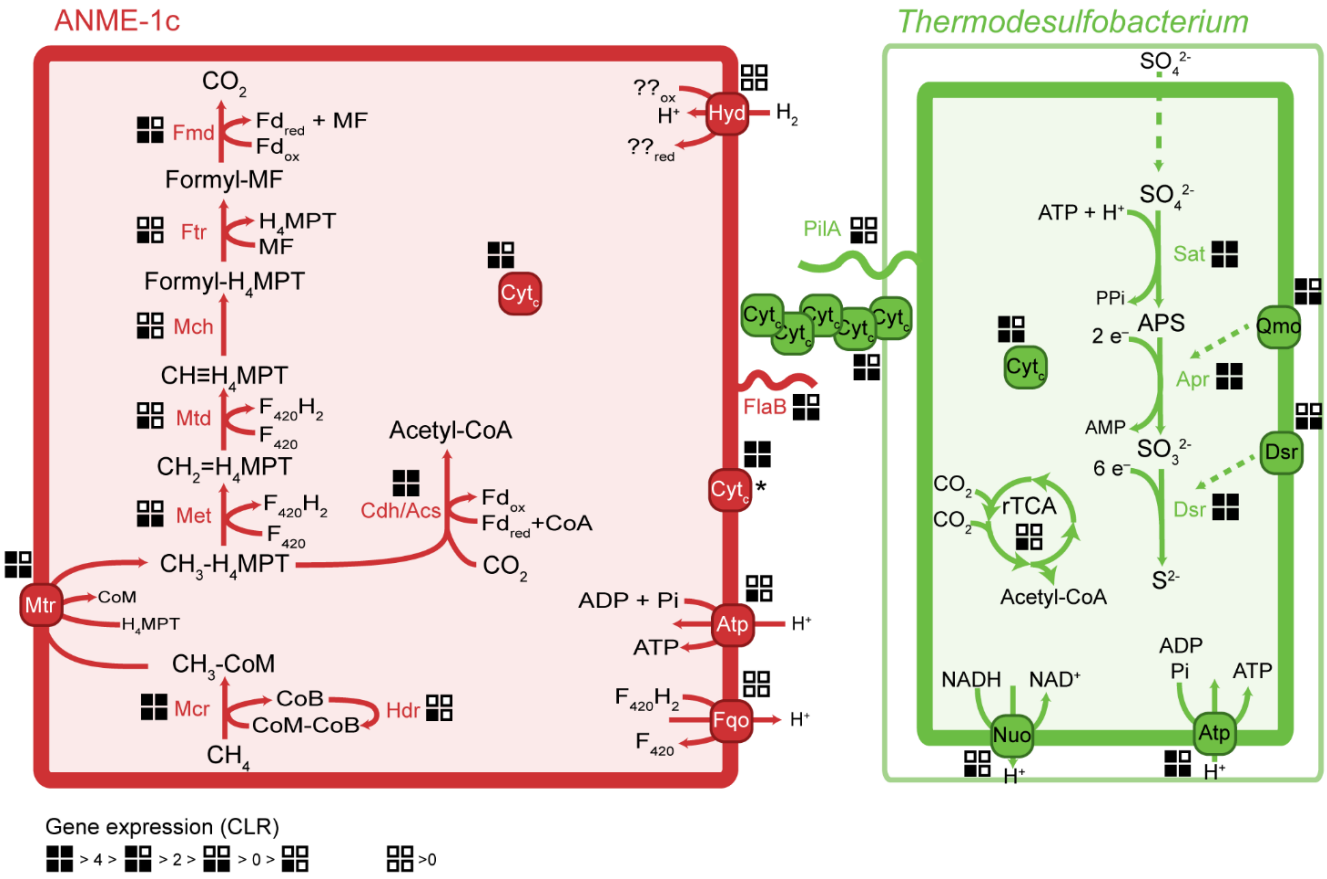

Figure 3. Key metabolic pathways in ANME-1c and *Ca.* Thermodesulfobacterium torris and metatranscriptomic expression during AOM. Gene expression values were normalized to centered-log ratios (CLR). A CLR value of 0 represents the mean expression of all genes in a genome. The asterisk next to the ANME-1c cytochrome indicates unknown cell localization. Abbreviations: H_4MPT, tetrahydromethanopterin; MF, methanofuran; Fd, ferredoxin; Mcr, methyl-coenzyme M reductase; Mtr, tetrahydromethanopterin S-methyltransferase; Met, 5,10-methylenetetrahydrofolate reductase; Mtd, methylenetetrahydromethanopterin dehydrogenase; Mch, methenyltetrahydromethanopterin cyclohydrolase; Ftr, formylmethanofuran-tetrahydromethanopterin formyltransferase; Fmd, formylmethanofuran dehydrogenase; Cdh/Acs, CO dehydrogenase/acetyl-coenzyme A synthase complex; rTCA, reductive tricarboxylic acid cycle; Sat, sulfate adenylyltransferase; Apr, adenylylsulfate reductase; Dsr, dissimilatory sulfate reductase; Fqo, ferredoxin:quinone oxidoreductase; Atp, ATP synthase; Hyd, hydrogenase; Qmo, quinone-modifying oxidoreductase; Nuo, NADH:ubiquinone oxidoreductase; Cyt_c, multiheme cytochrome *c*-like protein; PilA, bacterial pilus protein; FlaB, archaeal flagellum protein (archaellum).

Phylogeny and environmental distribution of AOM-associated *Thermodesulfobacteria*

We compared the *Thermodesulfobacterium* MAG in AOM70 cultures with the *Thermodesulfobacteria* MAGs from Pescadero Basin and to MAGs retrieved from databases (NCBI and JGI). Our AOM70 *Thermodesulfobacterium* shares >95% ANI with a MAG of a *Thermodesulfobacterium* from Pescadero Basin (Laso-Pérez et al., 2022; Speth et al., 2022) (Supplementary Figure 7). Based on 16S rRNA phylogeny (Supplementary Figure 6), the *Thermodesulfobacterium* AOM70 sequences form a cluster with sequences originating from Guaymas Basin and Pescadero Basin hydrothermal seeps (McKay et al., 2016; Lagostina et al., 2021; Pérez Castro et al., 2021; Speth et al., 2022). Several species of *Thermodesulfobacterium* have been isolated from hot springs (Zeikus et al., 1983; Sonne-Hansen and Ahring, 1999; Hamilton-Brehm et al., 2013), petroleum reservoirs (Rozanova and Khudiakova, 1974) and hydrothermal vents (Jeanthon et al., 2002; Moussard et al., 2004). The 16S rRNA gene sequence of our AOM70 *Thermodesulfobacterium* is 96% identical to the closest cultured representative, *Thermodesulfobacterium geofontis*, isolated from Obsidian Pool, Yellowstone National Park (Hamilton-Brehm et al., 2013). Considering an ANI <83% for distinct species and >95% for same species (Jain et al., 2018) the *Thermodesulfobacteria* MAG from the AOM70 culture metagenome and the Pescadero MAG are a new candidate species in the genus *Thermodesulfobacterium* (Supplementary Figure 8). We propose the taxon name *Candidatus* Thermodesulfobacterium torris (torris "firebrand" referring to the thermophilic lifestyle and the formation of black aggregates in the cultures).

Metabolism of the partner bacteria *Thermodesulfobacteria*

Members of the *Thermodesulfobacteria* family have not been previously reported as partner bacteria in AOM. All *Thermodesulfobacteria* isolates are sulfate-reducing (hyper)thermophiles with growth optima between 65°C and 90°C. They differ in the range of electron donors or carbon sources they use, which include molecular hydrogen, formate, lactate and pyruvate (Zeikus et al., 1983; Sonne-Hansen and Ahring, 1999; Jeanthon et al., 2002; Moussard et al., 2004). Similar to other members, *Ca*. T. torris encodes a complete dissimilatory sulfate reduction pathway, including sulfate adenylyltransferase (*sat*), adenylylsulfate reductase (*apr*) and dissimilatory sulfite reductase (*dsr*). In *Ca.* T. torris this pathway is highly expressed during AOM (average CLR values between 4.0 and 6.5, Supplementary Table 4). In addition, *Ca.* T. torris contains and expresses the Dsr-associated membrane complex (*dsr*KMOP) which takes up electrons from the periplasmic cytochrome *c* pool to reduce a disulfide bond in the cytoplasmic DsrC (Pereira et al., 2011; Venceslau et al., 2014). The quinone-modifying oxidoreductase (*qmo*ABC) genes are present in an operon together with the Apr genes. In fact, the Qmo membrane complex interacts

with Apr through a third unknown protein and channels electrons from the membrane ubiquinones via electron confurcation (Ramos et al., 2012). Both the *dsr*KMOP and the *qmo*ABC transcripts have high expression (Supplementary Table 4). Other cytoplasmic enzymes commonly associated with heterodisulfide reductases, such as the methylviologen reducing hydrogenase (Mvh/Hdr), were not found in the dataset. For energy conservation, *Ca.* T. torris uses a membrane-bound NADH:ubiquinone oxidoreductase (Nuo) and an ATP synthase (Atp). Nuo couples the reduction of NAD^+ by reduced ubiquinones in the cytoplasmic membrane to the translocation of protons to the periplasmic space. The proton gradient generated enables oxidative phosphorylation in the ATP synthase.

The reductive acetyl-CoA pathway (Wood-Ljungdahl pathway) for carbon fixation is incomplete in the genome. *Ca.* T. torris does not encode a formate dehydrogenase (*fdh*) or a carbon monoxide dehydrogenase/acetyl-CoA complex (*cdh*/*acs*), but it encodes the enzymes catalyzing C_1-tetrahydrofolate transformations. These reactions are necessary for several cell processes including nucleic acid biosynthesis (Ducker and Rabinowitz, 2017). Instead, *Ca.* T. torris likely fixes carbon via the rTCA cycle. The genome codes for an almost complete rTCA cycle, lacking a succinyl-CoA synthetase. This enzyme is likely substituted by a putative acetyl-CoA synthetase encoded in the genome and highly expressed (CLR= 3.39, locus MW689_000791). Acetyl-CoA synthetases have sequence homology with succinyl-CoA synthetases and are also active towards succinate with reduced affinity (Sánchez et al., 2000). Similarly, the thermophilic partner bacterium *Ca.* Desulfofervidus auxilii and other non-symbiotic thermophilic SRB fix carbon via the rTCA cycle (Schauder et al., 1987; Krukenberg et al., 2016). By contrast, meso- and psychrophilic AOM partner bacteria fix carbon using the Wood-Ljungdahl pathway (Skennerton et al., 2017).

We aimed to enrich *Ca.* T. torris by incubating aliquots of the AOM70 culture with H_2, formate, lactate or pyruvate as electron donors. None of the substrates resulted in immediate sulfide production (Supplementary Figure 9). Pyruvate caused sulfide production after 15 days, which likely indicates the growth of originally rare microorganisms, similar as shown for mesophilic AOM cultures (Zhu et al., 2022). These incubations suggest that *Ca.* T. torris is an obligate syntrophic bacterium that fully depends on the transfer of reducing equivalents in AOM.

Transfer of reducing equivalents between ANME-1c and *Thermodesulfobacteria*

Because ANME have no own respiratory pathways, they need to transfer the reducing equivalents liberated during AOM to their sulfate-reducing partners. Multiple mechanisms have been proposed for syntrophic fermentation, including interspecies hydrogen transfer (Schink, 1997). A canonical syntrophy

based on interspecies hydrogen transfer would require membrane-bound hydrogenases in both partners. Notably, the ANME-1c MAGs code for a complete nickel-iron hydrogenase, a feature that is rare in other ANME-1 genomes. The hydrogenase database (HydDB) annotation classifies this hydrogenase within the group 1g of hydrogenases that are typically found in thermophilic organisms (Brock et al., 1972; Fischer et al., 1983; Huber et al., 2000; Laska et al., 2003). Yet this hydrogenase is only poorly expressed (CLR < –0.3, Supplementary Table 4). In contrast, the *Ca.* T. torris MAG lacks hydrogenases. The addition of molecular hydrogen to the culture did not stimulate sulfide production in the AOM culture, which confirms that *Ca.* T. torris cannot grow on hydrogen. Based on these observations we exclude hydrogen as electron carrier from ANME-1c towards *Ca.* T. torris. Our results confirm thermodynamic models which excluded hydrogen exchange in AOM consortia (Sørensen et al., 2001). Most other AOM partner bacteria such as SeepSRB-1a and SeepSRB2 are also obligate syntrophs and do not encode hydrogenases (Nauhaus et al., 2002; Wegener et al., 2016; Krukenberg et al., 2018). *Ca.* D. auxilii, performs DIET when growing as partner in AOM or short-chain alkane oxidation at 50-60°C (Wegener et al., 2015; Laso-Pérez et al., 2016; Krukenberg et al., 2018; Hahn et al., 2020), but it also shows growth on hydrogen (Krukenberg et al., 2016). It has been shown that DIET allows more efficient growth than interspecies hydrogen transfer (Summers et al., 2010).

In AOM and short-chain alkane-oxidizing consortia, cells are densely packed and the intercellular space contains cytochromes and nanowire-like structures (McGlynn et al., 2015; Wegener et al., 2015; Laso-Pérez et al., 2016; Krukenberg et al., 2018). In these mesophilic and thermophilic consortia, both partners express cytochrome and *pil*A genes (Laso-Pérez et al., 2016; Krukenberg et al., 2018). The genes *pil*A (bacterial pilin) in *Ca*. T. torris and *fla*B (archaeal flagellin) in ANME-1c show a high expression in the metatranscriptomes (CLR values of 1.8 and 3.2, respectively, Supplementary Table 4). The archaeal flagellum (archaellum) is highly similar to bacterial type IV pili (Albers and Jarrell, 2015) and might also be involved in electron transfer over longer distances. The conductivity of the archaellum from the methanogen *Methanospirillum hungatei* was demonstrated, yet its possible role in interspecies electron transfer is unclear (Walker et al., 2019). Conductive filaments that enable the transport of electrons across long distances towards extracellular electron acceptors have been widely studied in *Geobacter* (Reguera et al., 2005; Malvankar et al., 2011; Shrestha et al., 2013; Adhikari et al., 2016). Reguera et al. (2005) showed that pilus-deficient *Geobacter* mutants could not transfer electrons to extracellular electron acceptors, suggesting an involvement of pilin proteins in this process (Reguera et al., 2005).

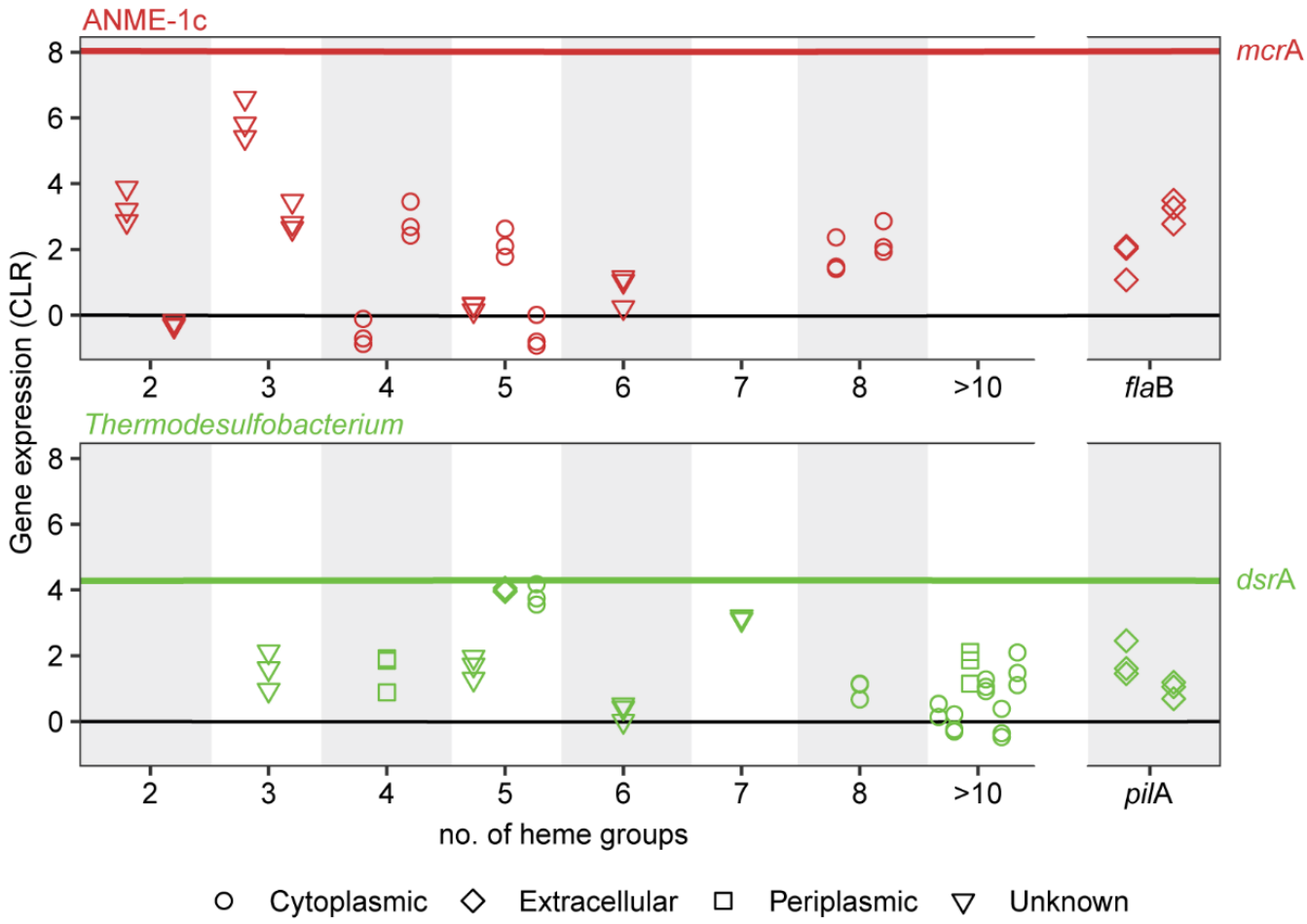

Figure 4. **Expression and subcellular localization of multiheme cytochromes and cellular appendages in ANME-1c (top) and *Thermodesulfobacterium* (bottom) in AOM70 cultures.** Gene expression is noted as centered-log ratio values, with 0 as the mean expression of all genes in each genome. *mcr*A and *dsr*A mean CLR values are displayed as a reference (red and green lines, respectively). Symbols show the predicted subcellular localization of cytochromes (PSORTb). Three symbols in a vertical line correspond to CLR values of a specific locus in triplicate metatranscriptomes.

The molecular basis of DIET in sulfate-dependent AOM has been intensively discussed in the past years (McGlynn et al., 2015; Wegener et al., 2015; Chadwick et al., 2022; Yu et al., 2022). McGlynn et al. (2015) proposed a model based on direct interspecies electron transfer via multiheme cytochromes for AOM consortia, using evidence from single-cell activities, microscopic observations and genomics (McGlynn et al., 2015). Krukenberg et al. (2018) showed that both partners highly express cytochromes with a low number of heme groups (3-5 heme binding motifs) during thermophilic AOM (Krukenberg et al., 2018). In AOM consortia at 60°C, it was observed that SRB Ca. Desulfofervidus auxilii expressed pili genes and that the intercellular space was filled with nanowire structures similar to syntrophic consortia of *Geobacter* (Wegener et al., 2015). Indeed it was recently shown that the filaments in *Geobacter*

sulfurreducens are not formed by pilin proteins (PilA), but rather by stacked OmcS hexaheme cytochromes (Wang et al., 2019). Instead, PilA might be involved in secretion of OmcS cytochromes (Gu et al., 2021). Both ANME-1c and *Ca.* T. torris encode several multiheme cytochromes. ANME-1c codes for several proteins with 2 to 8 heme-binding motifs (Figure 4 and Supplementary Table 4). A cytochrome c7 and a protein without annotation, both with 3 heme groups, are among the top expressed genes (CLR values of 5.9 and 2.96, respectively, Supplementary Table 4). However, the predicted subcellular localizations of these putative cytochromes are unknown, as reported by PSORTb. Interestingly, these cytochromes are highly similar to extracellular cytochromes that were highly expressed in ANME-1 during AOM at 60°C (Supplementary Table 4) (Krukenberg et al., 2018). *Ca.* T. torris also contains numerous multiheme cytochromes, with up to 26 heme-binding motifs. A cytochrome-like gene with five heme-binding motifs and predicted extracellular localization shows high expression levels similar to the *dsr*A (CLR value of 4.0, Figure 4). This putative pentaheme cytochrome shares high sequence identity (<40% identity) with a *Ca.* Desulfofervidus auxilii OmcS-like protein (Wegener et al., 2015; Krukenberg et al., 2018) (locus tag HS1_000170, Supplementary Figure 10). We hypothesize that the extracellular pentaheme cytochromes from *Ca.* T. torris are likely involved in receiving electrons derived from methane oxidation. ANME-1c cytochromes with undetermined cell localization might also be involved in interspecies electron transfer.

Alternative roles of the membrane-bound hydrogenase in ANME-1c

Some ANME-1c MAGs code for a NiFe membrane-bound hydrogenase, which is an uncommon feature in most ANME genomes (Stokke et al., 2012; Wegener et al., 2015; Krukenberg et al., 2018). This hydrogenase forms a clade with those of *Ca*. Syntrophoarchaeum and *Ca.* Alkanophagales (Figure 2B and Supplementary Figure 11) (Laso-Pérez et al., 2016; Wang et al., 2021). In *Ca*. Syntrophoarchaeum the hydrogenase is highly expressed during anaerobic propane and butane oxidation, albeit its function is also unknown (Laso-Pérez et al., 2016). In contrast, in ANME-1c the NiFe-hydrogenase has low expression (Figure 3 and Supplementary Table 4). A recent study described the ANME-1c as an ancestral clade at the base of ANME-1a/1b and as a sister branch of *Ca.* Syntrophoarchaeales (Laso-Pérez et al., 2022). ANME-1c were proposed to be facultative methanogens based on the encoded hydrogenase and the unclear association with partner bacteria in environmental samples (Laso-Pérez et al., 2022). The capability of ANME-1 to perform methanogenesis has been repeatedly suggested (Seifert et al., 2006; Treude et al., 2007; Orcutt et al., 2008). ANME-1 16S rRNA and *mcr*A genes and transcripts were found in methanogenic sediment horizons at White Oak River estuary and in the sulfate-methane transition zone (Lloyd et al., 2011; Kevorkian et al., 2021). The authors weighted this as an argument for a potential role

of ANME-1 in methanogenesis. There is no genomic evidence that ANME-1 from these environment contain hydrogenases, which are required to perform methanogenesis from CO_2, and this question should be addressed in future metagenomic studies. To test whether ANME-1c are capable of methanogenesis, we transferred AOM70 culture aliquots to sulfate-free medium and exchanged the methane in the headspace with an H_2/CO_2 atmosphere. Hydrogen addition did not stimulate production of methane in AOM70 cultures in the course of 4-month incubations (Supplementary Figure 12). According to these results, ANME-1c are incapable of hydrogenotrophic methanogenesis. The habitable zones of the hydrothermally-heated sediments in Guaymas Basin are rich in sulfate due to hydrothermal circulation and seawater advection (Ramírez et al., 2021). This provides additional evidence for ANME-1c being obligate methane oxidizers that depend on syntrophic partnerships with sulfate-reducers. The hydrogenase in ANME-1c might be a remnant from the common ancestor of the Ca. Syntrophoarchaeum/Ca. Alkanophagales/ANME-1 clade. These ancestral alkanotrophic archaea might have performed interspecies electron transfer based on hydrogen transfer. In the course of evolution that capability was replaced by an apparently more efficient DIET mechanism via extracellular multiheme cytochromes (Summers et al., 2010).

Conclusion

Here we cultured a thermophilic AOM consortium at 70°C consisting of methane-oxidizing archaea from the ANME-1c clade with *Thermodesulfobacteria* as sulfate-reducing partner bacteria. Our study bridges the temperature gap between AOM activity previously observed by pore water profiles and tracer experiments, and its *in-vitro* demonstration in cultures. ANME-1c is a basal lineage to the ANME-1a/b clade. Interestingly, ANME-1c MAGs encode a hydrogenase operon that is not present in the ANME-1a/b clades. ANME-1c neither produces nor consumes hydrogen. The hydrogenase genes have low expression and this enzyme is likely a remnant of the ancestor of the *Ca*. Syntrophoarchaeia, an organism that was likely a multi-carbon alkane oxidizer. The function of this hydrogenase in ANME-1, but also other members of the Syntrophoarchaeia is unresolved. Based on indirect evidence ANME-1 were repeatedly suggested to be facultative methanogens (Seifert et al., 2006; Treude et al., 2007; Orcutt et al., 2008; Lloyd et al., 2011; Kevorkian et al., 2021). Here we demonstrated that even ANME-1c that encode a hydrogenase are not able to reverse their metabolism towards net methanogenesis. Cultivation-based approaches should be used to test whether the ANME-1a/b that encode hydrogenases are capable of methanogenesis.

Most likely, ANME and their partners interact via DIET. The partner *Thermodesulfobacterium* encodes an extracellular pentaheme *c*-type cytochrome with high expression. This cytochrome is highly similar to

Ca. Desulfofervidus auxilii cytochromes that have high expression during AOM at 60°C. This evidence suggests a central role of this pentaheme cytochrome of *Thermodesulfobacteria* in DIET. In addition, multiheme cytochromes and flagella from ANME-1c are highly expressed under AOM conditions. However, the role of these cytochromes with unknown subcellular location in DIET needs further investigation.

Our study provides culture-based evidence for the feasibility of AOM at high-temperature conditions and the versatility and evolutionary diversity of the organisms mediating AOM in marine environments. To our knowledge, this is the first report of syntrophic consortia of ANME and *Thermodesulfobacteria.* ANME-1c and *Ca.* T. torris co-occur in environmental samples from the Guaymas Basin and Pescadero Basin (Gulf of California) (Laso-Pérez et al., 2022; Speth et al., 2022). This limited geographical distribution is likely a result of undersampling of heated methane-rich environments. Apart from the rather rare methane-rich hydrothermal vents, consortia of these phylotypes might inhabit deep sulfate-methane interfaces. Indeed, these sulfate-methane interfaces occur at depths up to 150 m below the seafloor and at temperatures of up to 80°C (Teske et al., 2021; Beulig et al., 2022). The question of whether these sulfate-methane interfaces are a habitat for AOM needs to be addressed. Future studies should aim to search for the ANME-1c and *Thermodesulfobacteria* co-occurring in such deep-sea sediments.

Data Availability Statement

The metagenome-assembled genomes (MAGs) and metagenomic contigs are available on NCBI under BioProject PRJNA805391. Assembled metagenomic contigs are available under BioSample ID SAMN30121676. ANME-1c and *Ca.* Thermodesulfobacterium torris annotated genomes are available under BioSample IDs SAMN27514932 and SAMN27514933, respectively.

Author Contributions

DBM and GW designed the study. GW did sampling on board. AT planned and organized the cruise. DBM and HZ did cultivation experiments. DBM performed laboratory experiments and ‘omics analyses and wrote the manuscript with contributions from all coauthors. All authors contributed to the article and approved the submitted version.

Funding

The study was funded by the Max Planck Society and the DFG under Germany’s Excellence Intiative/Strategy through the Clusters of Excellence EXC 2077 “The Ocean Floor–Earth’s Uncharted

Interface" (project no. 390741601). The Guaymas Basin expedition was supported by the National Science Foundation, Biological Ocenography grant no. 1357238 to A. T. (Collaborative Research: Microbial Carbon cycling and its interactions with Sulfur and Nitrogen transformations in Guaymas Basin hydrothermal sediments).

Acknowledgements

The authors thank the captain and crew of R/V *Atlantis*, and the *Alvin* group for excellent work during Expedition AT42-05. We thank Susanne Menger for technical support in the laboratory. We thank Rafael Laso Pérez for providing ANME-1c MAGs from Pescadero Basin.

Conflict of Interest

The authors declare that the research was conducted in the absence of any commercial or financial relationships that could be construed as a potential conflict of interest.

The handling editor S. Emil Ruff declared past co-authorships with one of the authors GW.

Publisher's note

Supplementary Material

The Supplementary material for this article can be found online at:

https://www.frontiersin.org/articles/10.3389/fmicb.2022.988871/full#supplementary-material

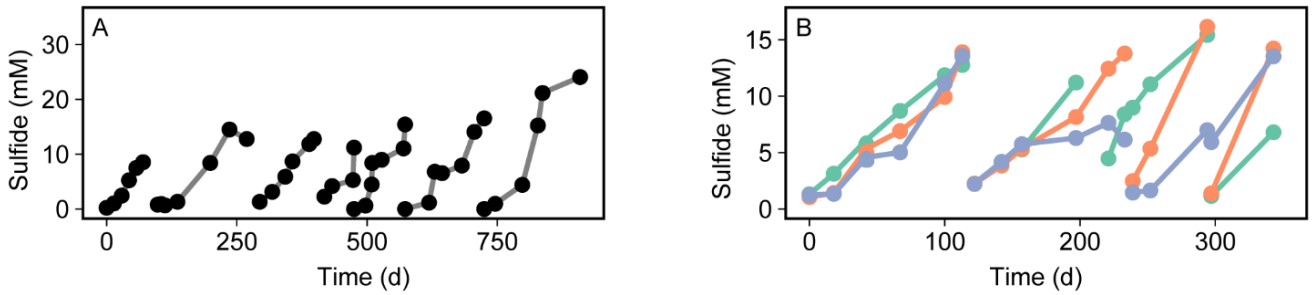

Supplementary Figure 1. Sulfide production in initial sediment slurry and in AOM cultures at 70°C. A. Sulfide production from sediment slurry was monitored over 800 days. Every drop in sulfide levels indicates when the slurry was diluted 1/10 with fresh medium. **B.** Sulfide production from three AOM70 cultures over 400 days. Every drop in sulfide levels indicates when the medium was replaced with fresh sulfate-reducer medium (no dilutions were made in established cultures).

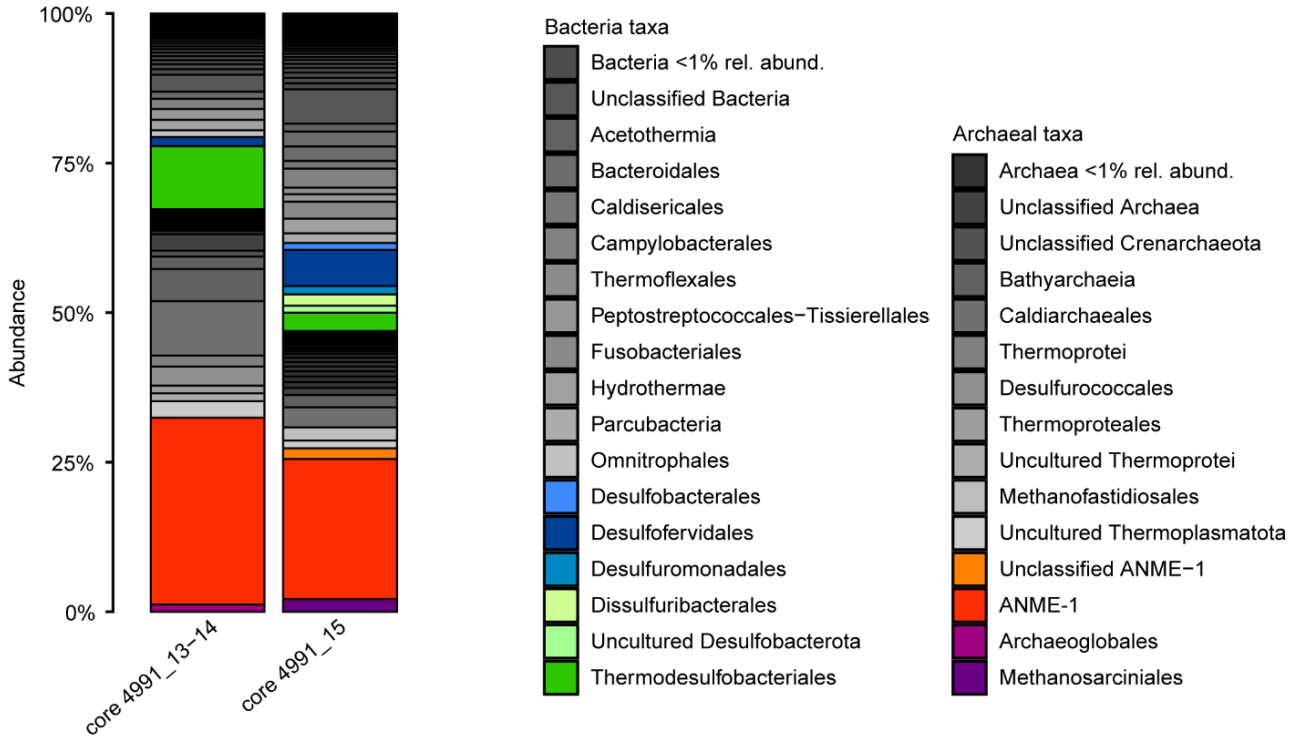

Supplementary Figure 2. 16S rRNA community composition of original sediments. Community composition of original sediments based on 16S rRNA gene read. fragments recruited from metagenomes. Data from two sediment core metagenomes are shown (core 4991_13-14 and core 4991_15). The 16S rRNA gene reads were extracted, mapped and classified with phyloFlash (Gruber-Vodicka et al., 2020). Bacterial sulfate reducers of the Desulfobacterota phylum and the archaeal phylum Halobacterota are highlighted in colours. Thermodesulfobacteria were found in both sediment cores. Unclassified ANME-1

(ANME-1c) were only found in one core with relative abundances over 1%. The ANME-1c and *Thermodesulfobacteria* 16S rRNA sequences reconstructed from sediment core metagenomes are also shown in the phylogenetic tree in Supplementary Figure 4 and Supplementary Figure 6, respectively.

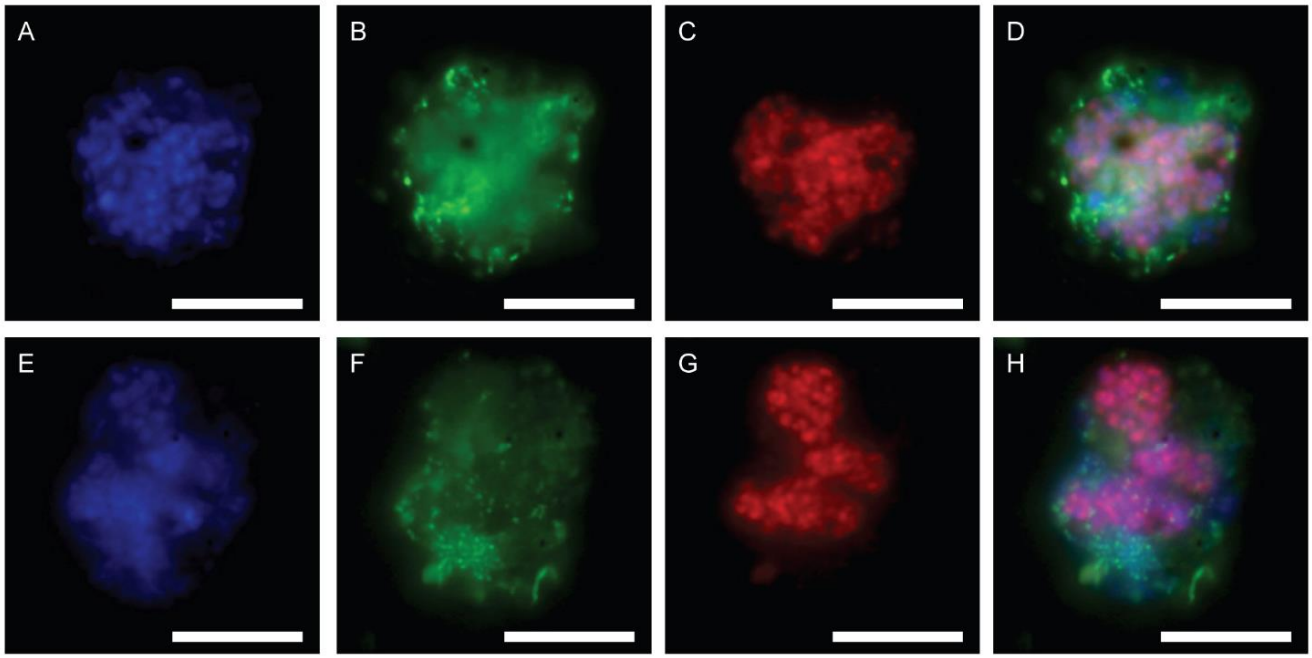

Supplementary Figure 3. CARD-FISH micrographs of the AOM culture at 70°C. Micrographs of two different aggregates of ANME-1c and *Ca.* Thermodesulfobacterium torris. A, E: DAPI staining; B, F: general bacterial probe mix (EUB338 I-III): C, G: ANME-1c specific probe (ANME-1-389); D, H: merged images of DAPI, EUB338 and ANME-1-389. Scale bar: 10 µm.

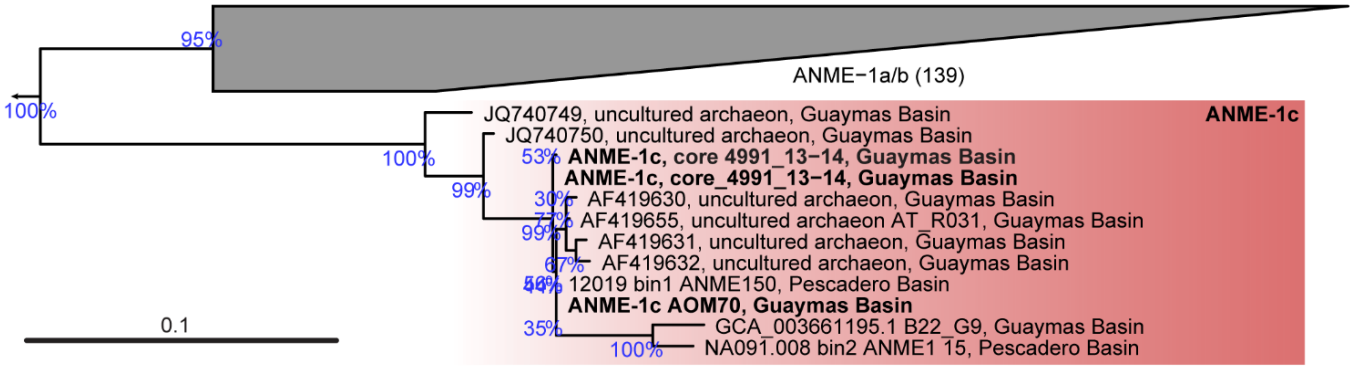

Supplementary Figure 4. 16S rRNA phylogeny of ANME-1c. Maximum likelihood tree of selected ANME-1 16S rRNA gene sequences from SILVA release 138.1 and reference NCBI genomes. *Methanonatronarchaea* sequences served as outgroup (not shown). Blue numbers at branching points shown support values based on 1000 bootstraps. ANME-1c 16S rRNA genes (red shading) form a basal clade to ANME-1a/b. The 16S rRNA gene sequences of ANME-1c from AOM70 culture and sediment samples appear in bold.

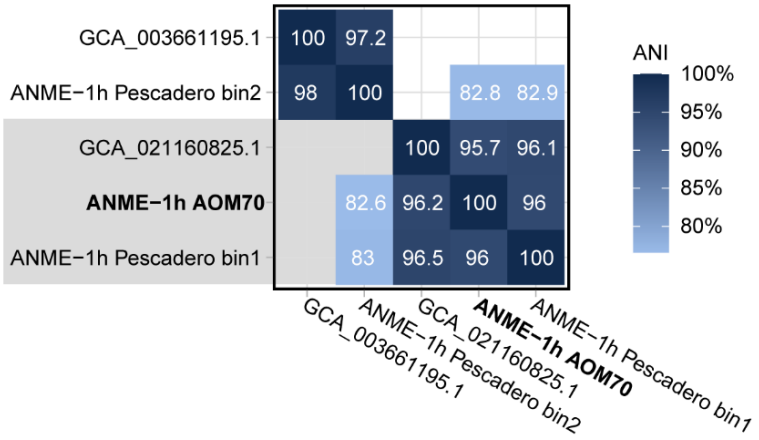

Supplementary Figure 5. Average nucleotide identity of ANME-1c genomes. The ANME-1c clade includes five MAGs distributed in 2 species (>95% ANI, grey shading). ANME-1c from AOM70 enrichment (this study) belongs to the same species as another MAG from the Guaymas Basin.

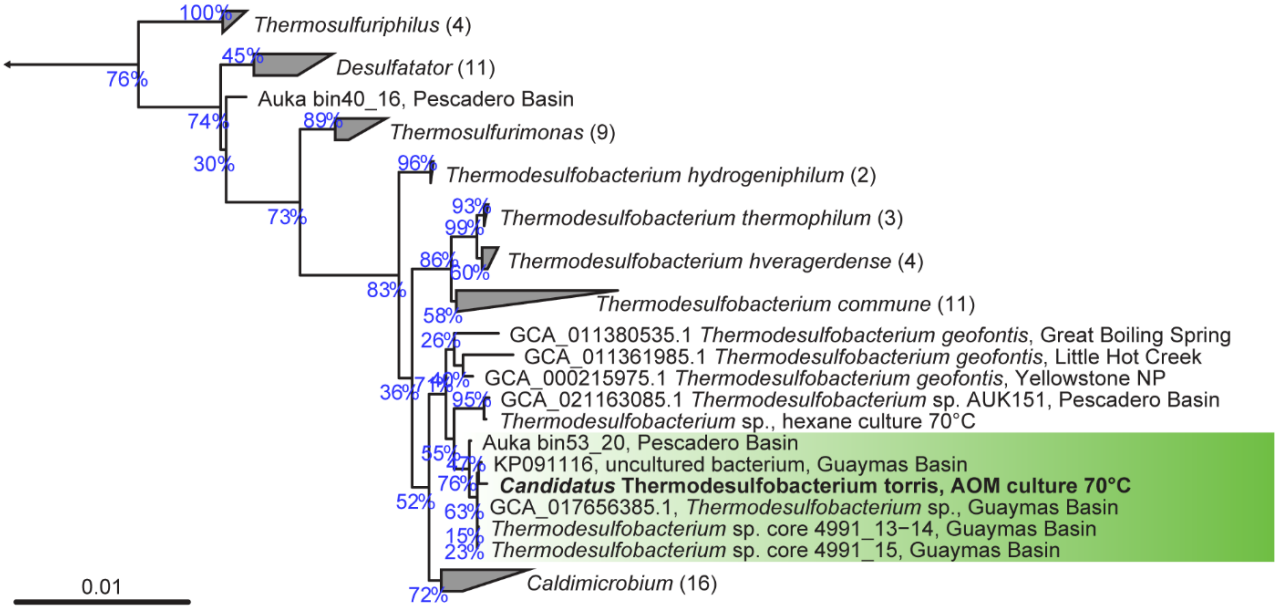

Supplementary Figure 6. 16S rRNA gene phylogeny of *Thermodesulfobacteria*. Maximum likelihood tree of selected *Thermodesulfobacteria* 16S rRNA gene sequences from SILVA 138.1 and reference NCBI genomes. *Ca.* Desulfofervidus sequences served as outgroup (not shown). Blue numbers at branching points shown support values based on 1000 bootstraps. The 16S rRNA gene sequences of *Thermodesulfobacteria* from AOM70 culture and sediment samples appear in bold. The *Ca.* Thermodesulfobacterium torris clade (green shading) contains sequences with similarities >99%. *Ca.* T. torris 16S rRNA is 97% identical to the closest cultured representative, *Thermodesulfobacterium geofontis*.

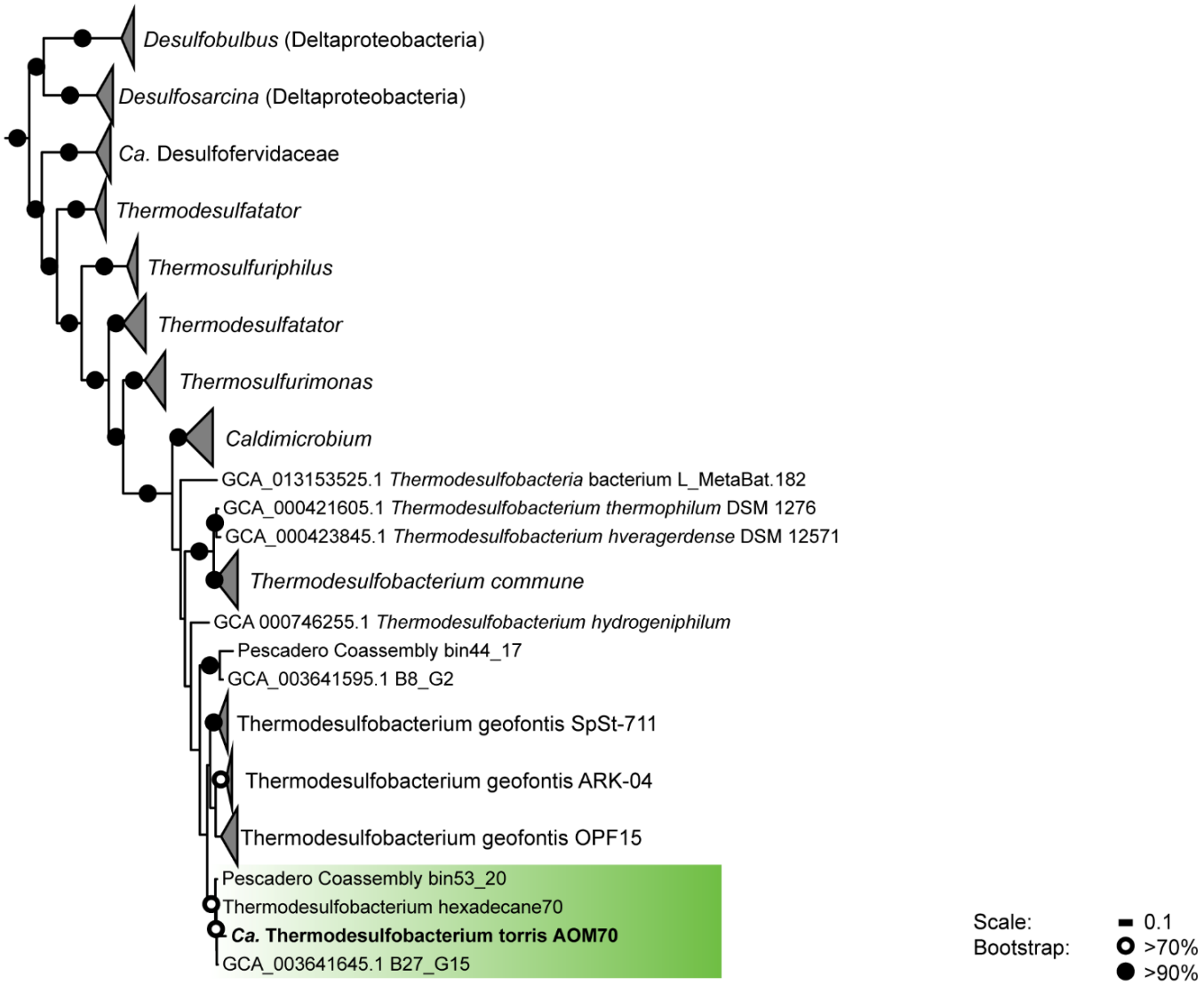

Supplementary Figure 7. Phylogenomic tree of *Thermodesulfobacteria*. Maximum likelihood tree based on a concatenated alignment of 71 bacterial marker genes (Rinke et al., 2013) (Supplementary Table 2). Bootstrap support is based on 500 iterations.

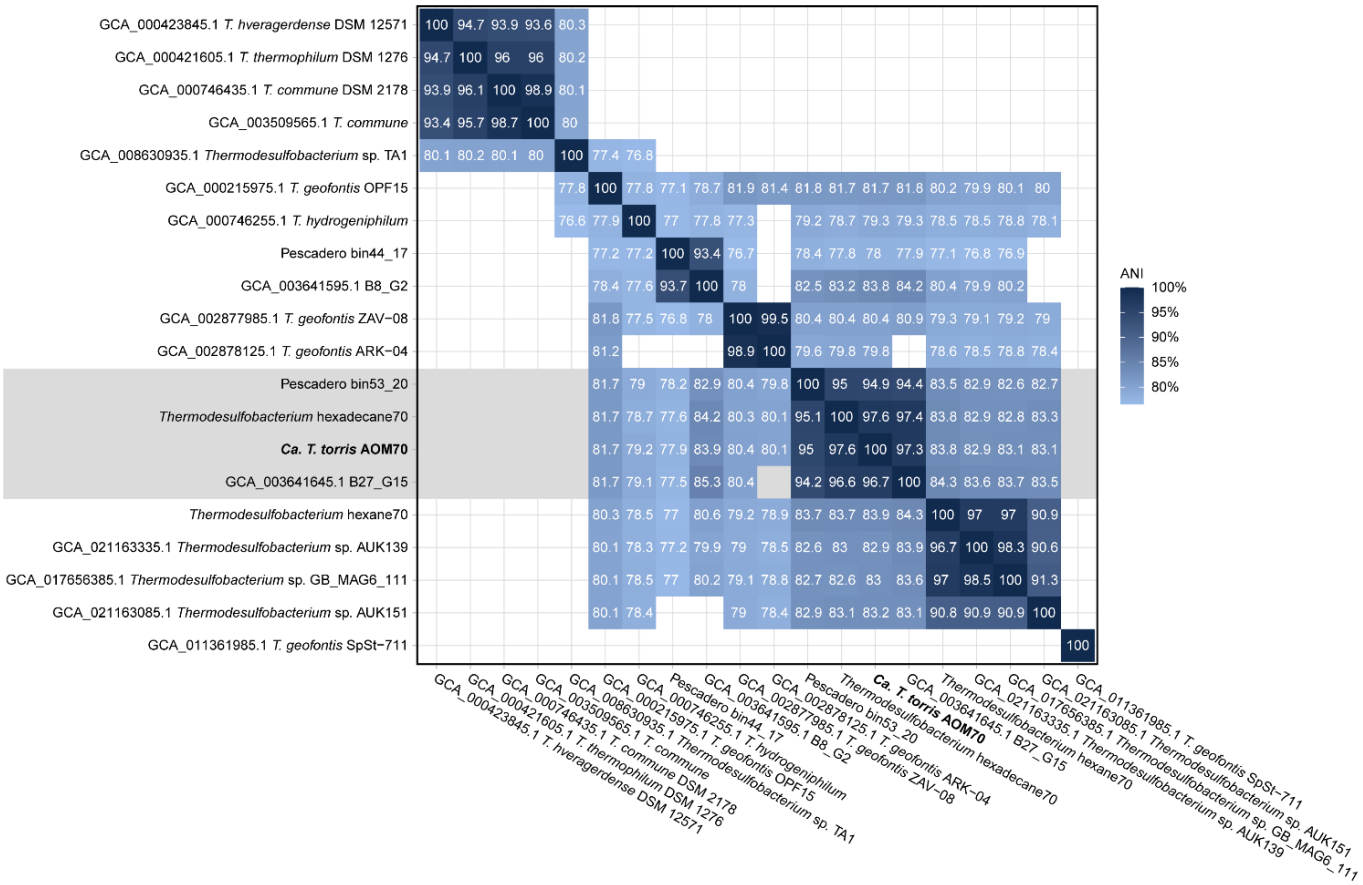

Supplementary Figure 8. Average nucleotide identity of selected *Thermodesulfobacteria* genomes. *Ca.* Thermodesulfobacterium torris (in bold) species cluster (>95% ANI, grey shading) includes 4 genomes: two MAGs originating from Pescadero Basin (Laso-Pérez et al., 2022; Speth et al., 2022), a MAG from a hexadecane-degrading enrichment at 70 °C from Guaymas Basin (Benito Merino, unpublished) and the MAG from the AOM70 enrichment from Guaymas Basin (this study).

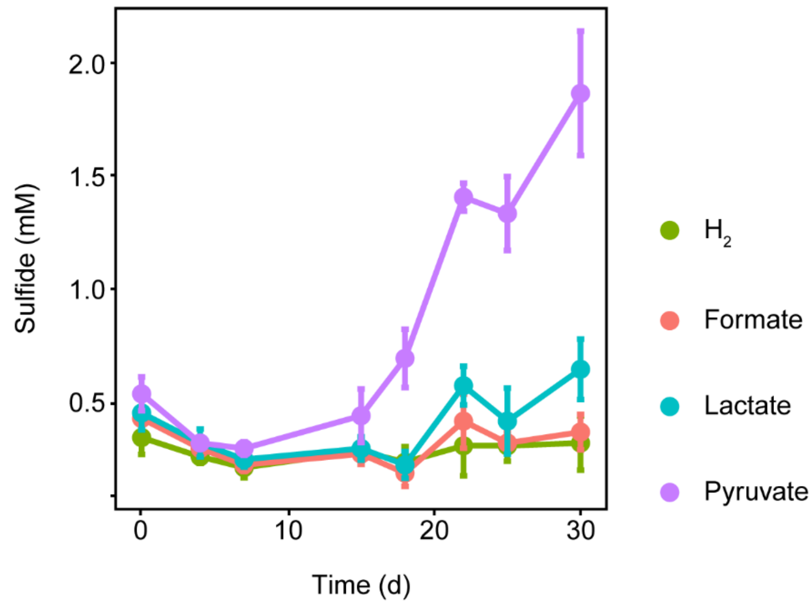

Supplementary Figure 9. Sulfide production in incubations with substrates for *Thermodesulfobacteria*. AOM70 culture aliquots were incubated with formate (10 mM), lactate (10 mM), pyruvate (10 mM) or hydrogen (2 atm H_2:CO_2 20:80 headspace). Substantial substrate-dependent sulfide oxidation was only observed in incubations with pyruvate after 15 days, most likely caused by ancillary heterotrophic microorganisms and not by *Thermodesulfobacteria*.

Supplementary Figure 10. Alignment of *Ca*. Thermodesulfobacterium torris and partner sulfate-reducing bacteria multiheme cytochromes likely involved in interspecies electron transfer. *Ca.* T. torris cytochromes: 6237 (locus tag MW689_000279, extracellular, 5 heme), 6222 (locus tag MW689_000264, unknown location, 7 heme), 6225 (locus tag MW689_000267, unknown location, 5 heme). *Ca*. D. auxilii cytochrome: AMM39976.1 (locus tag HS1_000170). Seep-SRB2 (E20 culture) cytochrome: PXF57827.1 (locus tag C4B58_08455). Seep-SRB2 (G37 culture) cytochrome: PXF54082.1 (locus tag: C4B57_08635). Putative heme-binding motifs (CxxCH) highlighted in red have conserved positions within the alignment.

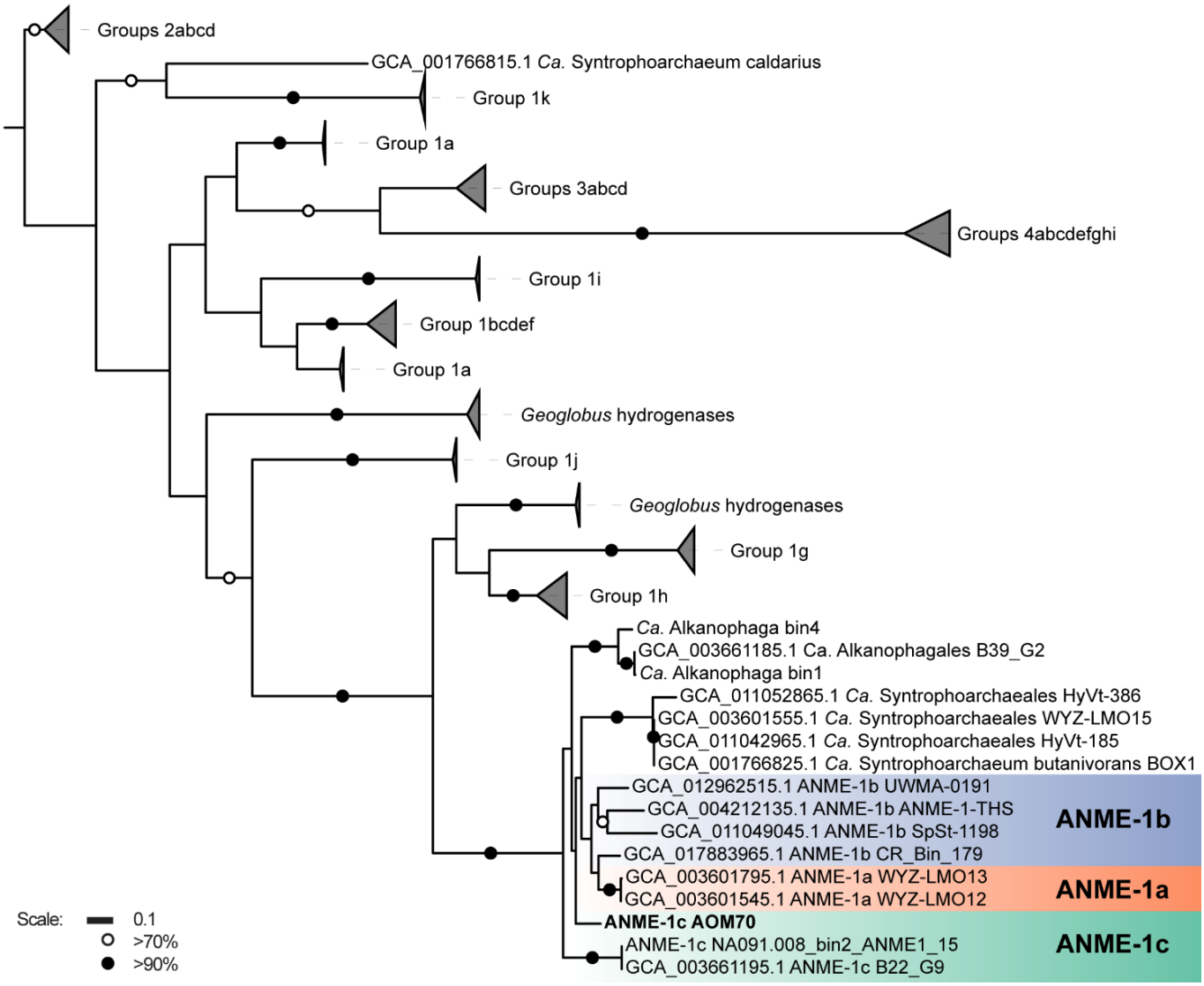

Supplementary Figure 11. NiFe hydrogenase tree including ANME-1 hydrogenases. All ANME-1 and related Syntrophoarchaeales and Alkanophagales hydrogenases form a cluster at the base of groups 1g and 1h NiFe hydrogenases. The low bootstrap support (>70%) explains the spread of the hydrogenases of the ANME-1c.

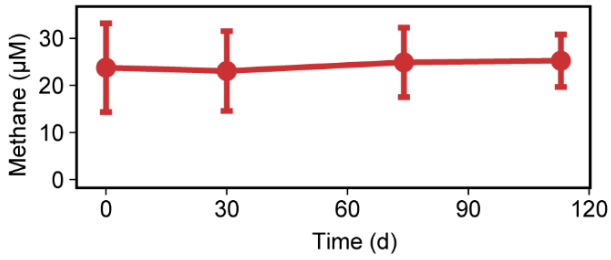

Supplementary Figure 12. The AOM70 enrichment does not produce methane under methanogenesis conditions. Triplicate aliquots of AOM70 cultures were transferred to sulfate-free medium with an H_2/CO_2 headspace. We did not observe methane formation over time. The ~24 µM methane in the headspace was residual methane from the original AOM70 culture.

Supplementary Table 1. Abundance and length distribution of PacBio metagenomic long reads.

Read length	Abundance	Total length (bp)
>100 bp	15,363	143,242,211
>250 bp	15,154	143,199,554
>500 bp	14,335	142,905,803
>1 Kbp	13,602	142,378,411
>2.5 Kbp	11,677	139,017,257
>5 Kbp	9,104	129,533,143
>10 Kbp	5,899	106,112,415
>25 Kbp	817	24,768,328
>50 Kbp	4	204,380

Supplementary Table 2. CARD-FISH probes used in this study.

Probe	Target group	[FA]	Probe sequence (5' to 3')	Reference	Hybridization
Arch915	Most archaea	35%	GTG CTC CCC CGC CAA TTC CT	(Amann et al., 1990)	Hybridized with ANME-1c.
EUB338 I-III	Most bacteria	35%	I: GCT GCC TCC CGT AGG AGT II: GCA GCC ACC CGT AGG TGT III: GCT GCC ACC CGT AGG TGT	(Daims et al., 1999)	Hybridized with SRB.
ANME-1-350	ANME-1	40%	AGT TTT CGC GCC TGA TGC	(Boetius et al., 2000)	Did not hybridize with ANME-1c.
ANME-1-260	ANME-1c	30%	GGC TTG TCG GTC CGT TAA	This study.	Hybridized with ANME-1c.
ANME-1-389	ANME-1c	40%	CAC TCA GCG TCC CCT CAT	This study.	Hybridized with ANME-1c.
Tds201	Thermodesulfo-bacteria	-	GCT TGC TAT GCA GAG GCC	This study.	No hybridization
Tds725	Thermodesulfo-bacteria	-	CCA GCT GGC CGG CTT CCC	This study.	No hybridization
Tds991	Thermodesulfo-bacteria	-	ACA ACC CTG GCA TGT CAA	This study.	No hybridization

Supplementary Table 3. Genomes and conserved marker genes used for archaeal/bacterial phylogenomic tree calculation.

Supplementary Table 4. Annotation and metatranscriptomic expression of main pathways of ANME-1c and *Ca. Thermodesulfobacterium torris* discussed in the main text.

Supplementary Table 5. Reference NiFe-hydrogenases accession numbers used for hydrogenase phylogenetic tree calculation.

References

Adams, M. M., Hoarfrost, A. L., Bose, A., Joye, S. B., and Girguis, P. R. (2013). Anaerobic oxidation of short-chain alkanes in hydrothermal sediments: potential influences on sulfur cycling and microbial diversity. *Front. Microbiol.* 4, 110. doi: 10.3389/fmicb.2013.00110.

Adhikari, R. Y., Malvankar, N. S., Tuominen, M. T., and Lovley, D. R. (2016). Conductivity of individual *Geobacter* pili. *RSC Adv.* 6, 8354–8357. doi: 10.1039/C5RA28092C.

Albers, S. V., and Jarrell, K. F. (2015). The archaellum: how Archaea swim. *Front. Microbiol.* 6, 1–12. doi: 10.3389/FMICB.2015.00023.

Altschul, S. F., Gish, W., Miller, W., Myers, E. W., and Lipman, D. J. (1990). Basic local alignment search tool. *J. Mol. Biol.* 215, 403–410. doi: 10.1016/S0022-2836(05)80360-2.

Amann, R. I., Krumholz, L., and Stahl, D. A. (1990). Fluorescent-oligonucleotide probing of whole cells for determinative, phylogenetic, and environmental studies in microbiology. *J. Bacteriol.* 172, 762. doi: 10.1128/JB.172.2.762-770.1990.

Bengtsson-Palme, J., Hartmann, M., Eriksson, K. M., Pal, C., Thorell, K., Larsson, D. G. J., et al. (2015). metaxa2: improved identification and taxonomic classification of small and large subunit rRNA in metagenomic data. *Mol. Ecol. Resour.* 15, 1403–1414. doi: 10.1111/1755-0998.12399.

Beulig, F., Schubert, F., Adhikari, R. R., Glombitza, C., Heuer, V. B., Hinrichs, K.-U., et al. (2022). Rapid metabolism fosters microbial survival in the deep, hot subseafloor biosphere. *Nat. Commun. 2022 131* 13, 1–9. doi: 10.1038/s41467-021-27802-7.

Biddle, J. F., Cardman, Z., Mendlovitz, H., Albert, D. B., Lloyd, K. G., Boetius, A., et al. (2012). Anaerobic oxidation of methane at different temperature regimes in Guaymas Basin hydrothermal sediments. *ISME J.* 6, 1018–1031. doi: 10.1038/ismej.2011.164.

Boetius, A., and Knittel, K. (2010). "Habitats of Anaerobic Methane Oxidizers," in *Handbook of Hydrocarbon and Lipid Microbiology*, ed. K. N. Timmis (Berlin, Heidelberg: Springer Berlin Heidelberg), 2193–2202. doi: 10.1007/978-3-540-77587-4_159.

Boetius, A., Ravenschlag, K., Schubert, C. J., Rickert[2], D., Widdel, F., Gieseke, A., et al. (2000). A marine microbial consortium apparently mediating anaerobic oxidation of methane. *Nature* 407, 623–626.

Borrel, G., Adam, P. S., McKay, L. J., Chen, L.-X., Sierra-García, I. N., Sieber, C. M. K., et al. (2019). Wide diversity of methane and short-chain alkane metabolisms in uncultured archaea. *Nat. Microbiol.*, 1. doi: 10.1038/s41564-019-0363-3.

Brock, T. D., Brock, K. M., Belly, R. T., and Weiss, R. L. (1972). *Sulfolobus*: a new genus of sulfur-oxidizing bacteria living at low pH and high temperature. *Arch. für Mikrobiol. 1972 841* 84, 54–68. doi: 10.1007/BF00408082.

Chadwick, G. L., Skennerton, C. T., Laso-Pérez, R., Leu, A. O., Speth, D. R., Yu, H., et al. (2022). Comparative genomics reveals electron transfer and syntrophic mechanisms differentiating methanotrophic and methanogenic archaea. *PLOS Biol.*, 1–70. doi: 10.1371/journal.pbio.3001508.

Chernomor, O., Von Haeseler, A., and Minh, B. Q. (2016). Terrace aware data structure for phylogenomic inference from supermatrices. *Syst. Biol.* 65, 997–1008. doi: 10.1093/SYSBIO/SYW037.

Cord-Ruwisch, R. (1985). A quick method for the determination of dissolved and precipitated sulfides in cultures of sulfate-reducing bacteria. *J. Microbiol. Methods* 4, 33–36.

Daims, H., Brühl, A., Amann, R., Schleifer, K.-H., and Wagner, M. (1999). The domain-specific probe EUB338 is insufficient for the detection of all Bacteria: Development and evaluation of a more comprehensive probe set. *Syst. Appl. Microbiol.* 22, 434–444. doi: 10.1016/S0723-2020(99)80053-8.

Darling, A. E., Jospin, G., Lowe, E., Matsen, F. A., Bik, H. M., and Eisen, J. A. (2014). PhyloSift: phylogenetic analysis of genomes and metagenomes. *PeerJ* 2, e243. doi: 10.7717/peerj.243.

Dekas, A. E., Connon, S. A., Chadwick, G. L., Trembath-Reichert, E., and Orphan, V. J. (2015). Activity and interactions of methane seep microorganisms assessed by parallel transcription and FISH-

NanoSIMS analyses. *ISME J. 2016 103* 10, 678–692. doi: 10.1038/ismej.2015.145.

Dekas, A. E., Poretsky, R. S., and Orphan, V. J. (2009). Deep-sea archaea fix and share nitrogen in methane-consuming microbial consortia. *Science (80-.).* 326, 422–426. doi: 10.1126/science.1178223/.

Dombrowski, N., Seitz, K. W., Teske, A. P., and Baker, B. J. (2017). Genomic insights into potential interdependencies in microbial hydrocarbon and nutrient cycling in hydrothermal sediments. *Microbiome* 5, 106. doi: 10.1186/s40168-017-0322-2.

Dombrowski, N., Teske, A. P., and Baker, B. J. (2018). Expansive microbial metabolic versatility and biodiversity in dynamic Guaymas Basin hydrothermal sediments. *Nat. Commun.* 9, 4999. doi: 10.1038/s41467-018-07418-0.

Dowell, F., Cardman, Z., Dasarathy, S., Kellermann, M. Y., Lipp, J. S., Ruff, S. E., et al. (2016). Microbial communities in methane- and short chain alkane-rich hydrothermal sediments of Guaymas Basin. *Front. Microbiol.* 7, 17. doi: 10.3389/fmicb.2016.00017.

Ducker, G. S., and Rabinowitz, J. D. (2017). One-carbon metabolism in health and disease. *Cell Metab.* 25, 27. doi: 10.1016/J.CMET.2016.08.009.

Edgar, R. C. (2004). MUSCLE: A multiple sequence alignment method with reduced time and space complexity. *BMC Bioinformatics* 5, 1–19. doi: 10.1186/1471-2105-5-113/FIGURES/16.

Eren, A. M., Esen, Ö. C., Quince, C., Vineis, J. H., Morrison, H. G., Sogin, M. L., et al. (2015). Anvi'o: an advanced analysis and visualization platform for 'omics data. *PeerJ* 3, e1319. doi: 10.7717/peerj.1319.

Eren, A. M., Kiefl, E., Shaiber, A., Veseli, I., Miller, S. E., Schechter, M. S., et al. (2020). Community-led, integrated, reproducible multi-omics with anvi'o. *Nat. Microbiol. 2020 61* 6, 3–6. doi: 10.1038/s41564-020-00834-3.

Ermler, U., Grabarse, W., Shima, S., Goubeaud, M., and Thauer, R. K. (1997). Crystal structure of methyl-coenzyme M reductase: The key enzyme of biological methane formation. *Science (80-.).* 278, 1457–1462. doi: 10.1126/science.278.5342.1457.

Fischer, F., Zillig, W., Stetter, K. O., and Schreiber, G. (1983). Chemolithoautotrophic metabolism of anaerobic extremely thermophilic archaebacteria. *Nat. 1983 3015900* 301, 511–513. doi: 10.1038/301511a0.

Friedmann, H. C., Klein, A., and Thauer, R. K. (1990). Structure and function of the nickel porphinoid, coenzyme F430 and of its enzyme, methyl coenzyme M reductase. *FEMS Microbiol. Rev.* 7, 339–348. doi: 10.1111/J.1574-6968.1990.TB04934.X.

Galperin, M. Y., Makarova, K. S., Wolf, Y. I., and Koonin, E. V. (2015). Expanded microbial genome coverage and improved protein family annotation in the COG database. *Nucleic Acids Res.* 43, D261–D269. doi: 10.1093/NAR/GKU1223.

Gruber-Vodicka, H. R., Seah, B. K. B., and Pruesse, E. (2020). phyloFlash: Rapid small-subunit rRNA profiling and targeted assembly from metagenomes. *mSystems* 5. doi: 10.1128/mSystems.00920-20.

Gu, Y., Srikanth, V., Salazar-Morales, A. I., Jain, R., O'Brien, J. P., Yi, S. M., et al. (2021). Structure of *Geobacter* pili reveals secretory rather than nanowire behaviour. *Nat. 2021 5977876* 597, 430–434. doi: 10.1038/s41586-021-03857-w.

Haft, D. H., Loftus, B. J., Richardson, D. L., Yang, F., Eisen, J. A., Paulsen, I. T., et al. (2001). TIGRFAMs: a protein family resource for the functional identification of proteins. *Nucleic Acids Res.* 29, 41–43. doi: 10.1093/NAR/29.1.41.

Hahn, C. J., Laso-Pérez, R., Vulcano, F., Vaziourakis, K.-M., Stokke, R., Steen, I. H., et al. (2020). "*Candidatus* Ethanoperedens," a thermophilic genus of archaea mediating the anaerobic oxidation of ethane. *MBio* 11, 1–18. doi: 10.1128/mBio.00600-20.

Hallam, S. J., Putnam, N., Preston, C. M., Detter, J. C., Rokhsar, D., Richardson, P. M., et al. (2004). Reverse Methanogenesis: Testing the Hypothesis with Environmental Genomics. *Science (80-.).* 305, 1457–1462. doi: 10.1126/science.1100025.

Hamilton-Brehm, S. D., Gibson, R. A., Green, S. J., Hopmans, E. C., Schouten, S., van der Meer, M. T. J., et al. (2013). *Thermodesulfobacterium geofontis* sp. nov., a hyperthermophilic, sulfate-reducing bacterium isolated from Obsidian Pool, Yellowstone National Park. *Extremophiles* 17, 251–263. doi: 10.1007/S00792-013-0512-1.

Hao, L., McIlroy, S. J., Kirkegaard, R. H., Karst, S. M., Fernando, W. E. Y., Aslan, H., et al. (2018). Novel prosthecate bacteria from the candidate phylum Acetothermia. *ISME J. 2018 129* 12, 2225–2237. doi: 10.1038/s41396-018-0187-9.

Haroon, M. F., Hu, S., Shi, Y., Imelfort, M., Keller, J., Hugenholtz, P., et al. (2013). Anaerobic oxidation of methane coupled to nitrate reduction in a novel archaeal lineage. *Nat. 2013 5007464* 500, 567–570. doi: 10.1038/nature12375.

Hinrichs, K.-U., and Boetius, A. (2002). "The Anaerobic Oxidation of Methane: New Insights in Microbial Ecology and Biogeochemistry," in *Ocean Margin Systems* (Berlin, Heidelberg: Springer Berlin Heidelberg), 457–477. doi: 10.1007/978-3-662-05127-6_28.

Hoehler, T. M., Alperin, M. J., Albert, D. B., and Martens, C. S. (1994). Field and laboratory studies of methane oxidation in an anoxic marine sediment: Evidence for a methanogen-sulfate reducer consortium. *Global Biogeochem. Cycles* 8, 451–463. doi: 10.1029/94GB01800.

Holler, T., Wegener, G., Knittel, K., Boetius, A., Brunner, B., Kuypers, M. M. M., et al. (2009). Substantial $^{13}C/^{12}C$ and D/H fractionation during anaerobic oxidation of methane by marine consortia enriched *in vitro*. *Environ. Microbiol. Rep.* 1, 370–376. doi: 10.1111/J.1758-2229.2009.00074.X.

Holler, T., Widdel, F., Knittel, K., Amann, R., Kellermann, M. Y., Hinrichs, K.-U., et al. (2011). Thermophilic anaerobic oxidation of methane by marine microbial consortia. *ISME J.* 5, 1946–1956. doi: 10.1038/ismej.2011.77.

Huber, H., Burggraf, S., Mayer, T., Wyschkony, I., Rachel, R., and Stetter, K. O. (2000). *Ignicoccus* gen. nov., a novel genus of hyperthermophilic, chemolithoautotrophic Archaea, represented by two new species, *Ignicoccus islandicus* sp. nov and *Ignicoccus pacificus* sp. nov. *Int. J. Syst. Evol. Microbiol.* 50 Pt 6, 2093–2100. doi: 10.1099/00207713-50-6-2093.

Hyatt, D., Chen, G. L., LoCascio, P. F., Land, M. L., Larimer, F. W., and Hauser, L. J. (2010). Prodigal: prokaryotic gene recognition and translation initiation site identification. *BMC Bioinformatics*, 1–11. doi: 10.1186/1471-2105-11-119.

Inagaki, F., Kuypers, M. M. M., Tsunogai, U., Ishibashi, J. I., Nakamura, K. I., Treude, T., et al. (2006). Microbial community in a sediment-hosted CO_2 lake of the southern Okinawa Trough hydrothermal system. *Proc. Natl. Acad. Sci. U. S. A.* 103, 14164–14169. doi: 10.1073/PNAS.0606083103.

Ishii, K., Mußmann, M., MacGregor, B. J., and Amann, R. (2004). An improved fluorescence *in situ* hybridization protocol for the identification of bacteria and archaea in marine sediments. *FEMS Microbiol. Ecol.* 50, 203–213. doi: 10.1016/J.FEMSEC.2004.06.015.

Jain, C., Rodriguez-R, L. M., Phillippy, A. M., Konstantinidis, K. T., and Aluru, S. (2018). High throughput ANI analysis of 90K prokaryotic genomes reveals clear species boundaries. *Nat. Commun. 2018 91* 9, 1–8. doi: 10.1038/s41467-018-07641-9.

Jeanthon, C., L'Haridon, S., Cueff, V., Banta, A., Reysenbach, A.-L., and Prieur, D. (2002). *Thermodesulfobacterium hydrogeniphilum* sp. nov., a thermophilic, chemolithoautotrophic, sulfate-reducing bacterium isolated from a deep-sea hydrothermal vent at Guaymas Basin, and emendation of the genus *Thermodesulfobacterium*. *Int. J. Syst. Evol. Microbiol.* 52, 765–772. doi: 10.1099/00207713-52-3-765.

Kallmeyer, J., and Boetius, A. (2004). Effects of temperature and pressure on sulfate reduction and anaerobic oxidation of methane in hydrothermal sediments of Guaymas Basin. *Appl. Environ. Microbiol.* 70, 1231–1233. doi: 10.1128/AEM.70.2.1231-1233.2004.

Kalyaanamoorthy, S., Minh, B. Q., Wong, T. K. F., Von Haeseler, A., and Jermiin, L. S. (2017). ModelFinder: fast model selection for accurate phylogenetic estimates. *Nat. Methods 2017 146* 14, 587–589. doi: 10.1038/nmeth.4285.

Kanehisa, M., and Goto, S. (2000). KEGG: Kyoto encyclopedia of genes and genomes. *Nucleic Acids Res.* 28, 27–30. doi: 10.1093/NAR/28.1.27.

Kellermann, M. Y., Wegener, G., Elvert, M., Yoshinaga, M. Y., Lin, Y.-S., Holler, T., et al. (2012). Autotrophy as a predominant mode of carbon fixation in anaerobic methane-oxidizing microbial communities. *Proc. Natl. Acad. Sci.* 109, 19321–19326. doi: 10.1073/pnas.1208795109.

Kevorkian, R. T., Callahan, S., Winstead, R., and Lloyd, K. G. (2021). ANME-1 archaea may drive methane accumulation and removal in estuarine sediments. *Environ. Microbiol. Rep.* 13, 185–194. doi: 10.1111/1758-2229.12926.

Knittel, K., Boetius, A., Lemke, A., Eilers, H., Lochte, K., Pfannkuche, O., et al. (2003). Activity, distribution, and diversity of sulfate reducers and other bacteria in sediments above gas hydrate (Cascadia margin, Oregon). *Geomicrobiol. J.* 20, 269–294. doi: 10.1080/01490450303896.

Knittel, K., Lösekann, T., Boetius, A., Kort, R., and Amann, R. (2005). Diversity and distribution of methanotrophic archaea at cold seeps. *Appl. Environ. Microbiol.* 71, 467–479. doi: 10.1128/AEM.71.1.467-479.2005.

Kolmogorov, M., Bickhart, D. M., Behsaz, B., Gurevich, A., Rayko, M., Shin, S. B., et al. (2020). metaFlye: scalable long-read metagenome assembly using repeat graphs. *Nat. Methods* 17, 1103–1110. doi: 10.1038/s41592-020-00971-x.

Krukenberg, V., Harding, K., Richter, M., Glöckner, F. O., Gruber-Vodicka, H. R., Adam, B., et al. (2016). *Candidatus* Desulfofervidus auxilii, a hydrogenotrophic sulfate-reducing bacterium involved in the thermophilic anaerobic oxidation of methane. *Environ. Microbiol.* 18, 3073–3091. doi: 10.1111/1462-2920.13283.

Krukenberg, V., Riedel, D., Gruber-Vodicka, H. R., Buttigieg, P. L., Tegetmeyer, H. E., Boetius, A., et al. (2018). Gene expression and ultrastructure of meso- and thermophilic methanotrophic consortia. *Environ. Microbiol.* 20, 1651–1666. doi: 10.1111/1462-2920.14077.

Lagesen, K., Hallin, P., Rødland, E. A., Stærfeldt, H. H., Rognes, T., and Ussery, D. W. (2007). RNAmmer: consistent and rapid annotation of ribosomal RNA genes. *Nucleic Acids Res.* 35, 3100. doi: 10.1093/NAR/GKM160.

Lagostina, L., Frandsen, S., MacGregor, B. J., Glombitza, C., Deng, L., Fiskal, A., et al. (2021). Interactions between temperature and energy supply drive microbial communities in hydrothermal sediment. *Commun. Biol. 2021 41* 4, 1–14. doi: 10.1038/s42003-021-02507-1.

Langmead, B., and Salzberg, S. L. (2012). Fast gapped-read alignment with Bowtie 2. *Nat. Methods 2012 94* 9, 357–359. doi: 10.1038/nmeth.1923.

Lanoil, B. D., Sassen, R., La Duc, M. T., Sweet, S. T., and Nealson, K. H. (2001). Bacteria and Archaea physically associated with Gulf of Mexico gas hydrates. *Appl. Environ. Microbiol.* 67, 5143–5153. doi: 10.1128/AEM.67.11.5143-5153.2001.

Laska, S., Lottspeich, F., and Kletzin, A. (2003). Membrane-bound hydrogenase and sulfur reductase of the hyperthermophilic and acidophilic archaeon *Acidianus ambivalens*. *Microbiology* 149, 2357–2371. doi: 10.1099/MIC.0.26455-0/CITE/REFWORKS.

Laso-Pérez, R., Krukenberg, V., Musat, F., and Wegener, G. (2018). Establishing anaerobic hydrocarbon-degrading enrichment cultures of microorganisms under strictly anoxic conditions. *Nat. Publ. Gr.* 13, 1310–1330. doi: 10.1038/nprot.2018.030.

Laso-Pérez, R., Wegener, G., Knittel, K., Widdel, F., Harding, K. J., Krukenberg, V., et al. (2016). Thermophilic archaea activate butane via alkyl-coenzyme M formation. *Nature* 539, 396–401. doi: 10.1038/nature20152.

Laso-Pérez, R., Wu, F., Crémière, A., Speth, D. R., Magyar, J. S., Krupovic, M., et al. (2022). Evolutionary diversification of methanotrophic *Ca.* Methanophagales (ANME-1) and their expansive virome. *bioRxiv*, 2022.07.04.498658. doi: 10.1101/2022.07.04.498658.

Letunic, I., and Bork, P. (2011). Interactive Tree of Life v2: Online annotation and display of phylogenetic trees made easy. *Nucleic Acids Res.* doi: 10.1093/nar/gkr201.

Li, H. (2018). Minimap2: pairwise alignment for nucleotide sequences. *Bioinformatics* 34, 3094–3100. doi: 10.1093/BIOINFORMATICS/BTY191.

Lloyd, K. G., Alperin, M. J., and Teske, A. (2011). Environmental evidence for net methane production and oxidation in putative ANaerobic MEthanotrophic (ANME) archaea. *Environ. Microbiol.* 13, 2548–2564. doi: 10.1111/j.1462-2920.2011.02526.x.

Lösekann, T., Knittel, K., Nadalig, T., Fuchs, B., Niemann, H., Boetius, A., et al. (2007). Diversity and abundance of aerobic and anaerobic methane oxidizers at the Haakon Mosby Mud Volcano, Barents Sea. *Appl. Environ. Microbiol.* 73, 3348–3362. doi: 10.1128/AEM.00016-07.

Ludwig, W., Strunk, O., Westram, R., Richter, L., Meier, H., Yadhukumar, A., et al. (2004). ARB: a software environment for sequence data. *Nucleic Acids Res.* 32, 1363–1371. doi: 10.1093/NAR/GKH293.

Malvankar, N. S., Vargas, M., Nevin, K. P., Franks, A. E., Leang, C., Kim, B. C., et al. (2011). Tunable metallic-like conductivity in microbial nanowire networks. *Nat. Nanotechnol. 2011 69* 6, 573–579. doi: 10.1038/nnano.2011.119.

McGlynn, S. E., Chadwick, G. L., Kempes, C. P., and Orphan, V. J. (2015). Single cell activity reveals direct electron transfer in methanotrophic consortia. *Nature*. doi: 10.1038/nature15512.

McKay, L. J. (2014). Microbial ecology of a manmade oil spill in the Gulf of Mexico and a natural, hydrothermal oil seep in the Gulf of California. Available at: http://search.proquest.com/docview/1613182914?accountid=14468%5Cnhttp://wx7cf7zp2h.search.serialssolutions.com/?ctx_ver=Z39.88-2004&ctx_enc=info:ofi/enc:UTF-8&rfr_id=info:sid/ProQuest+Dissertations+&+Theses+Global&rft_val_fmt=info:ofi/fmt:kev:mtx:dissertа.

McKay, L., Klokman, V. W., Mendlovitz, H. P., Larowe, D. E., Hoer, D. R., Albert, D., et al. (2016). Thermal and geochemical influences on microbial biogeography in the hydrothermal sediments of Guaymas Basin, Gulf of California. *Environ. Microbiol. Rep.* 8, 150–161. doi: 10.1111/1758-2229.12365.

Merkel, A. Y., Huber, J. A., Chernyh, N. A., Bonch-Osmolovskaya, E. A., and Lebedinsky, A. V (2013). Detection of putatively thermophilic anaerobic methanotrophs in diffuse hydrothermal vent fluids. doi: 10.1128/AEM.03034-12.

Meyerdierks, A., Kube, M., Kostadinov, I., Teeling, H., Glöckner, F. O., Reinhardt, R., et al. (2010). Metagenome and mRNA expression analyses of anaerobic methanotrophic archaea of the ANME-1 group. *Environ. Microbiol.* 12, 422–439. doi: 10.1111/J.1462-2920.2009.02083.X.

Michaelis, W., Seifert, R., Nauhaus, K., Treude, T., Thiel, V., Blumenberg, M., et al. (2002). Microbial reefs in the Black Sea fueled by anaerobic oxidation of methane. *Science* 297, 1013–1015. doi: 10.1126/SCIENCE.1072502.

Minh, B. Q., Schmidt, H. A., Chernomor, O., Schrempf, D., Woodhams, M. D., Von Haeseler, A., et al. (2020). IQ-TREE 2: new models and efficient methods for phylogenetic inference in the genomic era. *Mol. Biol. Evol.* 37, 1530–1534. doi: 10.1093/MOLBEV/MSAA015.

Mistry, J., Chuguransky, S., Williams, L., Qureshi, M., Salazar, G. A., Sonnhammer, E. L. L., et al. (2021). Pfam: The protein families database in 2021. *Nucleic Acids Res.* 49, D412–D419. doi: 10.1093/NAR/GKAA913.

Moore, S. J., Sowa, S. T., Schuchardt, C., Deery, E., Lawrence, A. D., Ramos, J. V., et al. (2017). Elucidation of the biosynthesis of the methane catalyst coenzyme F430. *Nat. 2017 5437643* 543, 78–82. doi: 10.1038/nature21427.

Moussard, H., L'Haridon, S., Tindall, B. J., Banta, A., Schumann, P., Stackebrandt, E., et al. (2004). *Thermodesulfatator indicus* gen. nov., sp. nov., a novel thermophilic chemolithoautotrophic sulfate-reducing bacterium isolated from the Central Indian Ridge. *Int. J. Syst. Evol. Microbiol.* 54, 227–233. doi: 10.1099/IJS.0.02669-0.

Nauhaus, K., Boetius, A., Krüger, M., and Widdel, F. (2002). *In vitro* demonstration of anaerobic

oxidation of methane coupled to sulphate reduction in sediment from a marine gas hydrate area. *Environ. Microbiol.* 4, 296–305. doi: 10.1046/J.1462-2920.2002.00299.X.

Niemann, H., Elvert, M., Hovland, M., Orcutt, B., Judd, A., Suck, I., et al. (2005). Methane emission and consumption at a North Sea gas seep (Tommeliten area). *Biogeosciences* 2, 335–351. doi: 10.5194/BG-2-335-2005.

Niemann, H., Lösekann, T., De Beer, D., Elvert, M., Nadalig, T., Knittel, K., et al. (2006). Novel microbial communities of the Haakon Mosby mud volcano and their role as a methane sink. *Nat. 2006 4437113* 443, 854–858. doi: 10.1038/nature05227.

Orcutt, B. N., Boetius, A., Lugo, S. K., MacDonald, I. R., Samarkin, V. A., and Joye, S. B. (2004). Life at the edge of methane ice: Microbial cycling of carbon and sulfur in Gulf of Mexico gas hydrates. *Chem. Geol.* 205, 239–251. doi: 10.1016/J.CHEMGEO.2003.12.020.

Orcutt, B., Samarkin, V., Boetius, A., and Joye, S. (2008). On the relationship between methane production and oxidation by anaerobic methanotrophic communities from cold seeps of the Gulf of Mexico. *Environ. Microbiol.* 10, 1108–1117. doi: 10.1111/j.1462-2920.2007.01526.x.

Orphan, V. J., Hinrichs, K.-U., Ussler, W., Paull, C. K., Taylor, L. T., Sylva, S. P., et al. (2001). Comparative analysis of methane-oxidizing archaea and sulfate-reducing bacteria in anoxic marine sediments. *Appl. Environ. Microbiol.* 67, 1922–1934. doi: 10.1128/AEM.67.4.1922-1934.2001.

Orphan, V. J., House, C. H., Hinrichs, K. U., McKeegan, K. D., and DeLong, E. F. (2002). Multiple archaeal groups mediate methane oxidation in anoxic cold seep sediments. *Proc. Natl. Acad. Sci. U. S. A.* 99, 7663–7668. doi: 10.1073/PNAS.072210299/ASSET/06C54137-68B2-457C-8C76-FEA01D3D60DE/ASSETS/GRAPHIC/PQ1122102003.JPEG.

Orphan, V. J., Turk, K. A., Green, A. M., and House, C. H. (2009). Patterns of 15N assimilation and growth of methanotrophic ANME-2 archaea and sulfate-reducing bacteria within structured syntrophic consortia revealed by FISH-SIMS. *Environ. Microbiol.* 11, 1777–1791. doi: 10.1111/J.1462-2920.2009.01903.X.

Parks, D. H., Imelfort, M., Skennerton, C. T., Hugenholtz, P., and Tyson, G. W. (2015). CheckM: Assessing the quality of microbial genomes recovered from isolates, single cells, and metagenomes. *Genome Res.* 25, 1043–1055. doi: 10.1101/gr.186072.114.

Pereira, I. A. C., Ramos, A. R., Grein, F., Marques, M. C., da Silva, S. M., and Venceslau, S. S. (2011). A Comparative Genomic Analysis of Energy Metabolism in Sulfate Reducing Bacteria and Archaea. *Front. Microbiol.* 2, 1–22. doi: 10.3389/fmicb.2011.00069.

Pérez Castro, S., Borton, M. A., Regan, K., Hrabe de Angelis, I., Wrighton, K. C., Teske, A. P., et al. (2021). Degradation of biological macromolecules supports uncultured microbial populations in Guaymas Basin hydrothermal sediments. *ISME J. 2021 1512* 15, 3480–3497. doi: 10.1038/s41396-021-01026-5.

Pernthaler, A., Pernthaler, J., and Amann, R. (2002). Fluorescence in situ hybridization and catalyzed reporter deposition for the identification of marine bacteria. *Appl. Environ. Microbiol.* 68, 3094–3101. doi: 10.1128/AEM.68.6.3094-3101.2002.

Pruesse, E., Peplies, J., and Glöckner, F. O. (2012). SINA: Accurate high-throughput multiple sequence alignment of ribosomal RNA genes. *Bioinformatics* 28, 1823–1829. doi: 10.1093/BIOINFORMATICS/BTS252.

Quast, C., Pruesse, E., Yilmaz, P., Gerken, J., Schweer, T., Yarza, P., et al. (2013). The SILVA ribosomal RNA gene database project: improved data processing and web-based tools. *Nucleic Acids Res.* 41, D590–D596. doi: 10.1093/NAR/GKS1219.

Ramírez, G. A., Mara, P., Sehein, T., Wegener, G., Chambers, C. R., Joye, S. B., et al. (2021). Environmental factors shaping bacterial, archaeal and fungal community structure in hydrothermal sediments of Guaymas Basin, Gulf of California. *PLoS One* 16, e0256321. doi: 10.1371/JOURNAL.PONE.0256321.

Ramos, A. R., Keller, K. L., Wall, J. D., and Cardoso Pereira, I. A. (2012). The membrane QmoABC

complex interacts directly with the dissimilatory adenosine 5′-phosphosulfate reductase in sulfate reducing bacteria. *Front. Microbiol.* 3, 1–10. doi: 10.3389/FMICB.2012.00137.

Reeburgh, W. S. (2007). Oceanic methane biogeochemistry. *Chem. Rev.* 107, 486–513. doi: 10.1021/cr050362v.

Regnier, P., Dale, A. W., Arndt, S., LaRowe, D. E., Mogollón, J., and Van Cappellen, P. (2011). Quantitative analysis of anaerobic oxidation of methane (AOM) in marine sediments: A modeling perspective. *Earth-Science Rev.* 106, 105–130. doi: 10.1016/J.EARSCIREV.2011.01.002.

Reguera, G., McCarthy, K. D., Mehta, T., Nicoll, J. S., Tuominen, M. T., and Lovley, D. R. (2005). Extracellular electron transfer via microbial nanowires. *Nat. 2005 4357045* 435, 1098–1101. doi: 10.1038/nature03661.

Rinke, C., Schwientek, P., Sczyrba, A., Ivanova, N. N., Anderson, I. J., Cheng, J. F., et al. (2013). Insights into the phylogeny and coding potential of microbial dark matter. *Nat. 2013 4997459* 499, 431–437. doi: 10.1038/nature12352.

Roussel, E. G., Bonavita, M. A. C., Querellou, J., Cragg, B. A., Webster, G., Prieur, D., et al. (2008). Extending the sub-sea-floor biosphere. *Science (80-.).* 320, 1046. doi: 10.1126/SCIENCE.1154545.

Rozanova, E., and Khudiakova, A. (1974). Novyĭ bessporovyĭ termofil'nyĭ organizm, vosstanavlivaiushchiĭ sul'faty, *Desulfovibrio thermophilus* nov. sp [A new non-spore forming thermophilic organism, reducing sulfates, *Desulfovibrio thermophilus* nov. sp]. *Mikrobiologiia* 43, 1069–75.

Ruff, S. E., Biddle, J. F., Teske, A. P., Knittel, K., Boetius, A., and Ramette, A. (2015). Global dispersion and local diversification of the methane seep microbiome. *Proc. Natl. Acad. Sci. U. S. A.* 112, 4015–20. doi: 10.1073/pnas.1421865112.

Sánchez, L. B., Galperin, M. Y., and Müller, M. (2000). Acetyl-CoA synthetase from the amitochondriate eukaryote Giardia lamblia belongs to the newly recognized superfamily of acyl-CoA synthetases (Nucleoside diphosphate-forming). *J. Biol. Chem.* 275, 5794–5803. doi: 10.1074/JBC.275.8.5794.

Schauder, R., Widdel, F., and Fuchs, G. (1987). Carbon assimilation pathways in sulfate-reducing bacteria II. Enzymes of a reductive citric acid cycle in the autotrophic *Desulfobacter hydrogenophilus*. *Arch. Microbiol. 1987 1483* 148, 218–225. doi: 10.1007/BF00414815.

Scheller, S., Goenrich, M., Boecher, R., Thauer, R. K., and Jaun, B. (2010). The key nickel enzyme of methanogenesis catalyses the anaerobic oxidation of methane. *Nat. 2010 4657298* 465, 606–608. doi: 10.1038/nature09015.

Schink, B. (1997). Energetics of syntrophic cooperation in methanogenic degradation. *Microbiol. Mol. Biol. Rev.* 61, 262. doi: 10.1128/MMBR.61.2.262-280.1997.

Schouten, S., Wakeham, S. G., Hopmans, E. C., and Damsté, J. S. S. (2003). Biogeochemical evidence that thermophilic archaea mediate the anaerobic oxidation of methane. *Appl. Environ. Microbiol.* 69, 1680–1686. doi: 10.1128/AEM.69.3.1680-1686.2003.

Seifert, R., Nauhaus, K., Blumenberg, M., Krüger, M., and Michaelis, W. (2006). Methane dynamics in a microbial community of the Black Sea traced by stable carbon isotopes in vitro. *Org. Geochem.* 37, 1411–1419. doi: 10.1016/J.ORGGEOCHEM.2006.03.007.

Shima, S., Krueger, M., Weinert, T., Demmer, U., Kahnt, J., Thauer, R. K., et al. (2012). Structure of a methyl-coenzyme M reductase from Black Sea mats that oxidize methane anaerobically. *Nature* 481, 98–101. doi: 10.1038/nature10663.

Shrestha, P. M., Rotaru, A.-E., Summers, Z. M., Shrestha, M., Liu, F., and Lovley, D. R. (2013). Transcriptomic and genetic analysis of direct interspecies electron transfer. *Appl. Environ. Microbiol.* 79, 2397–2404. doi: 10.1128/AEM.03837-12.

Skennerton, C. T., Chourey, K., Iyer, R., Hettich, R. L., Tyson, G. W., and Orphan, V. J. (2017). Methane-Fueled Syntrophy through Extracellular Electron Transfer: Uncovering the Genomic Traits Conserved within Diverse Bacterial Partners of Anaerobic Methanotrophic Archaea. *MBio* 8, 1–14. doi: 10.1128/mBio.00530-17.

Søndergaard, D., Pedersen, C. N. S., and Greening, C. (2016). HydDB: A web tool for hydrogenase classification and analysis. *Sci. Reports 2016 61* 6, 1–8. doi: 10.1038/srep34212.

Sonne-Hansen, J., and Ahring, B. K. (1999). *Thermodesulfobacterium hveragerdense* sp. nov., and *Thermodesulfovibrio islandicus* sp. nov., two thermophilic sulfate reducing bacteria isolated from a Icelandic hot spring. *Syst. Appl. Microbiol.* 22, 559–564. doi: 10.1016/S0723-2020(99)80009-5.

Sørensen, K. B., Finster, K., and Ramsing, N. B. (2001). Thermodynamic and kinetic requirements in anaerobic methane oxidizing consortia exclude hydrogen, acetate, and methanol as possible electron shuttles. *Microb. Ecol. 2001 421* 42, 1–10. doi: 10.1007/S002480000083.

Speth, D. R., Yu, F. B., Connon, S. A., Lim, S., Magyar, J. S., Peña-Salinas, M. E., et al. (2022). Microbial communities of Auka hydrothermal sediments shed light on vent biogeography and the evolutionary history of thermophily. *ISME J. 2022*, 1–15. doi: 10.1038/s41396-022-01222-x.

Stamatakis, A. (2014). RAxML version 8: a tool for phylogenetic analysis and post-analysis of large phylogenies. *Bioinformatics* 30, 1312–1313. doi: 10.1093/BIOINFORMATICS/BTU033.

Stokke, R., Roalkvam, I., Lanzen, A., Haflidason, H., and Steen, I. H. (2012). Integrated metagenomic and metaproteomic analyses of an ANME-1-dominated community in marine cold seep sediments. *Environ. Microbiol.* 14, 1333–1346. doi: 10.1111/J.1462-2920.2012.02716.X.

Summers, Z. M., Fogarty, H. E., Leang, C., Franks, A. E., Malvankar, N. S., and Lovley, D. R. (2010). Direct exchange of electrons within aggregates of an evolved syntrophic coculture of anaerobic bacteria. *Science (80-.).* 330, 1413–1415. doi: 10.1126/science.1196526.

Teske, A., Hinrichs, K.-U., Edgcomb, V., Gomez, A. D. V., Kysela, D., Sylva, S. P., et al. (2002). Microbial Diversity of Hydrothermal Sediments in the Guaymas Basin: Evidence for Anaerobic Methanotrophic Communities. *Appl. Environ. Microbiol.* 68, 1994–2007. doi: 10.1128/AEM.68.4.1994.

Teske, A., Lizarralde, D., and Höfig, T. W. (2021). Guaymas Basin tectonics and biosphere. *Proc. Int. Ocean Discov. Progr.* 385. doi: 10.14379/IODP.PROC.385.2021.

Thauer, R. K. (2011). Anaerobic oxidation of methane with sulfate: on the reversibility of the reactions that are catalyzed by enzymes also involved in methanogenesis from CO_2. *Curr. Opin. Microbiol.* 14, 292–299. doi: 10.1016/J.MIB.2011.03.003.

Treude, T., Krüger, M., Boetius, A., and Jørgensen, B. B. (2005). Environmental control on anaerobic oxidation of methane in the gassy sediments of Eckernförde Bay (German Baltic). *Limnol. Oceanogr.* 50, 1771–1786. doi: 10.4319/LO.2005.50.6.1771.

Treude, T., Orphan, V., Knittel, K., Gieseke, A., House, C. H., and Boetius, A. (2007). Consumption of Methane and CO 2 by Methanotrophic Microbial Mats from Gas Seeps of the Anoxic Black Sea. *Appl. Environ. Microbiol.* 73, 2271–2283. doi: 10.1128/AEM.02685-06.

Venceslau, S. S., Stockdreher, Y., Dahl, C., and Pereira, I. A. C. (2014). The "bacterial heterodisulfide" DsrC is a key protein in dissimilatory sulfur metabolism. *Biochim. Biophys. Acta* 1837, 1148–1164. doi: 10.1016/J.BBABIO.2014.03.007.

Walker, D. J. F., Martz, E., Holmes, D. E., Zhou, Z., Nonnenmann, S. S., and Lovley, D. R. (2019). The archaellum of *Methanospirillum hungatei* is electrically conductive. *MBio* 10, 1–6. doi: 10.1128/MBIO.00579-19.

Wang, F.-P., Zhang, Y., Chen, Y., He, Y., Qi, J., Hinrichs, K.-U., et al. (2014). Methanotrophic archaea possessing diverging methane-oxidizing and electron-transporting pathways. *ISME J.* 8, 1069–1078. doi: 10.1038/ismej.2013.212.

Wang, F., Gu, Y., O'Brien, J. P., Yi, S. M., Yalcin, S. E., Srikanth, V., et al. (2019). Structure of microbial nanowires reveals stacked hemes that transport electrons over micrometers. *Cell* 177, 361-369.e10. doi: 10.1016/j.cell.2019.03.029.

Wang, Y., Wegener, G., Williams, T. A., Xie, R., Hou, J., Tian, C., et al. (2021). A methylotrophic origin of methanogenesis and early divergence of anaerobic multicarbon alkane metabolism. *Sci. Adv.* 7, 1–12. doi: 10.1126/sciadv.abj1453.

Wegener, G., Krukenberg, V., Riedel, D., Tegetmeyer, H. E., and Boetius, A. (2015). Intercellular wiring enables electron transfer between methanotrophic archaea and bacteria. *Nature* 526, 587–590. doi: 10.1038/nature15733.

Wegener, G., Krukenberg, V., Ruff, S. E., Kellermann, M. Y., and Knittel, K. (2016). Metabolic capabilities of microorganisms involved in and associated with the anaerobic oxidation of methane. *Front. Microbiol.* 7, 1–16. doi: 10.3389/fmicb.2016.00046.

Whiticar, M. J. (1999). Carbon and hydrogen isotope systematics of bacterial formation and oxidation of methane. *Chem. Geol.* 161, 291–314. doi: 10.1016/S0009-2541(99)00092-3.

Widdel, F., and Bak, F. (1992). "Gram-negative mesophilic sulfate-reducing bacteria," in *The Prokaryotes* (Springer, New York, NY), 3352–3378. doi: 10.1007/978-1-4757-2191-1_21.

Wu, Y.-W., Simmons, B. A., and Singer, S. W. (2016). MaxBin 2.0: an automated binning algorithm to recover genomes from multiple metagenomic datasets. *Bioinformatics* 32, 605–607. doi: 10.1093/bioinformatics/btv638.

Yu, H., Skennerton, C. T., Chadwick, G. L., Leu, A. O., Aoki, M., Tyson, G. W., et al. (2022). Sulfate differentially stimulates but is not respired by diverse anaerobic methanotrophic archaea. *ISME J.* 16, 168–177. doi: 10.1038/S41396-021-01047-0.

Yu, N. Y., Wagner, J. R., Laird, M. R., Melli, G., Rey, S., Lo, R., et al. (2010). PSORTb 3.0: improved protein subcellular localization prediction with refined localization subcategories and predictive capabilities for all prokaryotes. *Bioinformatics* 26, 1608–1615. doi: 10.1093/bioinformatics/btq249.

Zeikus, J. G., Dawson, M. A., Thompson, T. E., Ingvorsen, K., and Hatchikian, E. C. (1983). Microbial ecology of volcanic sulphidogenesis: isolation and characterization of *Thermodesulfobacterium commune* gen. nov. and sp. nov. *Microbiology* 129, 1159–1169. doi: 10.1099/00221287-129-4-1159.

Zheng, K., Ngo, P. D., Owens, V. L., Yang, X., and Mansoorabadi, S. O. (2016). The biosynthetic pathway of coenzyme F430 in methanogenic and methanotrophic archaea. *Science (80-.).* 354, 339–342. doi: 10.1126/science.aag2947.

Zhou, J., Bruns, M. A., and Tiedje, J. M. (1996). DNA recovery from soils of diverse composition. *Appl. Environ. Microbiol.* 62, 316–322. doi: 10.1128/aem.62.2.316-322.1996.

Zhu, Q.-Z., Wegener, G., Hinrichs, K.-U., and Elvert, M. (2022). Activity of ancillary heterotrophic community members in anaerobic methane-oxidizing cultures. *Front. Microbiol.* 13, 1–12. doi: 10.3389/fmicb.2022.912299.

Anaerobic hexadecane degradation by a thermophilic Hadarchaeon from Guaymas Basin

David Benito Merino, Julius S. Lipp, Guillaume Borrel, Antje Boetius, Gunter Wegener

manuscript ready for submission to

ISME Journal

Anaerobic hexadecane degradation by a thermophilic Hadarchaeon from Guaymas Basin

David Benito Merino[1,2]*, Julius S. Lipp[3], Guillaume Borrel[4], Antje Boetius[1,3,5], Gunter Wegener[1,3]*

[1]Max Planck Institute for Marine Microbiology, Bremen, Germany

[2]Faculty of Geosciences, University of Bremen, Bremen, Germany

[3]MARUM, Center for Marine Environmental Sciences, University of Bremen, Bremen, Germany

[4]Department of Microbiology, Unit Evolutionary Biology of the Microbial Cell, Institut Pasteur, Paris, France

[5]Alfred Wegener Institute, Helmholtz Center for Polar and Marine Research, Bremerhaven, Germany

*** Correspondence:**

David Benito Merino, dbenito@mpi-bremen.de

Gunter Wegener, gwegener@mpi-bremen.de

Keywords: archaea, alkanes, hydrocarbons, anaerobic metabolism, evolution

Abstract

Hadarchaeota inhabit subsurface and hydrothermal environments but members of this phylum were not available in culture previous to this study. Hence, their metabolic traits remained inconclusive. Some Hadarchaeota metagenome-assembled genomes (MAGs) encode a non-canonical methyl-coenzyme M reductase (alkyl-coenzyme M reductase, Acr), suggesting that these organisms grow on multicarbon alkanes. Here, we established an anaerobic hexadecane-degrading culture at 70°C from hydrothermally heated sediments of the Guaymas Basin. This culture was enriched in a Hadarchaeon that we propose as *Candidatus* Cerberiarchaeum oleivorans. Genomic and chemical analyses indicate that this *Ca.* Cerberiarchaeum oleivorans uses an Acr to activate hexadecane to hexadecyl-coenzyme M. A β-oxidation pathway and a tetrahydromethanopterin (H_4MPT) methyl branch Wood-Ljungdahl (mWL) pathway allow the complete oxidation of the hexadecane to CO_2. Our results suggest a syntrophic lifestyle with sulfate reducers, as *Ca*. C. oleivorans does not have a canonical respiratory pathway for sulfate. A comparative genomic survey of Hadarchaeota shows that Acr, mWL and β-oxidation genes are restricted to one family of Hadarchaeota. Our phylogenetic analyses show that the mWL pathway was basal to all Hadarchaeota. In contrast, the carbon monoxide dehydrogenase/acetyl-coenzyme A synthase complex (Cdh/Acs) in this Hadarchaea family was likely acquired via horizontal gene transfer from Bathyarchaeia. The Acr and β-oxidation genes from Hadarchaea are highly similar to those of *Ca*. Methanoliparia and other alkane-oxidizing archaea, suggesting also horizontal gene transfer. Our results demonstrate that alkane metabolism appeared only in an isolated family of Hadarchaeota, which however inhabit varied environments. Our results emphasize the role of Acr-encoding archaea in shaping the geochemistry of petroleum reservoirs.

Introduction

The methyl-coenzyme M reductase (Mcr) is an enzyme unique to the domain Archaea. Originally, this enzyme was described from methanogens, strict anaerobes that form methane from various substrates such as CO_2, formate, acetate and methylated compounds (Thauer et al., 2008). Anaerobic methane-oxidizing archaea (ANME) use Mcr variants to activate methane to methyl-CoM (Shima et al., 2012), and they completely oxidize the carbon to CO_2 using a reverse methanogenesis pathway (Hallam et al., 2004). Related members of the Halobacteriota, namely *Candidatus* Syntrophoarchaeum, *Ca*. Alkanophaga, *Ca.* Ethanoperedens and *Ca.* Argoarchaeum thrive on short- and mid-chain alkanes (Laso-Pérez et al., 2016; Chen et al., 2019; Hahn et al., 2020; Zehnle et al., 2022). They activate alkanes with divergent Mcr types (alkyl-coenzyme M reductases, Acrs) and form the corresponding alkyl-CoM (Laso-Pérez et al., 2016; Chen et al., 2019; Hahn et al., 2020). Subsequently, these anaerobic multicarbon alkane degraders (ANKA, (Wang et al., 2020; Wegener et al., 2022)) convert the alkyl-CoM to acyl-CoA, which is completely oxidized to CO_2 via the β-oxidation and the Wood-Ljungdahl (WL) pathways (Laso-Pérez et al., 2016; Zehnle et al., 2022). In the case of Ca. Ethanoperedens and Ca. Argoarchaeum, they activate ethane to ethyl-CoM, convert it to acetyl-CoA and oxidize it to CO_2 via the WL pathway, without a β-oxidation pathway (Chen et al., 2019; Hahn et al., 2020). Most ANME and other short- and mid-chain alkane-oxidizing archaea do not possess respiratory pathways to couple the oxidation of their substrates to sulfate reduction (Boetius et al., 2000; Michaelis et al., 2002; Orphan et al., 2002; McGlynn et al., 2015; Wegener et al., 2015). Instead, they form syntrophic interactions with partner sulfate-reducing bacteria (SRB) of the phylum Desulfobacterota, such as members of the Seep-SRB, *Ca*. Desulfofervidus auxilii or Thermodesulfobacteria (Krukenberg et al., 2016; Laso-Pérez et al., 2016; Hahn et al., 2020; Benito Merino et al., 2022). In contrast, *Ca*. Methanoliparia are non-syntrophic ANKA. *Ca.* Methanoliparia couple the oxidation of alkanes via Acr activation to CO_2-reducing methanogenesis (Borrel et al., 2019; Laso-Pérez et al., 2019; Zhou et al., 2022). Thus, they encode both an Acr and an Mcr.

Recent metagenomic studies revealed the presence of either Mcr or Acr in MAGs of uncultured archaea related to classical methanogens such as Archaeoglobi, but also distant groups such as Bathyarchaeia, Helarchaeia and Hadarchaeia (Evans et al., 2015; Boyd et al., 2019; Seitz et al., 2019; Wang et al., 2019). Previous work suggests that gene duplication and horizontal gene transfer (HGT) events have been important in the evolution of Mcr/Acr and alkane metabolism in archaea (Wang et al., 2021). Yet, neither these Acr-containing organisms, nor close relatives have been cultured. Among them, Hadarchaea might have a globally relevant role, because of their wide distribution in subsurface environments (Baker et al., 2016). Hadarchaea were originally described as the South African Goldmine Miscellaneous Euryarchaeal

Group, which were found in alkaline sulfate-rich mining fissure waters (Takai et al., 2001). Hadarchaea inhabit diverse anoxic subsurface habitats such as hot springs, hydrothermal sediments, deep marine sediments, aquifers and cold seeps (Teske and Sørensen, 2008; Baker et al., 2016; Dombrowski et al., 2018; Probst et al., 2018; Wang et al., 2019; Dong et al., 2020). The high GC content and short branching in the sequenced rRNAs suggested that Hadarchaea are thermophiles (Takai et al., 2001). This lineage was recently proposed to be a phylum (Hadarchaeota, (Rinke et al., 2021)), including at least 30 MAGs from public repositories (Baker et al., 2016; Wang et al., 2019; Farag et al., 2020). Of these, some hot-spring Hadarchaea MAGs encode an Acr, but their alkane substrates have not been characterized (Wang et al., 2019).

In this study, we targeted the cultivation of long-chain alkane degrading microorganisms from hydrothermal vents of the Guaymas Basin, located in the Gulf of California at 3000 m depth (Simoneit et al., 1990). Here, hydrocarbon-rich fluids diffuse from deeper layers towards the sediment surface, where they fuel the metabolism of diverse microbial communities (Bazylinski et al., 1989; Rueter et al., 1994; Teske et al., 2002). Of these, we enriched anoxic microbes with hexadecane as substrate, and analyzed the microbial community and metabolism by ‘omics and metabolite analysis. We tested the hypothesis that members of the Hadarchaea are involved in alkane degradation in thermophilic anoxic environments and suggest that Hadarchaea acquired the necessary pathways for alkane metabolism horizontal gene transfer (HGT) from other archaea.

Materials and Methods

Sediment sampling and culture setup

For this study, we retrieved sediments from Guaymas Basin during R/V *Atlantis* cruises AT37-06 (Dec. 2016) and AT42-05 (Nov. 2018) with the submersible *Alvin*. On cruise AT37-06, the push cores were taken during *Alvin* dive 4869 (27° 0.45’ N 111° 24.54’ W, water depth 2001 m) from a site densely covered by an orange mat of large sulfur-oxidizing *Beggiatoaceae* bacteria. Below the mat, temperatures rapidly increased and reached 85°C at 50 cm depth (Teske et al., 2021). On cruise AT42-05, a push core was taken during *Alvin* dive 4991 (27° 0.69’ N, 111° 24.27’ W, water depth 2013 m) from a site covered with orange-white *Beggiatoaceae* mats. Temperatures at 50 cm depth reached at least 80°C. Both samples were immediately transferred to glass bottles sealed with butyl rubber stoppers, and the headspace was exchanged to argon. Bottled sediments were stored at room temperature until further processing in the

home laboratory. Anoxic sediment slurries were prepared as described before (Laso-Pérez et al., 2018). Homogenized sediment from 2 to 10 cm was mixed with synthetic sulfate-reducer medium (Widdel and Bak, 1992). This slurry was distributed into replicate cultivation vials and further diluted reaching a final density of approximately 1 g sediment per 100 ml. The slurries were amended with1 mL *n*-hexadecane (99% purity, Sigma-Aldrich) as carbon and energy source. The vials were sealed with butyl rubber stoppers and pressured with 2 atm N_2:CO_2 (90:10). The bottles were incubated upside down to avoid chemical reactions of the alkane substrate with the rubber stopper. Samples were incubated at 37, 50 and 70°C with mild agitation (rotation 40 rpm). As marker for anaerobic alkane degradation we followed the formation of sulfide using a colorimetric copper sulfate assay (Cord-Ruwisch, 1985). Cultures with hexadecane at 70°C (hexadecane70) were subsequently diluted (1:4 dilution steps) when sulfide concentrations reached between 5 and 10 mM.

DNA extraction and 16S rRNA amplicon sequencing

DNA was extracted from early enrichments at 37, 50 and 70°C using the MO BIO PowerSoil DNA isolation kit (Qiagen). 16S rRNA gene libraries were prepared according to the Illumina 16S metagenomic sequencing library preparation protocol*. We amplified the V3-V4 region for bacteria and the V4-V6 region for archaea. 16S amplicon libraries were sequenced at CeBiTec (Bielefeld, Germany) on an Illumina MiSeq (2×300-bp paired-end run, 100 000 reads per library). Sequences were analyzed in R** Statistical Software v 3.5.1 with DADA2 v. 1.14 (Callahan et al., 2016). DADA2 scripts used for 16S amplicon analysis are accessible on GitHub***.

DNA extraction and metagenome sequencing

DNA samples from hexadecane70 cultures were extracted at three different stages for AT37-06 samples (Feb. 2018, Sep. 2018 and Mar. 2020) and at one point for AT42-05 samples (Jun. 2021). For the sediment-free samples, 50 mL culture were concentrated on 0.2 µm pore polycarbonate filters (Millipore, type GTTP filters) applying gentle vacuum (–40 kPa). DNA was extracted using the DNeasy PowerWater Kit (Qiagen). Metagenomes from Feb. 2018 were sequenced at CeBiTec (Bielefeld, Germany) on an Illumina MiSeq (2×300-bp paired-end run, 2 Mio reads). Metagenomes from Sep. 2018 were sequenced at the Marine Biological Laboratory (Woods Hole, USA) on an Illumina HiSeq (2×150-bp paired-end run, 1.5

* support.illumina.com/documents/documentation/chemistry_documentation/16s/16s-metagenomic-library-prep-guide-15044223-b.pdf
** R-project.org/
*** github.com/dbenitom/Metagenomics_scripts/blob/main/dada2_archaea.R and github.com/dbenitom/Metagenomics_scripts/blob/main/dada2_bacteria.R

Mio reads). Metagenomes from Mar. 2020 and Jun. 2021 were sequenced at the Max-Planck-Genome-Centre (Cologne, Germany) on an Illumina MiSeq (2×250-bp paired-end run, 4 and 10 Mio reads, respectively).

Metagenomics analyses

Primers and adapter sequences were removed from raw metagenomic reads and they were quality trimmed with BBduk within the BBtools package* v. 35.68, with the parameters minlength=50 mink=6 hdist=1 qtrim=r trimq=20. Microbial community composition based on 16S rRNA gene abundance was calculated with phyloFlash v. 3.3b1 (Gruber-Vodicka et al., 2020). Quality-trimmed reads were co-assembled in metagenomic contigs with SPAdes v. 3.9.0 (Bankevich et al., 2012) with default parameters. Quality-trimmed reads were mapped to the co-assembly with Bowtie2 v. 2.3.2 (Langmead and Salzberg, 2012) with the parameters --local --q. Metagenomic contigs were imported into the 'omics analysis software anvi'o v. 6 (Eren et al., 2015, 2020). Gene prediction in metagenomic contigs was done with Prodigal v 2.6 (Hyatt et al., 2010). Coding sequences were annotated with Prokka v 1.11, PFAMs, TIGRFAMs, COGs, KEGGs and RNAmmer (Kanehisa and Goto, 2000; Haft et al., 2001; Lagesen et al., 2007; Seemann, 2014; Galperin et al., 2015; Mistry et al., 2021). CXXCH motifs in putative multiheme cytochromes were searched with a custom script**. Metagenomic binning was done with maxbin v. 2.2.7 (Wu et al., 2016). Bins obtained with maxbin were manually refined in anvi'o (Eren et al., 2015, 2020) by removing contigs whose coverage did not match the overall coverage of the bins. Average nucleotide identity (ANI) between our bins and reference genomes was calculated with fastANI v. 1.31 (Jain et al., 2018). Pfl and Ass proteins were searched in the Archaeoglobi MAGs by aligning Pfl of *Archaeoglobus fulgidus* and Ass of *Desulfatibacillum alkenivorans* against the proteins of our Archaeoglobi MAGs using BLASTp (Altschul et al., 1990).

Synthesis of authentic hexadecyl-CoM standards

One equivalent (0.3 g) of sodium 2-mercaptoethanesulfonate (≥98% coenzyme M sodium salt, Sigma-Aldrich) was mixed with 2 equivalents (0.62 mL) of 1-bromohexadecane (97%, Sigma-Aldrich) in 2.4 mL basic ammonia solution (30% NH_4OH pH ~12). The mix was incubated overnight at RT with gentle shaking in a vortex (500 rpm). The aqueous phase was transferred to a new vial and pH was adjusted to 7.0 with 37% HCl.

Metabolite sample extractions

30 mL of culture were centrifuged at 4000 rpm for 30 min at RT, keeping both the pellet and the supernatant. The supernatant was removed and filtered onto polycarbonate filters (0.22 μm pore size,

* sourceforge.net/projects/bbmap/

** github.com/dbenitom/Metagenomics_scripts/blob/main/CXXCH_search_anvio_import.sh

Merck Millipore) under gentle vacuum (>30 kPa). Filter pieces and pellet were transferred to bead beating tubes (Lysing Matrix E, MP Biomedicals) with 1 mL of acetonitrile:methanol:water (4:4:2, v:v:v). The tubes were vortexed for 10 min at maximum speed. Beads and debris were pelleted by centrifugation at 10,000 rpm for 20 min at RT. The clear supernatant was transferred to glass vials and stored at 4°C.

LC-MS of metabolite extracts and standards

Chemical analysis of metabolite extracts and alkyl-CoM was done as described previously (Zehnle et al., 2022). Culture extracts and hexadecyl-CoM standards were analyzed via high-resolution accurate-mass mass spectrometry on a Bruker maXis plus quadrupole time-of-flight mass spectrometer (Bruker Daltonics, Bremen, Germany) connected to a Thermo Dionex Ultimate 3000RS UHPLC system (Thermo Fisher Scientific, Bremen, Germany) via an electrospray ionization ion source. Sample aliquots (equivalent to 20% of total extract) were evaporated under a nitrogen stream and redissolved in 10 µL of methanol:water (1:1, v:v) before injection. Separation was done on an Acclaim C30 reversed phase column (Thermo Fisher Scientific, 3.0×250 mm, 3 µm particle size). The column oven was set to 40°C and the binary pump programmed with a flow rate of 0.35 mL/min and the following gradient of eluent A (acetonitrile:water:formic acid 5:95:0.1, v:v:v) and eluent B (2-propanol:acetonitrile:formic acid 90:10:0.1, v:v:v): 0% B at 0 min, ramp up to 100% B at 30 min, hold at 100% B until 50 min, and reequilibration at 0% B from 51 min until the end of the run at 60 min. Parameters for the electrospray ion source were set as described previously (Zehnle et al., 2022). The mass spectrometer was set to acquire alternating scans of full scan and broad-band collision induced dissociation spectra (25 eV collision energy) in a mass range of m/z 50-600 in negative ionization mode. Every analysis was mass-calibrated to reach mass accuracy of 1-3 ppm by loop injection of a calibration solution containing sodium formate cluster ions at the end of the analysis during the equilibration phase and using the high-precision calibration algorithm. Extracted ion chromatograms were generated using a mass window of 0.01 Da. Data processing was performed using the Compass Data Analysis software package version 5.0 (Bruker Daltonics, Bremen, Germany).

Phylogenomic and phylogenetic analyses

For archaeal phylogenomics, 289 archaeal genomes were used to build a tree based on 76 archaeal marker proteins (Table S1, (Rinke et al., 2013)). To build phylogenetic trees for formylmethanofuran dehydrogenase (FwdABC) and carbon monoxide dehydrogenase (CdhABCDE), we annotated the gene sequences using PFAMs for Fwd and custom hidden Markov models for Cdh (Adam et al., 2018). The amino acid sequences for each gene set were aligned and concatenated with the anvi'o software (Eren et

al., 2015, 2020), using muscle as alignment tool (Edgar, 2004). The alignments are available as Supplementary Material (keeper.mpdl.mpg.de/d/77dc106d349e446e9749/). Maximum likelihood trees for all protein sets with 100 bootstraps were calculated using IQTree v. 2.0.3, using the –test option to estimate the best substitution model for each protein (Kalyaanamoorthy et al., 2017; Minh et al., 2020). The phylogenetic trees were visualized and edited on the Interactive Tree of Life web server (Letunic and Bork, 2011).

Data availability

The 16S rRNA gene amplicons reads, raw metagenomic reads, metagenomic assembly and MAGs generated in this study are accessible under BioProject PRJNA891685.

Results

Enrichment of Hadarchaea from Guaymas Basin sediments

We obtained sediment cores from a hydrothermally vented area in Guaymas Basin covered by sulfur-oxidizing microbial mats (Teske et al., 2021). According to 16S rRNA gene amplicon sequencing (Figure 1A), the main archaeal lineages in the sediment core from cruise AT37-06 are ANME-1 (~25% relative abundance of archaeal 16S rRNA gene amplicons), Thermoplasmatota (~30% relative abundance), Methanofastidiosales (~20% relative abundance) and Woesearchaeales (~10% relative abundance). The most abundant bacteria were SRB Desulfobacterota (~30% relative abundance of bacterial 16S rRNA gene amplicons) and Campylobacterales (~30% relative abundance).

Anoxic sediment slurries in sulfate-reducer medium were supplemented with hexadecane as sole energy source and incubated at 37, 50 and 70°C. The cultures at 37°C and 50°C showed relatively slow increase of sulfide, reaching ~5 mM after 150 days (Figure 1B). They contained mostly sulfate-reducing Desulfobacterota (Figure 1A) (formerly Deltaproteobacteria). These have been described before as alkane degraders in marine hydrocarbon seeps (Jaekel et al., 2013; Stagars et al., 2016). Also, these enrichments contained large proportions of Thermoprofundales (phylum Thermoplasmatota) and Woesearchaeales (phylum Nanoarchaeota), and some methyl-reducing hydrogenotrophic methanogens of the order Methanofastidiosales, all corresponding to the groups that were present in the original sediments.

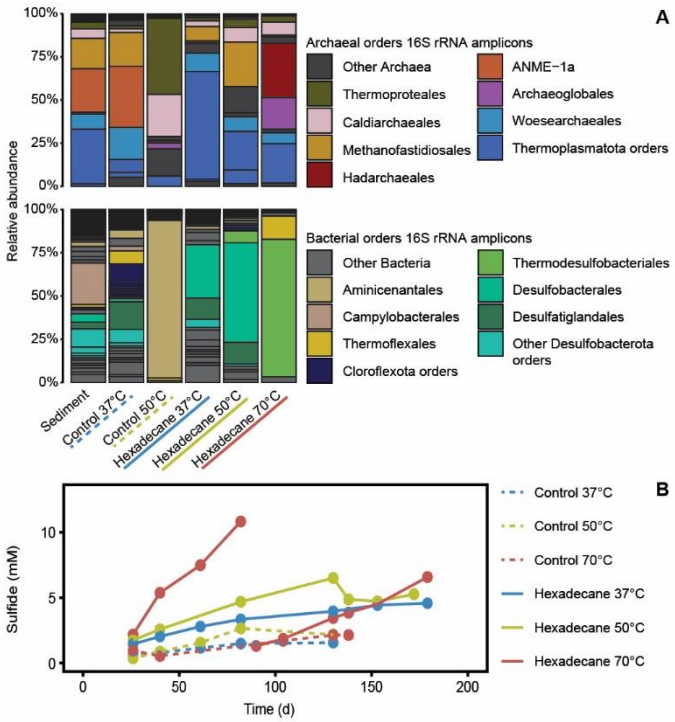

Figure 1. Community composition and sulfide formation in sediment slurries incubated with hexadecane. The results correspond to cruise AT37-06. **A.** Community composition based on archaeal and bacterial 16S rRNA gene amplicons. **B.** Sulfide production in early enrichments and control incubations. Control incubations did not show significant sulfide production over time. Enrichments with hexadecane at 37 and 50°C showed slow activities. Enrichments at 70°C grew faster and were diluted after 90 days of incubation.

In contrast, the incubation at 70°C produced 10 mM sulfide in 80 days and continued being active after a 1/5 dilution (Figure 1B). The archaeal amplicons consisted mostly of Hadarchaea, Archaeoglobi and Thermoplasmatota (JdFR-43) (Figure 1A). All three groups were rare in the control incubations at 70°C without hexadecane, or in incubations with hexadecane at lower temperatures. Archaeoglobi is a class that contains free-living sulfate reducers. *Archaeoglobus fulgidus* was suggested to grow on hexadecane as carbon and electron source and to activate this substrate via alkylsuccinate synthases of bacterial origin (Khelifi et al., 2014). The JdFR-43 family (order *Ca*. Thermoprofundales, phylum Thermoplasmatota) has been found in hydrothermal vents and is thought to utilize proteins and peptides for growth (Liu et al., 2022). In addition, the bacterial 16S rRNA gene amplicons of the 70°C culture differed remarkably from those of the lower temperature enrichments, and comprised Thermodesulfobacteriales (Figure 1). Thermodesulfobacteria are often autotrophs or grow on small organic molecules and are not known to degrade hydrocarbons (Zeikus et al., 1983; Sonne-Hansen and Ahring, 1999; Jeanthon et al., 2002; Moussard et al., 2004). However, recently they have been described as partners for thermophilic ANME-1c in the anaerobic oxidation of methane (AOM) and of *Ca*. Alkanophaga in the anaerobic oxidation of mid-chain alkanes, respectively (Benito Merino et al., 2022; Zehnle et al., 2022).

After two 1/5 dilutions, the 70°C cultures were almost sediment-free. We sequenced a metagenome of this culture to resolve its hexadecane-degrading community. Based on 16S rRNA genes recruited from this metagenome, the cultures were dominated by Archaea (>85% relative abundance, Figure 2). In two

independent enrichment cultures from different sampling, the early phase of the enrichments was characterized by dominance of Archaeoglobi (30% relative abundance), followed by Bathyarchaeia and Hadarchaeota (15-25% relative abundance; Figure 2). Acetothermia and Thermodesulfobacteriales sequences composed most of the bacterial fraction of the metagenome. In later culture dilutions, Hadarchaeota replaced the Archaeoglobi (40-50% relative abundance), suggesting an involvement of Hadarchaeota in hexadecane degradation. This enrichment consist of only two Hadarchaeota species as indicated by the 16S rRNA genes found in the metagenomes (Figure S1).

From the metagenomic co-assembly, we reconstructed 39 good-quality MAGs (completeness >50%, redundancy <15%, Table S2). A Hadarchaeota MAG recruited ~18% of the metagenomic reads in the latest stage of the culture (91% completeness, 0% redundancy, Table 1). This MAG encodes an Acr gene, leading to the hypothesis that these archaea may degrade hexadecane. Based on phylogenomics, our Hadarchaea MAG is related to a clade of Acr-encoding Hadarchaea described by Wang et al. (Wang et al., 2019). The average nucleotide identity (ANI) between our Hadarchaea MAG and the rest of the clade is below 75% (Figure S2). The ANI value of our MAG is also below 75% with the placeholder genome *Ca*. Hadarchaeum yellowstonense (Baker et al., 2016; Chuvochina et al., 2019). The hexadecane70 Hadarchaea MAG represents a novel genus. Based on its affiliation to Hadarchaeota and its metabolism (see results below), we propose the species name *Ca*. Cerberiarchaeum oleivorans (see Supplementary Text).

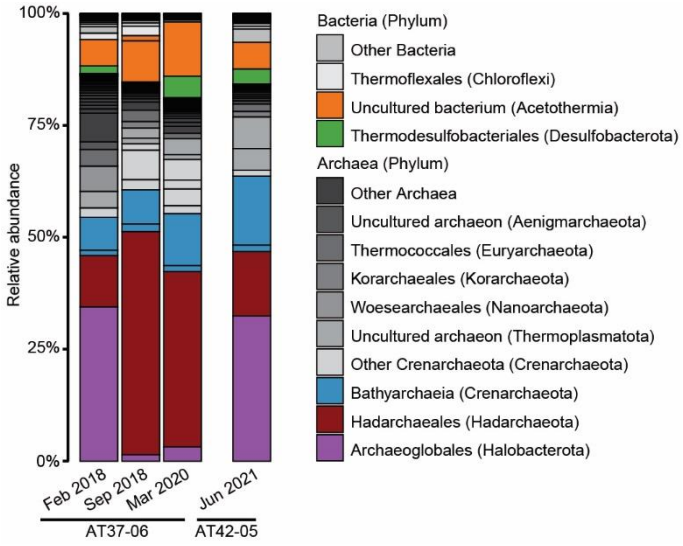

Figure 2. Community composition in Hexadecane70 cultures from AT37-06 and AT42-05. Relative abundance of microbial taxa based on 16S rRNA gene fragments recruited from the metagenome. Archaea dominate thermophilic alkane-degrading enrichments. Archaeoglobales were abundant in early sediment enrichments from the AT37-06 cruise (Feb 2018), and Hadarchaea became more dominant in later stages (Sep 2018, Mar 2020). The communities include heterotrophic Bathyarchaeia and Acetothermia, and sulfate-reducing Thermodesulfobacteriales. A second enrichment attempt from cruise AT42-05 showed similar results.

Function of Acr in Ca. Cerberiarchaeum oleivorans and Acr phylogeny

The genome of *Ca*. C. oleivorans harbors a single complete Acr operon. Based on the phylogenetic comparison of the catalytic alpha subunit, the Acr of *Ca*. C. oleivorans is closely related to those in MAGs

of Bathyarchaeia, Helarchaeota and *Ca*. Methanoliparia (Figure 3A) (Evans et al., 2015; Borrel et al., 2019; Laso-Pérez et al., 2019; Seitz et al., 2019; Wang et al., 2019; Zhou et al., 2022). To investigate the of *Ca*. C. oleivorans to activate hexadecane with Acr, we analyzed culture extracts from the hexadecane70 culture via liquid chromatography coupled to high-resolution mass spectrometry. A peak with the exact mass of hexadecyl-CoM eluted at the same retention time as an authentic hexadecyl-CoM standard (Figure 3B). A second peak eluted shortly before the hexadecyl-CoM standard. We hypothesize that this second compound is the product of hexadecane activation in the second carbon (2-methyl-pentadecyl-CoM, C_2-substituted hexadecyl), as previously described for the activation of butane (C_4 alkane) and dodecane (C_{12} alkane) (Laso-Pérez et al., 2016; Zehnle et al., 2022). In Hadarchaea, hexadecyl-CoM is the product of the activation of *n*-hexadecane by the Acr, as described for the anaerobic short- and mid-chain ANKA *Ca*. Ethanoperedens, *Ca*. Syntrophoarchaeum and *Ca*. Alkanophaga (Laso-Pérez et al., 2016; Chen et al., 2019; Hahn et al., 2020; Zehnle et al., 2022).

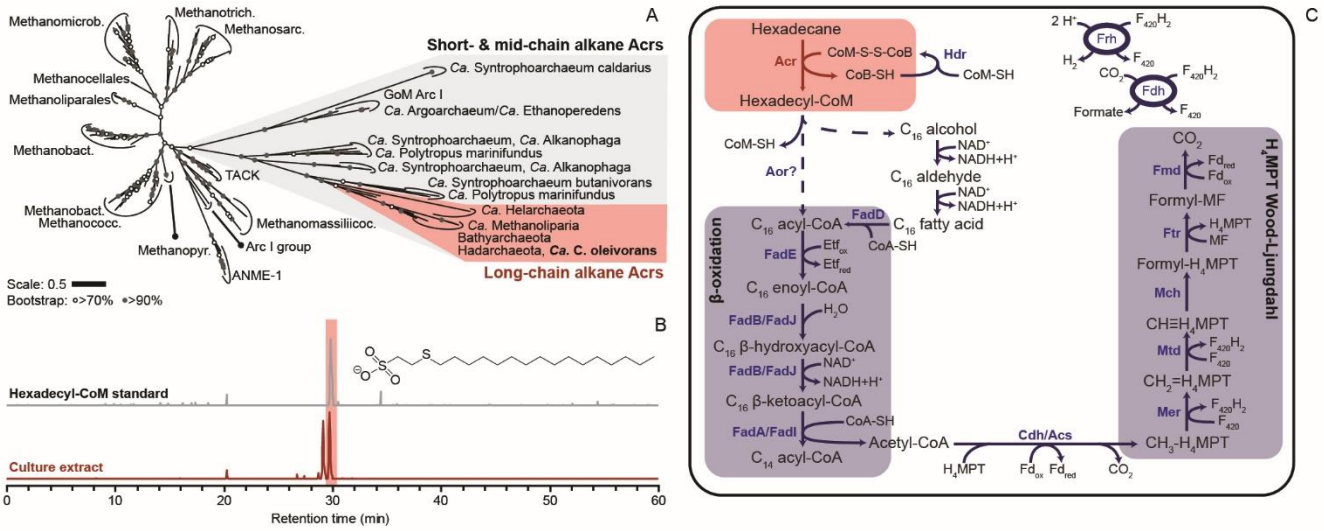

Figure 3. Methyl-/alkyl-coenzyme M reductase phylogeny, hexadecane activation by Acr and proposed metabolism for *Ca. Cerberiarchaeum oleivorans*. A. ML likelihood tree of McrA/AcrA alignment with 100 bootstraps. White circles and grey circles show bootstrap values of >70% and >90%, respectively. The clades shaded in grey include all Acr sequences (Mcr group IV, (Garcia et al., 2022)). The clade shaded in red includes putative long-chain alkane Acrs, including *Ca*. Cerberiarchaeum oleivorans Acr. **B.** *Ca*. C. oleivorans activates hexadecane to hexadecyl-CoM. LC-MS analysis of hexadecane70 culture extracts shows two dominant chromatographic peaks in extracted ion chromatograms of the exact mass of hexadecyl-CoM. These peaks likely represent coenzyme M-substituted alkyls resulting from activation of the alkane in the secondary and primary position, in order of elution time (Zehnle et al., 2022). **C.** Metabolic model for *Ca*. C. oleivorans. The Acr activates hexadecane to hexadecyl-CoM, which is then converted into a 16-carbon acyl-CoA (hexadecanoyl-CoA), possibly via Aor. Acyl-CoA is processed to acetyl-CoA units (β-oxidation pathway). Acetyl-CoA is incorporated into the downstream part of the H_4MPT mWL via the Cdh/Acs complex. The methyl group is completely oxidized to CO_2. The fate of the electrons released from this metabolism is unknown. $F_{420}H_2$ oxidation could be coupled to the production of H_2 via Frh or to the reduction of CO_2 to formate by a Fdh.

Complete alkane oxidation in Ca. Cerberiarchaeum oleivorans

Following Acr-dependent hexadecane activation, a conversion of hexadecyl-CoM to a hexadecanoyl-CoA (CoA-bound fatty acid) is necessary for the complete oxidation of the alkane (Figure 3C). This mechanism is so far unknown but for the related short-chain alkane oxidizers candidate enzymes have been proposed based on metagenomic and metatranscriptomic data (Laso-Pérez et al., 2016; Chen et al., 2019; Hahn et al., 2020). *Ca*. Syntrophoarchaeum butanivorans encodes a methylcobamide:CoM methyltransferase/corrinoid methyltransferase (MtaAC) that could be involved in the conversion of butyl-CoM into butyryl-CoA (Laso-Pérez et al., 2016). However, *Ca*. C. oleivorans MAG does not have the *mtaAC* genes. For *Ca*. E. thermophilum, a tungsten-containing aldehyde:ferredoxin oxidoreductase (Aor) has been proposed to catalyze this conversion, founded on the high expression of the gene in metatranscriptomes (Hahn et al., 2020). *Ca*. C. oleivorans encodes three copies of tungsten-containing Aor. –Future biochemical studies should target the function of these Aors in hexadecane degradation.

Ca. Ethanoperedens and *Ca*. Syntrophoarchaeum cannot form acyl-CoA from the corresponding fatty acid (acetate and butyrate), because they do not encode acyl-CoA synthetases. In contrast, *Ca. C. oleivorans* encodes acyl-CoA synthetases (*fadD*) and alcohol dehydrogenases. Therefore, *Ca.* C. oleivorans could use long-chain fatty acids or alcohols as carbon and energy source apart from long-chain alkanes. This ability was also suggested for *Ca*. Polytropus marinifundus (Boyd et al., 2019) and *Ca*. Methanoliparia (Borrel et al., 2019). Furthermore, *Ca. C. oleivorans* encodes a complete β-oxidation pathway, with multiple copies of some its genes (Table 2). The β-oxidation pathway allows the production of eight acetyl-CoA units from hexadecanoyl-CoA. Acetyl-CoA can be completely oxidized to CO_2 via the carbon monoxide dehydrogenase/acetyl-CoA synthase (Cdh/Acs) complex and the methanogenesis enzymes upstream of methyl transferase (Mtr), *i.e.*, the tetrahydromethanopterin (H_4MPT) methyl branch of the WL (mWL) pathway. In total, 16 CO_2 molecules are formed per each molecule of hexadecane, according to the following equation:

$$C_{16}H_{34} + 32\ H_2O \rightarrow 16\ CO_2 + 98\ H^+ + 98\ e^- \qquad \text{(eq. 1)}$$

The liberated electrons would reduce molecules such as coenzyme F_{420}, ferredoxin, NAD^+ and flavoproteins, which need to be reoxidized in respiratory pathways, or transfer their electrons to a syntrophic partner. In our culture, alkane degradation is likely coupled to sulfate reduction. Similar to other Hadarchaea containing Acrs, *Ca. C. oleivorans* does not encode a sulfate reduction pathway. Other syntrophic ANKA produce large amounts of multiheme cytochromes (MHC) that are likely mediating

direct interspecies electron transfer (DIET) (McGlynn et al., 2015; Wegener et al., 2015; Laso-Pérez et al., 2016; Hahn et al., 2020). *Ca*. C. oleivorans does not encode genes for MHC but it contains several genes encoding for pilus/flagellum that could aid in DIET with a sulfate-reducing partner (Wegener et al., 2015). Instead, it might channel the reducing equivalents in the form of molecular hydrogen produced by a NADH- or F_{420}-reducing NiFe-hydrogenase, or transfer small, reduced compounds like acetate and formate. The generation of hydrogen, formate and acetate could be thermodynamically feasible at in situ deep-sea conditions in the presence of syntrophic partners (Schink, 1997; Dong et al., 2019).

Possible sulfate-reducing partners and additional associated microorganisms

We screened the other MAGs retrieved from the hexadecane70 culture with a focus on potential sulfate-reducing partner of *Ca*. C. oleivorans (Table 1 and Table S2). The usual thermophilic partner for AOM and anaerobic oxidation of alkanes, *Ca*. Desulfofervidus auxilii, cannot thrive at 70°C (Krukenberg et al., 2016). Accordingly, we did not find it in the hexadecane70 cultures. However, Thermodesulfobacteriales (class Thermodesulfobacteria, phylum Desulfobacterota) were present throughout the different cultivation stages (Figure 2). *Ca*. Thermodesulfobacterium torris and *Ca*. Thermodesulfobacterium syntrophicum have been described as partner SRB for AOM and mid-chain alkane oxidation at 70°C, respectively (Benito Merino et al., 2022; Zehnle et al., 2022). We were able to retrieve a Thermodesulfobacteriales MAG in hexadecane70 metagenomes, present in low abundances (1-2% metagenomic reads map to the MAG, Table S2). This MAG corresponds to the species *Ca*. T. torris described at partners for AOM at 70°C (Benito Merino et al., 2022). *Ca*. T. torris encodes several putative MHC that would enable it to perform DIET with *Ca*. C. oleivorans. Despite their low abundances in the total community metagenome, *Thermodesulfobacteria* are the most likely partner SRB for hexadecane degradation at 70°C.

In early enrichments, Archaeoglobi were highly abundant (Figures 1 and 2) and several MAGs recruit between 1 and 10% of metagenomic reads (Table 1 and Table S2). The Archaeoglobi MAGs S5B4_HD70 and S5B11_HD70 encode a complete dissimilatory sulfate reduction pathway (Table S3) and are related to *Archaeoglobus fulgidus* (Figures S3 and S4). The cultured species of the genus *Archaeoglobus* are heterotrophic or chemolithotrophic sulfate reducers (Stetter, 1988; Burggraf et al., 1990; Stetter et al., 1993; Huber et al., 1997; Klenk et al., 1997; Mori et al., 2008; Steinsbu et al., 2010; von Jan et al., 2010; Stokke et al., 2013; Birkeland et al., 2017). Other Archaeoglobales genera (namely *Ferroglobus*, *Geoglobus* and *Ca*. Polytropus) are nitrate and ferric iron reducers (Anderson et al., 2011; Manzella et al., 2015; Mardanov et al., 2015; Boyd et al., 2019). We considered whether Archaeoglobi in the hexadecane70 culture could receive reducing equivalents from *Ca.* C. oleivorans. They do not encode

hydrogenases, making interspecies hydrogen exchange with *Ca*. C. oleivorans unlikely. They also do not code for proteins with multiple CXXCH heme-binding motifs (putative multiheme cytochromes, MHC). We thus suggest that Archaeoglobi in our culture could be competitive hexadecane oxidizers using alkylsuccinate synthases (Ass), a bacterial mechanism for activation of alkanes (Spormann and Widdel, 2000). *A. fulgidus* has been isolated from hydrothermal vents and oil reservoirs (Stetter et al., 1987) and encodes a pyruvate formate lyase (Pfl) with high similarity to alkylsuccinate synthase A (AssA) and benzylsuccinate synthase A (BssA) (Khelifi et al., 2014). (Khelifi et al., 2014). All Archaeoglobi MAGs retrieved encode proteins with high similarity to PflC/AssD, but lack the PflD/AssA that was highly expressed in *A. fulgidus* during growth on hexadecane (Figure S3). Interestingly, one Archaeoglobus MAG (Archaeoglobi archaeon S5B9_HD70, 83% completeness, 4% contamination, Table S2) encodes both a PflC/AssD and PflD/AssA with high sequence similarity to those of *A. fulgidus* and *D. alkenivorans*. In summary, the Archaeoglobi of the hexadecane70 culture are unlikely to play a role as partners of *Ca*. C. oleivorans. Instead, they might compete for the oxidation of the hexadecane, coupling it to sulfate reduction.

The culture also contains a bacterial MAG affiliated to the phyla Bipolaricaulota (formerly Acetothermia) that recruited 2-6% of the metagenomic reads (Table 1). Bipolaricaulota have been found in anoxic environments such as oil reservoirs and anaerobic digesters (Hu et al., 2016; Hao et al., 2018). These bacteria are described as generalists that ferment sugars, amino acids and peptides to acetate, formate and hydrogen (Takami et al., 2012; Hao et al., 2018), but do not encode MHC. In the culture, we also found a Bathyarchaeia MAG (phylum Thermoproteota) that recruited 1-3% of the metagenomic reads (Table 1). Bathyarchaeia are found in diverse environments such as deep-sea and freshwater sediments (Vetriani et al., 1999; Kubo et al., 2012; Lloyd et al., 2013; Meng et al., 2013). Unlike the Bathyarchaeia MAGs described by Evans et al. (Evans et al., 2015), this MAG did not encode Acrs and thus it is unlikely to be involved directly in hexadecane oxidation. Furthermore, a MAG belonging to Thermoprofundales (completeness <70%) recruits 1-2% of metagenomic reads (Table S2). Thermoprofundales are peptidolytic organisms that have been reported from hydrothermal environments and oil reservoirs and also co-occurring with Hadarchaea (Liu et al., 2022). The Bipolaricaulota, Bathyarchaeia and Thermoplasmatota described here appear to be heterotrophic generalists that might thrive on side metabolites of the alkane-oxidizing community such as peptides, acetate or formate (Kellermann et al., 2012; Zhu et al., 2022). None of these MAGs encoded for sulfate reduction genes, nor have they been previously reported as partners for AOM or anaerobic oxidation of alkanes. Overall, this community gives us insights on the complex metabolic networks that potentially operate in oil-rich environments.

Table 1. MAGs retrieved from hexadecane70 culture metagenomes (described in the main text). A complete list of MAGs can be found in Table S2**.**

	Candidatus **Cerberiarchaeum oleivorans**	**Bipolaricaulota bacterium S4B7_HD70**	**Bathyarchaeia archaeon S9B4_HD70**	**Archaeoglobi archaeon S5B11_HD70**	**Archaeoglobi archaeon S5B4_HD70**
Genome size	1.3 Mb	1.8 Mb	1.7 Mb	0.9 Mb	2.2 Mb
N50	44 kb	51 kb	1.7 Mb	15 kb	27 kb
Num. contigs	54	85	1	82	142
GC content	52%	62%	34%	46%	45%
Completeness	91%	79%	96%	68%	97%
Redundancy	0%	0%	0%	0%	3%
Read recruitment (Feb 2018)	3%	2%	1%	5%	5%
Read recruitment (Mar 2020)	18%	6%	3%	<1%	<1%
Closest relative (GTDB)	GCA_004347925.1	GCA_002010385.1	GCA_002254975.1	*Archaeoglobus fulgidus*	*Archaeoglobus fulgidus*

Table 2. Genes of the β-oxidation pathway in *Candidatus* Cerberiarchaeum oleivorans.

Pathway step	**Gene product**	**Number of copies (based on annotated COGs)**
Fatty acid:CoA ligation to form acyl-CoA	NDP-forming acyl-CoA synthetase (COG1042)	5
	AMP-forming acyl-CoA synthetase (COG0318)	3
Oxidation of acyl-CoA to enoyl-CoA	Acyl-CoA dehydrogenase (COG1960)	8
Hydration of enoyl-CoA to β-hydroxyacyl-CoA	Enoyl-CoA hydratase (COG1024)	1
Oxidation of β-hydroxyacyl-CoA to β-ketoacyl-CoA	β-hydroxyacyl-CoA dehydrogenase (COG1250)	2
Release of acetyl-CoA from β-ketoacyl-CoA	Acetyl-CoA acetyltransferase (COG0183)	5

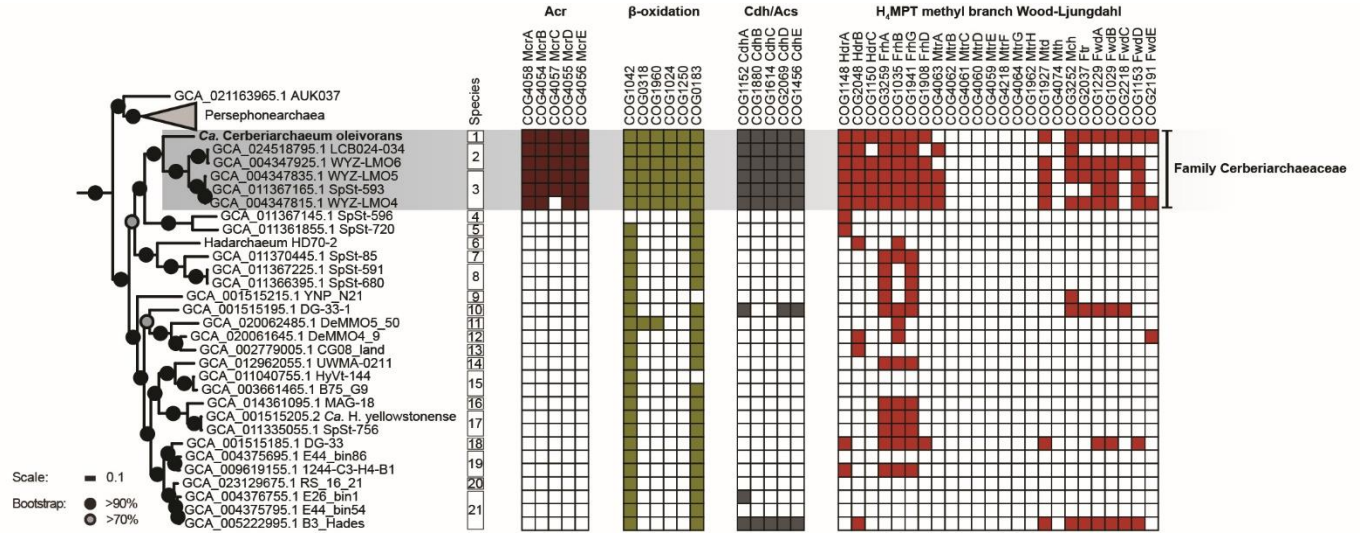

Figure 4. Pathways required for Acr-dependent alkane oxidation in Hadarchaeota. Subset of a phylogenomic tree of archaea showing Hadarchaeota (including Persephonearchaea), and occurrence of pathways for alkane degradation in the class Hadarchaeia. The 95% threshold in ANI defines the 21 species of Hadarchaeota. Colored squares indicate that the protein is encoded in the MAG. The Cerberiarchaeaceae family (grey shading) contains MAGs encoding an Acr, a complete β-oxidation pathway, a Cdh/Acs and a mWL pathway without methyl-H_4MPT:CoM methyltransferase (Mtr). The COGs in the β-oxidation pathway correspond to NDP-forming acyl-CoA synthetase (COG1042), AMP-forming acyl-CoA synthetase (COG0318), acyl-CoA dehydrogenase (COG1960), enoyl-CoA hydratase (COG1024), 3-hydroxyacyl-CoA dehydrogenase (COG1250) and acetyl-CoA acetyltransferase (COG0183).

Origin of alkane metabolism in Hadarchaea

To investigate the evolutionary history of Acr-based alkane metabolism in the Hadarchaea, we first determined the distribution Acr, β-oxidation and WL pathway genes in this class (Figure 4). As previously mentioned, these pathways are necessary for short- and mid-chain alkane-oxidation in *Ca*. Syntrophoarchaeum and *Ca*. Alkanophaga (Laso-Pérez et al., 2016; Zehnle et al., 2022), and long-chain alkane oxidation coupled to methanogenesis in *Ca*. Methanoliparia (Borrel et al., 2019; Laso-Pérez et al., 2019; Zhou et al., 2022). All Hadarchaea MAGs coding for an Acr belong to a single family (Figure 4) corresponding to WYZ-LMO6 in GTDB (Rinke et al., 2021), for which we propose the name *Ca*. Cerberiarchaeaceae. All MAGs from this family have a complete or almost complete pathway for alkane oxidation, including genes for β-oxidation, both branches of the WL pathway and HdrABC genes for the regeneration of CoM-CoB. Only two other Hadarachaeota outside of *Ca*. Cerbariarchaeaceae encode an almost complete WL pathway. To determine the origin of alkane oxidation in the Hadarchaea, we built a reference phylogeny of archaea and compared it to the phylogeny of enzymes of the two branches of the WL pathway (Figure 5). The phylogenies of the enzymes of the mWL pathway, i.e., formylmethanofuran dehydrogenase (FwdABC) (Figure 5B), formylmethanofuran—H_4MPT N-formyltransferase (Ftr; Figure

S6C) and methenyl-H_4MPT cyclohydrolase (Mch; Figure S6B), are mostly congruent with the reference phylogeny of Archaea (Figure 5A), supporting results of previous phylogenies (Adam et al., 2019). In particular, Hadesarchaea, Persephonearchaea and Theinoarchaea clades are closely related and form a separate clade from the Bathyarchaeota and Asgardarchaeota in Fwd and Mch phylogenies, similarly to the reference tree. Altogether this indicates that the mWL pathway was likely vertically inherited in the Hadarchaea. In contrast, for the carbonyl branch of the WL pathway (i.e., CdhABCDE), *Ca*. Cerbariarchaeaceae sequences are distantly related to those of Persephonearchaea and Theinoarchaea and branch within the Bathyarchaeota (Figure 5C). Very similar results were obtained for phylogenies based

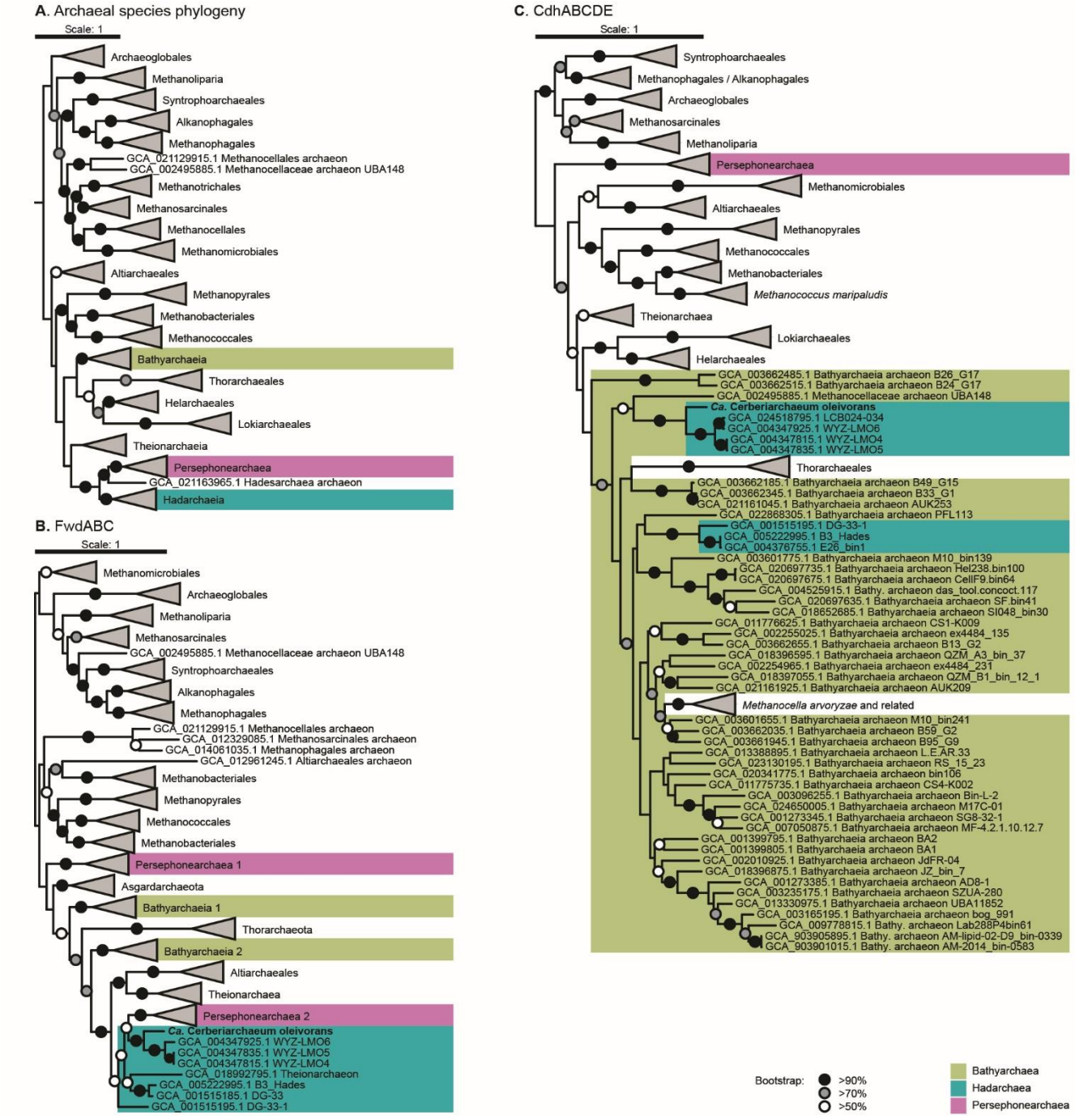

on individual Fwd and Cdh subunits (Figure S7 and Figure S8). Therefore, Hadarchaea most likely acquired the carbonyl branch of WL by HGT from Bathyarchaeota. The Acr from Hadarchaeota are closely related to sequences from two other phyla, Bathyarchaeota and Halobacterota (Ca. Methanoliparia), suggesting HGT between these lineages, but it is not possible to resolve the direction of the transfer. Based on BLASTp comparisons, the β-oxidation genes of *Ca*. C. oleivorans are also related to those of putative long-chain alkane oxidizers from phylogenetically distant lineages, such as Bathyarchaeia BA1/BA2 and *Ca*. Methanoliparia (Table S4) (Evans et al., 2015; Borrel et al., 2019). Similarly to Acr, this supports the existence of HGT between these lineages.

Discussion

Hadarchaeota was a phylum described exclusively from environmental MAGs before this study. Thus, there were no physiological studies available to link their genomic potential with growth in their ecological niches. Based on environmental MAGs and 16S rRNA sequences, Hadarchaeota are present in a broad range of subsurface anoxic environments. Many Hadarchaeota are likely extremophiles, suggested by the origin of most samples and the extremely high frequency of G-quadruplex-prone regions in their DNA, which is characteristic for heat-adapted microorganisms. (Brázda et al., 2020). Furthermore, Hadarchaea are often found at methane seeps, oil-rich and subsurface environments (Figure 6). MAGs of many Hadarchaea code for enzymes for CO and H_2 metabolism (Baker et al., 2016). Hydrogenogenic CO oxidation has been observed in microbes from heated environments (Wu et al., 2005). CO is produced geothermally or during fermentation and is an important carbon source in the subsurface (Brady et al., 2015; Colman et al., 2017). This supports the success of Hadarchaeota in such environments.

← Figure 5. Placement of Hadarchaea, Persephonearchaea and Bathyarchaeia in species genome tree, formylmethanofuran dehydrogenase (Fwd) phylogeny and carbon monoxide dehydrogenase/acetyl-CoA synthase complex (Cdh) phylogeny. Maximum-likelihood phylogenetic trees with 100 bootstraps based on concatenated alignment of 38 archaeal marker genes, FwdABC and CdhABCDE protein sequences. **A.** Hadarchaea and Persephonearchaea form a clade next to Theionarchaea. **B.** Hadarchaea Fwd sequences form a branch with the Persephonearchaea 2 sequences. **C.** Cdh sequences from the alkane-oxidising Hadarchaea clade cluster together and branch from Bathyarchaea sequences, probably as a consequence of an event of lateral gene transfer between subsurface alkane-oxidizing archaea.

The carbon metabolism in Hadarchaea seems to be highly diverse. Most Hadarchaea lack the WL pathway (Figure 4). Almost all Hadarchaea encode a gluconeogenesis pathway and the C_3-module of the glycolysis for synthesis of sugars and central building blocks, respectively. None of the Hadarchaea MAGs encodes a complete citric acid cycle or reductive citric acid cycle. Carbon assimilation might occur via the reductive pentose phosphate cycle (Pinheiro Alves de Souza and Soares Rosado, 2019). Respiratory pathways are rare in the Hadarchaeota. The dissimilatory sulfate reduction pathway is not present in Hadarchaeota. Some MAGs contain a nitrite reductase, which might be used for dissimilatory nitrite reduction to ammonia (DNRA) (Baker et al., 2016). Subsurface Hadarchaea might couple the oxidation of carbon monoxide to the reduction of H_2O to hydrogen or to DNRA, as proposed for Yellowstone MAGs (Baker et al., 2016). Because most Hadarchaea lack respiratory pathways, their predominant metabolism in deep anoxic and oil-rich environments should be the fermentation of organic compounds (Dong et al., 2019). Overall, we could not clearly resolve the metabolism of non-ANKA Hadarchaea and future research should aim to obtain cultured representatives and do further environmental mapping.

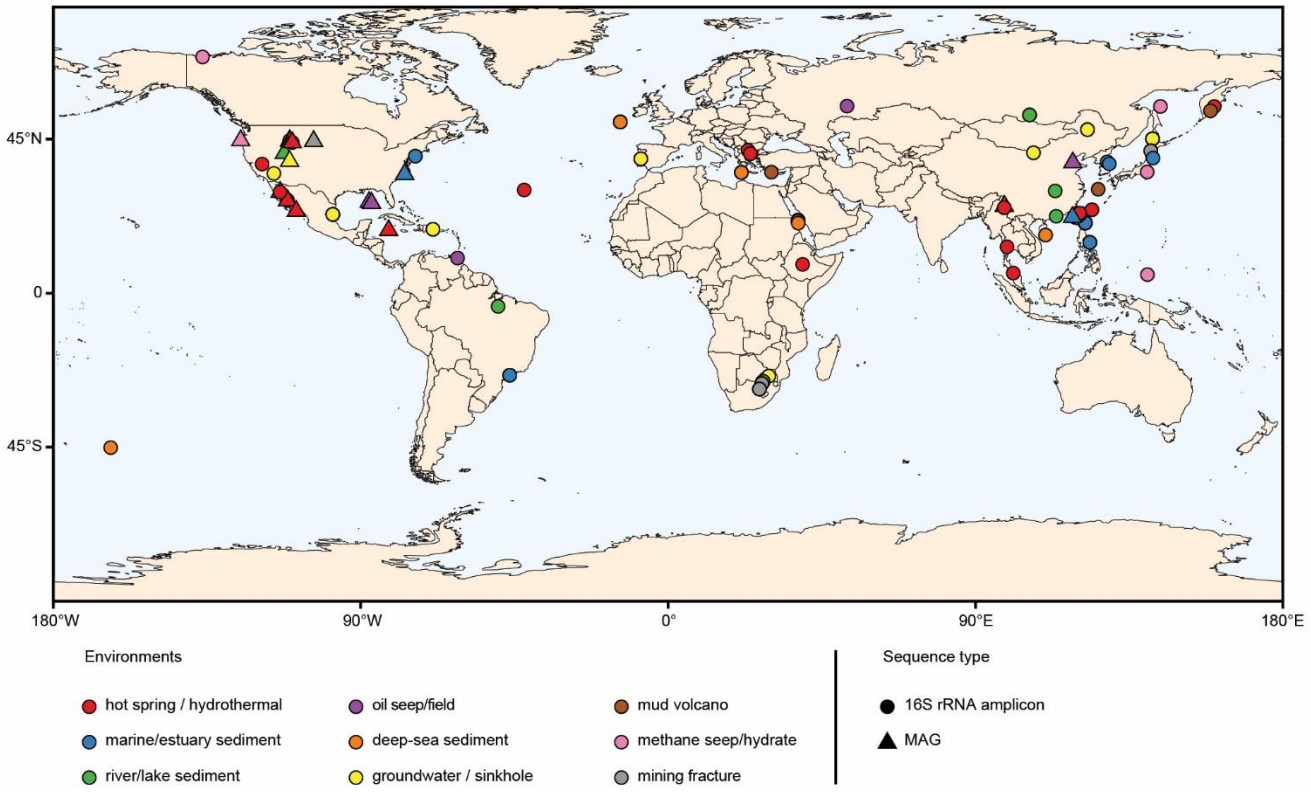

Figure 6. Global distribution of Hadarchaeota MAGs and 16S rRNA sequences. MAGs (triangles) and 16S rRNA sequences (circles) were retrieved from NCBI. Hadarchaea are globally distributed in anoxic subsurface environments and often associated with hydrothermal and alkane-rich environments.

The results of our enrichment study, together with other environmental data (Wang et al., 2019), now explain their presence in oil seeps and reservoirs. The genomic data along with the analysis of metabolites suggests that *Ca.* C. oleivorans uses an Acr to activate hexadecane to hexadecyl-CoM and can potentially oxidize the alkane completely to CO_2, supporting the proposed hypothesis for Acr-based alkane oxidation in Hadarchaea (Wang et al., 2019). This study of an enrichment culture of *Ca*. C. oleivorans suggests that it does not encode respiratory pathways or other electron sinking mechanisms. Syntrophic interactions based on transfer of molecular hydrogen or formate have been proposed (Schink, 1997). The most likely partner SRB in our culture is a *Thermodesulfobacterium*, as previously proposed for AOM and mid-chain alkane oxidation at 70°C (Benito Merino et al., 2022; Zehnle et al., 2022). Further cultivation efforts are needed to decipher this potential interaction between Hadarchaea and Thermodesulfobacteria aided by metatranscriptomics, physiological experiments and microscopy.

In the Mcr/Acr phylogeny we can distinguish four groups (Wang et al., 2020; Garcia et al., 2022). Group I contains Mcrs from CO_2-reducing methanogens and group II corresponds to methyl-reducing methanogens. Groups I and II also contain Mcrs involved in AOM. Group III contains TACK-like Mcr sequences from *Ca*. Verstraetearchaeota, *Ca*. Nezharchaeota, *Ca*. Korarchaeota, Thaumarchaeota and Archaeoglobi (Vanwonterghem et al., 2016; Colman et al., 2019; Hua et al., 2019; McKay et al., 2019; Wang et al., 2019). Group IV is a monophyletic clade including all Acrs. From cultivation of short- and medium-chain alkane-oxidizing archaea (Laso-Pérez et al., 2016; Chen et al., 2019; Hahn et al., 2020; Zehnle et al., 2022), we can infer that *Ca*. Polytropus marinifundus uses its Acr to activate alkanes within the range C_3-C_{14}, based on Acr phylogeny (Figure 3A, (Boyd et al., 2019)). Based on the results of Zhou et al. (Zhou et al., 2022) and our hexadecane70 enrichment culture, Acrs from the Hadarchaea/*Ca*. Methanoliparia clade are all likely responsible for the activation of long-chain alkanes (Figure 3A). Whether long-chain alkane Acrs are a monophyletic group should be investigated following cultivation of Bathyarchaeia and *Ca*. Helarchaeota from hydrocarbon-rich environments (Evans et al., 2015; Seitz et al., 2019).

We investigated the occurrence of pathways for Acr-based long-chain alkane oxidation in other Hadarchaeota MAGs available in public databases. Neither the WL pathway, nor the β-oxidation pathway are present in Hadarchaeota genomes outside of the *Ca*. Cerberiarchaeaceae, with the exception of two MAGs that encode an almost complete WL pathway (DG-33-1 and B3_Hades, Figure 4). In absence of the β-oxidation pathway and Acr, these two organisms might use their WL pathway for CO_2 fixation.

Previous studies suggested that Acr-based alkane-oxidation was transferred multiple times via HGTs in Archaea, but the direction of these transfers could not be resolved for most of the enzymes (Wang et al., 2021). However, we found that *Ca*. Cerberiarchaeaceae likely acquired the carbonyl branch of the WL pathway through HGT from Bathyarchaeota, similarly to what as already been proposed for *Methanocella arvoryzae* (Adam et al., 2018). Because this step is likely mandatory for the Acr-based alkane-oxidation, this transfer indicates that the last common ancestor of Hadarchaea was likely not an ANKA and that this metabolism was acquired by HGT, at the base of the *Ca*. Cerberiarchaeaceae. In this context, other steps of the Acr-based alkane-oxidation could have been gained by HGT in *Ca*. Cerberiarchaeaceae, and in particular Acr and the β-oxidation pathway. These genes might have been horizontally acquired from Bathyarchaeaota and/or Ca. Methanoliparia also dwelling in subsurface hydrothermal and oil-rich environments. In contrast, the mWL was vertically inherited from the LACA to Hadarchaeaota and lost in members of the phylum lacking the pathway.

Overall, our study highlights the need to sample new locations and to use cultivation-based approaches to understand the extension, evolution and physiology of Acr-based alkane metabolism in Hadarchaea and other archaea from extreme environments.

Acknowledgements

We thank Andreas Teske and the scientific party and the crews of RV Atlantis missions AT37-06 and AT42-05 with submarine Alvin for their outstanding work. We thank Halina Tegetmeyer for amplicon sequencing and Matthew Schechter for analysis. Furthermore, we thank Mirja Meiners and Susanne Menger for their assistance in laboratory work and cultivation.

Ethics Declarations

Competing interests

The authors declare no competing interests.

Author Contributions

GW and DBM designed the study. GW retrieved samples on board and established enrichment cultures. DBM did cultivation, laboratory experiments and bioinformatics analysis. JSL performed LC-MS analyses. DBM wrote the manuscript with contributions of all coauthors.

Funding

This study was funded by the Max Planck Society and the DFG under Germany's Excellence Intiative/Strategy through the Clusters of Excellence EXC 2077 "The Ocean Floor–Earth's Uncharted Interface" (project no. 390741601). The Guaymas Basin expeditions were supported by the National Science Foundation, Biological Ocenography grant no. 1357238 to Andreas Teske (Collaborative Research: Microbial Carbon cycling and its interactions with Sulfur and Nitrogen transformations in Guaymas Basin hydrothermal sediments). Metagenome sequencing was done in the frame of Census of Deep Life Phase 14 call (Deep Carbon Observatory) granted to DBM and GW.

Supplementary Information

All supplementary information is available under https://keeper.mpdl.mpg.de/d/7db3b61d55154ed09f71

Extended data. Alignments used for phylogenetic tree calculations.

Description of proposed species *Candidatus* Cerberiarchaeum oleivorans and family *Ca.* Cerberiarchaeaceae

Candidatus Cerberiarchaeum: Cer.be.ri.ar.chae'um. N.L. neut. n. *archaeum*, archaeon, from Gr. adj. archaios, ancient; N.L. neut. N. *Cerberiarchaeum*, archaeon named after Cerberus (gen. *Cerberi*), the three-headed hound that guards the gates of the Underworld in the Greek mythology, in relation with the affiliation of this organism with Hadarchaea. *Candidatus* Cerberiarchaeum oleivorans: o.le.i.vo'rans. N.L. neut. n. *oleum*, oil (gen. *olei*), and *vorans*, N.L. v., eating, devouring, oil-eating *Cerberiarchaeum*.

Family Cerberiarchaeaceae: Cer.be.ri.ar.chae.a'ce.ae. N.L. neut. N. *Cerberiarchaeum* and *–aceae*, a suffix for family; N.L. fem. pl. *Cerberiarchaeaceae*, the Cerberiarchaeum family.

Supplementary figures

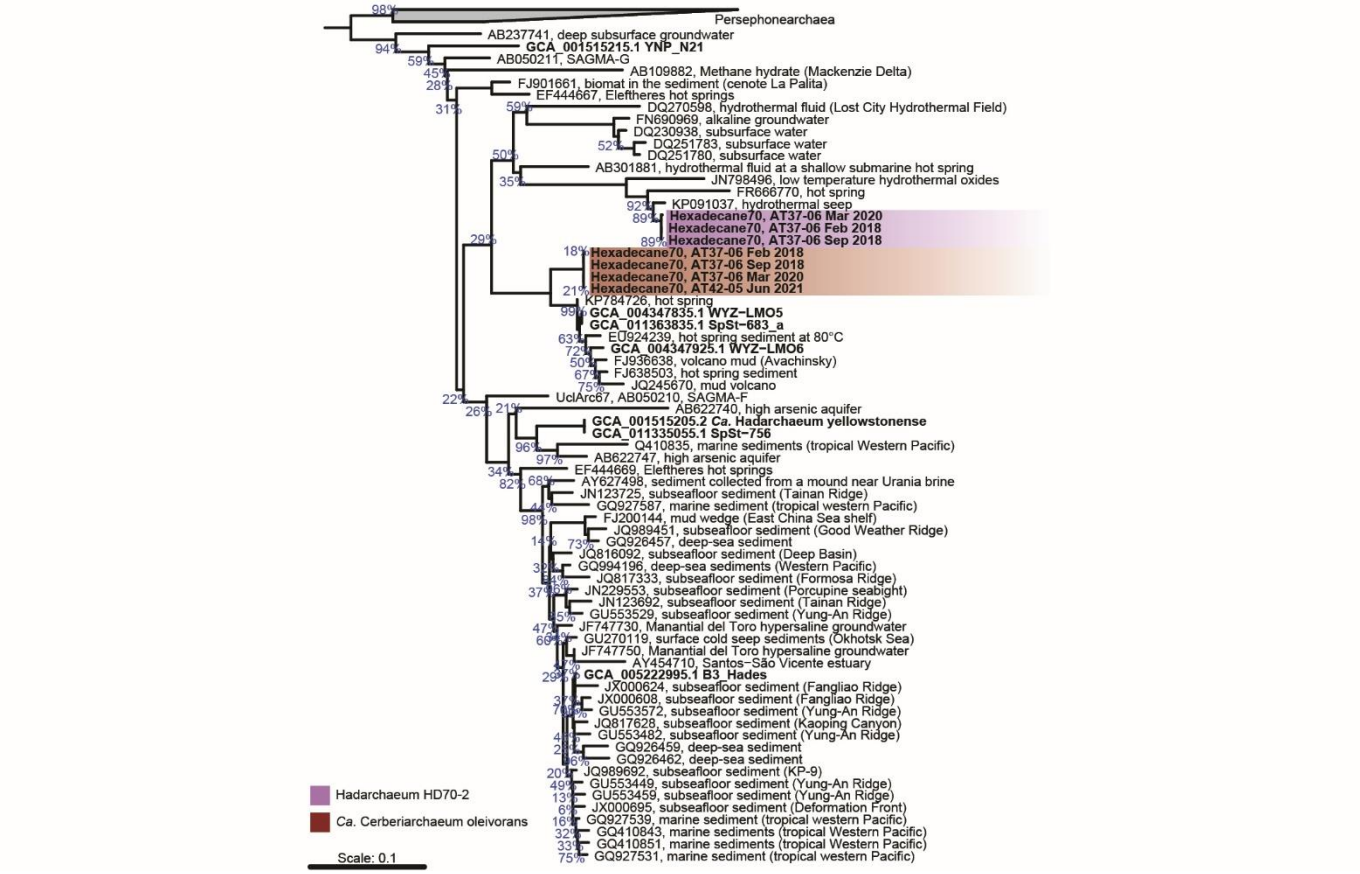

Figure S1. Placement of Hadarchaeota 16S rRNA genes in 16S rRNA gene phylogeny. Subset of 16S rRNA gene phylogeny of Archaea showing the Hadarchaeota and Persephonearchaea clades. Hadarchaeota sequences from 4 metagenomic samples of the hexadecane70 enrichment are shown in bold and highlighted in red squares. 16S rRNA genes of Hadarchaeota MAGs are shown in bold. Blue numbers at the branches indicate bootstrap support. 300 archaeal sequences from the SILVA database (Quast et al., 2013) were aligned with the SINA alignment tool (Pruesse et al., 2012). Maximum likelihood trees with 300 iterations were calculated with RAxML v. 7 (Stamatakis, 2014) and the tree was visualized with the ARB software (Ludwig et al., 2004).

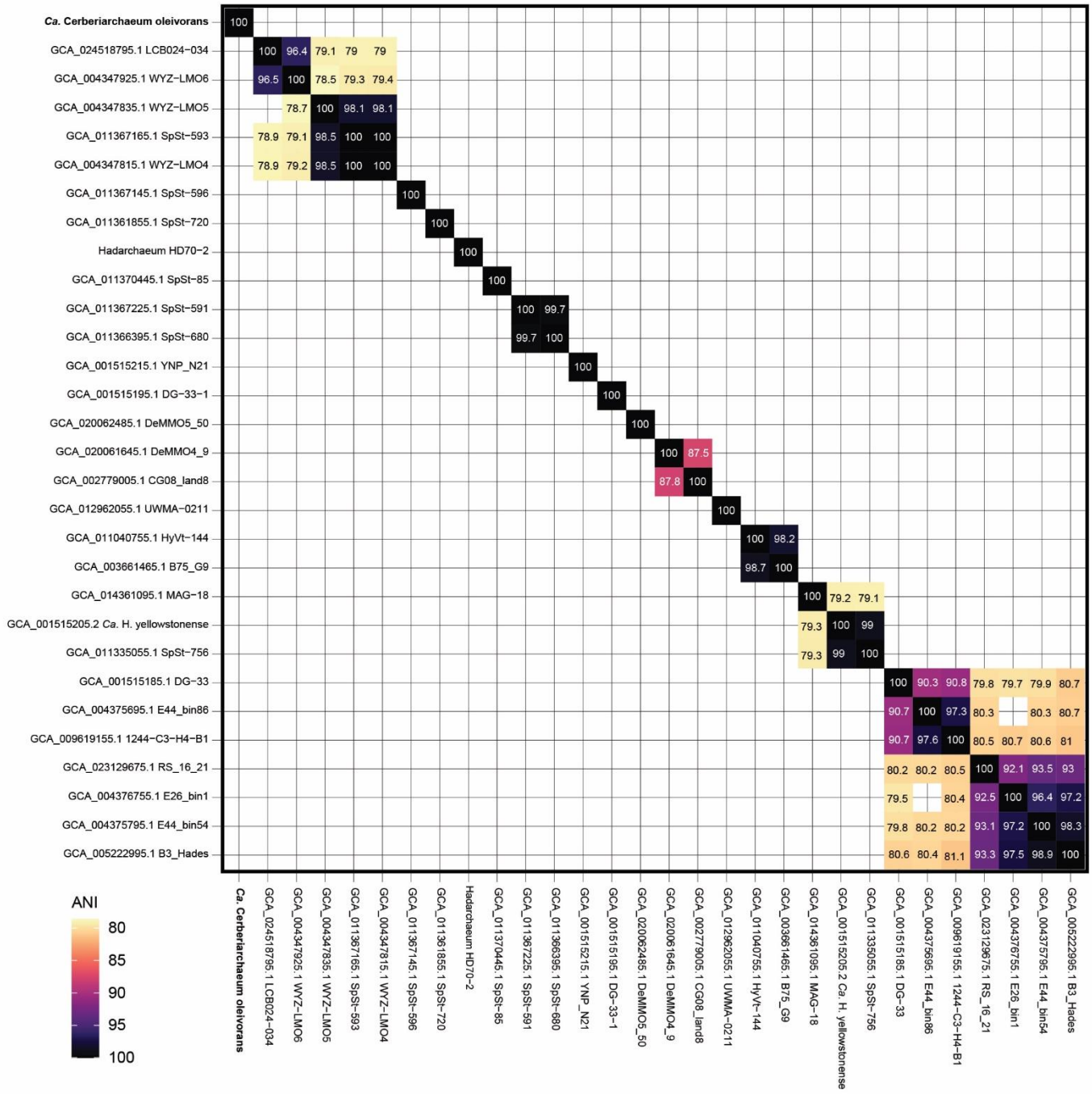

Figure S2. Average nucleotide identity between Hadarchaeota MAGs. ANI was calculated with FastANI (Jain et al., 2018). Values below 75% are not shown.

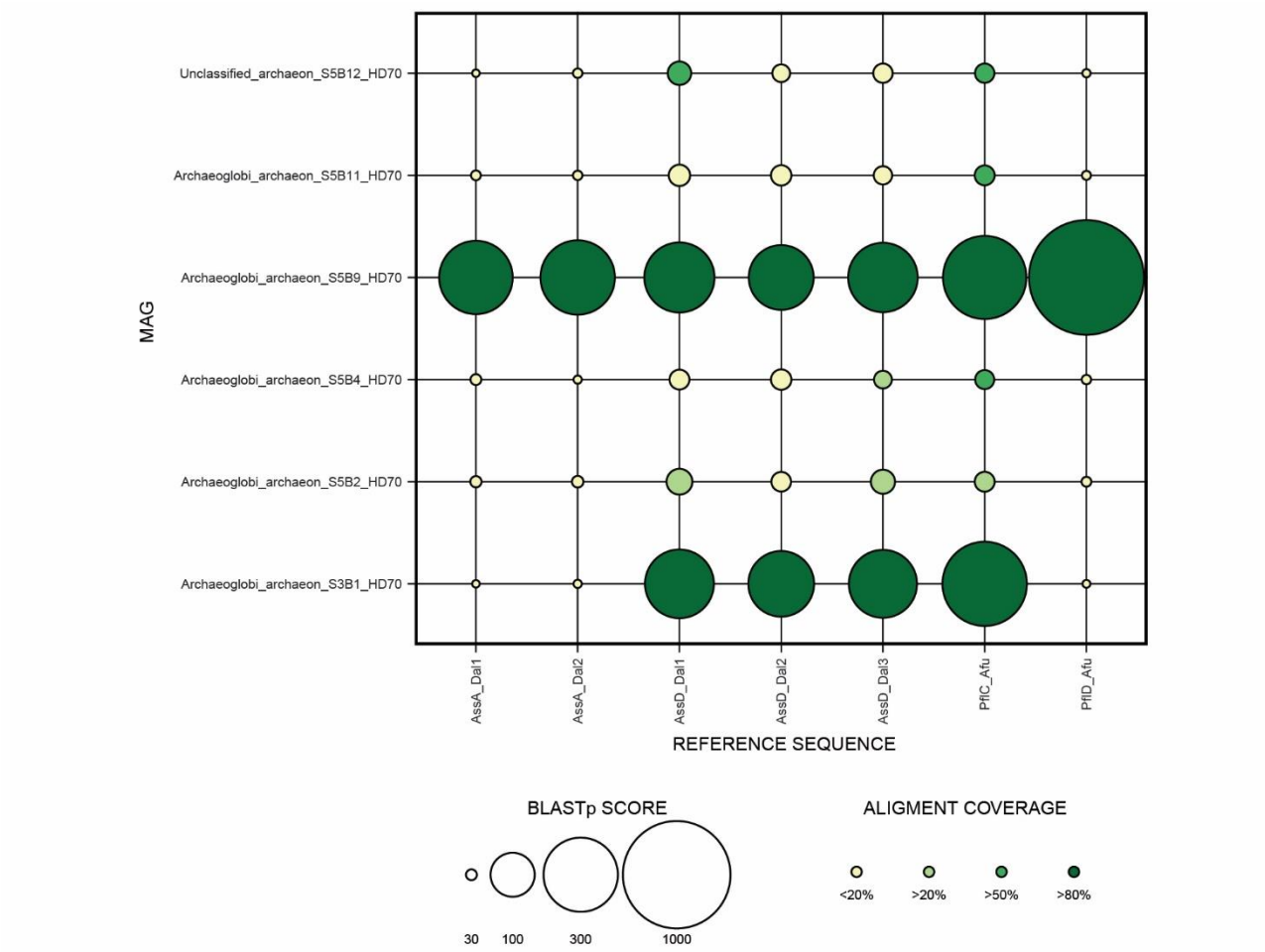

Figure S3. BLASTp search of Ass/Pfl genes in Archaeoglobi MAGs. The AssA and AssD of *Desulfatibacillum alkenivorans* and the PflC and PflD of *Archaeoglobus fulgidus* were queried against the proteins of Archaeoglobi MAGs. Darker colors represent longer sequence alignments and circle size represents higher BLASTp scores.

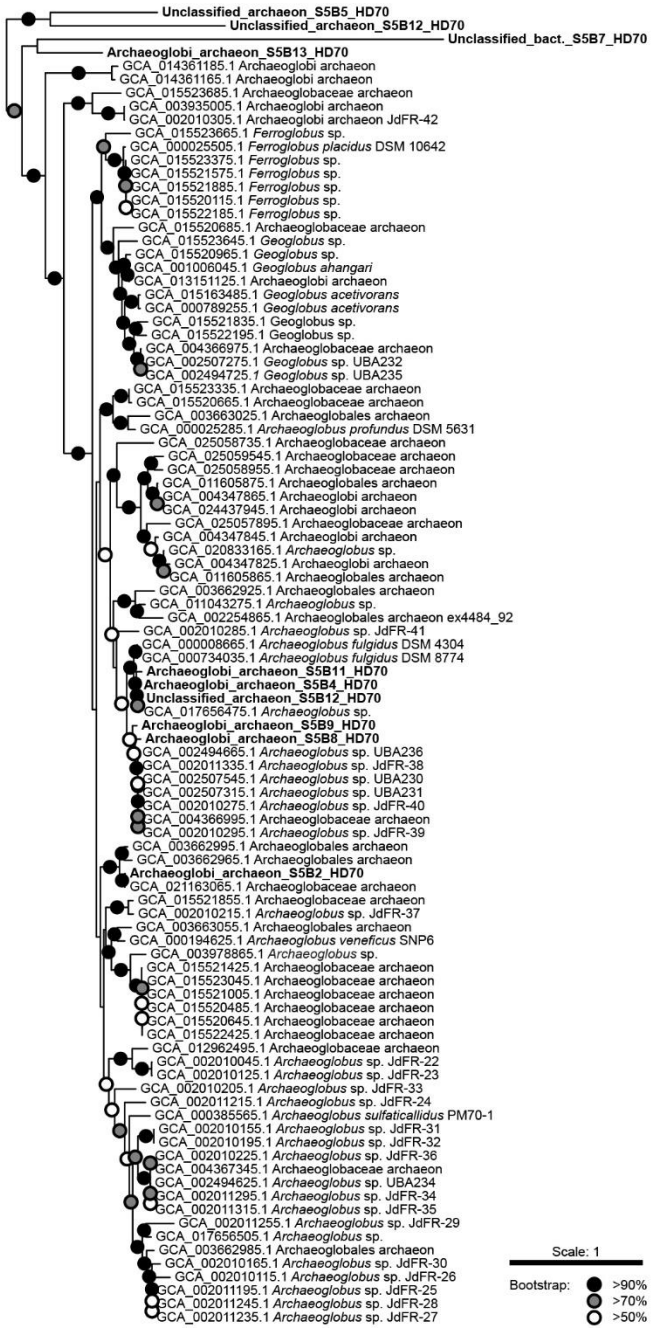

Figure S4. Placement of Archaeoglobi MAGs in phylogenomic species tree. Subset of species genome tree, showing Archaeoglobi and related MAGs. 38 archaeal marker proteins (Darling et al., 2014) were aligned with muscle (Edgar, 2004) and a concatenated alignment was generated in anvi'o v.6 (Eren et al., 2020). The maximum likelihood tree was calculated in IQTree using 100 bootstraps and the –test option to estimate the best substitution model for each protein (Minh et al., 2020).

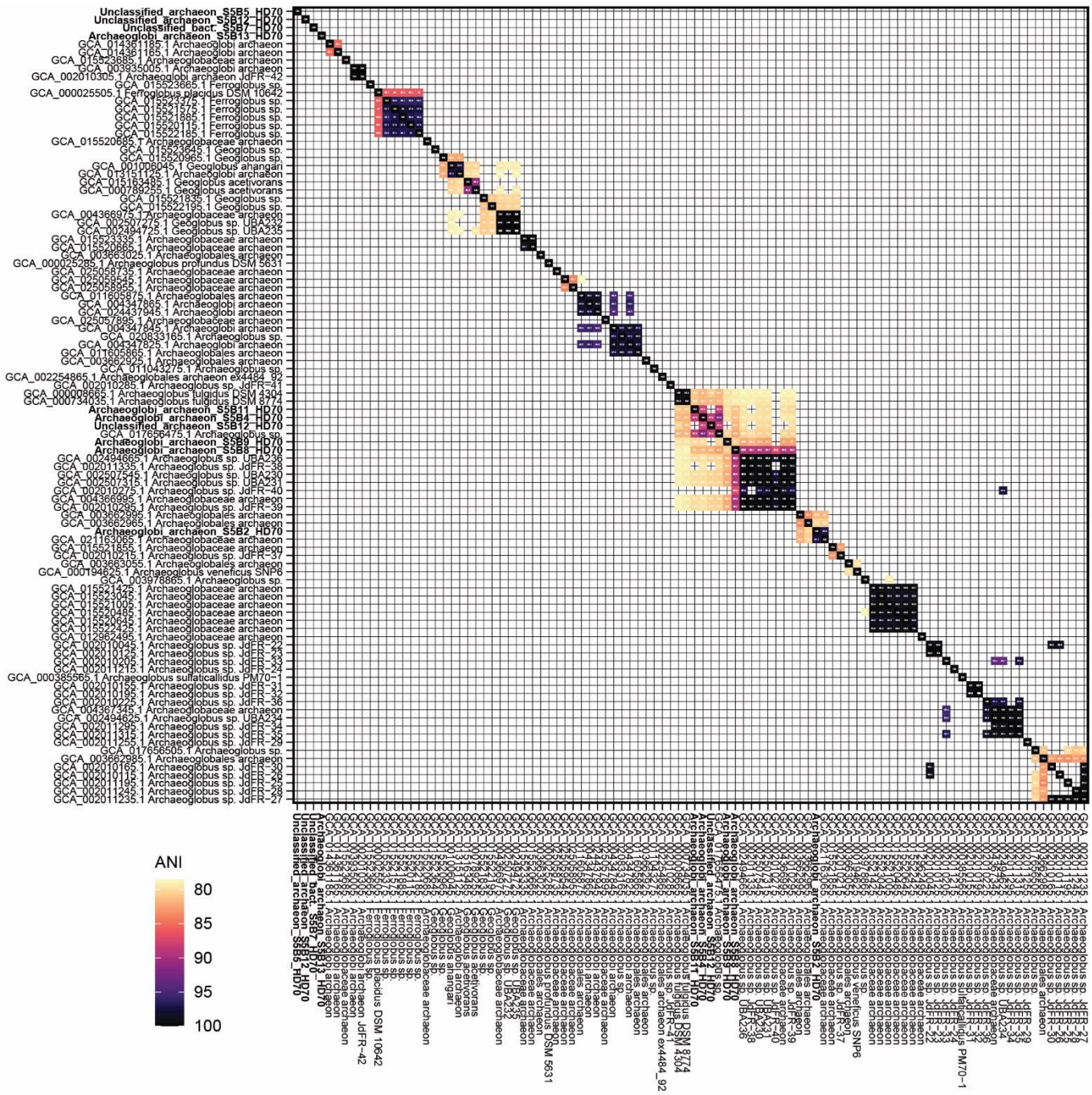

Figure S5. Average nucleotide identity between Archaeoglobi MAGs. The MAGs appear in the same order as in Figure S4. ANI was calculated with FastANI (Jain et al., 2018). Values below 75% are not shown.

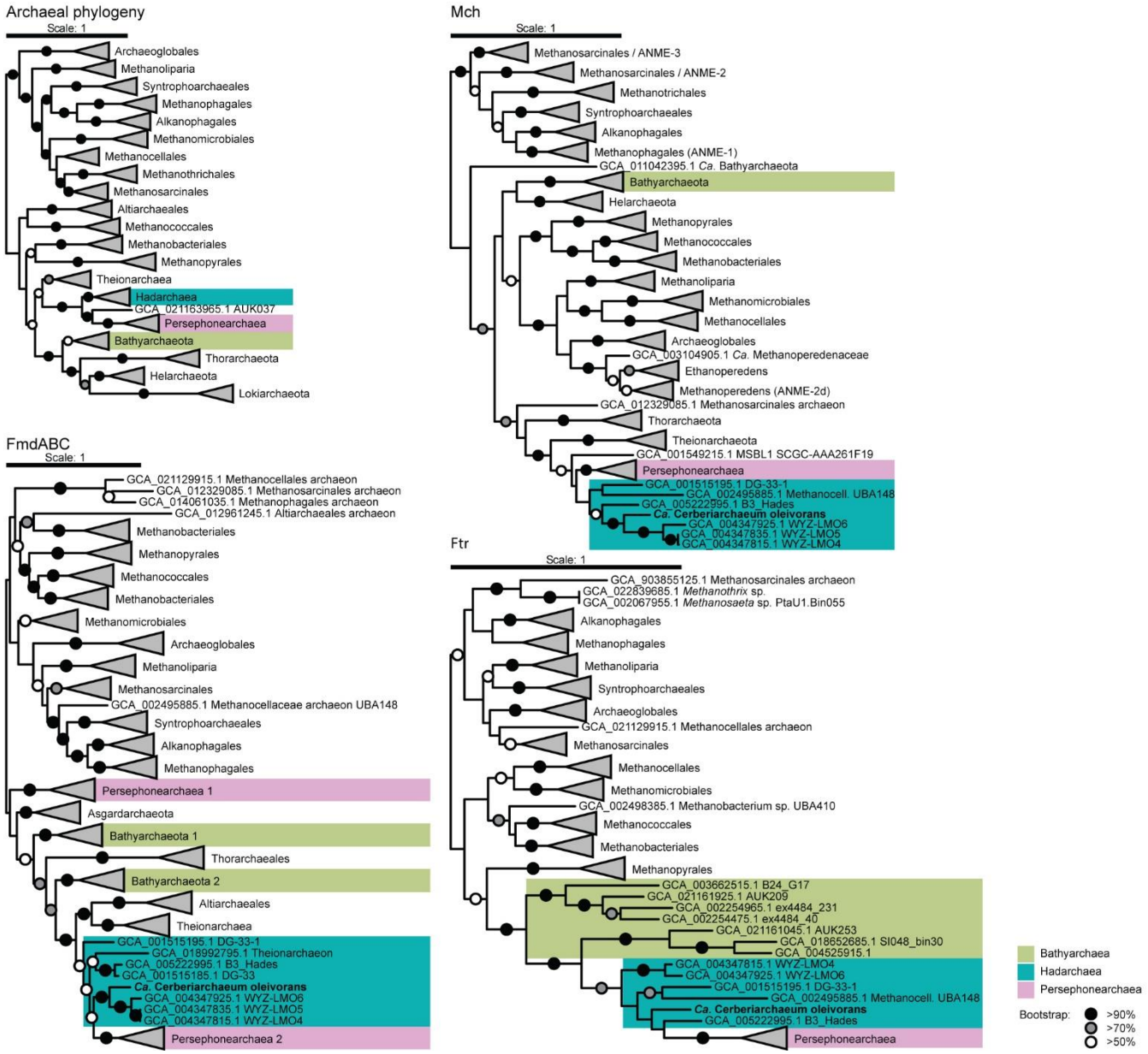

Figure S6. Placement of Hadarchaea in archaeal phylogenomic tree and in Mch, Fwd and Ftr phylogenies. Archaeal marker proteins and FwdABC phylogenies were done as in Figure S4. For Mch and Ftr, proteins predicted from PFAM models (Mistry et al., 2021) were aligned with muscle (Edgar, 2004). Maximum likelihood trees with 100 bootstraps were calculated with IQTree (Minh et al., 2020).

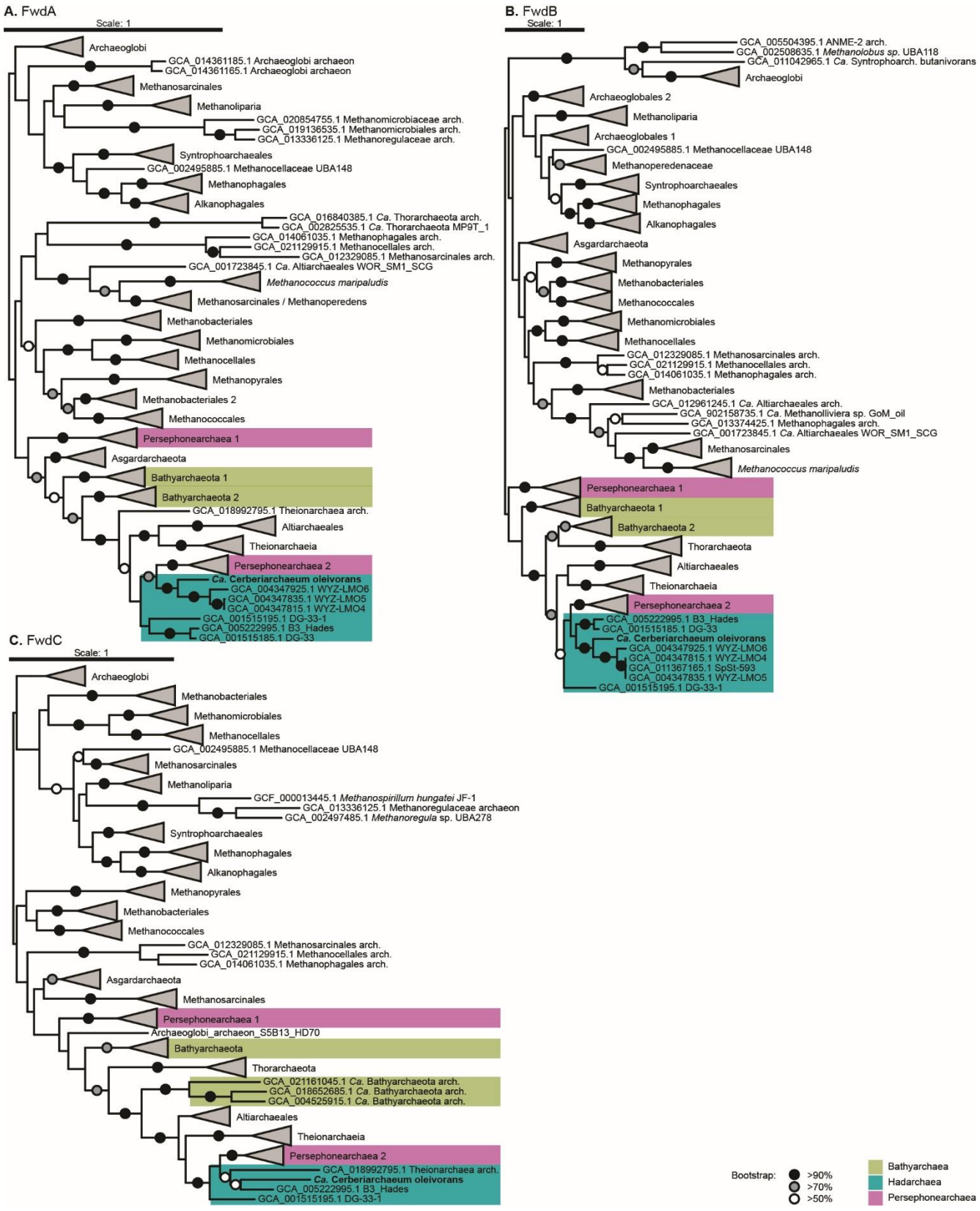

Figure S7. Phylogenies of formylmethanofuran dehydrogenase subunits A, B and C. The Fwd proteins were predicted using PFAMs (Mistry et al., 2021). Single proteins were aligned with muscle (Edgar, 2004) and the trees were calculated in IQTree with 100 bootstraps (Minh et al., 2020).

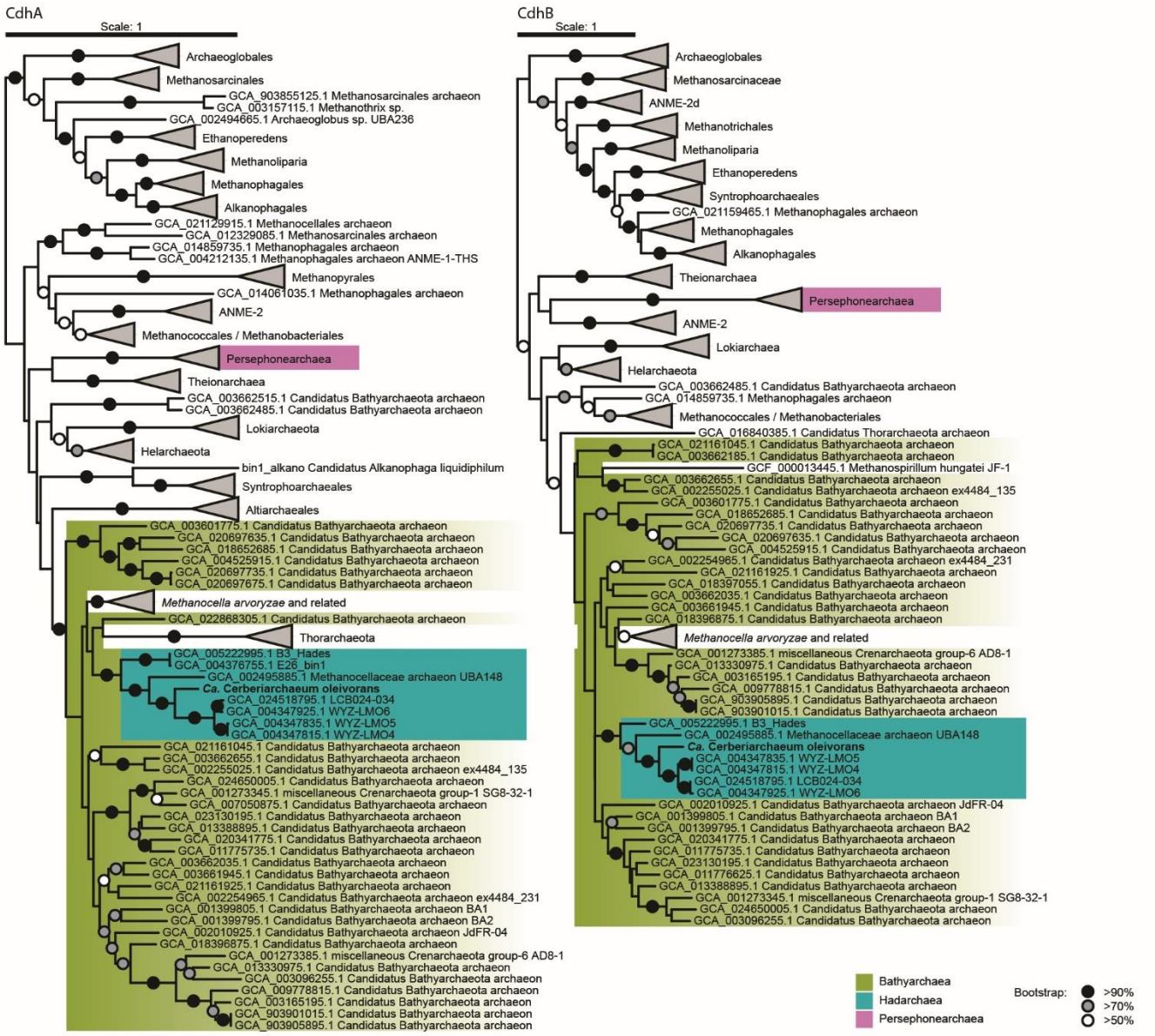

Figure S8. Phylogenies of Cdh subunits A, B, C, D and E. The Cdh proteins were predicted using custom hidden Markov models (Adam et al., 2018). Single proteins were aligned with muscle (Edgar, 2004) and the trees were calculated in IQTree with 100 bootstraps (Minh et al., 2020).

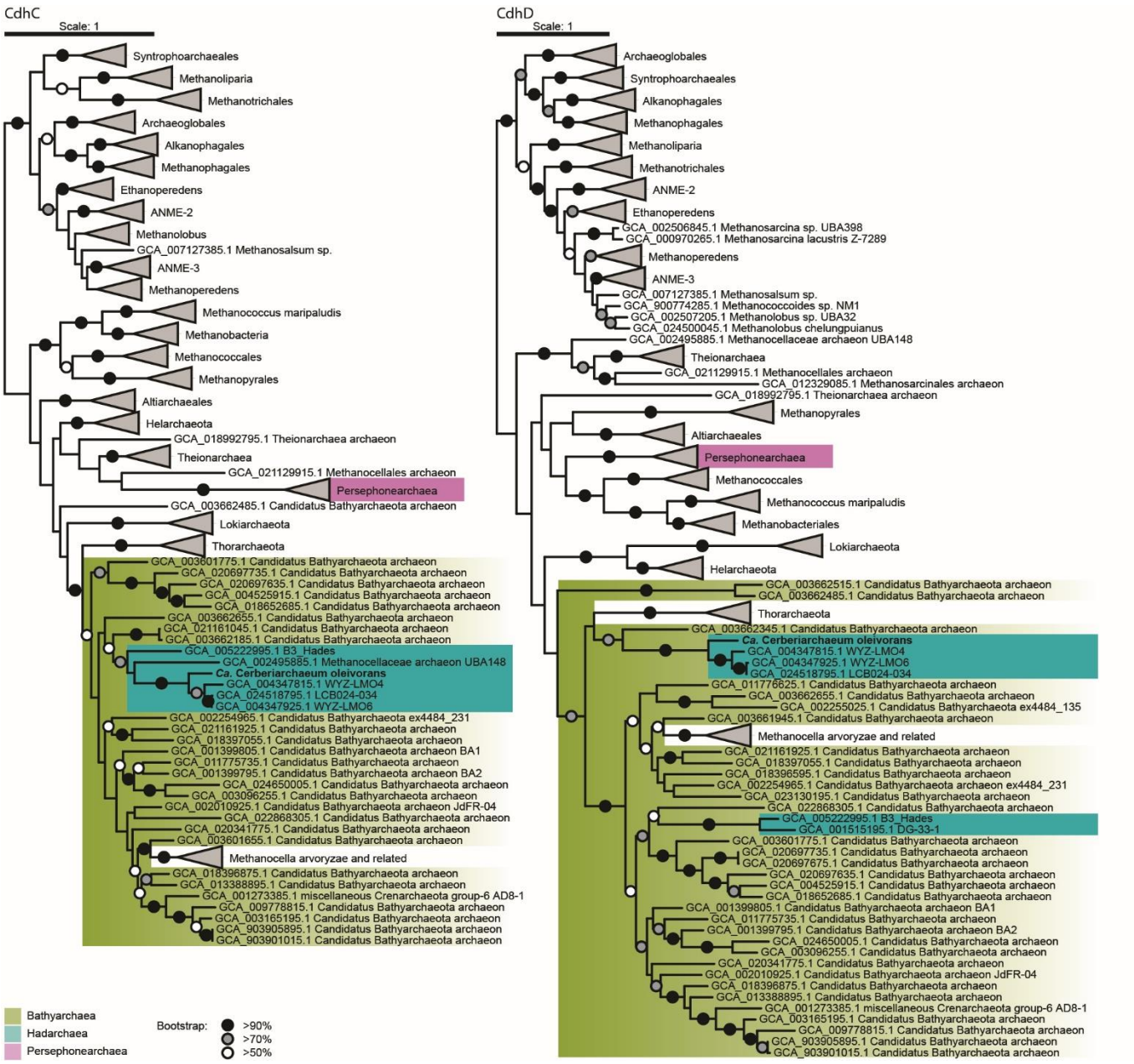

Figure S8 (continued). Phylogenies of Cdh subunits A, B, C, D and E.

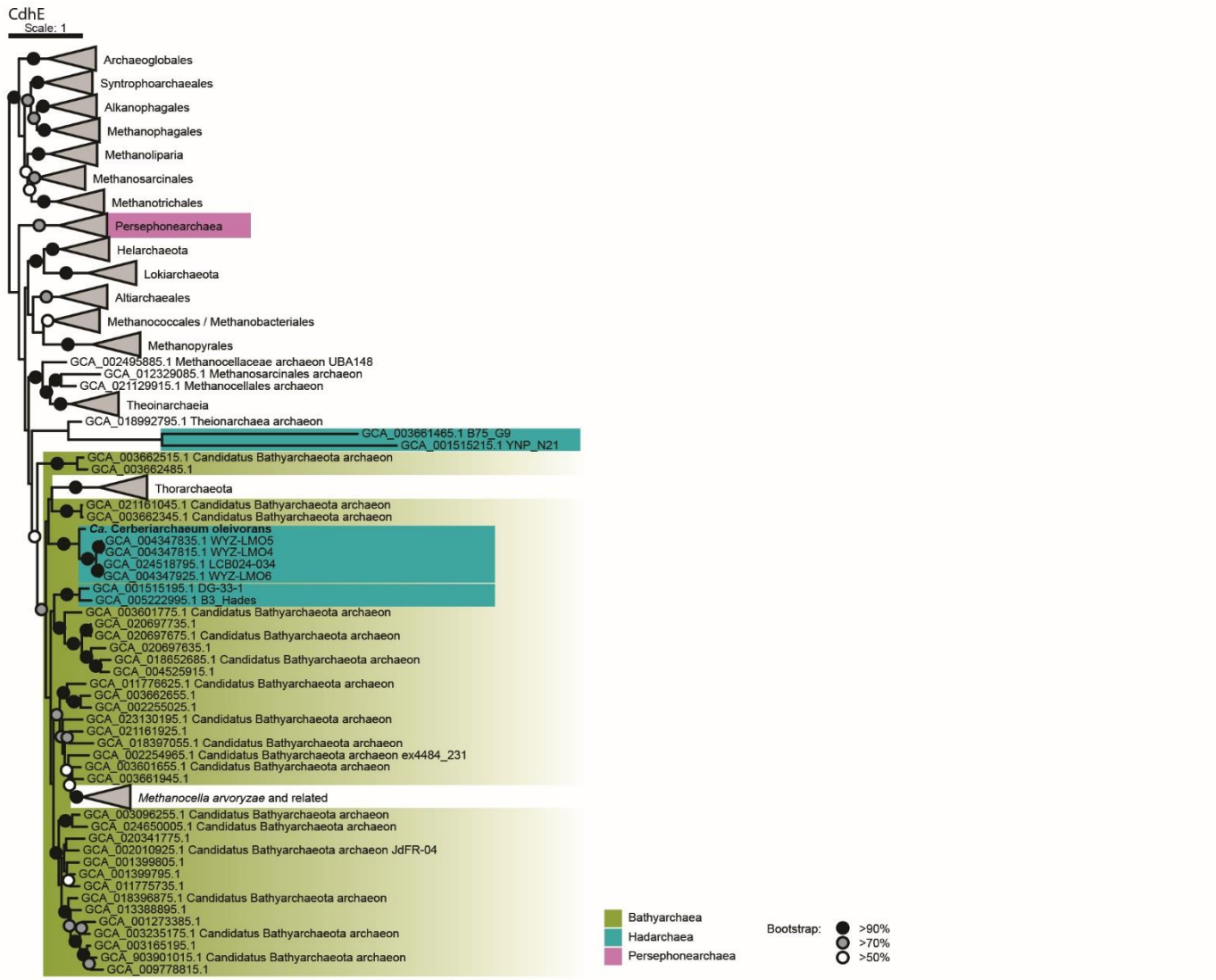

Figure S8 (continued). Phylogenies of Cdh subunits A, B, C, D and E.

Supplementary tables

Table S1. Genomes used in phylogenomics of Archaea and archaeal single copy marker genes.

Table S2. Metagenome-assembled genomes from hexadecane70 enrichment metagenomes.

Table S3. Annotation of MAGs described in the text.

Table S4. Best BLASTp hit of *Candidatus* Cerberiarchaeum oleivorans β-oxidation genes.

Gene locus	Selected BLASTp hits						
	Protein name	Organism	Accession	Total_score	Query_cover	E_value	%_identity
14623	Hypothetical protein EF807_00505	*Candidatus* Methanolliviera hydrocarbonicum	RZN73546.1	573	94%	0	59.44
29938	CoA-binding protein	Hadesarchaea archaeon	MCQ8898407.1	679	94%	0	76.19
	Succinyl-CoA ligase (ADP-forming) subunit alpha	*Candidatus* Methanolliviera sp. GoM_oil	VUT25164.1	622	94%	0	64.87
29950	Hypothetical protein DRO51_00170	*Candidatus* Bathyarchaeota archaeon	RLI33118.1	633	97%	0	64.36
34007	Hypothetical protein DSO02_04150	Hadesarchaea archaeon	TDA33499.1	761	98%	0	74.38
	Acetyl-CoA synthetase II (ACSII, ADP-forming) subunit alpha	*Candidatus* Bathyarchaeota archaeon BA2	KPV61898.1	496	93%	2.00E-169	53.1
63154	Acetyl-CoA synthetase	Hadesarchaea archaeon	TDA33370.1	361	99%	1.00E-123	72.03
	Acetyl-CoA synthetase	*Candidatus* Bathyarchaeota archaeon	HDO80133.1	279	96%	3.00E-91	58.95
28029	Long-chain fatty acid--CoA ligase	*Candidatus* Bathyarchaeota archaeon	RLI40557.1	546	84%	0	57.02
29725	Long-chain fatty acid--CoA ligase	Hadesarchaea archaeon	TDA32376.1	972	99%	0	80.67
	Acetyl-coenzyme A synthetase	*Candidatus* Bathyarchaeota archaeon BA2	KPV63969.1	647	98%	0	59.29
29759	Acyl--CoA ligase	Hadesarchaea archaeon	MCQ8898706.1	626	98%	0	62.2
	AMP-binding protein	*Candidatus* Bathyarchaeota archaeon	MBE0512054.1	369	94%	2.00E-118	43.33
29955	Acyl-CoA dehydrogenase family protein	Hadesarchaea archaeon	MCQ8898411.1	541	97%	0	67.52
	Acyl-CoA dehydrogenase family protein	*Candidatus* Bathyarchaeota archaeon	MCJ7455123.1	368	98%	2.00E-121	45.32

34889	Acyl-CoA/acyl-ACP dehydrogenase	Deltaproteobacteria bacterium	MBN1102166.1	256	91%	4.00E-78	44.2
	Acyl-CoA dehydrogenase	*Candidatus* Bathyarchaeota archaeon	RLI05015.1	244	91%	1.00E-73	42.54
34909	Acyl-CoA dehydrogenase family protein	*Candidatus* Bathyarchaeota archaeon	MCJ7455123.1	521	99%	0	58.75
34911	acyl-CoA dehydrogenase	Hadesarchaea archaeon	TDA32889.1	704	80%	0	81.95
	acyl-CoA dehydrogenase	*Candidatus* Bathyarchaeota archaeon	RLI00598.1	550	79%	0	65.74
44855	Hypothetical protein DSO04_05985	Hadesarchaea archaeon	TDA30402.1	756	100%	0	84.49
	acyl-CoA/acyl-ACP dehydrogenase	Deltaproteobacteria bacterium	MBP6939892.1	539	100%	0	59.86
45021	Acyl-CoA dehydrogenase	Hadesarchaea archaeon	TDA32016.1	715	100%	0	78.09
	acyl-CoA/acyl-ACP dehydrogenase	*Archaeoglobus* sp.	MBO8179407.1	453	99%	6.00E-154	54.08
49205	Acyl-CoA dehydrogenase	Hadesarchaea archaeon	TDA33325.1	668	100%	0	77.11
	Putative acyl-CoA dehydrogenase	*Candidatus* Bathyarchaeota archaeon BA2	KPV63971.1	631	100%	0	73.96
63115	Acyl-CoA dehydrogenase	Hadesarchaea archaeon	TDA35712.1	157	81%	2.00E-43	82.42
29763	Hypothetical protein DSO02_02765	Hadesarchaea archaeon	TDA34249.1	474	99%	3.00E-167	84.33
	Enoyl-CoA hydratase/isomerase family protein	*Candidatus* Bathyarchaeota archaeon	MBE0513307.1	389	96%	1.00E-133	70.3
16901	3-hydroxyacyl-CoA dehydrogenase	Hadesarchaea archaeon	MCQ8898368.1	437	95%	1.00E-148	57.14
	3-hydroxybutyryl-CoA dehydrogenase	*Candidatus* Bathyarchaeota archaeon	RLI31426.1	294	96%	2.00E-92	41.37
29764	3-hydroxyacyl-CoA dehydrogenase	Hadesarchaea archaeon	MCQ8898353.1	685	100%	0	82.49
	3-hydroxyacyl-CoA dehydrogenase	*Candidatus* Bathyarchaeota archaeon	MBE0512998.1	593	100%	0	71.07
16930	Thiolase domain-containing protein	Hadesarchaea archaeon	TDA32181.1	655	99%	0	83.16
23696	Acetyl-CoA C-acetyltransferase	Hadesarchaea archaeon	TDA33422.1	707	98%	0	83.42
	Acetyl-CoA C-acetyltransferase	*Candidatus* Methanolliviera hydrocarbonicum	RZN68012.1	540	99%	0	65.93
29946	Hypothetical protein DSO04_03510	Hadesarchaea archaeon	TDA31690.1	688	99%	0	81.82
	3-ketoacyl-CoA thiolase	*Candidatus* Bathyarchaeota archaeon	MBE0512076.1	641	100%	0	77.08

29958	Acetyl-CoA acetyltransferase	Hadesarchaea archaeon	TDA36457.1	713	99%	0	83.12
	Acetyl-CoA acetyltransferase	*Candidatus* Methanolliviera hydrocarbonicum	RZN68834.1	635	98%	0	73.67
40132	hypothetical protein DSO02_00745	Hadesarchaea archaeon	TDA36159.1	669	95%	0	80.3
	Putative acyltransferase	*Candidatus* Bathyarchaeota archaeon BA2	KPV62937.1	555	99%	0	66.02

References

Adam, P. S., Borrel, G., and Gribaldo, S. (2018). Evolutionary history of carbon monoxide dehydrogenase/acetyl-CoA synthase, one of the oldest enzymatic complexes. *Proc. Natl. Acad. Sci.* 115, E1166–E1173. doi: 10.1073/PNAS.1716667115.

Adam, P. S., Borrel, G., and Gribaldo, S. (2019). An archaeal origin of the Wood–Ljungdahl H4MPT branch and the emergence of bacterial methylotrophy. *Nat. Microbiol.* 4, 2155–2163. doi: 10.1038/s41564-019-0534-2.

Altschul, S. F., Gish, W., Miller, W., Myers, E. W., and Lipman, D. J. (1990). Basic local alignment search tool. *J. Mol. Biol.* 215, 403–410. doi: 10.1016/S0022-2836(05)80360-2.

Anderson, I., Risso, C., Holmes, D., Lucas, S., Copeland, A., Lapidus, A., et al. (2011). Complete genome sequence of Ferroglobus placidus AEDII12DO. *Stand. Genomic Sci.* 5, 50. doi: 10.4056/SIGS.2225018.

Baker, B. J., Saw, J. H., Lind, A. E., Lazar, C. S., Hinrichs, K. U., Teske, A. P., et al. (2016). Genomic inference of the metabolism of cosmopolitan subsurface Archaea, Hadesarchaea. *Nat. Microbiol.* 1, 1–7. doi: 10.1038/nmicrobiol.2016.2.

Bankevich, A., Nurk, S., Antipov, D., Gurevich, A. A., Dvorkin, M., Kulikov, A. S., et al. (2012). SPAdes: A New Genome Assembly Algorithm and Its Applications to Single-Cell Sequencing. *J. Comput. Biol.* 19, 455–477. doi: 10.1089/cmb.2012.0021.

Bazylinski, D. A., Wirsen, C. O., and Jannasch, H. W. (1989). Microbial Utilization of Naturally Occurring Hydrocarbons at the Guaymas Basin Hydrothermal Vent Site. *Appl. Environ. Microbiol.* 55, 2832–2836. doi: 10.1128/AEM.55.11.2832-2836.1989.

Benito Merino, D., Zehnle, H., Teske, A., and Wegener, G. (2022). Deep-branching ANME-1c archaea grow at the upper temperature limit of anaerobic oxidation of methane. *Front. Microbiol.* 13, 1–16. doi: 10.3389/fmicb.2022.988871.

Birkeland, N.-K., Schönheit, P., Poghosyan, L., Fiebig, A., and Klenk, H.-P. (2017). Complete genome sequence analysis of Archaeoglobus fulgidus strain 7324 (DSM 8774), a hyperthermophilic archaeal sulfate reducer from a North Sea oil field. *Stand. Genomic Sci.* 12, 1–9. doi: 10.1186/s40793-017-0296-5.

Boetius, A., Ravenschlag, K., Schubert, C. J., Rickert, D., Widdel, F., Gieseke, A., et al. (2000). A marine microbial consortium apparently mediating anaerobic oxidation of methane. *Nature* 407, 623–626. doi: 10.1038/35036572.

Borrel, G., Adam, P. S., McKay, L. J., Chen, L.-X., Sierra-García, I. N., Sieber, C. M. K., et al. (2019). Wide diversity of methane and short-chain alkane metabolisms in uncultured archaea. *Nat. Microbiol.* 4, 603–613. doi: 10.1038/s41564-019-0363-3.

Boyd, J. A., Jungbluth, S. P., Leu, A. O., Evans, P. N., Woodcroft, B. J., Chadwick, G. L., et al. (2019). Divergent methyl-coenzyme M reductase genes in a deep-subseafloor Archaeoglobi. *ISME J.*, 1. doi: 10.1038/s41396-018-0343-2.

Brady, A. L., Sharp, C. E., Grasby, S. E., and Dunfield, P. F. (2015). Anaerobic carboxydotrophic bacteria in geothermal springs identified using stable isotope probing. *Front. Microbiol.* 6, 1–10. doi: 10.3389/fmicb.2015.00897.

Brázda, V., Luo, Y., Bartas, M., Kaura, P., Porubiaková, O., Šťastný, J., et al. (2020). G-Quadruplexes in the Archaea Domain. *Biomolecules* 10, 1–23. doi: 10.3390/BIOM10091349.

Burggraf, S., Jannasch, H. W., Nicolaus, B., and Stetter, K. O. (1990). Archaeoglobus profundus sp. nov., Represents a New Species within the Sulfate-reducing Archaebacteria. *Syst. Appl. Microbiol.* 13, 24–28. doi: 10.1016/S0723-2020(11)80176-1.

Callahan, B. J., McMurdie, P. J., Rosen, M. J., Han, A. W., Johnson, A. J. A., and Holmes, S. P. (2016). DADA2: High-resolution sample inference from Illumina amplicon data. *Nat. Methods* 13, 581–583. doi: 10.1038/nmeth.3869.

Chen, S.-C., Musat, N., Lechtenfeld, O. J., Paschke, H., Schmidt, M., Said, N., et al. (2019). Anaerobic oxidation of ethane by archaea from a marine hydrocarbon seep. *Nat. 2019*, 1. doi: 10.1038/s41586-019-1063-0.

Chuvochina, M., Rinke, C., Parks, D. H., Rappé, M. S., Tyson, G. W., Yilmaz, P., et al. (2019). The importance of designating type material for uncultured taxa. *Syst. Appl. Microbiol.* 42, 15–21. doi: 10.1016/j.syapm.2018.07.003.

Colman, D. R., Lindsay, M. R., and Boyd, E. S. (2019). Mixing of meteoric and geothermal fluids supports hyperdiverse chemosynthetic hydrothermal communities. *Nat. Commun. 2019 101* 10, 1–13. doi: 10.1038/s41467-019-08499-1.

Colman, D. R., Poudel, S., Stamps, B. W., Boyd, E. S., and Spear, J. R. (2017). The deep, hot biosphere: Twenty-five years of retrospection. *Proc. Natl. Acad. Sci.* 114, 6895–6903. doi: 10.1073/pnas.1701266114.

Cord-Ruwisch, R. (1985). A quick method for the determination of dissolved and precipitated sulfides in cultures of sulfate-reducing bacteria. *J. Microbiol. Methods* 4, 33–36.

Darling, A. E., Jospin, G., Lowe, E., Matsen, F. A., Bik, H. M., and Eisen, J. A. (2014). PhyloSift: phylogenetic analysis of genomes and metagenomes. *PeerJ* 2, e243. doi: 10.7717/peerj.243.

Dombrowski, N., Teske, A. P., and Baker, B. J. (2018). Expansive microbial metabolic versatility and biodiversity in dynamic Guaymas Basin hydrothermal sediments. *Nat. Commun.* 9, 4999. doi: 10.1038/s41467-018-07418-0.

Dong, X., Greening, C., Rattray, J. E., Chakraborty, A., Chuvochina, M., Mayumi, D., et al. (2019). Metabolic potential of uncultured bacteria and archaea associated with petroleum seepage in deep-sea sediments. *Nat. Commun.* 10. doi: 10.1038/S41467-019-09747-0.

Dong, X., Rattray, J. E., Campbell, D. C., Webb, J., Chakraborty, A., Adebayo, O., et al. (2020). Thermogenic hydrocarbon biodegradation by diverse depth-stratified microbial populations at a Scotian Basin cold seep. *Nat. Commun.* 11, 1–14. doi: 10.1038/s41467-020-19648-2.

Edgar, R. C. (2004). MUSCLE: A multiple sequence alignment method with reduced time and space complexity. *BMC Bioinformatics* 5, 1–19. doi: 10.1186/1471-2105-5-113/FIGURES/16.

Eren, A. M., Esen, Ö. C., Quince, C., Vineis, J. H., Morrison, H. G., Sogin, M. L., et al. (2015). Anvi'o: an advanced analysis and visualization platform for 'omics data. *PeerJ* 3, e1319. doi: 10.7717/peerj.1319.

Eren, A. M., Kiefl, E., Shaiber, A., Veseli, I., Miller, S. E., Schechter, M. S., et al. (2020). Community-led, integrated, reproducible multi-omics with anvi'o. *Nat. Microbiol. 2020 61* 6, 3–6. doi: 10.1038/s41564-020-00834-3.

Evans, P. N., Parks, D. H., Chadwick, G. L., Robbins, S. J., Orphan, V. J., Golding, S. D., et al. (2015). Methane metabolism in the archaeal phylum Bathyarchaeota revealed by genome-centric metagenomics. *Science (80-.).* 350, 434–438. doi: 10.1126/science.aac7745.

Farag, I. F., Biddle, J. F., Zhao, R., Martino, A. J., House, C. H., and León-Zayas, R. I. (2020). Metabolic potentials of archaeal lineages resolved from metagenomes of deep Costa Rica sediments. *ISME J. 2020*, 1–14. doi: 10.1038/s41396-020-0615-5.

Galperin, M. Y., Makarova, K. S., Wolf, Y. I., and Koonin, E. V. (2015). Expanded microbial genome coverage and improved protein family annotation in the COG database. *Nucleic Acids Res.* 43, D261–D269. doi: 10.1093/NAR/GKU1223.

Garcia, P. S., Gribaldo, S., and Borrel, G. (2022). Diversity and Evolution of Methane-Related Pathways in Archaea. *Annu. Rev. Microbiol.* 76. doi: 10.1146/annurev-micro-041020-024935.

Gruber-Vodicka, H. R., Seah, B. K. B., and Pruesse, E. (2020). phyloFlash: Rapid small-subunit rRNA profiling and targeted assembly from metagenomes. *mSystems* 5. doi: 10.1128/mSystems.00920-20.

Haft, D. H., Loftus, B. J., Richardson, D. L., Yang, F., Eisen, J. A., Paulsen, I. T., et al. (2001). TIGRFAMs: a protein family resource for the functional identification of proteins. *Nucleic Acids Res.* 29, 41–43. doi: 10.1093/NAR/29.1.41.

Hahn, C. J., Laso-Pérez, R., Vulcano, F., Vaziourakis, K.-M., Stokke, R., Steen, I. H., et al. (2020). "*Candidatus* Ethanoperedens," a thermophilic genus of archaea mediating the anaerobic oxidation of ethane. *MBio* 11, 1–18. doi: 10.1128/mBio.00600-20.

Hallam, S. J., Putnam, N., Preston, C. M., Detter, J. C., Rokhsar, D., Richardson, P. M., et al. (2004). Reverse Methanogenesis: Testing the Hypothesis with Environmental Genomics. *Science (80-.).* 305, 1457–1462. doi: 10.1126/science.1100025.

Hao, L., McIlroy, S. J., Kirkegaard, R. H., Karst, S. M., Fernando, W. E. Y., Aslan, H., et al. (2018). Novel prosthecate bacteria from the candidate phylum Acetothermia. *ISME J.* 12, 2225–2237. doi: 10.1038/s41396-018-0187-9.

Hu, P., Tom, L., Singh, A., Thomas, B. C., Baker, B. J., Piceno, Y. M., et al. (2016). Genome-resolved metagenomic analysis reveals roles for candidate phyla and other microbial community members in biogeochemical transformations in oil reservoirs. *MBio* 7. doi: 10.1128/MBIO.01669-15/SUPPL_FILE/MBO001162636SF1F.TIF.

Hua, Z.-S., Wang, Y.-L., Evans, P. N., Qu, Y.-N., Goh, K. M., Rao, Y.-Z., et al. (2019). Insights into the ecological roles and evolution of methyl-coenzyme M reductase-containing hot spring Archaea. *Nat. Commun.* 10, 4574. doi: 10.1038/s41467-019-12574-y.

Huber, H., Jannasch, H., Rachel, R., Fuchs, T., and Stetter, K. O. (1997). Archaeoglobus veneficus sp. nov., a Novel Facultative Chemolithoautotrophic Hyperthermophilic Sulfite Reducer, Isolated from Abyssal Black Smokers. *Syst. Appl. Microbiol.* 20, 374–380. doi: 10.1016/S0723-2020(97)80005-7.

Hyatt, D., Chen, G. L., LoCascio, P. F., Land, M. L., Larimer, F. W., and Hauser, L. J. (2010). Prodigal: prokaryotic gene recognition and translation initiation site identification. *BMC Bioinformatics*, 1–11. doi: 10.1186/1471-2105-11-119.

Jaekel, U., Musat, N., Adam, B., Kuypers, M., Grundmann, O., and Musat, F. (2013). Anaerobic degradation of propane and butane by sulfate-reducing bacteria enriched from marine hydrocarbon cold seeps. *ISME J.* 7, 885–895. doi: 10.1038/ismej.2012.159.

Jain, C., Rodriguez-R, L. M., Phillippy, A. M., Konstantinidis, K. T., and Aluru, S. (2018). High throughput ANI analysis of 90K prokaryotic genomes reveals clear species boundaries. *Nat. Commun. 2018 91* 9, 1–8. doi: 10.1038/s41467-018-07641-9.

Jeanthon, C., L'Haridon, S., Cueff, V., Banta, A., Reysenbach, A.-L., and Prieur, D. (2002). Thermodesulfobacterium hydrogeniphilum sp. nov., a thermophilic, chemolithoautotrophic, sulfate-reducing bacterium isolated from a deep-sea hydrothermal vent at Guaymas Basin, and emendation of the genus Thermodesulfobacterium. *Int. J. Syst. Evol. Microbiol.* 52, 765–772. doi: 10.1099/00207713-52-3-765.

Kalyaanamoorthy, S., Minh, B. Q., Wong, T. K. F., Von Haeseler, A., and Jermiin, L. S. (2017). ModelFinder: fast model selection for accurate phylogenetic estimates. *Nat. Methods 2017 146* 14, 587–589. doi: 10.1038/nmeth.4285.

Kanehisa, M., and Goto, S. (2000). KEGG: Kyoto encyclopedia of genes and genomes. *Nucleic Acids Res.* 28, 27–30. doi: 10.1093/NAR/28.1.27.

Kellermann, M. Y., Wegener, G., Elvert, M., Yoshinaga, M. Y., Lin, Y.-S., Holler, T., et al. (2012). Autotrophy as a predominant mode of carbon fixation in anaerobic methane-oxidizing microbial communities. *Proc. Natl. Acad. Sci.* 109, 19321–19326. doi: 10.1073/pnas.1208795109.

Khelifi, N., Amin Ali, O., Roche, P., Grossi, V., Brochier-Armanet, C., Valette, O., et al. (2014). Anaerobic oxidation of long-chain n-alkanes by the hyperthermophilic sulfate-reducing archaeon, Archaeoglobus fulgidus. *ISME J.* 8, 2153–2166. doi: 10.1038/ismej.2014.58.

Klenk, H. P., Clayton, R. A., Tomb, J. F., White, O., Nelson, K. E., Ketchum, K. A., et al. (1997). The complete genome sequence of the hyperthermophilic, sulphate-reducing archaeon Archaeoglobus fulgidus. *Nat. 1997 3906658* 390, 364–370. doi: 10.1038/37052.

Krukenberg, V., Harding, K., Richter, M., Glöckner, F. O., Gruber-Vodicka, H. R., Adam, B., et al. (2016). *Candidatus* Desulfofervidus auxilii, a hydrogenotrophic sulfate-reducing bacterium involved in the

thermophilic anaerobic oxidation of methane. *Environ. Microbiol.* 18, 3073–3091. doi: 10.1111/1462-2920.13283.

Kubo, K., Lloyd, K. G., F Biddle, J., Amann, R., Teske, A., and Knittel, K. (2012). Archaea of the Miscellaneous Crenarchaeotal Group are abundant, diverse and widespread in marine sediments. *ISME J.* 6, 1949–1965. doi: 10.1038/ismej.2012.37.

Lagesen, K., Hallin, P., Rødland, E. A., Stærfeldt, H. H., Rognes, T., and Ussery, D. W. (2007). RNAmmer: consistent and rapid annotation of ribosomal RNA genes. *Nucleic Acids Res.* 35, 3100. doi: 10.1093/NAR/GKM160.

Langmead, B., and Salzberg, S. L. (2012). Fast gapped-read alignment with Bowtie 2. *Nat. Methods 2012 94* 9, 357–359. doi: 10.1038/nmeth.1923.

Laso-Pérez, R., Hahn, C., van Vliet, D. M., Tegetmeyer, H. E., Schubotz, F., Smit, N. T., et al. (2019). Anaerobic Degradation of Non-Methane Alkanes by "Candidatus Methanoliparia" in Hydrocarbon Seeps of the Gulf of Mexico. *MBio* 10, e01814-19. doi: 10.1128/mBio.01814-19.

Laso-Pérez, R., Krukenberg, V., Musat, F., and Wegener, G. (2018). Establishing anaerobic hydrocarbon-degrading enrichment cultures of microorganisms under strictly anoxic conditions. *Nat. Publ. Gr.* 13, 1310–1330. doi: 10.1038/nprot.2018.030.

Laso-Pérez, R., Wegener, G., Knittel, K., Widdel, F., Harding, K. J., Krukenberg, V., et al. (2016). Thermophilic archaea activate butane via alkyl-coenzyme M formation. *Nature* 539, 396–401. doi: 10.1038/nature20152.

Letunic, I., and Bork, P. (2011). Interactive Tree of Life v2: Online annotation and display of phylogenetic trees made easy. *Nucleic Acids Res.* doi: 10.1093/nar/gkr201.

Liu, Y. F., Yang, L., Liu, Z. L., Chen, J., Fang, B., Zhou, L., et al. (2022). Discovery of the non-cosmopolitan lineages in Candidatus Thermoprofundales. *Environ. Microbiol.* 24, 3063–3080. doi: 10.1111/1462-2920.15965.

Lloyd, K. G., Schreiber, L., Petersen, D. G., Kjeldsen, K. U., Lever, M. A., Steen, A. D., et al. (2013). Predominant archaea in marine sediments degrade detrital proteins. *Nature* 496, 215–218. doi: 10.1038/nature12033.

Ludwig, W., Strunk, O., Westram, R., Richter, L., Meier, H., Yadhukumar, A., et al. (2004). ARB: a software environment for sequence data. *Nucleic Acids Res.* 32, 1363–1371. doi: 10.1093/NAR/GKH293.

Manzella, M. P., Holmes, D. E., Rocheleau, J. M., Chung, A., Reguera, G., and Kashefi, K. (2015). The complete genome sequence and emendation of the hyperthermophilic, obligate iron-reducing archaeon "Geoglobus ahangari" strain 234T. *Stand. Genomic Sci.* 10. doi: 10.1186/S40793-015-0035-8.

Mardanov, A. V., Slododkina, G. B., Slobodkin, A. I., Beletsky, A. V., Gavrilov, S. N., Kublanov, I. V., et al. (2015). The Geoglobus acetivorans genome: Fe(III) reduction, acetate utilization, autotrophic growth, and degradation of aromatic compounds in a hyperthermophilic archaeon. *Appl. Environ. Microbiol.* 81, 1003–1012. doi: 10.1128/AEM.02705-14.

McGlynn, S. E., Chadwick, G. L., Kempes, C. P., and Orphan, V. J. (2015). Single cell activity reveals direct electron transfer in methanotrophic consortia. *Nature* 526, 531–535. doi: 10.1038/nature15512.

McKay, L. J., Dlakić, M., Fields, M. W., Delmont, T. O., Eren, A. M., Jay, Z. J., et al. (2019). Co-occurring genomic capacity for anaerobic methane and dissimilatory sulfur metabolisms discovered in the Korarchaeota. *Nat. Microbiol.*, 1. doi: 10.1038/s41564-019-0362-4.

Meng, J., Xu, J., Qin, D., He, Y., Xiao, X., and Wang, F. (2013). Genetic and functional properties of uncultivated MCG archaea assessed by metagenome and gene expression analyses. *ISME J. 2014 83* 8, 650–659. doi: 10.1038/ismej.2013.174.

Michaelis, W., Seifert, R., Nauhaus, K., Treude, T., Thiel, V., Blumenberg, M., et al. (2002). Microbial Reefs in the Black Sea Fueled by Anaerobic Oxidation of Methane. *Science (80-.).* 297, 1013–1015. doi: 10.1126/science.1072502.

Minh, B. Q., Schmidt, H. A., Chernomor, O., Schrempf, D., Woodhams, M. D., Von Haeseler, A., et al. (2020). IQ-TREE 2: new models and efficient methods for phylogenetic inference in the genomic era. *Mol. Biol. Evol.* 37, 1530–1534. doi: 10.1093/MOLBEV/MSAA015.

Mistry, J., Chuguransky, S., Williams, L., Qureshi, M., Salazar, G. A., Sonnhammer, E. L. L., et al. (2021). Pfam: The protein families database in 2021. *Nucleic Acids Res.* 49, D412–D419. doi: 10.1093/NAR/GKAA913.

Mori, K., Maruyama, A., Urabe, T., Suzuki, K. I., and Hanada, S. (2008). Archaeoglobus infectus sp. nov., a novel thermophilic, chemolithoheterotrophic archaeon isolated from a deep-sea rock collected at Suiyo Seamount, Izu-Bonin Arc, western Pacific Ocean. *Int. J. Syst. Evol. Microbiol.* 58, 810–816. doi: 10.1099/IJS.0.65422-0.

Moussard, H., L'Haridon, S., Tindall, B. J., Banta, A., Schumann, P., Stackebrandt, E., et al. (2004). Thermodesulfatator indicus gen. nov., sp. nov., a novel thermophilic chemolithoautotrophic sulfate-reducing bacterium isolated from the Central Indian Ridge. *Int. J. Syst. Evol. Microbiol.* 54, 227–233. doi: 10.1099/ijs.0.02669-0.

Orphan, V. J., House, C. H., Hinrichs, K.-U., McKeegan, K. D., and DeLong, E. F. (2002). Multiple archaeal groups mediate methane oxidation in anoxic cold seep sediments. *Proc. Natl. Acad. Sci.* 99, 7663–7668. doi: 10.1073/pnas.072210299.

Pinheiro Alves de Souza, Y., and Soares Rosado, A. (2019). "Opening the Black Box of Thermophilic Autotrophic Bacterial Diversity," in *Microbial Diversity in the Genomic Era* (Elsevier), 333–343. doi: 10.1016/B978-0-12-814849-5.00019-8.

Probst, A. J., Ladd, B., Jarett, J. K., Geller-Mcgrath, D. E., Sieber, C. M. K., Emerson, J. B., et al. (2018). Differential depth distribution of microbial function and putative symbionts through sediment-hosted aquifers in the deep terrestrial subsurface. *Nat. Microbiol.* 3, 328–336. doi: 10.1038/S41564-017-0098-Y.

Pruesse, E., Peplies, J., and Glöckner, F. O. (2012). SINA: Accurate high-throughput multiple sequence alignment of ribosomal RNA genes. *Bioinformatics* 28, 1823–1829. doi: 10.1093/BIOINFORMATICS/BTS252.

Quast, C., Pruesse, E., Yilmaz, P., Gerken, J., Schweer, T., Yarza, P., et al. (2013). The SILVA ribosomal RNA gene database project: improved data processing and web-based tools. *Nucleic Acids Res.* 41, D590–D596. doi: 10.1093/NAR/GKS1219.

Rinke, C., Chuvochina, M., Mussig, A. J., Chaumeil, P.-A., Davín, A. A., Waite, D. W., et al. (2021). A standardized archaeal taxonomy for the Genome Taxonomy Database. *Nat. Microbiol.* 6, 946–959. doi: 10.1038/s41564-021-00918-8.

Rinke, C., Schwientek, P., Sczyrba, A., Ivanova, N. N., Anderson, I. J., Cheng, J. F., et al. (2013). Insights into the phylogeny and coding potential of microbial dark matter. *Nat. 2013 4997459* 499, 431–437. doi: 10.1038/nature12352.

Rueter, P., Rabus, R., Wilkest, H., Aeckersberg, F., Rainey, F. A., Jannasch, H. W., et al. (1994). Anaerobic oxidation of hydrocarbons in crude oil by new types of sulphate-reducing bacteria. *Nat. 1994 3726505* 372, 455–458. doi: 10.1038/372455a0.

Schink, B. (1997). Energetics of syntrophic cooperation in methanogenic degradation. *Microbiol. Mol. Biol. Rev.* 61, 262–280. doi: 10.1128/mmbr.61.2.262-280.1997.

Seemann, T. (2014). Prokka: rapid prokaryotic genome annotation. *Bioinformatics* 30, 2068–2069. doi: 10.1093/bioinformatics/btu153.

Seitz, K. W., Dombrowski, N., Eme, L., Spang, A., Lombard, J., Sieber, J. R., et al. (2019). Asgard archaea capable of anaerobic hydrocarbon cycling. *Nat. Commun.* 10, 1822. doi: 10.1038/s41467-019-09364-x.

Shima, S., Krueger, M., Weinert, T., Demmer, U., Kahnt, J., Thauer, R. K., et al. (2012). Structure of a methyl-coenzyme M reductase from Black Sea mats that oxidize methane anaerobically. *Nature* 481, 98–101. doi: 10.1038/nature10663.

Simoneit, B. R. T., Lonsdale, P. F., Edmond, J. M., and Shanks, W. C. (1990). Deep-water hydrocarbon seeps in Guaymas Basin, Gulf of California. *Appl. Geochemistry* 5, 41–49. doi: 10.1016/0883-2927(90)90034-3.

Sonne-Hansen, J., and Ahring, B. K. (1999). Thermodesulfobacterium hveragerdense sp.nov., and Thermodesulfovibrio islandicus sp.nov., Two Thermophilic Sulfate Reducing Bacteria Isolated from a Icelandic Hot Spring. *Syst. Appl. Microbiol.* 22, 559–564. doi: 10.1016/S0723-2020(99)80009-5.

Spormann, A. M., and Widdel, F. (2000). Metabolism of alkylbenzenes, alkanes, and other hydrocarbons in anaerobic bacteria. *Biodegrad. 2000 112* 11, 85–105. doi: 10.1023/A:1011122631799.

Stagars, M. H., Ruff, S. E., Amann, R., and Knittel, K. (2016). High Diversity of Anaerobic Alkane-Degrading Microbial Communities in Marine Seep Sediments Based on (1-methylalkyl)succinate Synthase Genes. *Front. Microbiol.* 6, 1511. doi: 10.3389/fmicb.2015.01511.

Stamatakis, A. (2014). RAxML version 8: a tool for phylogenetic analysis and post-analysis of large phylogenies. *Bioinformatics* 30, 1312–1313. doi: 10.1093/BIOINFORMATICS/BTU033.

Steinsbu, B. O., Thorseth, I. H., Nakagawa, S., Inagaki, F., Lever, M. A., Engelen, B., et al. (2010). *Archaeoglobus sulfaticallidus* sp. nov., a thermophilic and facultatively lithoautotrophic sulfate-reducer isolated from black rust exposed to hot ridge flank crustal fluids. *Int. J. Syst. Evol. Microbiol.* 60, 2745–2752. doi: 10.1099/ijs.0.016105-0.

Stetter, K. O. (1988). Archaeoglobus fulgidus gen. nov., sp. nov.: a New Taxon of Extremely Thermophilic Archaebacteria. *Syst. Appl. Microbiol.* 10, 172–173. doi: 10.1016/S0723-2020(88)80032-8.

Stetter, K. O., Huber, R., Blöchl, E., Kurr, M., Eden, R. D., Fielder, M., et al. (1993). Hyperthermophilic archaea are thriving in deep North Sea and Alaskan oil reservoirs. *Nature* 365, 743–745. doi: 10.1038/365743a0.

Stetter, K. O., Lauerer, G., Thomm, M., and Neuner, A. (1987). Isolation of Extremely Thermophilic Sulfate Reducers: Evidence for a Novel Branch of Archaebacteria. *Science (80-.).* 236, 822–824. doi: 10.1126/science.236.4803.822.

Stokke, R., Hocking, W. P., Steinsbu, B. O., and Steen, I. H. (2013). Complete Genome Sequence of the Thermophilic and Facultatively Chemolithoautotrophic Sulfate Reducer Archaeoglobus sulfaticallidus Strain PM70-1T. *Genome Announc.* 1. doi: 10.1128/GENOMEA.00406-13.

Takai, K., Moser, D. P., DeFlaun, M., Onstott, T. C., and Fredrickson, J. K. (2001). Archaeal Diversity in Waters from Deep South African Gold Mines. *Appl. Environ. Microbiol.* 67, 5750–5760. doi: 10.1128/AEM.67.21.5750-5760.2001.

Takami, H., Noguchi, H., Takaki, Y., Uchiyama, I., Toyoda, A., Nishi, S., et al. (2012). A Deeply Branching Thermophilic Bacterium with an Ancient Acetyl-CoA Pathway Dominates a Subsurface Ecosystem. *PLoS One* 7, e30559. doi: 10.1371/JOURNAL.PONE.0030559.

Teske, A., Hinrichs, K.-U., Edgcomb, V., Gomez, A. D. V., Kysela, D., Sylva, S. P., et al. (2002). Microbial Diversity of Hydrothermal Sediments in the Guaymas Basin: Evidence for Anaerobic Methanotrophic Communities. *Appl. Environ. Microbiol.* 68, 1994–2007. doi: 10.1128/AEM.68.4.1994.

Teske, A., and Sørensen, K. B. (2008). Uncultured archaea in deep marine subsurface sediments: Have we caught them all? *ISME J.* 2, 3–18. doi: 10.1038/ismej.2007.90.

Teske, A., Wegener, G., Chanton, J. P., White, D., MacGregor, B., Hoer, D., et al. (2021). Microbial Communities Under Distinct Thermal and Geochemical Regimes in Axial and Off-Axis Sediments of Guaymas Basin. *Front. Microbiol.* 12, 110. doi: 10.3389/fmicb.2021.633649.

Thauer, R. K., Kaster, A. K., Seedorf, H., Buckel, W., and Hedderich, R. (2008). Methanogenic archaea: ecologically relevant differences in energy conservation. *Nat. Rev. Microbiol. 2008 68* 6, 579–591. doi: 10.1038/nrmicro1931.

Vanwonterghem, I., Evans, P. N., Parks, D. H., Jensen, P. D., Woodcroft, B. J., Hugenholtz, P., et al. (2016). Methylotrophic methanogenesis discovered in the archaeal phylum Verstraetearchaeota. *Nat.*

Microbiol. 1, 16170. doi: 10.1038/nmicrobiol.2016.170.

Vetriani, C., Jannasch, H. W., Macgregor, B. J., Stahl, D. A., and Reysenbach, A. L. (1999). Population Structure and Phylogenetic Characterization of Marine Benthic Archaea in Deep-Sea Sediments. *Appl. Environ. Microbiol.* 65, 4375. doi: 10.1128/AEM.65.10.4375-4384.1999.

von Jan, M., Lapidus, A., del Rio, T. G., Copeland, A., Tice, H., Cheng, J. F., et al. (2010). Complete genome sequence of Archaeoglobus profundus type strain (AV18). *Stand. Genomic Sci.* 2, 327–346. doi: 10.4056/SIGS.942153.

Wang, Y., Wegener, G., Hou, J., Wang, F., and Xiao, X. (2019). Expanding anaerobic alkane metabolism in the domain of Archaea. *Nat. Microbiol.* 4, 1. doi: 10.1038/s41564-019-0364-2.

Wang, Y., Wegener, G., Ruff, S. E., and Wang, F. (2020). Methyl/alkyl-coenzyme M reductase-based anaerobic alkane oxidation in archaea. *Environ. Microbiol.* 00. doi: 10.1111/1462-2920.15057.

Wang, Y., Wegener, G., Williams, T. A., Xie, R., Hou, J., Tian, C., et al. (2021). A methylotrophic origin of methanogenesis and early divergence of anaerobic multicarbon alkane metabolism. *Sci. Adv.* 7, 1–12. doi: 10.1126/sciadv.abj1453.

Wegener, G., Krukenberg, V., Riedel, D., Tegetmeyer, H. E., and Boetius, A. (2015). Intercellular wiring enables electron transfer between methanotrophic archaea and bacteria. *Nature* 526, 587–590. doi: 10.1038/nature15733.

Wegener, G., Laso-Pérez, R., Orphan, V. J., and Boetius, A. (2022). Anaerobic Degradation of Alkanes by Marine Archaea. *Annu. Rev. Microbiol.* 76, 553–577. doi: 10.1146/annurev-micro-111021-045911.

Widdel, F., and Bak, F. (1992). "Gram-negative mesophilic sulfate-reducing bacteria," in *The Prokaryotes* (Springer, New York, NY), 3352–3378. doi: 10.1007/978-1-4757-2191-1_21.

Wu, M., Ren, Q., Durkin, A. S., Daugherty, S. C., Brinkac, L. M., Dodson, R. J., et al. (2005). Life in Hot Carbon Monoxide: The Complete Genome Sequence of Carboxydothermus hydrogenoformans Z-2901. *PLoS Genet.* 1, e65. doi: 10.1371/journal.pgen.0010065.

Wu, Y.-W., Simmons, B. A., and Singer, S. W. (2016). MaxBin 2.0: an automated binning algorithm to recover genomes from multiple metagenomic datasets. *Bioinformatics* 32, 605–607. doi: 10.1093/bioinformatics/btv638.

Zehnle, H., Lipp, J., Teske, A., and Wegener, G. (2022). Candidatus Alkanophaga archaea from heated hydrothermal vent sediment oxidize petroleum alkanes. *Prepr. (Version 1) available Res. Sq.*, 1–33. doi: 10.21203/RS.3.RS-2096998/V1.

Zeikus, J. G., Dawson, M. A., Thompson, T. E., Ingvorsen, K., and Hatchikian, E. C. (1983). Microbial Ecology of Volcanic Sulphidogenesis: Isolation and Characterization of *Thermodesulfobacterium commune* gen. nov. and sp. nov. *Microbiology* 129, 1159–1169. doi: 10.1099/00221287-129-4-1159.

Zhou, Z., Zhang, C., Liu, P., Fu, L., Laso-Pérez, R., Yang, L., et al. (2022). Non-syntrophic methanogenic hydrocarbon degradation by an archaeal species. *Nature* 601, 257–262. doi: 10.1038/s41586-021-04235-2.

Zhu, Q.-Z., Wegener, G., Hinrichs, K.-U., and Elvert, M. (2022). Activity of ancillary heterotrophic community members in anaerobic methane-oxidizing cultures. *Front. Microbiol.* 13, 1–12. doi: 10.3389/fmicb.2022.912299.

Mechanisms for syntrophic interspecies electron transfer are widespread in genomes of Thermodesulfobacteria

David Benito Merino, Hanna Zehnle, Gunter Wegener

Manuscript in preparation

Mechanisms for syntrophic interspecies electron transfer are widespread in genomes of Thermodesulfobacteria

David Benito Merino[1,2]*, Hanna Zehnle[1,2,3], Gunter Wegener[1,3]*

[1]Max Planck Institute for Marine Microbiology, Bremen, Germany

[2]Faculty of Geosciences, University of Bremen, Bremen, Germany

[3]MARUM, Center for Marine Environmental Sciences, University of Bremen, Bremen, Germany

Keywords: sulfate-reducing bacteria, syntrophy, thermophily, direct interspecies electron transfer

Abstract

The Thermodesulfobacteria is a class of obligate thermophilic bacteria. According to modern phylogeny, they are part of the core phylum Desulfobacterota, which includes most sulfate reducers and all known partner bacteria of alkane-degrading archaea. Recently, two candidate species of *Thermodesulfobacterium* were found in consortia with anaerobic methane and mid-chain alkane oxidizing archaea. To resolve the molecular features of this possible syntrophy, we analysed the phylogeny and genomic capabilities of cultured members and metagenome assembled genome (MAGs) of this group. All Thermodesulfobacteria originate from heated environments or oil reservoirs, supporting obligate thermophily in this group. All encode the genes for dissimilatory sulfate reduction and the majority encodes a membrane-bound hydrogenase. In contrast to other Desulfobacterota, alkylsuccinate synthases for alkane activation are absent in Thermodesulfobacteria. Genome analysis revealed that group 1c hydrogenases were common to almost all Thermodesulfobacteria. Thermodesulfobacteria from hydrothermal vents also encoded cytochromes potentially involved in direct interspecies electron transfer (DIET). The AOM partner *Ca*. Thermodesulfobacterium torris encodes all the steps of the DIET pathway and lacks a hydrogenase. In contrast, other predicted syntrophic partner Thermodesulfobacteria lack an outer membrane cytochrome needed for DIET. The molecular prerequisites of sulfate reducing partners are still not resolved and, at this stage, we cannot predict putative syntrophic organisms by analyzing the cytochromes present in the genomes. However, many hydrothermal-vent Thermodesulfobacteria have a complete DIET pathway. This suggests a possible implication of the Thermodesulfobacteria as partners for anaerobic oxidation of methane and alkanes.

Introduction

In oxygen-depleted habitats, microorganisms couple the degradation of organic matter to the reduction of various alternative electron acceptors (Jørgensen, 2006). In marine sediments below the oxic layer, the most prevalent respiratory pathway is dissimilatory sulfate reduction, due to the high concentration of sulfate in seawater (28 mM) (Jørgensen, 1982). Dissimilatory sulfate reduction occurs in three steps, catalyzed sequentially by sulfate adenylyltransferase (Sat), adenylylsulfate reductase (AprAB) and dissimilatory sulfite reductase (DsrAB) (Rabus et al., 2013). Sulfate reduction is considered one of the most ancient pathways on Earth (Woese, 1987; Shen et al., 2001), having evolved probably after sulfate accumulated in substantial amounts (Canfield and Raiswell, 1999). After the establishment of oxygenic photosynthesis 2.7×10^9 years (2.7 Ga) ago, sulfate started to accumulate in greater amounts on Earth (Nisbet and Sleep, 2001) and sulfate concentrations in the ocean surpassed 1 mM by 2.3 Ga (Canfield and Raiswell, 1999). However, it is expected that hyperthermophilic sulfate-reducing bacteria were present in the environment much earlier, approximately 3.4 Ga ago (Canfield and Raiswell, 1999). In fact, the earliest evidence for sulfides of biological origin dates back to 3.47 Ga ago (Shen et al., 2001). The phylogeny of dissimilatory sulfite reductases also supported an early origin of sulfate reduction (Wagner et al., 1998). Early studies suggested that dissimilatory sulfate reduction was limited to a few prokaryotic lineages; however, genes coding for Dsr are widespread in Bacteria and Archaea (Anantharaman et al., 2018).

In marine sediments where methane and sulfate gradients overlap, i.e. sulfate-methane transition zones (SMTZs), anaerobic methanotrophic archaea (ANME) coexist with sulfate-reducing bacteria (SRB) of the phylum Desulfobacterota (formerly known as Deltaproteobacteria) (Boetius and Knittel, 2010). These microbes form microbial consortia to perform anaerobic oxidation of methane (AOM), where the archaeon oxidizes methane to CO_2 and passes on the resulting electrons to the partner SRB (Knittel and Boetius, 2010). Several types of such AOM consortia exist in deep-sea habitats such as hydrothermal sediments, cold seeps, mud volcanoes and methane hydrates (Niemann et al., 2006; Boetius and Knittel, 2010). The association of the different ANME groups (ANME-1, -2 and -3) with SRB is specific to a certain degree (Murali et al., 2022). SRB of the groups Seep-SRB1, Seep-SRB2 and Desulfobulbia have been detected in psychro- and mesophilic AOM consortia, both *in situ* and in enrichment cultures (Niemann et al., 2006; Schreiber et al., 2010; Skennerton et al., 2017; Krukenberg et al., 2018; Metcalfe et al., 2020; Yu et al., 2021). In thermophilic AOM cultures up to 60°C, the deep-branching species *Candidatus* Desulfofervidus auxilii forms consortia with ANME-1 (Holler et al., 2011; Krukenberg et al., 2018). *Ca*. D. auxilii also forms consortia with short-chain alkane-oxidizing archaea of the genera *Ca*. Syntrophoarchaeum and *Ca*. Ethanoperedens (Laso-Pérez et al., 2016; Hahn et al., 2020). Recently, methane- and mid-chain alkane-

oxidizing consortia growing at 70°C have been enriched (Benito Merino et al., 2022; Zehnle et al., 2022). In AOM at 70°C, deep-branching ANME-1c associate with *Ca*. Thermodesulfobacterium torris (class Thermodesulfobacteria, phylum Desulfobacterota) as partner SRB (Benito Merino et al., 2022). Similarly, *Ca*. T. syntrophicum form associations with *Ca*. Alkanophaga to oxidize alkanes from C_5 to C_{14} (Zehnle et al., 2022). Furthermore, anoxic hexadecane-oxidizing enrichment cultures containing Hadarchaea also contained *Ca*. T. torris (Benito Merino et al., in prep., Chapter 2). In general, Thermodesulfobacteria could be partners for methane and alkane degradation at 70°C, temperature at which the thermophilic *Ca*. D. auxilii does not survive (Krukenberg et al., 2016).

Direct interspecies electron transfer (DIET) is the most likely mechanism on which the syntrophy between alkane-oxidizing archaea and SRB relies (McGlynn et al., 2015). The genomic features that support DIET in syntrophic Seep-SRB and HotSeep-1 have been recently characterized (Murali et al., 2022). DIET between ANME and SRB is based on multiheme cytochromes that are produced by both partners (McGlynn et al., 2015; Krukenberg et al., 2018). Nanowire-like structures and heme groups appear in the intercellular space between ANME-1 and partner SRB (McGlynn et al., 2015; Wegener et al., 2015; Krukenberg et al., 2018). It has been proposed that the nanowires of *Geobacter sulfurreducens* are formed by outer membrane hexaheme cytochromes and that the export of these proteins to the extracellular space is mediated by pilus proteins (Wang et al., 2019; Gu et al., 2021). The DIET machinery apparently consists of a periplasmic cytochrome *c*, an outer-membrane porin and an extracellular cytochrome *c* lipoprotein (Murali et al., 2022).

The class Thermodesulfobacteria (phylum Desulfobacterota) (Parks et al., 2018) contains thermophilic and hyperthermophilic species isolated from hydrothermal vents (Jeanthon et al., 2002; Moussard et al., 2004; Alain et al., 2010; Slobodkin et al., 2012; Lai et al., 2016; Slobodkina et al., 2017; Frolova et al., 2018), hot springs (Zeikus et al., 1983; Henry et al., 1994; Sonne-Hansen and Ahring, 1999; Miroshnichenko et al., 2009; Hamilton-Brehm et al., 2013; Kojima et al., 2016) and oil reservoirs (Rozanova and Khudiakova, 1974). The class encompasses one order (the Thermodesulfobacteriales) and three families: the Thermodesulfatatoraceae (including the genus *Thermodesulfatator*), the Thermodesulfobacteriaceae (including the genera *Thermodesulfobacterium*, *Caldimicrobium* and *Thermosulfurimonas*) and ST65 (including the genus *Thermosulfuriphilus*) (Parks et al., 2018). Modern standardized bacterial taxonomy suggests that the genera and species nomenclature in the Thermodesulfobacteria class should be revised (Parks et al., 2018). In this manuscript, we use the terms Thermodesulfobacteria and *Thermodesulfobacterium* for the class and for the genus ranks, respectively.

Public repositories contain 60 genomes and metagenome-assembled genomes (MAGs) of Thermodesulfobacteria. Most of the studies on Thermodesulfobacteria reported on isolates or the presence of Thermodesulfobacteria in environmental samples. A systematic genomic comparison of this organism group in context of its role as free-living and syntrophic partner bacterium was lacking. To resolve the molecular basis of its multiple features, we generated a database with available Thermodesulfobacteria MAGs both from public repositories and from unpublished datasets. We did a phylogenetic and genomic comparison of the MAGs and searched for markers that could indicate a putative syntrophic lifestyle.

Materials and Methods

Origin of the Thermodesulfobacteria MAGs

Thermodesulfobacteria and Desulfobacterota MAGs used in this study were downloaded from public repositories (NCBI and GTDB) (Table S1). Furthermore, we included unpublished Thermodesulfobacteria MAGs (Table 1) retrieved from the Arctic Mid-Ocean Ridge (AMOR) (Vulcano et al., 2022) and the Pescadero Basin (Gulf of California, Mexico) (Laso-Pérez et al., 2022; Speth et al., 2022).

Genome annotation

All the MAGs were processed within anvi'o v. 7.1 (Eren et al., 2015, 2020). Protein and rRNA annotation was done with COGs, KEGGs, PFAMs and RNAmmer (Kanehisa and Goto, 2000; Lagesen et al., 2007; Galperin et al., 2015; Mistry et al., 2021). Annotation with motifs and custom protein datasets is detailed below.

Annotation of cytochromes

CXXCH heme-binding motifs were searched with a custom script* and were used as a proxy for the annotation of putative multiheme cytochrome (MHC) proteins. Putative extracellular and periplasmic cytochromes were searched with BLASTP (Altschul et al., 1990, 1997) using protein queries from known partner SRB (Murali et al., 2022). The query cytochromes and the BLASTP search parameters are summarized in Table S2. Protein localization was predicted with PSORTb v. 3.0 (Yu et al., 2010)

* github.com/dbenitom/Metagenomics_scripts/blob/main/CXXCH_search_anvio_import.sh

Annotation of hydrogenases

Hydrogenases were annotated with custom hidden Markov models (HMMs)* and with a list of COGs for several hydrogenases (Table S3). The affiliation of the hydrogenases was verified with the Hydrogenase Database (HydDB) (Søndergaard et al., 2016).

Phylogenomic classification

Thermodesulfobacteria MAG completeness and contamination were calculated with the "lineage_wf" workflow within CheckM v. 1.1.3 (Parks et al., 2015). The phylogenomic affiliation of the MAGs was determined with GTDB-Tk v. 1.5.1 with the "classify_wf" workflow (Chaumeil et al., 2020). Pairwise average nucleotide identity (ANI) between the MAGs was calculated with fastANI v. 1.32 (Jain et al., 2018). A set of single-copy bacterial marker proteins defined by Parks et al. (Parks et al., 2018) was used to reconstruct a bacterial phylogenomic tree with 156 genomes of Desulfobacterota and outgroups (Table S1). The amino acid sequences were aligned with muscle (Edgar, 2004). The alignments were produced in anvi'o with the command "anvi-get-sequences-for-hmm-hits", using the flags "--concatenate" and "--partition-file" to generate concatenated alignments and partition files** (Eren et al., 2015, 2020). Phylogenomic trees were calculated with and IQTree v. 2.0.3 (Minh et al., 2020). In IQTree, the flag "-m TEST" was used to estimate the best amino acid substitution model for each protein in the dataset (Chernomor et al., 2016). Trees were visualized in the Interactive Tree of Life web server (Letunic and Bork, 2011).

Phylogeny based on 16S rRNA genes

16S rRNA gene sequences were obtained from the SILVA database v. 138 (Table S4) (Quast et al., 2013). 16S rRNA gene sequences from the Thermodesulfobacteria MAGs were aligned to the SILVA sequences with the SINA alignment tool (Pruesse et al., 2012) integrated in the ARB software (Ludwig et al., 2004). Phylogenetic trees were calculated with IQTree v. 2.0.3 using 100 bootstraps (Stamatakis, 2014). Trees were visualized in the Interactive Tree of Life web server (Letunic and Bork, 2011).

* github.com/banfieldlab/metabolic-hmms

** github.com/dbenitom/Metagenomics_scripts/blob/main/Phylogenomic_alignment_bacteria

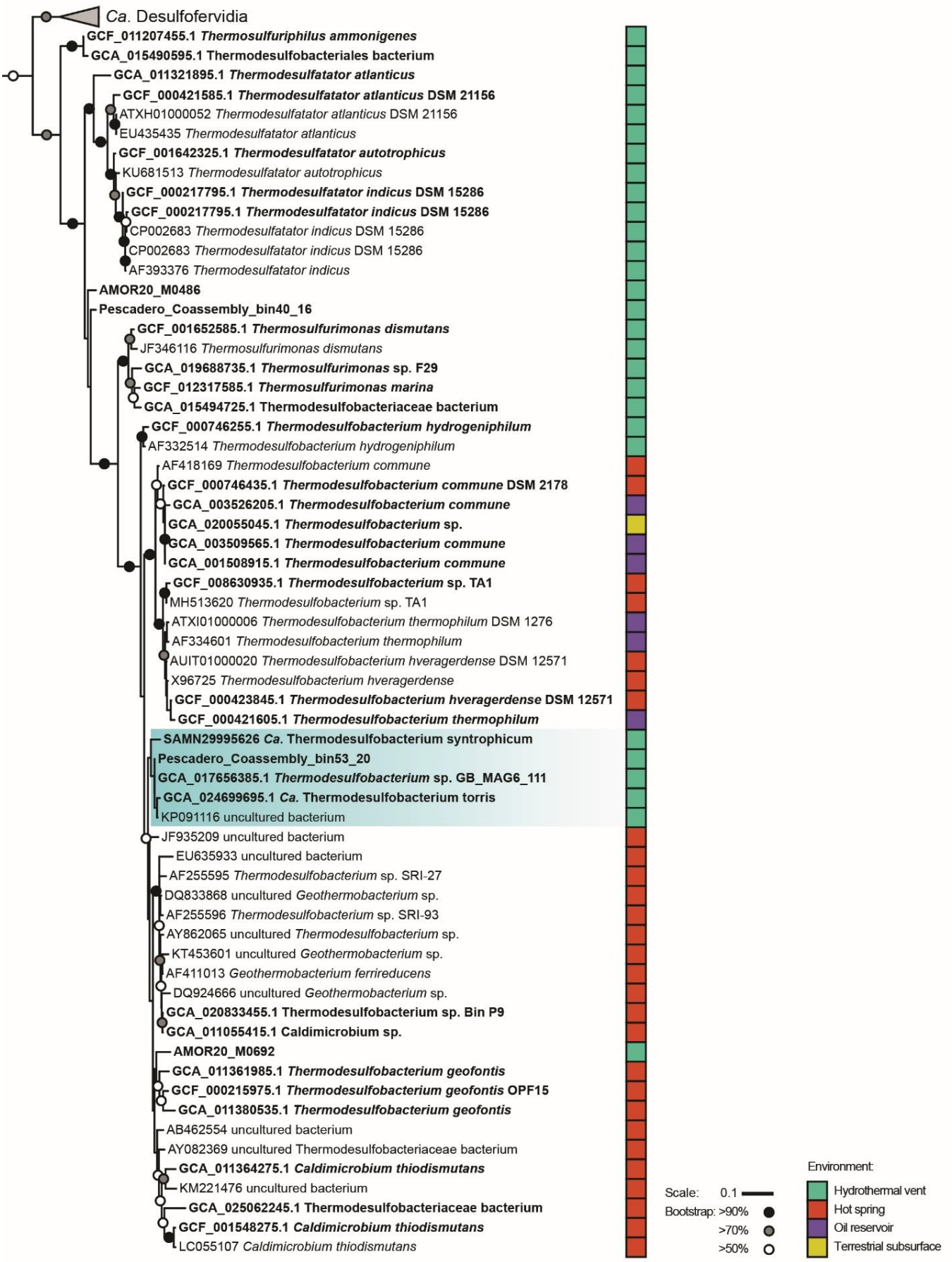
Ca. Desulfofervidia
GCF_011207455.1 Thermosulfuriphilus ammonigenes
GCA_015490595.1 Thermodesulfobacteriales bacterium
GCA_011321895.1 Thermodesulfatator atlanticus
GCF_000421585.1 Thermodesulfatator atlanticus DSM 21156
ATXH01000052 Thermodesulfatator atlanticus DSM 21156
EU435435 Thermodesulfatator atlanticus
GCF_001642325.1 Thermodesulfatator autotrophicus
KU681513 Thermodesulfatator autotrophicus
GCF_000217795.1 Thermodesulfatator indicus DSM 15286
GCF_000217795.1 Thermodesulfatator indicus DSM 15286
CP002683 Thermodesulfatator indicus DSM 15286
CP002683 Thermodesulfatator indicus DSM 15286
AF393376 Thermodesulfatator indicus
AMOR20_M0486
Pescadero_Coassembly_bin40_16
GCF_001652585.1 Thermosulfurimonas dismutans
JF346116 Thermosulfurimonas dismutans
GCA_019688735.1 Thermosulfurimonas sp. F29
GCF_012317585.1 Thermosulfurimonas marina
GCA_015494725.1 Thermodesulfobacteriaceae bacterium
GCF_000746255.1 Thermodesulfobacterium hydrogeniphilum
AF332514 Thermodesulfobacterium hydrogeniphilum
AF418169 Thermodesulfobacterium commune
GCF_000746435.1 Thermodesulfobacterium commune DSM 2178
GCA_003526205.1 Thermodesulfobacterium commune
GCA_020055045.1 Thermodesulfobacterium sp.
GCA_003509565.1 Thermodesulfobacterium commune
GCA_001508915.1 Thermodesulfobacterium commune
GCF_008630935.1 Thermodesulfobacterium sp. TA1
MH513620 Thermodesulfobacterium sp. TA1
ATXI01000006 Thermodesulfobacterium thermophilum DSM 1276
AF334601 Thermodesulfobacterium thermophilum
AUIT01000020 Thermodesulfobacterium hveragerdense DSM 12571
X96725 Thermodesulfobacterium hveragerdense
GCF_000423845.1 Thermodesulfobacterium hveragerdense DSM 12571
GCF_000421605.1 Thermodesulfobacterium thermophilum
SAMN29995626 Ca. Thermodesulfobacterium syntrophicum
Pescadero_Coassembly_bin53_20
GCA_017656385.1 Thermodesulfobacterium sp. GB_MAG6_111
GCA_024699695.1 Ca. Thermodesulfobacterium torris
KP091116 uncultured bacterium
JF935209 uncultured bacterium
EU635933 uncultured bacterium
AF255595 Thermodesulfobacterium sp. SRI-27
DQ833868 uncultured Geothermobacterium sp.
AF255596 Thermodesulfobacterium sp. SRI-93
AY862065 uncultured Thermodesulfobacterium sp.
KT453601 uncultured Geothermobacterium sp.
AF411013 Geothermobacterium ferrireducens
DQ924666 uncultured Geothermobacterium sp.
GCA_020833455.1 Thermodesulfobacterium sp. Bin P9
GCA_011055415.1 Caldimicrobium sp.
AMOR20_M0692
GCA_011361985.1 Thermodesulfobacterium geofontis
GCF_000215975.1 Thermodesulfobacterium geofontis OPF15
GCA_011380535.1 Thermodesulfobacterium geofontis
AB462554 uncultured bacterium
AY082369 uncultured Thermodesulfobacteriaceae bacterium
GCA_011364275.1 Caldimicrobium thiodismutans
KM221476 uncultured bacterium
GCA_025062245.1 Thermodesulfobacteriaceae bacterium
GCF_001548275.1 Caldimicrobium thiodismutans
LC055107 Caldimicrobium thiodismutans
Scale: 0.1
Bootstrap: >90%
>70%
>50%
Environment:
Hydrothermal vent
Hot spring
Oil reservoir
Terrestrial subsurface

Results and Discussion

Diversity and habitats of Thermodesulfobacteria

Our first task was to compile and annotate all publicly available Thermodesulfobacteria MAGs (Table S1) and MAGs from unpublished data (Table 1). We also downloaded the Thermodesulfobacteria 16S rRNA genes and metadata from the SILVA database (Table S4). Almost all the Thermodesulfobacteria originate from three types of environments – hydrothermal vents, hot springs and oil reservoirs (Figure 1). This confirms that Thermodesulfobacteria are obligate thermophiles and hyperthermophiles, in contrast to their Desulfobacterota relatives (Rabus et al., 2015).

We obtained MAGs that originated from a black smoker in the Loki's Castle vent field, located in the Arctic Mid-Ocean Ridge (AMOR) (Baumberger et al., 2016; Vulcano et al., 2022). The high-quality MAGs from the AMOR affiliated with the *Thermosulfurimonas* (two MAGs), the Thermodesulfatatoraceae (four MAGs) and Thermodesulfobacterium (four MAGs) (Table 1 and Figure 2). We also obtained MAGs from the Auka hydrothermal system in the southern Pescadero Basin (Gulf of California, Mexico) (Paduan et al., 2018; Speth et al., 2022). The MAGs from Pescadero Basin have lower quality estimates than the AMOR ones (Table 1). One Pescadero MAG affiliated broadly with the order Thermodesulfobacteriales whereas the other two MAGs were *Thermodesulfobacterium* (*Tb.*) species. Thermodesulfobacteria MAGs from alkane-degrading enrichment cultures from Guaymas Basin belong to the candidate species *Ca*. Tb. torris and *Ca*. Tb. syntrophicum (Benito Merino et al., 2022; Zehnle et al., 2022). All the new MAGs cover genera from most of the Thermodesulfobacteria families, with the exception of the ST65 family (*Thermosulfuriphilus* cluster) (Figure 2).

Thermodesulfobacteria MAGs and genomes related to oil reservoirs belong to a single clade based on 16S rRNA phylogeny (Figure 1) and genome phylogeny (Figure 2). *Tb. thermophilum*, isolated from a petroleum deposit (Rozanova and Khudiakova, 1974; Trüper, 2003), and several *Tb. commune* MAGs retrieved from oil-rich environments (Christensen et al., 1992; Parks et al., 2018) are included in this clade. The clade also includes isolates from hot springs such as *Tb. commune* and *Tb. hveragerdense* (Zeikus et al., 1983), and a MAG originating from of an hydraulically fractured gas well (GCA_020055045.1, marked as "subsurface" in Figures 1 and 2).

← Figure 1. 16S rRNA phylogeny of Thermodesulfobacteria. The tree is a ML phylogeny of 16S rRNA genes. Support values are based on 100 iterations. The sequences in bold ares the 16S rRNA genes extracted from MAGs and genomes. The clade highlighted in blue contains putative syntrophic Thermodesulfobacteria from (Benito Merino et al., 2022; Zehnle et al., 2022).

The Thermodesulfobacteria that originate from hydrothermal vents and from hot springs belong to separated clades. An exception to this is *Tb. hydrogeniphilum*, isolated from vents of the Guaymas Basin (Jeanthon et al., 2002). *Tb. hydrogeniphilum* branches at the base of the hot spring-associated *Tb. commune*, in a clade with >70% bootstrap support (Figure 2). While most Desulfobacterota SRB are mesophilic (Rabus et al., 2015), all Thermodesulfobacteria have optimal growth temperatures above 60°C (Table 2).

Table 1. Unpublished Thermodesulfobacteria MAGs used in this study. Completeness and contamination were estimated with CheckM (Parks et al., 2015).

MAG	Origin	Comp. (%)	Cont. (%)	GTDB taxonomy
AMOR20_M0463	Arctic Mid-Ocean Ridge	95.47	2.1	g__Thermosulfurimonas
AMOR20_M0464	Arctic Mid-Ocean Ridge	83.33	6.22	g__Thermosulfurimonas
AMOR20_M0483	Arctic Mid-Ocean Ridge	98.22	4.6	g__Thermodesulfatator
AMOR20_M0484	Arctic Mid-Ocean Ridge	94.72	2.14	g__Thermodesulfatator
AMOR20_M0485	Arctic Mid-Ocean Ridge	96.78	2.26	g__Thermodesulfatator_A
AMOR20_M0486	Arctic Mid-Ocean Ridge	99.04	1.23	f__Thermodesulfatatoraceae
AMOR20_M0690	Arctic Mid-Ocean Ridge	99.17	1.18	g__Thermodesulfobacterium
AMOR20_M0691	Arctic Mid-Ocean Ridge	99.09	1.25	g__Thermodesulfobacterium
AMOR20_M0692	Arctic Mid-Ocean Ridge	98.75	1.25	g__Thermodesulfobacterium
AMOR20_M0693	Arctic Mid-Ocean Ridge	87.45	3.12	g__Thermodesulfobacterium
Pescadero_bin40_16	Pescadero Basin	73.66	4.12	o__Thermodesulfobacteriales
Pescadero_bin44_17	Pescadero Basin	76.34	1.65	g__Thermodesulfobacterium
Pescadero_bin53_20	Pescadero Basin	77.45	1.88	s__Thermodesulfobacterium sp003641645
Ca. Tb. torris C16_70	Hexadecane culture at 70°C (Guaymas Basin)	90.14	2.82	s__Thermodesulfobacterium sp003641645
Ca. Tb.syntrophicum MCA70	Mid-chain alkane cultures at 70°C (Guaymas Basin)	98.75	0.83	s__Thermodesulfobacterium sp003641645

Presence of Thermodesulfobacteria in oil-rich environments

Because Thermodesulfobacteria are often present in oil reservoirs and gas-rich vents, we searched their genomes for putative alkyl-succinate synthases (Ass). This enzyme adds a molecule of fumarate to the secondary carbon of alkanes, to activate them to (1-methylalkyl)succinates (Grundmann et al., 2008; Callaghan et al., 2010; Widdel and Musat, 2010). None of the Thermodesulfobacteria genomes encodes Ass-like enzymes, strongly suggesting that they are unable to grow themselves on alkane or other hydrocarbons. Thermodesulfobacteria inhabiting oil reservoirs (e.g., *Tb. commune*) likely grow on the oxidation of fermentation products such as small organic molecules and H_2. We base this assumption on the substrates that Thermodesulfobacteria isolates metabolize (Table 2) and on the occurrence of Thermodesulfobacteria in enrichment cultures with anoxic marine sediments (Pérez Castro et al., 2021).

Table 2. Origin and metabolism of isolated Thermodesulfobacteria. Abbreviations: *Tb*., *Thermodesulfobacterium*; *C*., *Caldimicrobium*; *Tp*., *Thermosulfuriphilus*; *Tt*., *Thermodesulfatator*; *Tm*., *Thermosulfurimonas*; OT, optimal growth temperature; S^0, elemental sulfur.

Organism	Location	OGT (°C)	Description of metabolism	Reference
Tb. commune	Ink Pot hot spring (Yellowstone NP, USA)	70	Pyruvate, lactate and H_2 as electron donors; sulfate reduction.	(Zeikus et al., 1983)
Tb. thermophilum	Petroleum deposit (Caspian Sea)	65	Lactate as electron donor; sulfate reduction.	(Rozanova and Khudiakova, 1974)
Tb. hveragerdense	Hot spring (Hveragerdi, Iceland)	70-74	Pyruvate, lactate and H_2 as electron donors; sulfate and thiosulfate reduction.	(Sonne-Hansen and Ahring, 1999)
Tb. hydrogeniphilum	Guaymas Basin hydrothermal sediment (Mexico)	75	H_2 as electron donor; CO_2 as C source; sulfate reduction.	(Jeanthon et al., 2002)
Tb. geofontis	Obsidian Pool hot spring (Yellowstone NP, USA)	83	H_2 or formate as electron donor; CO_2 as C source; sulfate, thiosulfate and S^0 reduction	(Hamilton-Brehm et al., 2013)
C. thiodismutans	Nakabusa hot spring (Japan)	75	CO_2 as C source; S^0, thiosulfate and sulfite disproportionation.	(Kojima et al., 2016)
C. rimae	Uzon volcanic caldera (Kamchatka, Russia)	75	H_2 as electron donor; CO_2 as C source; S^0 and thiosulfate reduction.	(Miroshnichenko et al., 2009)
Tp. ammonigenes	Eastern Lau Spreading Centre (Pacific Ocean)	65	S^0 as electron donor; CO_2 as C source; nitrate reduction or S^0, thiosulfate or sulfite disproportionation.	(Slobodkina et al., 2017)
Tt. indicus	Kairei vent field (Indian Ocean)	70	H_2 as electron donor; CO_2 as C source; sulfate reduction.	(Moussard et al., 2004)
Tt. autotrophicus	Hydrothermal vent (Indian Ocean)	65-70	H_2 as electron donor; CO_2 as C source; sulfate reduction.	(Lai et al., 2016)
Tt. atlanticus	Rainbow hydrothermal vent (Atlantic Ocean)	65-70	H_2 as electron donor; CO_2, methylamine, peptone or yeast extract as C source; sulfate reduction.	(Alain et al., 2010)
Tm. dismutans	Eastern Lau Spreading Centre (Pacific Ocean)	74	S^0 as electron donor; CO_2 as C source; S^0, thiosulfate and sulfite disproportionation.	(Slobodkin et al., 2012)
Tm. marina	Shallow hydrothermal vent (Kunashir Island)	74	S^0 as electron donor; CO_2 as C source; S^0, thiosulfate and sulfite disproportionation.	(Frolova et al., 2018)

By this, Thermodesulfobacteria may contribute to the souring of reservoirs close to the limit of sterilization in oil reservoirs (i.e., approximately 80°C), thus outcompeting other meso- and thermophilic SRB (Connan, 1984). The limit for alkane oxidation was set around 50°C because most SRB cannot survive at higher temperatures. This, together with the inability of Thermodesulfobacteria to grow on alkanes, could favour the growth of anaerobic alkane-degrading archaea such as sulfate-reducing Archaeoglobi (Khelifi et al., 2014) or syntrophic alkane degraders like *Ca*. Syntrophoarchaeum (Laso-Pérez et al., 2016).

Energy conservation in free-living Thermodesulfobacteria

Like most Desulfobacterota, the majority of Thermodesulfobacteria are sulfate-reducing bacteria. This means that the transfer of electrons generates a charge potential in the cell membrane, that is then coupled to the oxidative phosphorylation of ATP (Cardoso Pereira et al., 2011). SRB encode a wide variety of cytochromes and membrane complexes that allows them to flexibly utilize different electron donors (Pereira et al., 2007). All the Thermodesulfobacteria encode a dissimilatory sulfate reduction pathway. While most Thermodesulfobacteria are SRB, some might use the pathway for disproportionation of sulfur compounds (Cypionka, 1995; Rabus et al., 2015). Although many SRB can disproportionate sulfur compounds, only a few species can utilize these reactions for growth (Krämer and Cypionka, 1989; Finster, 2008; Finster et al., 2013). In the Thermodesulfobacteria, four isolates are capable of elemental sulfur, thiosulfate or sulfite disproportionation.

Hydrogen metabolism is common in the Thermodesulfobacteria. All isolates utilize H_2 as energy source, with the exception of *Tb. thermophilum* and the sulfur-disproportionating *Thermosulfurimonas* and *Thermosulfuriphilus* (Table 2). Protein annotation with HMMs revealed that NiFe hydrogenases of the groups 1 and 4 are widespread in the Thermodesulfobacteria (Figure 2). All the group 4 hydrogenases predicted by HMMs were annotated as non-hydrogenases with the HydDB (Søndergaard et al., 2016). Therefore, we excluded this group from further discussion.

→

Figure 2. Phylogenomic tree of Thermodesulfobacteria, combined with presence-absence matrix for genes encoding specific cytochromes related to DIET and hydrogenases. ML phylogeny of bacterial single copy marker genes. Circles in the branches show bootstrap support based on 100 iterations. The genomes in bold are MAGs added to the Thermodesulfobacteria phylogeny in this study (Table 1). From left to right, the datasets show the origin of the genomes (same colour coding as Figure 1), completeness and contamination of the genomes, extracellular cytochromes (orange), outer membrane-associated conduit (blue), periplasmic cytochromes (lilac), inner membrane electron transfer complexes (yellow) and hydrogenases (divided by group, green). Species abbreviations: *Tb., Thermodesulfobacterium; C., Caldimicrobium; Tp., Thermosulfuriphilus; Tt., Thermodesulfatator; Tm., Thermosulfurimonas*. We define six Thermodesulfobacteria clusters without biological meaning for the purpose of discussion in the main text (right-most on the figure).

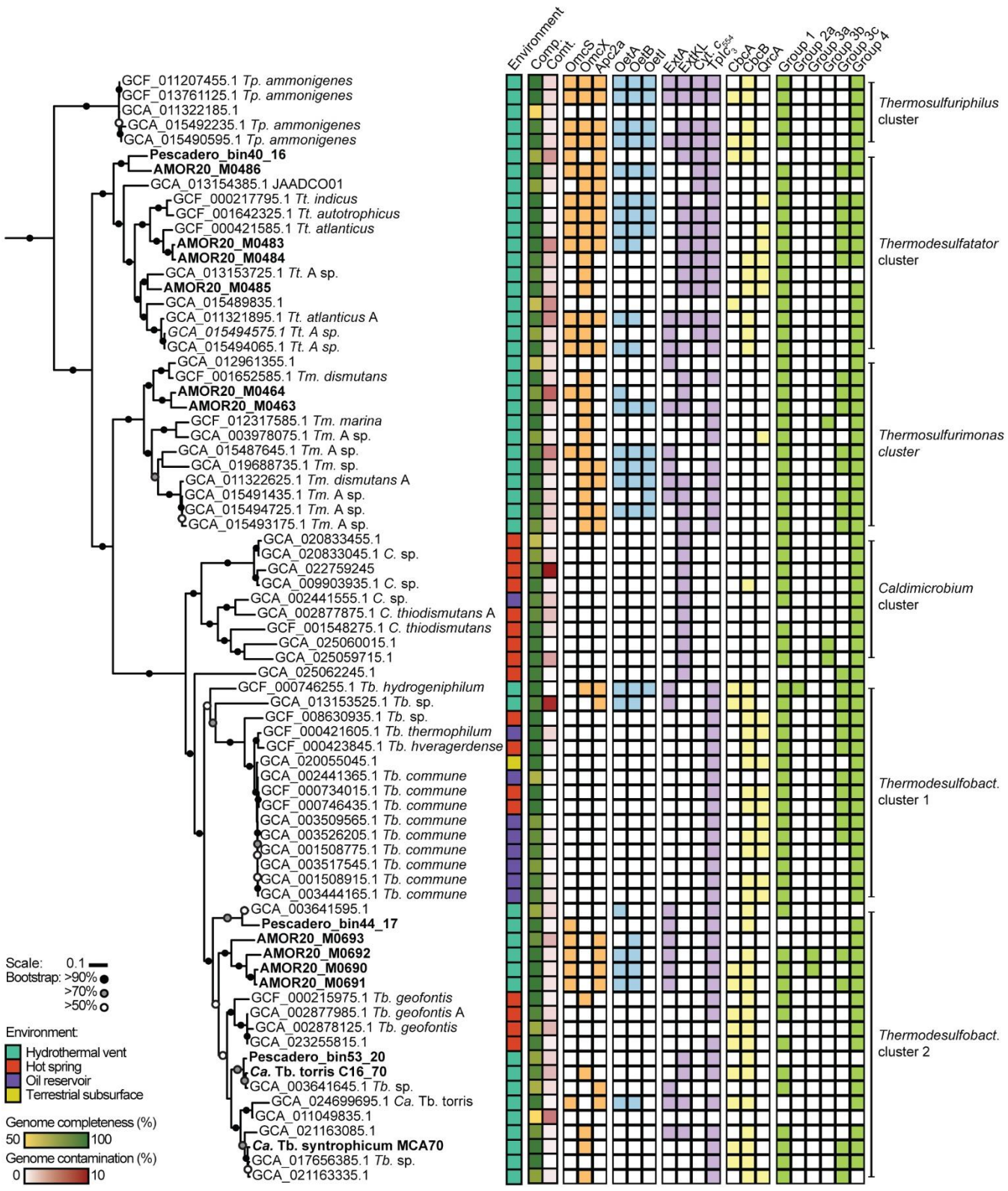

Group 1 refers to H_2 uptake hydrogenases that couple H_2 oxidation to the reduction of anaerobic electron acceptors, such as sulfate (Vignais and Billoud, 2007). Thermodesulfobacteria hydrogenases belong to the subgroup 1c (Søndergaard et al., 2016). In Thermodesulfobacteria and other hydrogenotrophic sulfate reducers, this hydrogenase transfers the electrons derived from H_2 oxidation to the quinone pool in the

inner membrane (Matias et al., 2005). The quinone-modifying oxidoreductase (Qmo) transfers the electrons from reduced quinones to AprAB, which then reduces adenylylsulfate (adenosine-5'-monophosphate) to sulfite in the cytoplasm (Figure 3) (Ramos et al., 2012). From the quinone pool, electrons can also flow to the Dsr-associated membrane complex (DsrJKMOP) which then reduces a disulfide bond in DsrC, located in the cytoplasm (Cardoso Pereira et al., 2011; Venceslau et al., 2014). DsrC directly interacts with DsrAB to reduce sulfite to sulfide (Venceslau et al., 2014).

Some Thermodesulfobacteria MAGs encode group 3c hydrogenases (Figure 2). These are cytoplasmic hydrogenases that function bidirectionally to reduce or oxidize cofactors such as F_{420}, NAD^+ or $NADP^+$ (Vignais and Billoud, 2007). In the hyperthermophilic archaeon *Pyrococcus furiosus*, a group 3 hydrogenase produces H_2 from the fermentation of organic molecules and it can also reduce elemental sulfur (S^0) to hydrogen sulfide (H_2S) (Ma et al., 1994). Group 3 hydrogenases are mainly encoded by *Thermodesulfatator* sp., *Thermosulfurimonas* sp., and *Thermodesulfobacterium* clade 1 (Figure 2). In *Thermosulfurimonas*, cytoplasmic hydrogenases could catalyze S^0 reduction. In hydrogenotrophic *Thermodesulfobacterium* and *Thermodesulfatator*, this hydrogenase could be reducing the heterodisulfide.

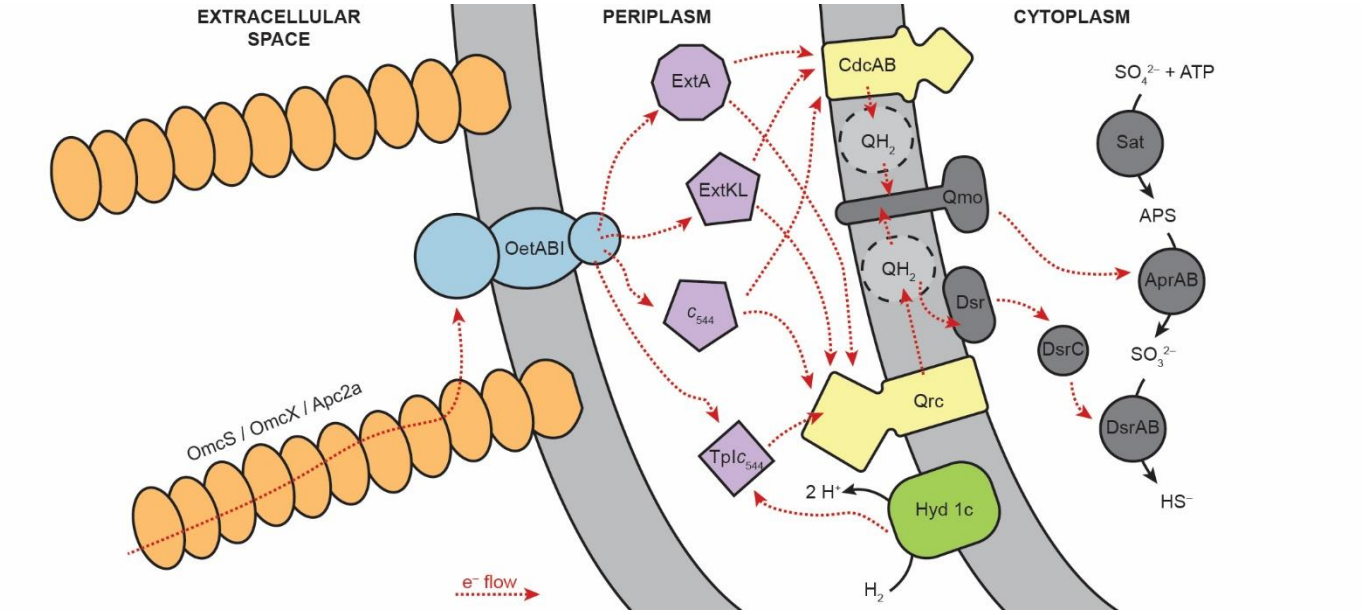

Figure 3. Schematic path of electrons from the extracelullar space to the sulfate reduction pathway. The flow of electrons is represented with dashed red arrows. The colour scheme maches the presence/absence matrix in Figure 2: extracellular cytochromes (orange), outer membrane-associated conduit (blue), periplasmic cytochromes (lilac), inner membrane electron transfer complexes (yellow) and group 1c hydrogenase (green). The sulfate reduction pathway and associated membrane complexes are depicted in grey. QH_2 refers to the inner membrane quinone/quinol pool. For detailed pathway description please refer to the text.

Our analyses show a wide distribution of group 1 hydrogenases in the Thermodesulfobacteria. Free-living Thermodesulfobacteria utilize membrane-bound hydrogenases for hydrogenotrophic growth. While the absence of hydrogenases in some MAGs might signify an obligate syntrophic lifestyle (see text below), other MAGs lacking hydrogenases could utilize other electron donors. Alternatively, low completeness values could explain this absence.

DIET-associated cytochromes

Recently, the mechanisms for energy conservation and DIET have been studied in partner SRB of the groups Seep-SRB1 (*Ca*. Syntrophophila and *Ca*. Desulfomelonium), Seep-SRB2 (*Ca*. Desulfomithrium) and HotSeep-1 (*Ca*. Desulfofervidus) (Murali et al., 2022). We aimed to clarify whether this pathway is also present in the Thermodesulfobacteria.

AOM-associated SRB receive electrons derived from AOM via conductive nanowire-like structures (Wegener et al., 2015), formed by outer-membrane cytochromes (OmcS and OmcX) (Shrestha et al., 2013; Wang et al., 2019; Yu et al., 2021; Murali et al., 2022) or a hexaheme cytochrome named Apc2a (Murali et al., 2022). The electrons are then transferred to an outer membrane-bound extracellular electron transfer conduit (OetABI) typical of syntrophic SRB and Geobacter (Leang et al., 2005; Murali et al., 2022). The OetABI is a conduit located in the outer membrane that transfers extracellular electrons from OmcS, OmcX and Apc2a to the periplasmic cytochromes (Figure 3). Homologs of *Geobacter sulfurreducens* cytochromes ExtA (Jiménez Otero et al., 2018) and ExtKL (Jahan et al., 2018), along with cytochrome TpIc_3 and cytochrome c_{554}, have been identified in syntrophic Desulfobacterota as DIET periplasmic cytochromes (Murali et al., 2022). These periplasmic cytochromes reduce quinones in the inner membrane. Reduced quinones pass on the electrons to the sulfate reduction pathway, as described above.

Interestingly, only Thermodesulfobacteria from hydrothermal vents encode all or some of the following: outer-membrane cytochromes (OmcS-like, OmcX and Apc2a), the Oet conduit and periplasmic cytochromes (ExtA-like, ExtKL, c_{554} and TpIc_3) (Figure 2). This could indicate a possible role of these SRB in DIET, as discussed in the following section.

Periplasmic cytochromes transfer electrons to protein complexes in the inner cellular membrane. For AOM-associated SRB, the quinone reductase complex (Qrc) or a *bc*-type cytochrome (CbcAB) were proposed as inner-membrane complexes (Venceslau et al., 2010; Rabus et al., 2015; Joshi et al., 2021; Murali et al., 2022). These complexes reduce quinones in the inner membrane. Almost all

Thermodesulfobacteria encode one or two Cbc subunits (Figure 2). The presence of Qrc is rare in the Thermodesulfobacteria.

Putative syntrophic Thermodesulfobacteria

Ca. Tb. torris is the partner bacterium of ANME-1c in AOM at 70°C (Benito Merino et al., 2022). *Ca.* Tb. torris encodes all the steps in the DIET pathway from the extracellular cytochromes to the inner membrane-associated complexes, except for the subunit OetI. We attribute the lack of OetI to inefficient protein annotation, because the cytochrome queries used in BLASTP originate from SRB outside of the Thermodesulfobacteria (Table S2). Interestingly, the membrane bound group 1c hydrogenase is absent in *Ca*. Tb. torris (Figure 2). The predicted group 4 hydrogenase was classified as a non-hydrogenase by HydDB (Søndergaard et al., 2016). Growth of *Ca*. Tb. torris on hydrogen or other electron donors has not been observed (Benito Merino et al., 2022). With this information, *Ca*. Tb. torris could be an obligate syntroph in AOM and anaerobic oxidation of alkanes (AOA).

The MAGs that do not code for a hydrogenase (other than *Ca*. Tb. torris) do not have a complete DIET pathway. In the case of the neighbouring genome of Ca. Tb. torris (GCA_011049835.1), the lack of hydrogenase and DIET pathway could be due to the low genome completeness. Interestingly, the rest of the MAGs in the clade of *Ca*. Tb. torris all encode this hydrogenase. The other two putative syntrophic Thermodesulfobacteria (*Ca*. Tb. syntrophicum and *Ca*. Tb. torris C16_70; (Zehnle et al., 2022) and Benito Merino, in prep., Chapter 3) in this clade encode a hydrogenase but not the Oet conduit. This could mean that these Thermodesulfobacteria interact with alkane-oxidizing archaea with interspecies transfer of hydrogen or other reduced compounds (Schink, 1997). The syntrophy mechanisms of alkanotrophic archaea and Thermodesulfobacteria needs further research.

The DIET pathway is conserved in some genomes of the *Thermosulfuriphilus* cluster, the *Thermodesulfatator* cluster and the *Thermosulfurimonas* cluster (Figure 2). In contrast, it is absent from the *Caldimicrobium* cluster and from most of the genomes of *Thermodesulfobacterium* cluster 1, i.e., the two clusters that comprise genomes from hot spring and oil reservoirs (Figure 2). The Thermodesulfobacteria from hydrothermal vents encoding extracellular, periplasmic and inner-membrane cytochromes could be putative syntrophic partners for AOA or AOM.

Conclusion and outlook

The class Thermodesulfobacteria contains the most thermophilic organisms in the phylum Desulfobacterota (Rabus et al., 2015). Growing in the thermophilic-hyperthermophilic range (between 50

and 90°C), Thermodesulfobacteria define the upper temperature limit for bacterial sulfate reducers. Based on our analyses, almost all of the Thermodesulfobacteria MAGs could grow on hydrogen, thanks to membrane-bound hydrogenases (Figure 2). This supports observations on isolated Thermodesulfobacteria species. Most of the isolates grow autotrophically and some of them grow heterotrophically on small organic molecules such as lactate or pyruvate (Table 2). These are common metabolisms in Desulfobacterota SRB (Rabus et al., 2015). However, an extensive analysis of the central carbon metabolism in Thermodesulfobacteria should be done to understand which pathways are used for autotrophy.

Our knowledge on SRB cytochromes mediating DIET in AOM has recently expanded (Murali et al., 2022). Many of the cytochromes of the DIET pathway are present in Thermodesulfobacteria genomes. Syntrophic interactions between anaerobic alkane- and methane-oxidizing archaea and Thermodesulfobacteria might be frequent in heated marine environments. Alternatively, the cytochromes might have other functions in free-living species. Future research should aim at disentangling the role of the extracellular and periplasmic cytochromes encoded by hydrothermal vent Thermodesulfobacteria. Comparative transcriptome analysis of putative syntrophic MAGs with isolates could aid us in clarifying the functions of the DIET pathway, extracellular cell appendages and hydrogenases in Thermodesulfobacteria.

With this study, we put the focus on the previously overlooked Thermodesulfobacteria, which could have a significant role as partners for sulfate-dependent alkane degradation or in souring of oil reservoirs at high temperatures.

Acknowledgements

We thank Francesca Vulcano and Emily Maria Denny for providing MAGs and metadata from AMOR. We thank Rafael Laso Pérez for providing MAGs and metadata from Pescadero Basin. We thank Ranjani Murali for providing protein queries of periplasmic and extracellular cytochromes.

Author Contributions

DBM and HZ designed the study with contributions of GW. HZ created the database of MAGs and metadata. HZ and DBM performed bioinformatics analyses. DBM wrote the manuscript with contributions of GW.

Funding

The study was funded by the Max Planck Society and the DFG under Germany's Excellence Intiative/Strategy through the Clusters of Excellence EXC 2077 "The Ocean Floor–Earth's Uncharted Interface" (project no. 390741601).

Supplementary Information

Supplementary Figures

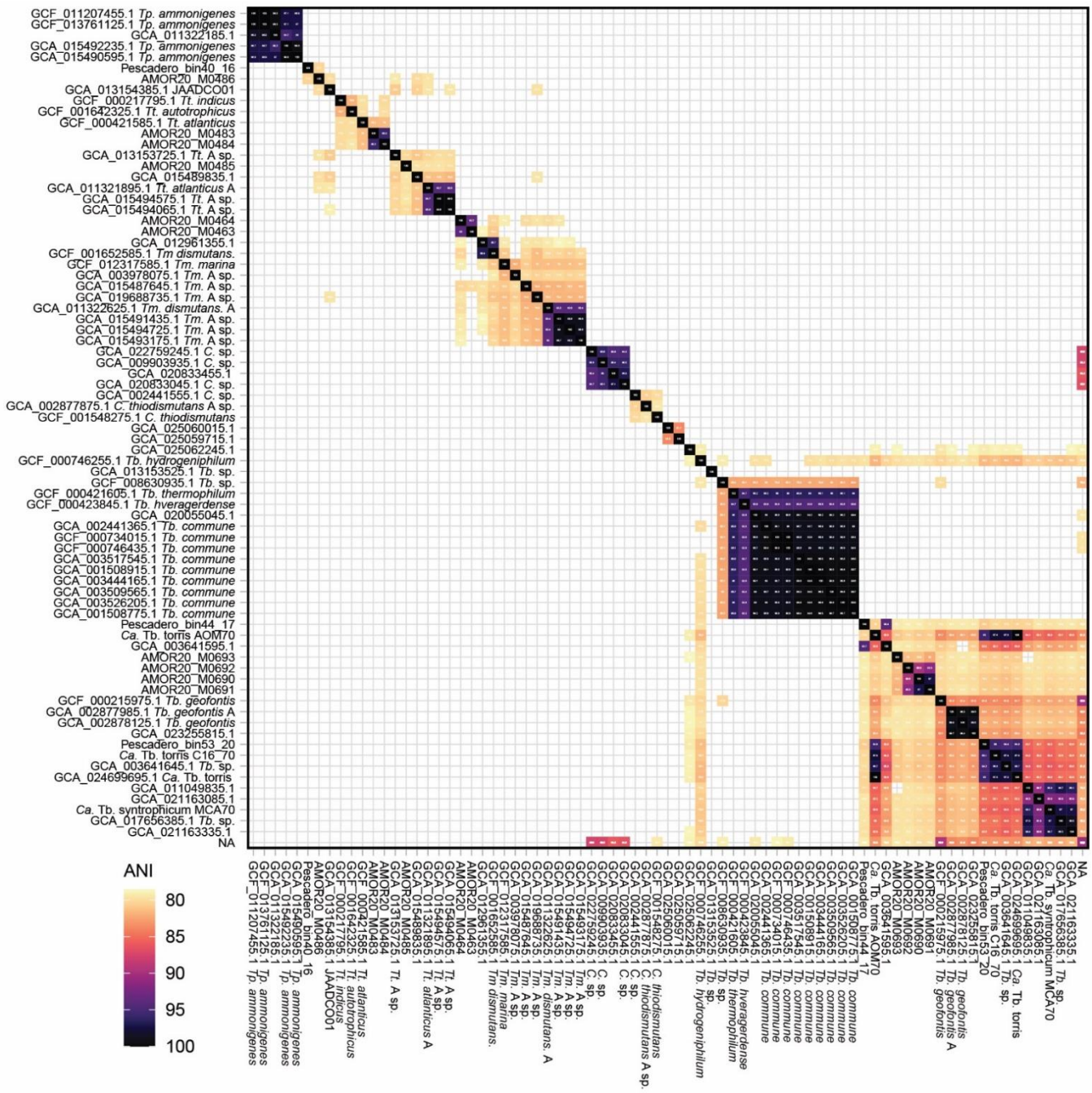

Figure S1. ANI of Thermodesulfobacteria genomes.

Supplementary Tables

Table S1. Thermodesulfobacteria genomes used in this study.

Assembly accession	BioProject	BioSample	Organism name	isolate / infraspecific name
GCA_001508095.1	PRJNA278302	SAMN03445130	Thermodesulfobacterium commune	37_1485
GCA_001508915.1	PRJNA278302	SAMN03445142	Thermodesulfobacterium commune	37_35
GCA_002441365.1	PRJNA348753	SAMN06455986	Thermodesulfobacterium commune	UBA6246
GCA_003444165.1	PRJNA417962	SAMN08017432	Thermodesulfobacterium commune	UBA12529
GCA_003509565.1	PRJNA417962	SAMN08019213	Thermodesulfobacterium commune	UBA12541
GCA_003517545.1	PRJNA417962	SAMN08019505	Thermodesulfobacterium commune	UBA12172
GCA_003526205.1	PRJNA417962	SAMN08020314	Thermodesulfobacterium commune	UBA12519
GCA_011321895.1	PRJNA480137	SAMN09638743	Thermodesulfatator atlanticus	HyVt-533
GCA_011322625.1	PRJNA480137	SAMN09638687	Thermosulfurimonas dismutans	HyVt-483
GCA_002877985.1	PRJNA419931	SAMN08107317	Thermodesulfobacterium geofontis	ZAV-08
GCA_002878125.1	PRJNA419931	SAMN08107297	Thermodesulfobacterium geofontis	ARK-04
GCA_011049835.1	PRJNA480137	SAMN09638550	Thermodesulfobacterium geofontis	HyVt-36
GCA_023255815.1	PRJNA419239	SAMN17914481	Thermodesulfobacterium geofontis	KUB_Bin04
GCA_001508775.1	PRJNA278302	SAMN03445117	Thermodesulfobacterium sp. 37_54	37_54
GCA_002877875.1	PRJNA419931	SAMN08107324	Caldimicrobium thiodismutans	ZAV-15
GCA_003978075.1	PRJNA454888	SAMN09407893	Thermodesulfatator sp.	MAG 95
GCA_011322185.1	PRJNA480137	SAMN09638719	Thermodesulfatator sp.	HyVt-511
GCA_002441555.1	PRJNA348753	SAMN06454325	Thermodesulfobacteriaceae bacterium UBA6232	UBA6232
GCA_017656385.1	PRJNA635695	SAMN15049711	Thermodesulfobacterium sp.	GB_MAG6_111
GCA_020055045.1	PRJNA308326	SAMN17087351	Thermodesulfobacterium sp.	WD_2_bin.24
GCA_020833455.1	PRJNA568221	SAMN18939781	Thermodesulfobacterium sp.	Bin P9
GCA_021163085.1	PRJNA713414	SAMN18353647	Thermodesulfobacterium sp.	AUK151
GCA_021163335.1	PRJNA713414	SAMN18353635	Thermodesulfobacterium sp.	AUK139
GCA_022759245.1	PRJNA669531	SAMN16495486	Thermodesulfobacterium sp.	2016_B01_C_8
GCA_009903935.1	PRJNA600296	SAMN13824555	Caldimicrobium sp.	EvPrim.Bin5
GCA_020833045.1	PRJNA568220	SAMN18938191	Caldimicrobium sp.	Bin S4
GCA_025059715.1	PRJNA761511	SAMN30304897	Caldimicrobium sp.	SKYB6

GCA_025060015.1	PRJNA761511	SAMN30304920	Caldimicrobium sp.	SKYB93
GCA_015487645.1	PRJNA546572	SAMN12876343	Thermosulfurimonas sp.	S012_5
GCA_015491435.1	PRJNA546572	SAMN12876512	Thermosulfurimonas sp.	S140_59
GCA_015493175.1	PRJNA546572	SAMN12876746	Thermosulfurimonas sp.	S146_100
GCA_003641595.1	PRJNA362212	SAMN09215085	Thermodesulfobacteria bacterium	B8_G2
GCA_003641645.1	PRJNA362212	SAMN09214901	Thermodesulfobacteria bacterium	B27_G15
GCA_013153525.1	PRJNA557557	SAMN12405692	Thermodesulfobacteria bacterium	L_MetaBat.182
GCA_013153725.1	PRJNA557557	SAMN12405693	Thermodesulfobacteria bacterium	L_MetaBat.13
GCA_013154385.1	PRJNA557557	SAMN12405695	Thermodesulfobacteria bacterium	L_MaxBin.001
GCA_024699695.1	PRJNA805391	SAMN27514933	Thermodesulfobacteria bacterium	AOM70-2
GCA_015490595.1	PRJNA546572	SAMN12876563	Thermodesulfobacteriales bacterium	S141_54
GCA_015492235.1	PRJNA546572	SAMN12876745	Thermodesulfobacteriales bacterium	S146_83
GCA_012961355.1	PRJNA522654	SAMN10967585	Thermodesulfobacteriaceae bacterium	UWMA-0247
GCA_015489835.1	PRJNA546572	SAMN12876647	Thermodesulfobacteriaceae bacterium	S143_105
GCA_015494065.1	PRJNA546572	SAMN12876665	Thermodesulfobacteriaceae bacterium	S144_47_esom
GCA_015494575.1	PRJNA546572	SAMN12876648	Thermodesulfobacteriaceae bacterium	S143_86
GCA_015494725.1	PRJNA546572	SAMN12876649	Thermodesulfobacteriaceae bacterium	S143_67
GCA_025062245.1	PRJNA761511	SAMN30304844	Thermodesulfobacteriaceae bacterium	SKYB108
GCA_019688735.1	PRJNA753696	SAMN20704186	Thermosulfurimonas sp. F29	strain=F29
GCF_000746255.1	PRJNA224116	SAMN02744824	Thermodesulfobacterium hydrogeniphilum	strain=DSM 14290
GCF_000734015.1	PRJNA224116	SAMN02934663	Thermodesulfobacterium commune DSM 2178	strain=DSM 2178
GCF_000746435.1	PRJNA224116	SAMN02744091	Thermodesulfobacterium commune DSM 2178	strain=DSM 2178
GCF_000217795.1	PRJNA224116	SAMN02232057	Thermodesulfatator indicus DSM 15286	strain=DSM 15286
GCF_000215975.1	PRJNA224116	SAMN02232058	Thermodesulfobacterium geofontis OPF15	strain=OPF15
GCF_001652585.1	PRJNA224116	SAMN04623574	Thermosulfurimonas dismutans	strain=S95
GCF_000421585.1	PRJNA224116	SAMN02440586	Thermodesulfatator atlanticus DSM 21156	strain=DSM 21156
GCF_000423845.1	PRJNA224116	SAMN02441489	Thermodesulfobacterium hveragerdense DSM 12571	strain=DSM 12571
GCF_000421605.1	PRJNA224116	SAMN02441582	Thermodesulfobacterium thermophilum DSM 1276	strain=DSM 1276
GCF_001548275.1	PRJNA224116	SAMD00039083	Caldimicrobium thiodismutans	strain=TF1
GCF_001642325.1	PRJNA224116	SAMN04478079	Thermodesulfatator autotrophicus	strain=S606

GCF_011207455.1	PRJNA224116	SAMN14116118	Thermosulfuriphilus ammonigenes	strain=ST65
GCF_013761125.1	PRJNA224116	SAMN14908362	Thermosulfuriphilus ammonigenes	strain=DSM 102941
GCF_012317585.1	PRJNA224116	SAMN12566302	Thermosulfurimonas marina	strain=SU872
GCF_008630935.1	PRJNA224116	SAMN12730809	Thermodesulfobacterium sp. TA1	strain=TA1

Table S2. Queries used for BLASTP annotations of DIET cytochromes and related proteins.

Protein	Query accession	Organism (BioSample)	E-value (BLASTP)
Apc2a	AMM40354.1	Candidatus Desulfofervidus auxilii (SAMN03372543)	1.00E-60
CbcA	PXF54667.1	Deltaproteobacteria bacterium (SAMN08434994)	1.00E-60
CbcB	PXF54668.1	Deltaproteobacteria bacterium (SAMN08434994)	1.00E-20
Cyt_c544	AMM39990.1	Candidatus Desulfofervidus auxilii (SAMN03372543)	1.00E-60
ExtA	MBC2719022.1	Desulfobacteraceae bacterium (SAMN14584927)	1.00E-20
ExtK / ExtL	KPJ65526.1	Syntrophobacter sp. DG_60 (SAMN03994151)	1.00E-20
OetA	OEU53798.1	Desulfobacterales bacterium C00003106 (SAMN05301625)	1.00E-60
OetB	OEU53799.1	Desulfobacterales bacterium C00003106 (SAMN05301625)	1.00E-60
OetI	LWX02_11375	Seep-SRB1a sp. 2 CR9063A (SAMN21396826)	1.00E-20
	OEU57520.1	Desulfobacterales bacterium C00003104 (SAMN05263723)	1.00E-20
	WP_140396645.1	Desulfuromonas acetexigens	1.00E-20
	WP_014551859.1	Geobacter sulfurreducens	1.00E-20
OmcS	AMM40351.1	Candidatus Desulfofervidus auxilii (SAMN03372543)	1.00E-60
OmcX	AMM39993.1	Candidatus Desulfofervidus auxilii (SAMN03372543)	1.00E-60
QrcA	AMM40483.1	Candidatus Desulfofervidus auxilii (SAMN03372543)	1.00E-05
TpIc3	AMM41048.1	Candidatus Desulfofervidus auxilii (SAMN03372543)	1.00E-05

Table S3. Hydrogenase COGs.

COG	Protein
COG0374	Ni,Fe-hydrogenase I large subunit
COG1740	Ni,Fe-hydrogenase I small subunit
COG5557	Ni/Fe-hydrogenase 2 integral membrane subunit HybB
COG3260	Ni,Fe-hydrogenase III small subunit
COG3261	Ni,Fe-hydrogenase III large subunit
COG3262	Ni,Fe-hydrogenase III component G
COG1969	Ni,Fe-hydrogenase I cytochrome b subunit
COG3658	Cytochrome b subunit of Ni2+-dependent hydrogenase
COG1142	Fe-S-cluster-containing hydrogenase component 2
COG1035	Coenzyme F420-reducing hydrogenase, beta subunit
COG1908	Coenzyme F420-reducing hydrogenase, delta subunit
COG1941	Coenzyme F420-reducing hydrogenase, gamma subunit
COG3259	Coenzyme F420-reducing hydrogenase, alpha subunit
COG4042	Energy-converting hydrogenase Eha subunit A
COG4041	Energy-converting hydrogenase Eha subunit B
COG4040	Energy-converting hydrogenase Eha subunit C
COG4039	Energy-converting hydrogenase Eha subunit D
COG4038	Energy-converting hydrogenase Eha subunit E
COG4037	Energy-converting hydrogenase Eha subunit F
COG4036	Energy-converting hydrogenase Eha subunit G
COG4078	Energy-converting hydrogenase Eha subunit H
COG4035	Energy-converting hydrogenase Eha subunit L
COG4084	Energy-converting hydrogenase A subunit M
COG4074	5,10-methenyltetrahydromethanopterin hydrogenase
COG4624	Iron only hydrogenase large subunit, C-terminal domain

Table S4. 16S rRNA genes accessions including Thermodesulfobacteria and outgroups. The sequences were used for reconstruction of 16S rRNA phylogenies.

Accession	Organism
EU435435	Thermodesulfatator atlanticus
ATXH01000052	Thermodesulfatator atlanticus DSM 21156
KU681513	Thermodesulfatator autotrophicus
AF393376	Thermodesulfatator indicus
CP002683	Thermodesulfatator indicus DSM 15286
CP002683	Thermodesulfatator indicus DSM 15286
X96725	Thermodesulfobacterium hveragerdense
JF346116	Thermosulfurimonas dismutans
MH513620	Thermodesulfobacterium sp. TA1
AF255595	Thermodesulfotobacterium sp. SRI-27
AF332514	Thermodesulfobacterium hydrogeniphilum
AF334601	Thermodesulfobacterium thermophilum
AF418169	Thermodesulfobacterium commune
JF935209	uncultured bacterium
EU635933	uncultured bacterium
KP091116	uncultured bacterium
ATXI01000006	Thermodesulfobacterium thermophilum DSM 1276
AUIT01000020	Thermodesulfobacterium hveragerdense DSM 12571
LC055107	Caldimicrobium thiodismutans
AB462554	uncultured bacterium
AF255596	Thermodesulfotobacterium sp. SRI-93
AF411013	Geothermobacterium ferrireducens
AY082369	uncultured Thermodesulfobacteriaceae bacterium
KM221476	uncultured bacterium
DQ833868	uncultured Geothermobacterium sp.
DQ924666	uncultured Geothermobacterium sp.
AY862065	uncultured Thermodesulfobacterium sp.
KT453601	uncultured Geothermobacterium sp.
AJ237604	Desulfomicrobium macestii
AJ237601	Desulfatiglans anilini
AJ251623	Desulfomicrobium orale
AJ277894	Desulfomicrobium baculatum
AJ277886	Desulfomicrobium escambiense
AJ237605	Syntrophobacter sp.
U41561	Geobacter chapellei
U48244	Desulfohalobium retbaense
U64865	Desulfomicrobium apsheronum
CP013015	Candidatus Desulfofervidus auxilii
X70905	Syntrophobacter wolinii
X82874	Syntrophobacter fumaroxidans
AJ582755	Desulfovibrio idahonensis

X82875	Syntrophobacter pfennigii
X95180	Desulfobulbus elongatus
X99235	Desulfohalobium retbaense
X83274	Desulforhabdus amnigena
FJ225426	Desulfovibrio legallii
X99236	Desulfovibrio africanus
FJ491989	Desulfosoma caldarium
JQ414031	Dissulfuribacter thermophilus
AB179691	uncultured bacterium
X85131	Syntrophus buswellii
AM086646	Desulfomonile tiedjei
FO203522	Desulfovibrio hydrothermalis AM13 = DSM 14728
X85132	Syntrophus gentianae
FR733678	Desulfovibrio simplex
L42613	Desulforhopalus vacuolatus
HM056226	Desulfosoma profundi
AB110541	Pseudodesulfovibrio portus
AY464939	Desulfomicrobium thermophilum
AB447633	uncultured bacterium
KM462058	Desulfobulbus sp. feline oral taxon 096
AB110549	Desulfobulbus japonicus
EU020016	Desulfatiglans anilini
AY574979	Desulfovibrio putealis
FJ810575	uncultured bacterium
AB212873	Syntrophorhabdus aromaticivorans
AB303305	Desulfovibrio butyratiphilus
AP010904	Desulfovibrio magneticus RS-1
AB294142	Desulfovibrio vulgaris
KT159733	Dissulfurimicrobium hydrothermale
HM750216	Desulfobulbus alkaliphilus
AY653549	Geobacter psychrophilus
KJ569657	uncultured bacterium
AB603520	Desulfovibrio simplex
AY651787	Syntrophobacter sulfatireducens
AB763347	Desulfatiglans parachlorophenolica
AB626715	uncultured bacterium
KU051627	Dissulfurirhabdus thermomarina
GU993263	Syntrophus aciditrophicus
KC259658	uncultured bacterium
AE017285	Desulfovibrio vulgaris str. Hildenborough
AF053752	Desulfovibrio burkinensis
AE017285	Desulfovibrio vulgaris str. Hildenborough
AF002671	Desulfobacca acetoxidans
CP000478	Syntrophobacter fumaroxidans MPOB
AB746665	uncultured bacterium

AF050101	Desulfovibrio fructosivorans JJ
AF067964	Desulfovibrio aminophilus
AF118453	Desulforhopalus singaporensis
AF192153	Desulfovibrio desulfuricans
U12253	Desulfobulbus rhabdoformis
KU845305	Desulfobulbus oligotrophicus
AF177276	Desulfovibrio inopinatus
AB806696	uncultured bacterium
AF192152	Desulfovibrio piger
AB806670	uncultured bacterium
AF230531	Desulfomonile limimaris
AF354663	Desulfobulbus mediterraneus
HE604070	uncultured bacterium
AF418172	Pseudodesulfovibrio profundus
FM179871	uncultured delta proteobacterium
CP001629	Desulfomicrobium baculatum DSM 4028
CP001734	Desulfohalobium retbaense DSM 5692
CP001734	Desulfohalobium retbaense DSM 5692
AF354156	uncultured delta proteobacterium
CP001649	Desulfovibrio salexigens DSM 2638
CP001940	Desulfurivibrio alkaliphilus AHT 2
CP002431	Pseudodesulfovibrio aespoeensis Aspo-2
CP002364	Desulfobulbus propionicus DSM 2032
AF507840	uncultured delta proteobacterium
AECZ01000068	Desulfovibrio fructosivorans JJ
CP002629	Desulfobacca acetoxidans DSM 11109
EU037213	uncultured bacterium
CP003360	Desulfomonile tiedjei DSM 6799
GU180164	uncultured bacterium
AM404378	uncultured delta proteobacterium
AJ306772	uncultured bacterium
AM167955	uncultured Microgenomates group bacterium
EU104847	uncultured delta proteobacterium
AY216442	uncultured bacterium
FR667800	uncultured bacterium
AY592579	uncultured bacterium
FR667402	uncultured bacterium
EU246116	uncultured organism
CR933289	uncultured Syntrophorhabdaceae bacterium
FR682639	uncultured delta proteobacterium
FR682650	uncultured delta proteobacterium
KM410576	uncultured prokaryote
JQ668617	uncultured bacterium
JQ723604	uncultured Desulfobacterales bacterium
FR682645	uncultured delta proteobacterium

KM356386	uncultured bacterium
JX000637	uncultured bacterium
JQ668569	uncultured Syntrophus sp.
EU644240	uncultured bacterium
FR682648	uncultured delta proteobacterium
DQ404843	uncultured bacterium
JX222100	uncultured bacterium
HM245642	uncultured bacterium
JX223633	uncultured bacterium
JX000648	uncultured bacterium
JX000639	uncultured bacterium
JX224892	uncultured bacterium
KM356302	uncultured bacterium
CU924798	uncultured bacterium
DQ521786	uncultured bacterium
KF268888	uncultured bacterium
KR814200	uncultured Desulfobulbaceae bacterium
KT308299	uncultured Desulfobulbus sp.
EF018817	uncultured bacterium
JN439980	uncultured organism
JX223369	uncultured bacterium
JN466207	uncultured organism
GQ181289	uncultured bacterium
GQ181528	uncultured bacterium
JN441849	uncultured organism
KP091244	uncultured bacterium
KX097369	uncultured bacterium
GQ181311	uncultured bacterium
MICL01000055	Syntrophobacterales bacterium RBG_19FT_COMBO_59_10
KX812787	uncultured bacterium
JN662185	uncultured delta proteobacterium
KX812786	uncultured bacterium
FJ462062	uncultured bacterium
KX812792	uncultured bacterium
FJ484787	uncultured delta proteobacterium
KX823820	uncultured bacterium
FJ462076	uncultured bacterium
JN626569	uncultured bacterium
MFZZ01000045	Candidatus Roizmanbacteria bacterium RIFCSPHIGHO2_12_FULL_38_13
AUBQ01000027	Desulfovibrio putealis DSM 16056
GQ402720	uncultured bacterium
LQBF01000029	delta proteobacterium ML8_D
FJ712508	uncultured bacterium
JF268398	uncultured bacterium
ATUZ01000009	Desulfovibrio desulfuricans subsp. desulfuricans DSM 642

AUCW01000075	Desulfobulbus mediterraneus DSM 13871
MAXQ01000429	Desulfobulbaceae bacterium C00003063
FJ516909	uncultured Desulfobacteraceae bacterium
LMZU01000026	Microgenomates bacterium OLB23
DQ186200	Desulfovibrio carbinoliphilus
LC124613	uncultured bacterium
FPLK01000706	metagenome
DQ122124	Desulfovibrio oxamicus
ARB_46D4CF55	AF419676.1 Uncultured bacterium a2b002 16S ribosomal RNA gene, partial sequence
ARB_B4CE3AA0	AF419677.1 Uncultured bacterium a2b033 16S ribosomal RNA gene, partial sequence

References

Alain, K., Postec, A., Grinsard, E., Lesongeur, F., Prieur, D., and Godfroy, A. (2010). Thermodesulfatator atlanticus sp. nov., a thermophilic, chemolithoautotrophic, sulfate-reducing bacterium isolated from a Mid-Atlantic Ridge hydrothermal vent. *Int. J. Syst. Evol. Microbiol.* 60, 33–38. doi: 10.1099/ijs.0.009449-0.

Altschul, S. F., Gish, W., Miller, W., Myers, E. W., and Lipman, D. J. (1990). Basic local alignment search tool. *J. Mol. Biol.* 215, 403–410. doi: 10.1016/S0022-2836(05)80360-2.

Altschul, S. F., Madden, T. L., Schäffer, A. A., Zhang, J., Zhang, Z., Miller, W., et al. (1997). Gapped BLAST and PSI-BLAST: a new generation of protein database search programs. *Nucleic Acids Res.* 25, 3389–3402. doi: 10.1093/nar/25.17.3389.

Anantharaman, K., Hausmann, B., Jungbluth, S. P., Kantor, R. S., Lavy, A., Warren, L. A., et al. (2018). Expanded diversity of microbial groups that shape the dissimilatory sulfur cycle. *ISME J.* 12, 1715–1728. doi: 10.1038/s41396-018-0078-0.

Baumberger, T., Früh-Green, G. L., Thorseth, I. H., Lilley, M. D., Hamelin, C., Bernasconi, S. M., et al. (2016). Fluid composition of the sediment-influenced Loki's Castle vent field at the ultra-slow spreading Arctic Mid-Ocean Ridge. *Geochim. Cosmochim. Acta* 187, 156–178. doi: 10.1016/j.gca.2016.05.017.

Benito Merino, D., Zehnle, H., Teske, A., and Wegener, G. (2022). Deep-branching ANME-1c archaea grow at the upper temperature limit of anaerobic oxidation of methane. *Front. Microbiol.* 13, 1–16. doi: 10.3389/fmicb.2022.988871.

Boetius, A., and Knittel, K. (2010). "Habitats of Anaerobic Methane Oxidizers," in *Handbook of Hydrocarbon and Lipid Microbiology*, ed. K. N. Timmis (Berlin, Heidelberg: Springer Berlin Heidelberg), 2193–2202. doi: 10.1007/978-3-540-77587-4_159.

Callaghan, A. V., Davidova, I. A., Savage-Ashlock, K., Parisi, V. A., Gieg, L. M., Suflita, J. M., et al. (2010). Diversity of Benzyl- and Alkylsuccinate Synthase Genes in Hydrocarbon-Impacted Environments and Enrichment Cultures. *Environ. Sci. Technol.* 44, 7287–7294. doi: 10.1021/es1002023.

Canfield, D. E., and Raiswell, R. (1999). The evolution of the sulfur cycle. *Am. J. Sci.* 299, 697–723. doi: 10.2475/ajs.299.7-9.697.

Cardoso Pereira, I. A., Ramos, A. R., Grein, F., Coimbra Marques, M., Marques da Silva, S., and Santos Venceslau, S. (2011). A Comparative Genomic Analysis of Energy Metabolism in Sulfate Reducing Bacteria and Archaea. *Front. Microbiol.* 2, 1–22. doi: 10.3389/fmicb.2011.00069.

Chaumeil, P. A., Mussig, A. J., Hugenholtz, P., and Parks, D. H. (2020). GTDB-Tk: a toolkit to classify genomes with the Genome Taxonomy Database. *Bioinformatics* 36, 1925–1927. doi: 10.1093/BIOINFORMATICS/BTZ848.

Chernomor, O., Von Haeseler, A., and Minh, B. Q. (2016). Terrace aware data structure for phylogenomic inference from supermatrices. *Syst. Biol.* 65, 997–1008. doi: 10.1093/SYSBIO/SYW037.

Christensen, B., Torsvik, T., and Lien, T. (1992). Immunomagnetically Captured Thermophilic Sulfate-Reducing Bacteria from North Sea Oil Field Waters. *Appl. Environ. Microbiol.* 58, 1244–1248. doi: 10.1128/AEM.58.4.1244-1248.1992.

Connan, J. (1984). "Biodegradation of Crude Oils in Reservoirs," in *Advances in Petroleum Geochemistry* (Elsevier), 299–335. doi: 10.1016/B978-0-12-032001-1.50011-0.

Cypionka, H. (1995). "Solute Transport and Cell Energetics," in *Sulfate-Reducing Bacteria* (Boston, MA: Springer US), 151–184. doi: 10.1007/978-1-4899-1582-5_6.

Edgar, R. C. (2004). MUSCLE: A multiple sequence alignment method with reduced time and space complexity. *BMC Bioinformatics* 5, 1–19. doi: 10.1186/1471-2105-5-113/FIGURES/16.

Eren, A. M., Esen, Ö. C., Quince, C., Vineis, J. H., Morrison, H. G., Sogin, M. L., et al. (2015). Anvi'o: an advanced analysis and visualization platform for 'omics data. *PeerJ* 3, e1319. doi:

10.7717/peerj.1319.

Eren, A. M., Kiefl, E., Shaiber, A., Veseli, I., Miller, S. E., Schechter, M. S., et al. (2020). Community-led, integrated, reproducible multi-omics with anvi'o. *Nat. Microbiol. 2020 61* 6, 3–6. doi: 10.1038/s41564-020-00834-3.

Finster, K. (2008). Microbiological disproportionation of inorganic sulfur compounds. *J. Sulfur Chem.* 29, 281–292. doi: 10.1080/17415990802105770.

Finster, K. W., Kjeldsen, K. U., Kube, M., Reinhardt, R., Mussmann, M., Amann, R., et al. (2013). Complete genome sequence of Desulfocapsa sulfexigens, a marine deltaproteobacterium specialized in disproportionating inorganic sulfur compounds. *Stand. Genomic Sci.* 8, 58–68. doi: 10.4056/sigs.3777412.

Frolova, A. A., Slobodkina, G. B., Baslerov, R. V., Novikov, A. A., Bonch-Osmolovskaya, E. A., and Slobodkin, A. I. (2018). Thermosulfurimonas marina sp. nov., an Autotrophic Sulfur-Disproportionating and Nitrate-Reducing Bacterium Isolated from a Shallow-Sea Hydrothermal Vent. *Microbiology* 87, 502–507. doi: 10.1134/S0026261718040082.

Galperin, M. Y., Makarova, K. S., Wolf, Y. I., and Koonin, E. V. (2015). Expanded microbial genome coverage and improved protein family annotation in the COG database. *Nucleic Acids Res.* 43, D261–D269. doi: 10.1093/NAR/GKU1223.

Grundmann, O., Behrends, A., Rabus, R., Amann, J., Halder, T., Heider, J., et al. (2008). Genes encoding the candidate enzyme for anaerobic activation of n-alkanes in the denitrifying bacterium, strain HxN1. *Environ. Microbiol.* 10, 376–385. doi: 10.1111/j.1462-2920.2007.01458.x.

Gu, Y., Srikanth, V., Salazar-Morales, A. I., Jain, R., O'Brien, J. P., Yi, S. M., et al. (2021). Structure of *Geobacter* pili reveals secretory rather than nanowire behaviour. *Nat. 2021 5977876* 597, 430–434. doi: 10.1038/s41586-021-03857-w.

Hahn, C. J., Laso-Pérez, R., Vulcano, F., Vaziourakis, K.-M., Stokke, R., Steen, I. H., et al. (2020). "*Candidatus* Ethanoperedens," a thermophilic genus of archaea mediating the anaerobic oxidation of ethane. *MBio* 11, 1–18. doi: 10.1128/mBio.00600-20.

Hamilton-Brehm, S. D., Gibson, R. A., Green, S. J., Hopmans, E. C., Schouten, S., van der Meer, M. T. J., et al. (2013). *Thermodesulfobacterium geofontis* sp. nov., a hyperthermophilic, sulfate-reducing bacterium isolated from Obsidian Pool, Yellowstone National Park. *Extremophiles* 17, 251–263. doi: 10.1007/S00792-013-0512-1.

Henry, E. A., Devereux, R., Maki, J. S., Gilmour, C. C., Woese, C. R., Mandelco, L., et al. (1994). Characterization of a new thermophilic sulfate-reducing bacterium - Thermodesulfovibrio yellowstonii, gen. nov. and sp. nov.: its phylogenetic relationship to Thermodesulfobacterium commune and their origins deep within the bacterial domain. *Arch. Microbiol.* 161, 62–69. doi: 10.1007/BF00248894.

Holler, T., Widdel, F., Knittel, K., Amann, R., Kellermann, M. Y., Hinrichs, K.-U., et al. (2011). Thermophilic anaerobic oxidation of methane by marine microbial consortia. *ISME J.* 5, 1946–1956. doi: 10.1038/ismej.2011.77.

Jahan, M. I., Tobe, R., and Mihara, H. (2018). Characterization of a Novel Porin-Like Protein, ExtI, from Geobacter sulfurreducens and Its Implication in the Reduction of Selenite and Tellurite. *Int. J. Mol. Sci.* 19, 809. doi: 10.3390/ijms19030809.

Jain, C., Rodriguez-R, L. M., Phillippy, A. M., Konstantinidis, K. T., and Aluru, S. (2018). High throughput ANI analysis of 90K prokaryotic genomes reveals clear species boundaries. *Nat. Commun. 2018 91* 9, 1–8. doi: 10.1038/s41467-018-07641-9.

Jeanthon, C., L'Haridon, S., Cueff, V., Banta, A., Reysenbach, A.-L., and Prieur, D. (2002). Thermodesulfobacterium hydrogeniphilum sp. nov., a thermophilic, chemolithoautotrophic, sulfate-reducing bacterium isolated from a deep-sea hydrothermal vent at Guaymas Basin, and emendation of the genus Thermodesulfobacterium. *Int. J. Syst. Evol. Microbiol.* 52, 765–772. doi: 10.1099/00207713-52-3-765.

Jiménez Otero, F., Chan, C. H., and Bond, D. R. (2018). Identification of Different Putative Outer Membrane Electron Conduits Necessary for Fe(III) Citrate, Fe(III) Oxide, Mn(IV) Oxide, or Electrode Reduction by Geobacter sulfurreducens. *J. Bacteriol.* 200, 347–365. doi: 10.1128/JB.00347-18.

Jørgensen, B. B. (1982). Mineralization of organic matter in the sea bed—the role of sulphate reduction. *Nature* 296, 643–645. doi: 10.1038/296643a0.

Jørgensen, B. B. (2006). "Bacteria and Marine Biogeochemistry," in *Marine Geochemistry*, eds. H. D. Schulz and M. Zabel (Berlin/Heidelberg: Springer), 169–206. doi: 10.1007/3-540-32144-6_5.

Joshi, K., Chan, C. H., and Bond, D. R. (2021). Geobacter sulfurreducens inner membrane cytochrome CbcBA controls electron transfer and growth yield near the energetic limit of respiration. *Mol. Microbiol.* 116, 1124–1139. doi: 10.1111/mmi.14801.

Kanehisa, M., and Goto, S. (2000). KEGG: Kyoto encyclopedia of genes and genomes. *Nucleic Acids Res.* 28, 27–30. doi: 10.1093/NAR/28.1.27.

Khelifi, N., Amin Ali, O., Roche, P., Grossi, V., Brochier-Armanet, C., Valette, O., et al. (2014). Anaerobic oxidation of long-chain n-alkanes by the hyperthermophilic sulfate-reducing archaeon, Archaeoglobus fulgidus. *ISME J.* 8, 2153–2166. doi: 10.1038/ismej.2014.58.

Knittel, K., and Boetius, A. (2010). "Anaerobic Methane Oxidizers," in *Handbook of Hydrocarbon and Lipid Microbiology* (Berlin, Heidelberg: Springer Berlin Heidelberg), 2023–2032. doi: 10.1007/978-3-540-77587-4_147.

Kojima, H., Umezawa, K., and Fukui, M. (2016). Caldimicrobium thiodismutans sp. nov., a sulfur-disproportionating bacterium isolated from a hot spring, and emended description of the genus Caldimicrobium. *Int. J. Syst. Evol. Microbiol.* 66, 1828–1831. doi: 10.1099/ijsem.0.000947.

Krämer, M., and Cypionka, H. (1989). Sulfate formation via ATP sulfurylase in thiosulfate- and sulfite-disproportionating bacteria. *Arch. Microbiol.* 151, 232–237. doi: 10.1007/BF00413135.

Krukenberg, V., Harding, K., Richter, M., Glöckner, F. O., Gruber-Vodicka, H. R., Adam, B., et al. (2016). *Candidatus* Desulfofervidus auxilii, a hydrogenotrophic sulfate-reducing bacterium involved in the thermophilic anaerobic oxidation of methane. *Environ. Microbiol.* 18, 3073–3091. doi: 10.1111/1462-2920.13283.

Krukenberg, V., Riedel, D., Gruber-Vodicka, H. R., Buttigieg, P. L., Tegetmeyer, H. E., Boetius, A., et al. (2018). Gene expression and ultrastructure of meso- and thermophilic methanotrophic consortia. *Environ. Microbiol.* 20, 1651–1666. doi: 10.1111/1462-2920.14077.

Lagesen, K., Hallin, P., Rødland, E. A., Stærfeldt, H. H., Rognes, T., and Ussery, D. W. (2007). RNAmmer: consistent and rapid annotation of ribosomal RNA genes. *Nucleic Acids Res.* 35, 3100. doi: 10.1093/NAR/GKM160.

Lai, Q., Cao, J., Dupont, S., Shao, Z., Jebbar, M., and Alain, K. (2016). Thermodesulfatator autotrophicus sp. nov., a thermophilic sulfate-reducing bacterium from the Indian Ocean. *Int. J. Syst. Evol. Microbiol.* 66, 3978–3982. doi: 10.1099/ijsem.0.001297.

Laso-Pérez, R., Wegener, G., Knittel, K., Widdel, F., Harding, K. J., Krukenberg, V., et al. (2016). Thermophilic archaea activate butane via alkyl-coenzyme M formation. *Nature* 539, 396–401. doi: 10.1038/nature20152.

Laso-Pérez, R., Wu, F., Crémière, A., Speth, D. R., Magyar, J. S., Krupovic, M., et al. (2022). Evolutionary diversification of methanotrophic *Ca.* Methanophagales (ANME-1) and their expansive virome. *bioRxiv*, 2022.07.04.498658. doi: 10.1101/2022.07.04.498658.

Leang, C., Adams, L. A., Chin, K.-J., Nevin, K. P., Meth , B. A., Webster, J., et al. (2005). Adaptation to Disruption of the Electron Transfer Pathway for Fe(III) Reduction in Geobacter sulfurreducens. *J. Bacteriol.* 187, 5918–5926. doi: 10.1128/JB.187.17.5918-5926.2005.

Letunic, I., and Bork, P. (2011). Interactive Tree of Life v2: Online annotation and display of phylogenetic trees made easy. *Nucleic Acids Res.* doi: 10.1093/nar/gkr201.

Ludwig, W., Strunk, O., Westram, R., Richter, L., Meier, H., Yadhukumar, A., et al. (2004). ARB: a

software environment for sequence data. *Nucleic Acids Res.* 32, 1363–1371. doi: 10.1093/NAR/GKH293.

Ma, K., Hao, Z., and Adams, M. W. W. (1994). Hydrogen production from pyruvate by enzymes purified from the hyperthermophilic archaeon, Pyrococcus furiosus : A key role for NADPH. *FEMS Microbiol. Lett.* 122, 245–250. doi: 10.1111/j.1574-6968.1994.tb07175.x.

Matias, P. M., Pereira, I. A. C., Soares, C. M., and Carrondo, M. A. (2005). Sulphate respiration from hydrogen in Desulfovibrio bacteria: a structural biology overview. *Prog. Biophys. Mol. Biol.* 89, 292–329. doi: 10.1016/j.pbiomolbio.2004.11.003.

McGlynn, S. E., Chadwick, G. L., Kempes, C. P., and Orphan, V. J. (2015). Single cell activity reveals direct electron transfer in methanotrophic consortia. *Nature* 526, 531–535. doi: 10.1038/nature15512.

Metcalfe, K. S., Murali, R., Mullin, S. W., Connon, S. A., and Orphan, V. J. (2020). Experimentally-validated correlation analysis reveals new anaerobic methane oxidation partnerships with consortium-level heterogeneity in diazotrophy. *ISME J. 2020 152* 15, 377–396. doi: 10.1038/s41396-020-00757-1.

Minh, B. Q., Schmidt, H. A., Chernomor, O., Schrempf, D., Woodhams, M. D., Von Haeseler, A., et al. (2020). IQ-TREE 2: new models and efficient methods for phylogenetic inference in the genomic era. *Mol. Biol. Evol.* 37, 1530–1534. doi: 10.1093/MOLBEV/MSAA015.

Miroshnichenko, M. L., Lebedinsky, A. V., Chernyh, N. A., Tourova, T. P., Kolganova, T. V., Spring, S., et al. (2009). Caldimicrobium rimae gen. nov., sp. nov., an extremely thermophilic, facultatively lithoautotrophic, anaerobic bacterium from the Uzon Caldera, Kamchatka. *Int. J. Syst. Evol. Microbiol.* 59, 1040–1044. doi: 10.1099/IJS.0.006072-0.

Mistry, J., Chuguransky, S., Williams, L., Qureshi, M., Salazar, G. A., Sonnhammer, E. L. L., et al. (2021). Pfam: The protein families database in 2021. *Nucleic Acids Res.* 49, D412–D419. doi: 10.1093/NAR/GKAA913.

Moussard, H., L'Haridon, S., Tindall, B. J., Banta, A., Schumann, P., Stackebrandt, E., et al. (2004). Thermodesulfatator indicus gen. nov., sp. nov., a novel thermophilic chemolithoautotrophic sulfate-reducing bacterium isolated from the Central Indian Ridge. *Int. J. Syst. Evol. Microbiol.* 54, 227–233. doi: 10.1099/ijs.0.02669-0.

Murali, R., Yu, H., Speth, D. R., Wu, F., Metcalfe, K. S., Crémière, A., et al. (2022). Physiological adaptation of sulfate reducing bacteria in syntrophic partnership with anaerobic methanotrophic archaea. *bioRxiv* 2022.11.23. doi: 10.1101/2022.11.23.517749.

Niemann, H., Lösekann, T., De Beer, D., Elvert, M., Nadalig, T., Knittel, K., et al. (2006). Novel microbial communities of the Haakon Mosby mud volcano and their role as a methane sink. *Nat. 2006 4437113* 443, 854–858. doi: 10.1038/nature05227.

Nisbet, E. G., and Sleep, N. H. (2001). The habitat and nature of early life. *Nature* 409, 1083–1091. doi: 10.1038/35059210.

Paduan, J. B., Zierenberg, R. A., Clague, D. A., Spelz, R. M., Caress, D. W., Troni, G., et al. (2018). Discovery of Hydrothermal Vent Fields on Alarcón Rise and in Southern Pescadero Basin, Gulf of California. *Geochemistry, Geophys. Geosystems* 19, 4788–4819. doi: 10.1029/2018GC007771.

Parks, D. H., Chuvochina, M., Waite, D. W., Rinke, C., Skarshewski, A., Chaumeil, P.-A., et al. (2018). A standardized bacterial taxonomy based on genome phylogeny substantially revises the tree of life. *Nat. Biotechnol.*, 1–9. doi: 10.1101/256800.

Parks, D. H., Imelfort, M., Skennerton, C. T., Hugenholtz, P., and Tyson, G. W. (2015). CheckM: Assessing the quality of microbial genomes recovered from isolates, single cells, and metagenomes. *Genome Res.* 25, 1043–1055. doi: 10.1101/gr.186072.114.

Pereira, I. A. C., Haveman, S. A., and Voordouw, G. (2007). "Biochemical, genetic and genomic characterization of anaerobic electron transport pathways in sulphate-reducing Delta proteobacteria," in *Sulphate-Reducing Bacteria*, eds. L. L. Barton and W. A. Hamilton (Cambridge: Cambridge University Press), 215–240. doi: 10.1017/CBO9780511541490.008.

Pérez Castro, S., Borton, M. A., Regan, K., Hrabe de Angelis, I., Wrighton, K. C., Teske, A. P., et al. (2021). Degradation of biological macromolecules supports uncultured microbial populations in Guaymas Basin hydrothermal sediments. *ISME J. 2021 1512* 15, 3480–3497. doi: 10.1038/s41396-021-01026-5.

Pruesse, E., Peplies, J., and Glöckner, F. O. (2012). SINA: Accurate high-throughput multiple sequence alignment of ribosomal RNA genes. *Bioinformatics* 28, 1823–1829. doi: 10.1093/BIOINFORMATICS/BTS252.

Quast, C., Pruesse, E., Yilmaz, P., Gerken, J., Schweer, T., Yarza, P., et al. (2013). The SILVA ribosomal RNA gene database project: improved data processing and web-based tools. *Nucleic Acids Res.* 41, D590–D596. doi: 10.1093/NAR/GKS1219.

Rabus, R., Hansen, T. A., and Widdel, F. (2013). "Dissimilatory Sulfate- and Sulfur-Reducing Prokaryotes," in *The Prokaryotes* (Berlin, Heidelberg: Springer Berlin Heidelberg), 309–404. doi: 10.1007/978-3-642-30141-4_70.

Rabus, R., Venceslau, S. S., Wöhlbrand, L., Voordouw, G., Wall, J. D., and Pereira, I. A. C. (2015). "A Post-Genomic View of the Ecophysiology, Catabolism and Biotechnological Relevance of Sulphate-Reducing Prokaryotes," in *Advances in Microbial Physiology*, 55–321. doi: 10.1016/bs.ampbs.2015.05.002.

Ramos, A. R., Keller, K. L., Wall, J. D., and Cardoso Pereira, I. A. (2012). The membrane QmoABC complex interacts directly with the dissimilatory adenosine 5′-phosphosulfate reductase in sulfate reducing bacteria. *Front. Microbiol.* 3, 1–10. doi: 10.3389/FMICB.2012.00137.

Rozanova, E., and Khudiakova, A. (1974). Novyĭ bessporovyĭ termofil'nyĭ organizm, vosstanavlivaiushchiĭ sul'faty, *Desulfovibrio thermophilus* nov. sp [A new non-spore forming thermophilic organism, reducing sulfates, *Desulfovibrio thermophilus* nov. sp]. *Mikrobiologiia* 43, 1069–75.

Schink, B. (1997). Energetics of syntrophic cooperation in methanogenic degradation. *Microbiol. Mol. Biol. Rev.* 61, 262–280. doi: 10.1128/mmbr.61.2.262-280.1997.

Schreiber, L., Holler, T., Knittel, K., Meyerdierks, A., and Amann, R. (2010). Identification of the dominant sulfate-reducing bacterial partner of anaerobic methanotrophs of the ANME-2 clade. *Environ. Microbiol.* 12, no-no. doi: 10.1111/j.1462-2920.2010.02275.x.

Shen, Y., Buick, R., and Canfield, D. E. (2001). Isotopic evidence for microbial sulphate reduction in the early Archaean era. *Nature* 410, 77–81. doi: 10.1038/35065071.

Shrestha, P. M., Rotaru, A.-E., Summers, Z. M., Shrestha, M., Liu, F., and Lovley, D. R. (2013). Transcriptomic and genetic analysis of direct interspecies electron transfer. *Appl. Environ. Microbiol.* 79, 2397–2404. doi: 10.1128/AEM.03837-12.

Skennerton, C. T., Chourey, K., Iyer, R., Hettich, R. L., Tyson, G. W., and Orphan, V. J. (2017). Methane-Fueled Syntrophy through Extracellular Electron Transfer: Uncovering the Genomic Traits Conserved within Diverse Bacterial Partners of Anaerobic Methanotrophic Archaea. *MBio* 8, 1–14. doi: 10.1128/mBio.00530-17.

Slobodkin, A. I., Reysenbach, A.-L., Slobodkina, G. B., Baslerov, R. V, Kostrikina, N. A., Wagner, I. D., et al. (2012). Thermosulfurimonas dismutans gen. nov., sp. nov., an extremely thermophilic sulfur-disproportionating bacterium from a deep-sea hydrothermal vent. *Int. J. Syst. Evol. Microbiol.* 62, 2565–2571. doi: 10.1099/ijs.0.034397-0.

Slobodkina, G. B., Reysenbach, A.-L., Kolganova, T. V, Novikov, A. A., Bonch-Osmolovskaya, E. A., and Slobodkin, A. I. (2017). Thermosulfuriphilus ammonigenes gen. nov., sp. nov., a thermophilic, chemolithoautotrophic bacterium capable of respiratory ammonification of nitrate with elemental sulfur. *Int. J. Syst. Evol. Microbiol.* 67, 3474–3479. doi: 10.1099/ijsem.0.002142.

Søndergaard, D., Pedersen, C. N. S., and Greening, C. (2016). HydDB: A web tool for hydrogenase classification and analysis. *Sci. Reports 2016 61* 6, 1–8. doi: 10.1038/srep34212.

Sonne-Hansen, J., and Ahring, B. K. (1999). Thermodesulfobacterium hveragerdense sp.nov., and

Thermodesulfovibrio islandicus sp.nov., Two Thermophilic Sulfate Reducing Bacteria Isolated from a Icelandic Hot Spring. *Syst. Appl. Microbiol.* 22, 559–564. doi: 10.1016/S0723-2020(99)80009-5.

Speth, D. R., Yu, F. B., Connon, S. A., Lim, S., Magyar, J. S., Peña-Salinas, M. E., et al. (2022). Microbial communities of Auka hydrothermal sediments shed light on vent biogeography and the evolutionary history of thermophily. *ISME J. 2022*, 1–15. doi: 10.1038/s41396-022-01222-x.

Stamatakis, A. (2014). RAxML version 8: a tool for phylogenetic analysis and post-analysis of large phylogenies. *Bioinformatics* 30, 1312–1313. doi: 10.1093/BIOINFORMATICS/BTU033.

Trüper, H. G. (2003). Valid publication of the genus name *Thermodesulfobacterium* and the species names *Thermodesulfobacterium commune* (Zeikus *et al*. 1983) and *Thermodesulfobacterium thermophilum* (ex *Desulfovibrio thermophilus* Rozanova and Khu. *Int. J. Syst. Evol. Microbiol.* 53, 927–927. doi: 10.1099/ijs.0.02494-0.

Venceslau, S. S., Lino, R. R., and Pereira, I. A. C. (2010). The Qrc Membrane Complex, Related to the Alternative Complex III, Is a Menaquinone Reductase Involved in Sulfate Respiration. *J. Biol. Chem.* 285, 22774–22783. doi: 10.1074/jbc.M110.124305.

Venceslau, S. S., Stockdreher, Y., Dahl, C., and Pereira, I. A. C. (2014). The "bacterial heterodisulfide" DsrC is a key protein in dissimilatory sulfur metabolism. *Biochim. Biophys. Acta - Bioenerg.* 1837, 1148–1164. doi: 10.1016/j.bbabio.2014.03.007.

Vignais, P. M., and Billoud, B. (2007). Occurrence, Classification, and Biological Function of Hydrogenases: An Overview. *Chem. Rev.* 107, 4206–4272. doi: 10.1021/cr050196r.

Vulcano, F., Hahn, C. J., Roerdink, D., Dahle, H., Reeves, E. P., Wegener, G., et al. (2022). Phylogenetic and functional diverse ANME-1 thrive in Arctic hydrothermal vents. *FEMS Microbiol. Ecol.* 98, 1–11. doi: 10.1093/femsec/fiac117.

Wagner, M., Roger, A. J., Flax, J. L., Brusseau, G. A., and Stahl, D. A. (1998). Phylogeny of Dissimilatory Sulfite Reductases Supports an Early Origin of Sulfate Respiration. *J. Bacteriol.* 180, 2975–2982. doi: 10.1128/JB.180.11.2975-2982.1998.

Wang, F., Gu, Y., O'Brien, J. P., Yi, S. M., Yalcin, S. E., Srikanth, V., et al. (2019). Structure of microbial nanowires reveals stacked hemes that transport electrons over micrometers. *Cell* 177, 361-369.e10. doi: 10.1016/j.cell.2019.03.029.

Wegener, G., Krukenberg, V., Riedel, D., Tegetmeyer, H. E., and Boetius, A. (2015). Intercellular wiring enables electron transfer between methanotrophic archaea and bacteria. *Nature* 526, 587–590. doi: 10.1038/nature15733.

Widdel, F., and Musat, F. (2010). "Diversity and Common Principles in Enzymatic Activation of Hydrocarbons," in *Handbook of Hydrocarbon and Lipid Microbiology* (Berlin, Heidelberg: Springer Berlin Heidelberg), 981–1009. doi: 10.1007/978-3-540-77587-4_70.

Woese, C. R. (1987). Bacterial evolution. *Microbiol. Rev.* 51, 221–271. doi: 10.1128/MMBR.51.2.221-271.1987.

Yu, H., Skennerton, C. T., Chadwick, G. L., Leu, A. O., Aoki, M., Tyson, G. W., et al. (2021). Sulfate differentially stimulates but is not respired by diverse anaerobic methanotrophic archaea. *ISME J.* 16, 168–177. doi: 10.1038/s41396-021-01047-0.

Yu, N. Y., Wagner, J. R., Laird, M. R., Melli, G., Rey, S., Lo, R., et al. (2010). PSORTb 3.0: improved protein subcellular localization prediction with refined localization subcategories and predictive capabilities for all prokaryotes. *Bioinformatics* 26, 1608–1615. doi: 10.1093/bioinformatics/btq249.

Zehnle, H., Lipp, J., Teske, A., and Wegener, G. (2022). Candidatus Alkanophaga archaea from heated hydrothermal vent sediment oxidize petroleum alkanes. *Prepr. (Version 1) available Res. Sq.*, 1–33. doi: 10.21203/RS.3.RS-2096998/V1.

Zeikus, J. G., Dawson, M. A., Thompson, T. E., Ingvorsen, K., and Hatchikian, E. C. (1983). Microbial Ecology of Volcanic Sulphidogenesis: Isolation and Characterization of *Thermodesulfobacterium commune* gen. nov. and sp. nov. *Microbiology* 129, 1159–1169. doi: 10.1099/00221287-129-4-1159.

Discussion and future perspectives

5.1. General discussion

At the end of the 19th century, Microbiologists of the Delft School in the Netherlands began to study aerobic and anaerobic biochemical pathways of bacteria (and yet-unknown archaea) (La Rivière, 1997). Since then, the variety of biochemical tricks in microbial metabolisms has fascinated biologists. Among these processes, methanogenesis has a stark impact in carbon biogeochemistry (Conrad, 2009). Methanogenesis is a metabolism exclusively found in the domain Archaea and occurs in many anoxic marine sediments (Jørgensen, 2006). In the same sediments, the reverse process, the AOM greatly restrains the release of methane into the atmosphere (Reeburgh, 2007; Knittel and Boetius, 2009). Sequencing technologies and bioinformatics have changed the way we study these processes, enabling us to find many methanogens and methanotrophs based on the occurrence of *mcr* genes in the environment. This included the hallmark finding of highly divergent *mcr* genes in Bathyarchaeia (Evans et al., 2015). Environmental metagenomics alone provide broad suggestions of for known metabolic pathways in MAGs. Novel genomic information can only be correctly understood when complementing such *in silico* analyses with cultivation-based techniques.

Shortly before I started my PhD, my new colleagues discovered a novel pathway for anaerobic short-chain alkane degradation in archaea based on divergent Mcr variants (Acrs) (Laso-Pérez et al., 2016). The same mechanism was then found in archaea from ethane-degrading cultures (Chen et al., 2019; Hahn et al., 2020). At the same time, a growing number of Mcr- and Acr-encoding environmental MAGs became available, for which we lacked cultures (Evans et al., 2015; Vanwonterghem et al., 2016; Borrel et al., 2019; Boyd et al., 2019; Hua et al., 2019; Laso-Pérez et al., 2019; Seitz et al., 2019; Wang et al., 2019). We also noted that microorganisms mediating AOM and AOA at temperatures above 60°C had not been cultured. These culture conditions could select for the enrichment of novel thermophilic alkane-oxidizing archaea.

The objective of my thesis was to obtain anoxic cultures from marine sediments to characterize novel methanotrophic and alkanotrophic archaea. For this, I established high-temperature anoxic cultures with methane or hexadecane as electron donors and sulfate as electron acceptor. In both cases, the enriched archaea and bacteria opened interesting questions on the evolution of alkane metabolism and adaptations to syntrophic partnerships that I discuss in the following sections.

5.2. The temperature limit to anaerobic oxidation of methane and alkanes

When I started my thesis, the most thermophilic AOM culture from the Guaymas Basin grew at 60°C and was composed of ANME-1a and *Ca.* Desulfofervidus auxilii (Holler et al., 2011; Wegener et al., 2016; Krukenberg et al., 2018). However, radiotracer experiments and porewater methane isotopes suggested that AOM may occur at temperatures up to 80°C (Holler et al., 2011; McKay et al., 2016).

During my thesis work, I have obtained cultured AOM performing microorganism at 70°C (Chapter 2). The methanotroph in the culture belongs to the ANME-1c clade, a basal lineage of *Ca.* Methanophagaceae (ANME-1). Recently, two names have been proposed for the ANME-1c family: *Ca*. Methanoxibalbaceae (Laso-Pérez et al., 2022) and *Ca*. Veteranomethanophagaceae (Vulcano et al., 2022). The partner SRB *Ca.* Thermodesulfobacterium torris (class Thermodesulfobacteria) had not been observed before in AOM. This association has raised questions on the adaptation of AOM-mediating microbes to high temperatures.

The class that comprises *Ca*. Methanophagaceae, *Ca*. Alkanophagaceae and *Ca*. Syntrophoarchaeaceae (i.e., class *Ca*. Syntrophoarchaeia) includes thermophilic ANKA that grow above 50°C (Laso-Pérez et al., 2016; Wegener et al., 2016; Krukenberg et al., 2018; Zehnle et al., 2022). The origin of alkane and methane metabolisms in the class *Ca*. Syntrophoarchaeia is discussed in detail in section 5.4. Mesophilic ANME belong to the groups ANME-1a and -1b (Meyerdierks et al., 2005; Wegener et al., 2016; Krukenberg et al., 2018). Because thermophilic ANME-1c, *Ca*. Alkanophagaceae and *Ca*. Syntrophoarchaeaceae are basal to the ANME-1a/b clade (Figure 1), I infer that the common ancestor of *Ca*. Syntrophoarchaeia was thermophilic. Some ANME-1a and -1b might have adapted later to mesophilic and psychrophilic AOM. In fact, the optimal growth temperature predicted for MAGs in *Ca*. Syntrophoarchaeia decreases with evolutionary distance to the common ancestor (Laso-Pérez et al., 2022).

Ca. Desulfofervidus auxilii grows optimally at 60°C and only while growing on hydrogen can it stand temperatures up to 70°C (Krukenberg et al., 2016). The association of ANME with SRB is somewhat specific but appears to be governed by the temperature at which the partners can grow (Murali et al., 2022). Thermophilic ANME-1c are associated to the newly described *Ca*. Thermodesulfobacterium torris. I discuss the involvement of Thermodesulfobacteria in AOM and AOA in section 5.5.

The description of a Hadarchaeon capable of long-chain alkane degradation (Chapter 3) is also relevant for considerations on thermophily. In anaerobic incubations with Guaymas Basin sediments amended with hexadecane and at different temperature regimes (37, 50 and 70°C), the lower temperatures selected for SRB, likely alkanotrophs. At 70°C, the incubations were dominated by thermophilic archaea (Hadarchaea

and Archaeoglobi), as seen in enrichment culture metagenomes. Alkanotrophic Archaeoglobi had been observed before in thermophilic cultures (Mbadinga et al., 2012; Khelifi et al., 2014). Furthermore, *Ca*. Methanoliparum sp., the only ANKA enriched on long-chain alkanes before my work, grow optimally at 55°C (Zhou et al., 2022). My and other data suggest that ANKA and Archaeoglobi outcompete modern alkanotrophic Desulfobacterota at high temperatures.

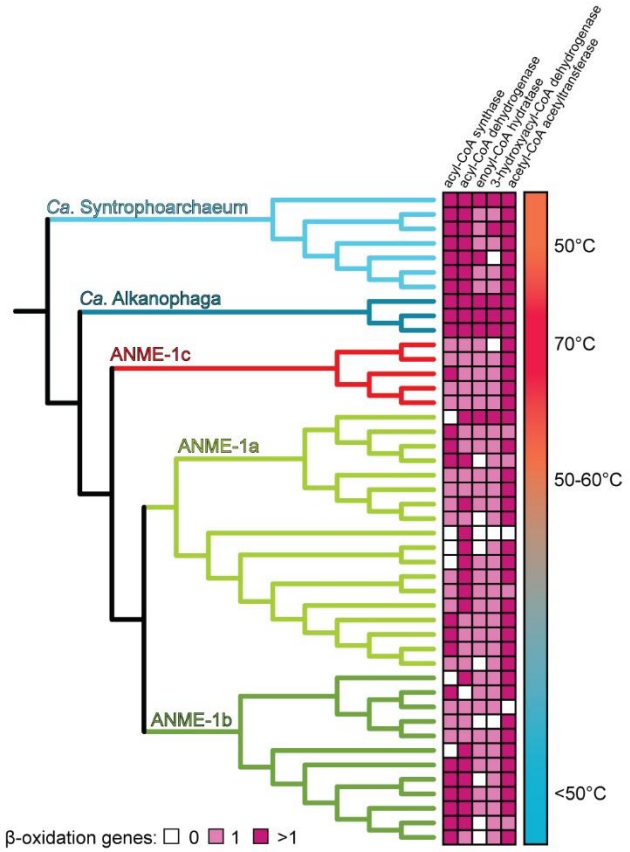

Figure 1. Phylogeny of class *Ca*. Syntrophoarchaeia, occurrence of β-oxidation genes and approximate growth temperature. The class comprises the alkane degraders *Ca*. Syntrophoarchaeum and *Ca*. Alkanophaga, and the methane oxidizers ANME-1a, b and c. The β-oxidation pathway is present in genomes of the whole class. The optimal growth temperature (the values represented are schematic) predicted decreases with evolutionary distance to the common

5.3. An Acr branch for the activation of petroleum alkanes

The discovery of Acrs involved in the activation of alkanes has been a revolution in the field of Archaea and anaerobic metabolisms. When I started my thesis, the evidence for Acrs catalysing long-chain alkane activation was environmental, because *Ca*. Methanoliparia had been observed associated with oil droplets in samples from the Gulf of Mexico (Laso-Pérez et al., 2019). *Ca*. Methanoliparia were later cultivated from oil field samples (Zhou et al., 2022). With the enrichment of Acr-encoding Hadarchaea, I extended this evidence of long-chain metabolism by archaea.

All known Acrs sequences fall in a divergent branch of the Mcr/Acr phylogeny (Figure 2). Both *Ca*. Syntrophoarchaeum caldarius and *Ca*. Syntrophoarchaeum butanivorans encode four Acr operons (Laso-

Pérez et al., 2016). One Acr of *Ca*. S. caldarius clusters with sequences from *Ca*. Ethanoperedens and GoM-Arc I that have been shown to activate ethane (Chen et al., 2019; Hahn et al., 2020, 2021). One Acr of *Ca*. S. butanivorans is located at the base of the *Ca*. Methanoliparia cluster (including Bathyarchaeia, Helarchaeales, *Ca*. Methanoliparia and Hadarchaeota Acrs). The different Acrs in *Ca*. Syntrophoarchaeum could provide them with flexibility to activate alkanes of different chain lengths. However, incubations of *Ca*. Syntrophoarchaeum enrichments with C_1 to C_6 alkanes other than propane and *n*-butane were inactive (Laso Pérez, 2018). *Ca*. Syntrophoarchaeales remains thus as a clade of solely propane and butane oxidizers. Differential gene expression analysis of *Ca*. Syntrophoarchaeum cultured with propane and butane did not resolve the substrate specificity of the different Acrs (Laso Pérez, 2018). Recently, cultures of *Ca*. Alkanophagaceae were obtained that grow on mid-chain alkanes longer than C_4 and shorter than C_{15} (Zehnle et al., 2022). *Ca*. Alkanophaga volatiphilum and *Ca*. A. liquidiphilum also encode three Acr operons each. *Ca.* Alkanophaga apparently employ one Acr for alkane activation, independently of alkane length (Zehnle et al., 2022). The Acrs are not specific towards particular substrates. All these Acrs are located at the base of the *Ca*. Methanoliparia cluster.

Interestingly, excluding one Acr from *Ca.* S. caldarius, the longest branches in the Acr clade correspond to the *Ca*. Methanoliparia cluster (Figure 2). Cultivation of oil-associated *Ca*. Methanoliparia proved the activation a wide range of long-chain alkanes from C_{16} to C_{22}, including alkyl-substituted cyclohexanes and benzenes (Zhou et al., 2022). Furthermore, alkanes up to C_{38} were depleted in *Ca*. Methanoliparia cultures in comparison with reference oil samples (Zhou et al., 2022). During my thesis work, I described *Ca*. Cerberiarchaeum oleivorans (Hadarchaeota) that activates hexadecane to hexadecyl-CoM (Chapter 3). With this evidence, I hypothesize that the *Ca*. Methanoliparia cluster contains Acrs specialized in long-chain alkane activation.

In the crystal structure of ethyl-CoM reductase (Ecr, Acr of *Ca*. Ethanoperedens thermophilum), the active site is substantially larger than the active site of Mcrs from methanogens and ANME (Hahn et al., 2021). In general, the active site of Ecr and Mcr is a channel delimited by hydrophobic amino acids (Ermler et al., 1997). In Mcrs, this channel is blocked when the CoM and CoB are bound and thus the space in the active site is limited for small molecules such as methane (Ermler et al., 1997). The Ecr of *Ca*. E. thermophilum contains an additional side hydrophobic tunnel, which could channel the bulkier ethane molecule into the active site (Hahn et al., 2021). The presence of a similar additional molecular path had been proposed for the Acrs of *Ca*. Methanoliparia and *Ca*. Syntrophoarchaeum (Laso Pérez, 2018). However, certain amino acid insertions that generate the hydrophobic tunnel are missing in the Acrs of

Ca. Methanoliparia and *Ca*. Syntrophoarchaeum (Lemaire and Wagner, 2022). Besides, the size of alkanes longer than ethane would limit their diffusion through the channel (Lemaire and Wagner, 2022). Structural modelling of *Ca*. Methanoliparia and *Ca*. Syntrophoarchaeum Acrs with Alphafold2 revealed the presence of an open cavity, caused by a single amino acid deletion (Lemaire and Wagner, 2022). Because alkanes are activated at the terminal or subterminal carbon atoms (Laso-Pérez et al., 2016; Zehnle et al., 2022), only this part of the molecule would need to be near the active site of Acr. The open cavity would enable the entry of long-chain alkanes, regardless of their chain length. This may explain the unexpected substrate "promiscuity" of the Acr of *Ca*. Methanoliparia (Zhou et al., 2022), but future research should aim to

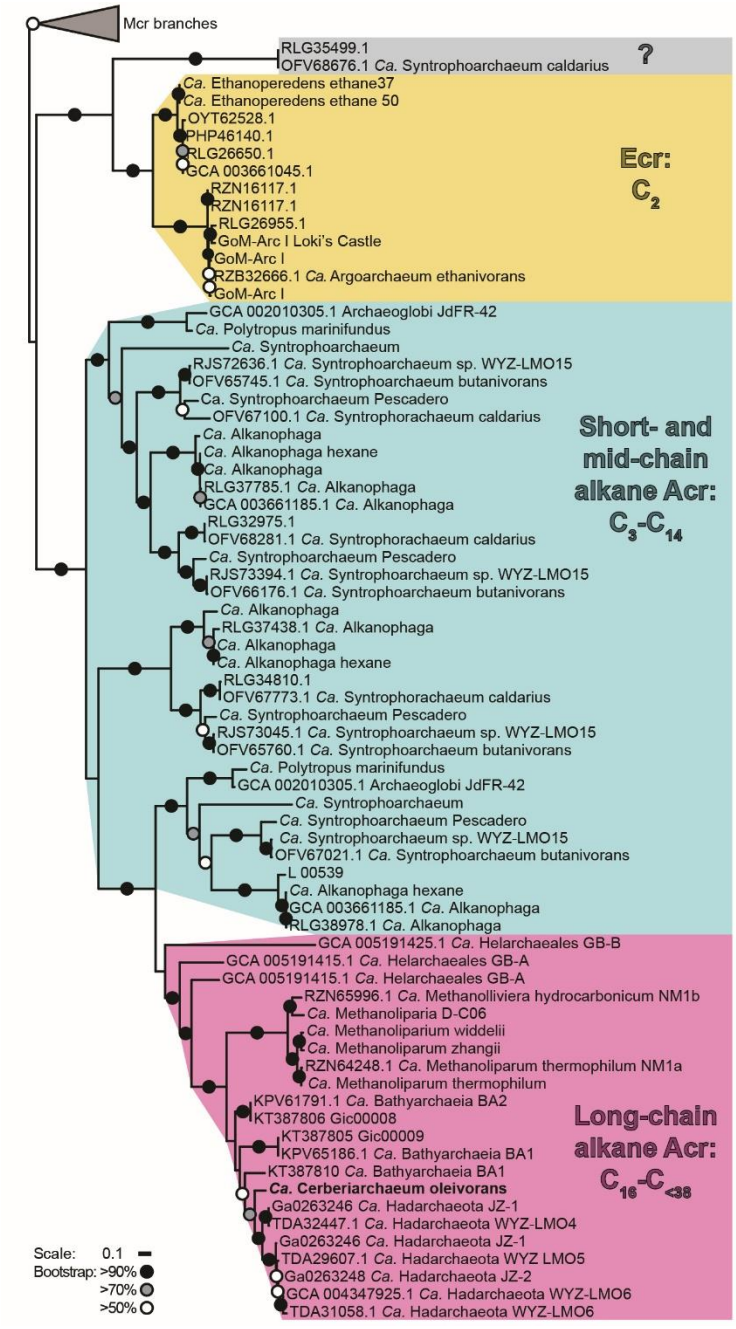

Figure 2. Phylogeny of alkyl-coenzyme M reductases. The tree is a ML phylogeny of McrA/AcrA. The yellow clade includes Ecrs from *Ca*. Ethanoperedens and *Ca* Argoarchaeum, confirmed to activate ethane. The blue clades correspond to Acrs from short-chain alkane degraders *Ca*. Syntrophoarchaeum and mid-chain alkane degraders *Ca*. Alkanophaga. The pink clade encompasses long-chain alkane oxidizers. Long-chain alkane activation via Acr has been confirmed for *Ca*. Methanoliparia and *Ca*. Hadarchaeota.

crystallize long-chain alkane Acrs. Unfortunately, structural modelling of the Acr from *Ca*. C. oleivorans was impossible because the metagenomic Acr sequence was incomplete. *Ca*. C. oleivorans might be an ideal candidate for crystallography studies because it encodes a single long-chain alkane-activating Acr.

5.4. Acquisition of alkane and methane metabolisms

Methanogenesis is an ancient metabolism that originated soon after the diversification of prokaryotes on the early Earth (Woese, 1987; Ueno et al., 2006). The diversification of methane-related metabolisms, including Acr-based alkane metabolism, in Archaea poses a challenge for evolutionary research.

In the species tree, ANME-2 and -3 belong to the Methanosarcinales order, whereas ANME-1 is included in the order *Ca*. Methanophagales. It is surprising that, in the Mcr/Acr phylogeny, ANME-1 sequences do not cluster with the ones of ANME-2/3. This indicates that methanotrophic Mcrs could have originated independently at least twice from mutations in methanogenic Mcrs. The differing Mcrs and the genomic distance between *Ca*. Methanophagales and ANME-2/3 suggests different evolutionary history of methanotrophy in these groups (Garcia et al., 2022). As discussed in section 5.2., the common ancestor of *Ca*. Syntrophoarchaeia, including *Ca*. Methanophagales, was likely a thermophile. The ancestral clades of *Ca*. Syntrophoarchaeia (i.e., *Ca*. Syntrophoarchaea and *Ca*. Alkanophaga) encode Acrs, that are absent in ANME-1 genomes. Nevertheless, all ANME-1 groups (a, b and c) encode β-oxidation genes (Figure 1), which might be evolutionary remnants (Chapter 2) (Wang et al., 2021). This suggests that the ancestral *Ca*. Syntrophoarchaeia was a thermophilic alkane degrader. ANME-1 would have become a methanotroph after losing the Acr and acquiring an Mcr from the *Ca.* Methanofastidiosa or *Ca*. Nuwarchaeia (Borrel et al., 2019; Wang et al., 2021).

In Chapter 3, I describe *Ca*. Cerberiarchaeum oleivorans, a thermophilic Hadarchaeon encoding a long-chain alkane Acr. When I explored the distribution of Acrs in the Hadarchaeota, I realized that only six MAGs (three species) that form a single clade encode this enzyme. As *Ca*. C. oleivorans is the MAG with the highest quality in this family-level clade, I propose the name *Ca*. Cerberiarchaeaceae. Interestingly, the other pathways needed for Acr-based alkane degradation, namely the β-oxidation pathway and the Wood-Ljungdahl pathway (WL, including carbonyl and methyl branches), are also only present in *Ca*. Cerberiarchaeaceae.

The WL or reductive acetyl-CoA pathway is a carbon fixation pathway with an early origin on Earth (Wood, 1991; Ljungdahl, 2009; Peretó, 2012; Martin, 2020). In the methyl branch, CO_2 is sequentially reduced to form a methyl-tetrahydromethanopterin (H_4MPT) (Ljungdhal, 1986). In the carbonyl branch,

CO_2 is reduced to CO and then the carbon monoxide dehydrogenase/acetyl-CoA synthase (Cdh/Acs) complex incorporates the CO to the methyl-H_4MPT to form acetyl-CoA (Ljungdhal, 1986). In some microorganisms, the WL pathway functions in reverse to oxidize acetate to CO_2 (Schauder et al., 1988; Hattori et al., 2005). This is the case for ANKA like *Ca*. Syntrophoarchaeum (Laso-Pérez et al., 2016) and *Ca*. C. oleivorans.

To understand the origin of the WL pathway in Hadarchaeota, I reconstructed phylogenies of its enzymes. While the phylogenetic trees were being calculated, I found previous studies that dealt with the evolution of the methanogenesis pathway, the WL pathway and the Cdh/Acs complex (Borrel et al., 2016; Adam et al., 2018, 2019). For the methyl-branch WL pathway, my phylogeny of the formylmethanofuran dehydrogenase (Fwd) including Hadarchaeota sequences matched the one presented in a previous study (Adam et al., 2019). The authors pointed out that the H_4MPT methyl-branch of the WL pathway was probably present the last archaeal common ancestor (LACA) (Adam et al., 2019). My phylogenetic reconstruction supports this hypothesis. I propose that non-alkanotrophic Hadarchaeota selectively lost the WL pathway in their adaptations to subsurface environments. In the future, cultivation-based approaches should aid us in understanding the physiology of these organisms.

Stunningly, the carbonyl-branch WL pathway has a different evolutionary history. Adam and colleagues showed that the Cdh phylogeny greatly matches the archaeal species phylogeny (Adam et al., 2018). However, they noted that two HGT events might have happened. One of them is the transfer of Cdh from Bathyarchaeia to some Methanomicrobiales and to *Methanocella arvoryzae* (Adam et al., 2018). These methanogens use the Cdh in the catabolic direction to assimilate acetate for growth (Sakai et al., 2010; Bräuer et al., 2011; Yashiro et al., 2011). Likewise, *Ca*. Cerberiarchaeum oleivorans uses the Cdh in the catabolic direction. In my updated Cdh phylogeny including Hadarchaeota, the Cdh sequences of *Ca*. Cerberiarchaeaceae also branch within the Bathyarchaeia sequences. I propose that the origin of Cdh in the *Ca*. Cerberiarchaeaceae is also due to a HGT event. Similarly, *Ca*. Cerberiarchaeaceae could have acquired the β-oxidation pathway from other ANKA such as Bathyarchaeia or *Ca*. Methanoliparia.

5.5. Novel partner bacteria for anaerobic oxidation of alkanes

Syntrophic organisms have evolved molecular mechanisms to form specific symbiotic associations (Kouzuma et al., 2015). The association of different ANME/ANKA with SRB seems to be specific to a certain degree, at least based on the growth temperatures of both partners. For example, *Ca*. Desulfofervidus auxilii is the common partner for all ANME/ANKA that grow at 50-60°C (Krukenberg et al., 2016, 2018; Laso-Pérez et al., 2016; Hahn et al., 2020).

Because some of the cytochromes involved in DIET are common to partner SRB, the association might not be specific on them. Instead, SRB interact with ANME based on extracellular polysaccharides (Murali et al., 2022). The biosynthetic pathway for secreted polysaccharide was upregulated when ANME-2 grew without a syntrophic partner (Yu et al., 2021). It has been suggested that the presence of this biosynthesis pathway in a genome could be a good marker for a syntrophic lifestyle (Murali et al., 2022).

During this thesis, I discovered the new AOM partner *Ca*. Thermodesulfobacterium torris (Chapter 2). This organism encodes a DIET pathway but lacks a H_2-uptake hydrogenase (Chapter 4). This was surprising because hydrogenases are a common trait in Thermodesulfobacteria. I did not observe growth of *Ca*. T. torris with H_2 or other common electron donors for SRB. Based on these observations, I propose that *Ca*. T. torris adapted to obligate syntrophy and lost the capability to grow with H_2 as electron donor.

Predicting a putative syntrophic lifestyle is complicated based solely on genomics (Chapter 4). However, we now have e better understanding on the molecular basis of DIET between ANME and SRB. My preliminary genomic analysis of the Thermodesulfobacteria showed that cytochromes for the DIET pathway are present in many genomes. This suggests that these bacteria have the potential to mediate thermophilic AOA in marine environments.

5.6. Global distribution of novel ANME and ANKA

ANME have been cultured from a psychro-, meso- and thermophilic environments (Boetius and Knittel, 2010). Specifically, MAGs of ANME-1a and -1b (family *Ca*. Methanophagaceae) also have a global distribution (Laso-Pérez et al., 2022). In contrast, MAGs of ANME-1c have been found only in three locations: the Guaymas Basin (Chapter 2 and (Dombrowski et al., 2018)), the South Pescadero Basin (Gulf of California) (Laso-Pérez et al., 2022) and the Arctic Mid Ocean Ridge (Vulcano et al., 2022). Future efforts should aim to determine whether thermophilic AOM catalyzed by ANME-1c occurs in other hydrothermal systems.

Many cultured ANKA such as *Ca*. Syntrophoarchaeum, *Ca*. Ethanoperedens and *Ca*. Alkanophaga, are thermophilic and originate from the Guaymas Basin (Gulf of California, Mexico) (Laso-Pérez et al., 2016; Hahn et al., 2020; Zehnle et al., 2022). Other putative ANKA originate from Guaymas Basin (*Ca*. Helarchaeales) (Seitz et al., 2019) and the Juan de Fuca Ridge in the Pacific Ocean (*Ca*. Polytropus marinifundus, Archaeoglobi) (Boyd et al., 2019). *Ca*. Argoarchaeum ethanivorans originates from cold seeps in the Gulf of Mexico and was enriched at 12°C (Chen et al., 2019). *Ca*. Methanoliparia spp. were enriched at 55°C from oily sludge obtained from an oil facility in eastern China (Zhou et al., 2022). *Ca*.

Methanoliparia had been originally reported from oil-related environments from Brazil, Santa Barbara Channel (USA) and the Gulf of Mexico (Borrel et al., 2019; Laso-Pérez et al., 2019). The wide geographic distribution of ANKA surprised me when I was writing this thesis.

Focusing on the family *Ca*. Cerberiarchaeaceae in the phylum Hadarchaeota, it comprises three species respectively from the Guaymas Basin (Chapter 3), the Jinze Hot Spring (China) and a hot spring from Yellowstone National Park (USA) (NCBI BioProjects PRJNA475882, PRJNA475886, PRJNA480137 and PRJNA859922; (Wang et al., 2019) and unpublished data). Considering this distribution of the *Ca*. Cerberiarchaeaceae in remote locations, I presume that they have a broader role in oil-rich environments than what we currently appreciate. Locations like Yellowstone National Park or the Guaymas Basin have been sampled recurrently due to an ease to reach terrestrial sampling sites (the former) or the frequent sampling campaigns on board of R/V *Atlantis* (the latter). Another possibility is that current ANKA are the vestiges of Acr-based oil degradation when it was a widespread metabolism in the domain Archaea. Regardless, metagenomic sequencing of hydrothermal vents, hot springs, oil reservoirs and oil-degrading cultures will certainly help us widen our vision of the distribution of alkane metabolism.

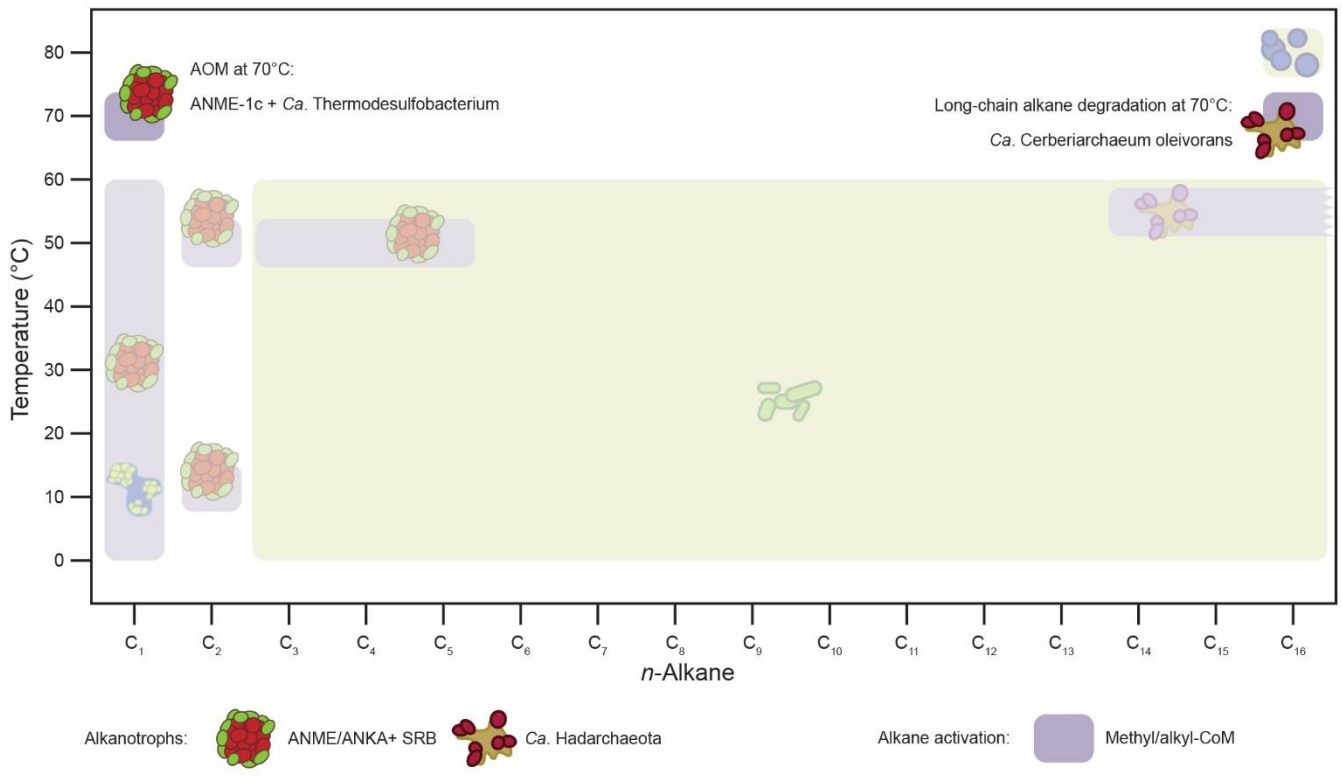

Figure 3. Summary of the thermophilic alkane-degrading archaea and associated bacteria presented in this thesis.

5.7. Concluding remarks and future perspectives

In my thesis, I have uncovered new groups of Archaea and Bacteria that perform anaerobic oxidation of methane and long-chain alkanes (Figure 3). More importantly, I have characterized *Ca*. Cerberiarchaeum oleivorans, the first confirmed ANKA outside of the Halobacteriota phylum.

Cultivation of Acr-encoding archaea is of great interest for understanding the ecological niches of these organisms. Based on the knowledge from cultivation of *Ca*. Methanoliparia (Zhou et al., 2022) and from my thesis, Acrs from *Ca*. Helarchaeales, *Ca*. Bathyarchaeia and *Ca*. Polytropus marinifundus could activate long-chain alkanes. Future research should aim to cultivate these archaea and test this hypothesis.

Further, more research is needed to resolve the pathways for interspecies electron transfer in archaea that lack multiheme cytochromes. In the case of Acr-encoding *Ca*. Bathyarchaeia and *Ca*. Helarchaeales, cultivation would also help resolve possible mechanisms for interspecies electron transfer. These ANKA could transfer small organic molecules or H_2 to syntrophic partners. This type of interaction has been observed in methanogenic alkane degradation (Jones et al., 2008) and has been proposed as the basis for the interaction of *Ca*. Helarchaeales with SRB (Zhao and Biddle, 2021).

The crystal structure of Ecr from *Ca*. Ethanoperedens thermophilum has enabled us to understand the archaeal pathway for the activation of alkanes at the molecular level (Hahn et al., 2021). Acrs need structural modifications in order to accommodate alkanes longer than ethane (Lemaire and Wagner, 2022). While structural modelling is a good approach to explore the proteins of uncultivated microorganisms, upcoming efforts should seek to crystallize Acrs. The multiple Acrs in *Ca*. Syntrophoarchaeum and *Ca*. Alkanophaga could co-crystallize and thus hinder the resolution of the structure. *Ca*. Cerberiarchaeaum is a good candidate for crystallography studies, because it only encodes one Acr. For this, the cultivation of *Ca*. C. oleivorans should be optimized to yield sufficient Acr for crystallization.

References

Adam, P. S., Borrel, G., and Gribaldo, S. (2018). Evolutionary history of carbon monoxide dehydrogenase/acetyl-CoA synthase, one of the oldest enzymatic complexes. *Proc. Natl. Acad. Sci.* 115, E1166–E1173. doi: 10.1073/PNAS.1716667115.

Adam, P. S., Borrel, G., and Gribaldo, S. (2019). An archaeal origin of the Wood–Ljungdahl H4MPT branch and the emergence of bacterial methylotrophy. *Nat. Microbiol.* 4, 2155–2163. doi: 10.1038/s41564-019-0534-2.

Boetius, A., and Knittel, K. (2010). "Habitats of Anaerobic Methane Oxidizers," in *Handbook of Hydrocarbon and Lipid Microbiology*, ed. K. N. Timmis (Berlin, Heidelberg: Springer Berlin Heidelberg), 2193–2202. doi: 10.1007/978-3-540-77587-4_159.

Borrel, G., Adam, P. S., and Gribaldo, S. (2016). Methanogenesis and the Wood-Ljungdahl Pathway: An Ancient, Versatile, and Fragile Association. *Genome Biol. Evol.* 8, 1706–11. doi: 10.1093/gbe/evw114.

Borrel, G., Adam, P. S., McKay, L. J., Chen, L.-X., Sierra-García, I. N., Sieber, C. M. K., et al. (2019). Wide diversity of methane and short-chain alkane metabolisms in uncultured archaea. *Nat. Microbiol.* 4, 603–613. doi: 10.1038/s41564-019-0363-3.

Boyd, J. A., Jungbluth, S. P., Leu, A. O., Evans, P. N., Woodcroft, B. J., Chadwick, G. L., et al. (2019). Divergent methyl-coenzyme M reductase genes in a deep-subseafloor Archaeoglobi. *ISME J.*, 1. doi: 10.1038/s41396-018-0343-2.

Bräuer, S. L., Cadillo-Quiroz, H., Ward, R. J., Yavitt, J. B., and Zinder, S. H. (2011). Methanoregula boonei gen. nov., sp. nov., an acidiphilic methanogen isolated from an acidic peat bog. *Int. J. Syst. Evol. Microbiol.* 61, 45–52. doi: 10.1099/ijs.0.021782-0.

Chen, S.-C., Musat, N., Lechtenfeld, O. J., Paschke, H., Schmidt, M., Said, N., et al. (2019). Anaerobic oxidation of ethane by archaea from a marine hydrocarbon seep. *Nat. 2019*, 1. doi: 10.1038/s41586-019-1063-0.

Conrad, R. (2009). The global methane cycle: recent advances in understanding the microbial processes involved. *Environ. Microbiol. Rep.* 1, 285–292. doi: 10.1111/j.1758-2229.2009.00038.x.

Dombrowski, N., Teske, A. P., and Baker, B. J. (2018). Expansive microbial metabolic versatility and biodiversity in dynamic Guaymas Basin hydrothermal sediments. *Nat. Commun.* 9, 4999. doi: 10.1038/s41467-018-07418-0.

Ermler, U., Grabarse, W., Shima, S., Goubeaud, M., and Thauer, R. K. (1997). Crystal structure of methyl-coenzyme M reductase: The key enzyme of biological methane formation. *Science (80-.).* 278, 1457–1462. doi: 10.1126/science.278.5342.1457.

Evans, P. N., Parks, D. H., Chadwick, G. L., Robbins, S. J., Orphan, V. J., Golding, S. D., et al. (2015). Methane metabolism in the archaeal phylum Bathyarchaeota revealed by genome-centric metagenomics. *Science (80-.).* 350, 434–438. doi: 10.1126/science.aac7745.

Garcia, P. S., Gribaldo, S., and Borrel, G. (2022). Diversity and Evolution of Methane-Related Pathways in Archaea. *Annu. Rev. Microbiol.* 76. doi: 10.1146/annurev-micro-041020-024935.

Hahn, C. J., Laso-Pérez, R., Vulcano, F., Vaziourakis, K.-M., Stokke, R., Steen, I. H., et al. (2020). "*Candidatus* Ethanoperedens," a thermophilic genus of archaea mediating the anaerobic oxidation of ethane. *MBio* 11, 1–18. doi: 10.1128/mBio.00600-20.

Hahn, C. J., Lemaire, O. N., Kahnt, J., Engilberge, S., Wegener, G., and Wagner, T. (2021). Crystal structure of a key enzyme for anaerobic ethane activation. *Science (80-.).* 373, 118–121. doi: 10.1126/science.abg1765.

Hattori, S., Galushko, A. S., Kamagata, Y., and Schink, B. (2005). Operation of the CO Dehydrogenase/Acetyl Coenzyme A Pathway in both Acetate Oxidation and Acetate Formation by the Syntrophically Acetate-Oxidizing Bacterium Thermacetogenium phaeum. *J. Bacteriol.* 187, 3471–3476. doi: 10.1128/JB.187.10.3471-3476.2005.

Holler, T., Widdel, F., Knittel, K., Amann, R., Kellermann, M. Y., Hinrichs, K.-U., et al. (2011). Thermophilic anaerobic oxidation of methane by marine microbial consortia. *ISME J.* 5, 1946–1956. doi: 10.1038/ismej.2011.77.

Hua, Z.-S., Wang, Y.-L., Evans, P. N., Qu, Y.-N., Goh, K. M., Rao, Y.-Z., et al. (2019). Insights into the ecological roles and evolution of methyl-coenzyme M reductase-containing hot spring Archaea. *Nat. Commun.* 10, 4574. doi: 10.1038/s41467-019-12574-y.

Jones, D. M., Head, I. M., Gray, N. D., Adams, J. J., Rowan, A. K., Aitken, C. M., et al. (2008). Crude-oil biodegradation via methanogenesis in subsurface petroleum reservoirs. *Nature* 451, 176–180. doi: 10.1038/nature06484.

Jørgensen, B. B. (2006). "Bacteria and Marine Biogeochemistry," in *Marine Geochemistry*, eds. H. D. Schulz and M. Zabel (Berlin/Heidelberg: Springer), 169–206. doi: 10.1007/3-540-32144-6_5.

Khelifi, N., Amin Ali, O., Roche, P., Grossi, V., Brochier-Armanet, C., Valette, O., et al. (2014). Anaerobic oxidation of long-chain n-alkanes by the hyperthermophilic sulfate-reducing archaeon, Archaeoglobus fulgidus. *ISME J.* 8, 2153–2166. doi: 10.1038/ismej.2014.58.

Knittel, K., and Boetius, A. (2009). Anaerobic Oxidation of Methane: Progress with an Unknown Process. *Annu. Rev. Microbiol.* doi: 10.1146/annurev.micro.61.080706.093130.

Kouzuma, A., Kato, S., and Watanabe, K. (2015). Microbial interspecies interactions: recent findings in syntrophic consortia. *Front. Microbiol.* 6, 1–8. doi: 10.3389/fmicb.2015.00477.

Krukenberg, V., Harding, K., Richter, M., Glöckner, F. O., Gruber-Vodicka, H. R., Adam, B., et al. (2016). *Candidatus* Desulfofervidus auxilii, a hydrogenotrophic sulfate-reducing bacterium involved in the thermophilic anaerobic oxidation of methane. *Environ. Microbiol.* 18, 3073–3091. doi: 10.1111/1462-2920.13283.

Krukenberg, V., Riedel, D., Gruber-Vodicka, H. R., Buttigieg, P. L., Tegetmeyer, H. E., Boetius, A., et al. (2018). Gene expression and ultrastructure of meso- and thermophilic methanotrophic consortia. *Environ. Microbiol.* 20, 1651–1666. doi: 10.1111/1462-2920.14077.

La Rivière, J. W. M. (1997). The Delft School of Microbiology in historical perspective. *Antonie Van Leeuwenhoek* 71, 3–13. doi: 10.1023/A:1000153724109.

Laso-Pérez, R., Hahn, C., van Vliet, D. M., Tegetmeyer, H. E., Schubotz, F., Smit, N. T., et al. (2019). Anaerobic Degradation of Non-Methane Alkanes by "Candidatus Methanoliparia" in Hydrocarbon Seeps of the Gulf of Mexico. *MBio* 10, e01814-19. doi: 10.1128/mBio.01814-19.

Laso-Pérez, R., Wegener, G., Knittel, K., Widdel, F., Harding, K. J., Krukenberg, V., et al. (2016). Thermophilic archaea activate butane via alkyl-coenzyme M formation. *Nature* 539, 396–401. doi: 10.1038/nature20152.

Laso-Pérez, R., Wu, F., Crémière, A., Speth, D. R., Magyar, J. S., Krupovic, M., et al. (2022). Evolutionary diversification of methanotrophic *Ca.* Methanophagales (ANME-1) and their expansive virome. *bioRxiv*, 2022.07.04.498658. doi: 10.1101/2022.07.04.498658.

Laso Pérez, R. (2018). A novel mechanism for the anaerobic degradation of non-methane hydrocarbons in archaea. Available at: http://nbn-resolving.de/urn:nbn:de:gbv:46-00107156-15 [Accessed December 13, 2022].

Lemaire, O. N., and Wagner, T. (2022). A Structural View of Alkyl-Coenzyme M Reductases, the First Step of Alkane Anaerobic Oxidation Catalyzed by Archaea. *Biochemistry* 61, 805–821. doi: 10.1021/acs.biochem.2c00135.

Ljungdahl, L. G. (2009). A Life with Acetogens, Thermophiles, and Cellulolytic Anaerobes. *Annu. Rev. Microbiol.* 63, 1–25. doi: 10.1146/annurev.micro.091208.073617.

Ljungdhal, L. G. (1986). The Autotrophic Pathway of Acetate Synthesis in Acetogenic Bacteria. *Annu. Rev. Microbiol.* 40, 415–450. doi: 10.1146/annurev.mi.40.100186.002215.

Martin, W. F. (2020). Older Than Genes: The Acetyl CoA Pathway and Origins. *Front. Microbiol.* 11, 817. doi: 10.3389/fmicb.2020.00817.

Mbadinga, S. M., Li, K.-P., Zhou, L., Wang, L.-Y., Yang, S.-Z., Liu, J.-F., et al. (2012). Analysis of

alkane-dependent methanogenic community derived from production water of a high-temperature petroleum reservoir. *Appl. Microbiol. Biotechnol.* 96, 531–542. doi: 10.1007/s00253-011-3828-8.

McKay, L., Klokman, V. W., Mendlovitz, H. P., LaRowe, D. E., Hoer, D. R., Albert, D., et al. (2016). Thermal and geochemical influences on microbial biogeography in the hydrothermal sediments of Guaymas Basin, Gulf of California. *Environ. Microbiol. Rep.* 8, 150–161. doi: 10.1111/1758-2229.12365.

Meyerdierks, A., Kube, M., Lombardot, T., Knittel, K., Bauer, M., Glöckner, F. O., et al. (2005). Insights into the genomes of archaea mediating the anaerobic oxidation of methane. *Environ. Microbiol.* 7, 1937–1951. doi: 10.1111/J.1462-2920.2005.00844.X.

Murali, R., Yu, H., Speth, D. R., Wu, F., Metcalfe, K. S., Crémière, A., et al. (2022). Physiological adaptation of sulfate reducing bacteria in syntrophic partnership with anaerobic methanotrophic archaea. *bioRxiv* 2022.11.23. doi: 10.1101/2022.11.23.517749.

Peretó, J. (2012). Out of fuzzy chemistry: from prebiotic chemistry to metabolic networks. *Chem. Soc. Rev.* 41, 5394. doi: 10.1039/c2cs35054h.

Reeburgh, W. S. (2007). Oceanic methane biogeochemistry. *Chem. Rev.* 107, 486–513. doi: 10.1021/cr050362v.

Sakai, S., Conrad, R., Liesack, W., and Imachi, H. (2010). Methanocella arvoryzae sp. nov., a hydrogenotrophic methanogen isolated from rice field soil. *Int. J. Syst. Evol. Microbiol.* 60, 2918–2923. doi: 10.1099/ijs.0.020883-0.

Schauder, R., Preuß, A., Jetten, M., and Fuchs, G. (1988). Oxidative and reductive acetyl CoA/carbon monoxide dehydrogenase pathway in Desulfobacterium autotrophicum. *Arch. Microbiol.* 151, 84–89. doi: 10.1007/BF00444674.

Seitz, K. W., Dombrowski, N., Eme, L., Spang, A., Lombard, J., Sieber, J. R., et al. (2019). Asgard archaea capable of anaerobic hydrocarbon cycling. *Nat. Commun.* 10, 1822. doi: 10.1038/s41467-019-09364-x.

Ueno, Y., Yamada, K., Yoshida, N., Maruyama, S., and Isozaki, Y. (2006). Evidence from fluid inclusions for microbial methanogenesis in the early Archaean era. *Nature* 440, 516–519. doi: 10.1038/nature04584.

Vanwonterghem, I., Evans, P. N., Parks, D. H., Jensen, P. D., Woodcroft, B. J., Hugenholtz, P., et al. (2016). Methylotrophic methanogenesis discovered in the archaeal phylum Verstraetearchaeota. *Nat. Microbiol.* 1, 16170. doi: 10.1038/nmicrobiol.2016.170.

Vulcano, F., Hahn, C. J., Roerdink, D., Dahle, H., Reeves, E. P., Wegener, G., et al. (2022). Phylogenetic and functional diverse ANME-1 thrive in Arctic hydrothermal vents. *FEMS Microbiol. Ecol.* 98, 1–11. doi: 10.1093/femsec/fiac117.

Wang, Y., Wegener, G., Hou, J., Wang, F., and Xiao, X. (2019). Expanding anaerobic alkane metabolism in the domain of Archaea. *Nat. Microbiol.* 4, 1. doi: 10.1038/s41564-019-0364-2.

Wang, Y., Wegener, G., Williams, T. A., Xie, R., Hou, J., Tian, C., et al. (2021). A methylotrophic origin of methanogenesis and early divergence of anaerobic multicarbon alkane metabolism. *Sci. Adv.* 7, 1–12. doi: 10.1126/sciadv.abj1453.

Wegener, G., Krukenberg, V., Ruff, S. E., Kellermann, M. Y., and Knittel, K. (2016). Metabolic capabilities of microorganisms involved in and associated with the anaerobic oxidation of methane. *Front. Microbiol.* 7, 1–16. doi: 10.3389/fmicb.2016.00046.

Woese, C. R. (1987). Bacterial evolution. *Microbiol. Rev.* 51, 221–271. doi: 10.1128/MMBR.51.2.221-271.1987.

Wood, H. G. (1991). Life with CO or CO2 and H2 as a source of carbon and energy. *FASEB J.* 5, 156–163. doi: 10.1096/fasebj.5.2.1900793.

Yashiro, Y., Sakai, S., Ehara, M., Miyazaki, M., Yamaguchi, T., and Imachi, H. (2011). Methanoregula formicica sp. nov., a methane-producing archaeon isolated from methanogenic sludge. *Int. J. Syst. Evol. Microbiol.* 61, 53–59. doi: 10.1099/ijs.0.014811-0.

Yu, H., Skennerton, C. T., Chadwick, G. L., Leu, A. O., Aoki, M., Tyson, G. W., et al. (2021). Sulfate differentially stimulates but is not respired by diverse anaerobic methanotrophic archaea. *ISME J.* 16, 168–177. doi: 10.1038/s41396-021-01047-0.

Zehnle, H., Lipp, J., Teske, A., and Wegener, G. (2022). Candidatus Alkanophaga archaea from heated hydrothermal vent sediment oxidize petroleum alkanes. doi: 10.21203/RS.3.RS-2096998/V1.

Zhao, R., and Biddle, J. F. (2021). Helarchaeota and co-occurring sulfate-reducing bacteria in subseafloor sediments from the Costa Rica Margin. *ISME Commun.* 1, 25. doi: 10.1038/s43705-021-00027-x.

Zhou, Z., Zhang, C., Liu, P., Fu, L., Laso-Pérez, R., Yang, L., et al. (2022). Non-syntrophic methanogenic hydrocarbon degradation by an archaeal species. *Nature* 601, 257–262. doi: 10.1038/s41586-021-04235-2.

Additional work

Tenacious sulfide tolerant sulfur-disproportionating bacteria retrieved from anaerobic methanotrophic enrichment cultures

Viola Krukenberg[1*#], David Benito Merino[1] Halina E. Tegetmeyer[2,3] and Gunter Wegener[1,4*]

[1]Max-Planck Institute for Marine Microbiology, Bremen, Germany;
[2]Alfred Wegener Institute, Helmholtz Center for Polar and Marine Research, Bremerhaven, Germany;
[3]Center for Biotechnology, Bielefeld University, Bielefeld, Germany;
[4]MARUM, Center for Marine Environmental Sciences, University Bremen, Germany
*Corresponding authors. Email viola.krukenberg@montana.edu, gwegener@mpi-bremen.de
#Present address: Montana State University, Bozeman, MT-59717, USA

Running title: novel marine sulfur-disproportionating bacteria

Abstract

The microbial transformation of inorganic sulfur species is essential to the biogeochemical sulfur cycle, and sulfur disproportionation is presumed among the most ancient modes of metabolism. However, few isolates of sulfur disproportionating bacteria exist, which all thrive at very low sulfide concentrations (i.e., provided by sulfide sinks). We here describe two novel marine sulfur disproportionating Deltaproteobacteria, *Candidatus* Desulfolitus althalia and *Candidatus* Desulfovarians guaymasii, enriched with zero-valent sulfur as sole energy source from long-term anaerobic methane-oxidizing enrichment cultures. Our cultures of *Ca.* D. althalia and *Ca.* D. guaymasii grow without a sulfur sink under autotrophic sulfur disproportionating conditions to sulfide concentrations up to 5 and 7 mM suggesting that in the environment sulfur disproportion may proceed at an extended range of sulfide concentrations by specialized sulfide-tolerant species. Interestingly *Ca.* D. guaymasii also thrives as hydrogen-dependent sulfur or sulfate reducer without observed increase in its growth efficiency. The generated draft genomes of both organisms encode for all essential cytoplasmic and membrane-bound enzyme complexes of the dissimilatory sulfate reduction pathway, several membrane-associated molybdopterin-containing oxidoreductases and cytoplasmic heterodisulfide reductase complexes as well as periplasmic and

cytoplasmic hydrogenases. Together these components may support sulfur disproportionation, or sulfur and sulfate reduction. Our study shows that slow growing metabolically specialized microorganisms such as sulfur disproportionating bacteria, sustain as minor population in long-term anaerobic marine enrichment cultures and are readily isolated with selective growth conditions.

List of manuscripts and declaration of contributions

Manuscript I:

Title: Deep-branching ANME-1c archaea grow at the upper temperature limit of anaerobic oxidation of methane

Authors: David Benito Merino, Hanna Zehnle, Andreas Teske, Gunter Wegener

Journal: Frontiers in Microbiology (2022)
DOI: 10.3389/fmicb.2022.819187

Contribution of the candidate of the total workload:

Experimental concept and design:	80%
Experimental work and acquisition of the data:	100%
Data analysis and interpretation:	90%
Preparation of figures and tables:	100%
Drafting of the manuscript:	80%

Manuscript II:

Title: Anaerobic hexadecane degradation by a thermophilic Hadarchaeon from Guaymas Basin

Authors: David Benito Merino, Julius S. Lipp, Guillaume Borrel, Antje Boetius, Gunter Wegener

Journal: ready for submission to ISME Journal

Contribution of the candidate of the total workload:

Experimental concept and design:	80%
Experimental work and acquisition of the data:	90%
Data analysis and interpretation:	90%
Preparation of figures and tables:	95%
Drafting of the manuscript:	80%

Manuscript III:

Title: Mechanisms for syntrophic interspecies electron transfer are widespread in genomes of Thermodesulfobacteria

Authors: David Benito Merino, Hanna Zehnle, Gunter Wegener.

Journal: to be decided, manuscript in preparation

Contribution of the candidate of the total workload:

Experimental concept and design:	50%
Experimental work and acquisition of the data:	70%
Data analysis and interpretation:	80%
Preparation of figures and tables:	100%
Drafting of the manuscript:	90%

Acknowledgements

I think life is beautiful because we learn things. My fascination for biology started during high school thanks to my teacher **Ana María**. She explained this complex science in a simple way and with a great sense of humour. I am grateful to many other teachers and professors that accompanied me since then. This PhD was a process that taught me to teach things to myself, but this is hard and I still can't do it that well! Therefore, I'd like to thank many people that gave me support during the journey. I will do this without mentioning academic titles but with profound respect.

Antje thank you for welcoming me in the friendly Habitat group, which you manage so well despite your busy calendar. I am grateful for your valuable feedback during committee meetings and for reviewing my thesis.

Cornelia, thank you for agreeing to review my thesis. I hope you make it until here and you like it! Thanks to **Kai-Uwe** and **Florence** for being part of the examination committee. **Maggie**, thank you for being the student representative in the committee.

Gunter, thank you! You have so much knowledge in so many different topics. It is always fun to discuss science with you and I am sure we could do it much better in a world without deadlines. Thanks for your support during the last four years and for being a fast reader! Also thank you for introducing me to Fusion.

Thank you to **Guillaume**, **Katrin** and **Tristan** for your scientific input during committee meetings. Thanks to **Andreas**, **Guillaume**, **Hanna** and **Julius** who contributed during manuscript preparation. Big thanks to **Batu**, **Hanna**, **Miri** and **Tina** who helped with thesis proofreading

Thanks to my **office mates –** you made work really enjoyable. **Rafa**, gracias por mostrarme el mundo de las arqueas y los alcanos, por tu ayuda cuando era un doctorando bebé y por los buenos momentos. **Batu**, thank you for reminding us to drink coffee regularly and for many nice conversations in the office. I am sorry for torturing you with my music. **Hanna**, thank you and gracias for listening to me complain about everything in two languages. I enjoy the scientific and non-scientific talks. I hope I will help you as much as you did. Where is **Lewen**? You were only briefly in the Habitat group, but we still remember you for all the fun we had.

Thank you to all current and former Habitants: **Magda**, **Christina**, **Teresa**, **Massi**, **Eddie**, **Felix**, **Pier**, **Raïssa**, **Matthias**, **Francesca**, **Cedric** and **Stian**. You are a very friendly crew and I really enjoyed social events with you. Also thanks to the technicians and especially to **Susanne** who maintains a very organized

lab despite our chaotic practices. Thanks to all **colleagues** that made times at the MPI enjoyable. Thanks especially to my dear PhD reps: **Elisa**, **Tina**, **Chiara** and **Bledina**. We had a lot of fun organizing events. Thank you to **Alexandra Elbakyan** for making science accessible for everyone.

Gracias a **Ingrid** por enseñarme a mantener mi posición pisando fuerte. Estoy muy agradecido porque me ha enseñado a relativizar las cosas durante el último año y medio. Gracias, danke.

Life is also beautiful because I made **friends** in …

… Bremen. Thank you **Cora** and **Matt** for starting this journey together and for the good times in Bremen. I still think you shouldn't have moved to other cities! **Andrea**, mi motomami favorita, gracias por todo tu apoyo, por las risas, por los cotilleos, por las noches en que nos perdimos en Heartbreak Hotel o en Bermuda Dreieck. **Carsten**, thank you for creating two homes in Viertel, one covered in Hemelinger stickers and a fancier one. **Chiara** and **Malte**, thanks for the fun times at Werdersee. Danke an alle Volleyball Mitspielern: ihr seid ein Grund dafür, Stahlbeinen zu haben! **Elisa**, **Chiara** and **Tina**, thank you for many dinners and many chats to complain about the PhD life. **Niek**, thank you for the films, for the conversations and silences, and for the rock climbing sessions. Vielen Dank an **Leo**, meine halbe Orange, für die virtuellen und realen Erfahrungen mit Kosmetika, Martini und LoL. Danke auch für die logistische Unterstützung während der letzten Woche. **Vitor**, you are fun and calmness, contradiction and logic. Now I am curious to get to know you more, obrigado!

… Burgos. A **Irene** y **Clara**, porque os conozco desde que éramos adolescentes con acné. Hacéis que quiera ir a casa para tomar un calimocho rememorando viejos tiempos o un vermú riéndonos del presente. Irene, ojalá fuera la mitad de trabajador que tú: habría acabado la tesis mucho antes. Clara, quizás adopto tu perro homosexual, aún me lo estoy pensando. Me encantó que me visitarais en Bremen. ¡Gracias!

… Barna. A **Alberto**, **Cèsar**, **Edgar**, **Enric**, **Marc**, **Ot**, **Pol** y **Tolo**. He terminado esta tesis con la falsa esperanza de tener más tiempo para veros. Gracias por las risas y por los viajes juntos. A **Ot**, por enseñarme que se puede ser feliz siendo organizado, por las llamadas, por las risas y por aguantar mis ralladitas varias. Gràcies! A **Alba**, gracias por las llamadas interminables, por esos momentos en los que nos vemos físicamente y exprimimos cada rato juntos. Eres la persona más sensible y empática que conozco, tengo mucha suerte de tenerte como amiga.

I am lucky to have a supportive **family**. A mi padre y a mi madre, que son mis raíces. **Papa**, **mama**: gracias por vuestra paciencia más o menos infinita, por creer en mis hermanos y en mí, por querernos con

nuestras diferencias, que entiendo que no es fácil. Aunque a veces no os llame tan a menudo como querríais, siempre estáis en mi mente y en mis historias. Gracias por los valores que me habéis transmitido y que me esfuerzo en defender como buen testarudo que soy. Me siento muy orgulloso de vuestra sencillez y de vuestra complejidad. A mis tías, **Carmenchu** y **Mª. Ángeles**, que son maravillosas. Gracias por vuestros cuidados y todo vuestro cariño. A mis hermanos, Gonzalo, Cristina y Laura: no sé cómo de adolescentes accedíais a hacer de canguros con vuestro hermano pequeño, pero estoy muy agradecido porque me habéis llevado a mil sitios. **Gon**, gracias por la música, por las poesías y por la rebeldía. Eres como un libro abierto, de las personas más inteligentes que conozco. **Cris**, gracias por tus cuidados, por tu talento para hacer regalos y que usas complacer a todos los que te rodean. Con tus viajes hiciste que me llamase la atención salir a ver el mundo. **Lau**, gracias por encontrar siempre la risa, por las llamadas largas, por escucharme y por entenderme tan bien. Ojalá pudiéramos vernos todos los días. Gracias **Marcos** y **Pedro** por ser parte de la familia y cuidar a mis hermanas.

Por último, a mis sobrinos **Aitana**, **Álvaro**, **Carmen**, **Paula** y **Pedro**. Sois refrescantes, enérgicos, novedosos. Espero que podamos construir un mundo que esté a vuestra altura (de momento bajita) y en el que seáis felices. Al menos tanto como lo soy yo cuando aprendo lo que vais aprendiendo.

Versicherung an Eides Statt / *Affirmation in lieu of an oath*

gem. § 5 Abs. 5 der Promotionsordnung vom 18.06.2018 /

according to § 5 (5) of the Doctoral Degree Rules and Regulations of 18 June, 2018

Ich / *I*, _____

(Vorname / *First name*, Name / *Name*, Anschrift / *Address*, ggf. Matr.-Nr. / *student ID no., if applicable*)

versichere an Eides Statt durch meine Unterschrift, dass ich die vorliegende Dissertation selbständig und ohne fremde Hilfe angefertigt und alle Stellen, die ich wörtlich dem Sinne nach aus Veröffentlichungen entnommen habe, als solche kenntlich gemacht habe, mich auch keiner anderen als der angegebenen Literatur oder sonstiger Hilfsmittel bedient habe und die zu Prüfungszwecken beigelegte elektronische Version (PDF) der Dissertation mit der abgegebenen gedruckten Version identisch ist. / *With my signature I affirm in lieu of an oath that I prepared the submitted dissertation independently and wit hout illicit assistance from third parties, that I appropriately referenced any text or content from other sources, that I used only literature and resources listed in the dissertation, and that the electronic (PDF) and printed versions of the dissertation are identical.*

Ich versichere an Eides Statt, dass ich die vorgenannten Angaben nach bestem Wissen und Gewissen gemacht habe und dass die Angaben der Wahrheit entsprechen und ich nichts verschwiegen habe. / *I affirm in lieu of an oath that the information provided herein to the best of my knowledge is true and complete.*

Die Strafbarkeit einer falschen eidesstattlichen Versicherung ist mir bekannt, namentlich die Strafandrohung gemäß § 156 StGB bis zu drei Jahren Freiheitsstrafe oder Geldstrafe bei vorsätzlicher Begehung der Tat bzw. gemäß § 161 Abs. 1 StGB bis zu einem Jahr Freiheitsstrafe oder Geldstrafe bei fahrlässiger Begehung. / *I am aware that a false affidavit is a criminal offence which is punishable by law in accordance with § 156 of the German Criminal Code (StGB) with up to three years imprisonment or a fine in ca se of intention, or in accordance with § 161 (1) of the German Criminal Code with up to one year imprisonment or a fine in case of negligence.*

_____ _____

Ort / *Place*, Datum / *Date* Unterschrift / *Signature*